Universitat Politècnica de Catalunya

ESCOLA TÈCNICA SUPERIOR D'ENGINYERS DE CAMINS, CANALS I PORTS DE BARCELONA.

DEPARTAMENT D'ENGINYERIA DE LA CONSTRUCCIÓ
CONSTRUCTION ENGINEERING DEPARTMENT

"DYNAMIC ASSESSMENT OF STRUCTURAL BUILDING COMPONENTS"

PH.D. THESIS
BY
JUAN CARLOS ARAIZA GARAYGORDÓBIL

PROMOTED BY
PERE ROCA I FABREGAT

BARCELONA, SPAIN. FEBRUARY 2003.

A Lílian

y a mis padres Juan Carlos y Griselda.

ACKNOWLEDGMENTS

"DYNAMIC ASSESSMENT OF STRUCTURAL BUILDING COMPONENTS"

Ph. D. Thesis by. **Juan Carlos Araiza Garaygordóbil**
Directed by. **Pere Roca i Fabregat**

Construction Engineering Department, Technical University of Catalonia, Spain.

Summary

The development of methods that correlate the measure of dynamic parameters with the condition of the structure has received a considerable attention from the engineering community in the last few years.

In the field of structural assessment of buildings, dynamic testing can be a valuable tool to extend the inspection to every structural component, covering the gaps left by other more complex techniques (such as core extraction or load testing). The information obtained by dynamic means is not restricted only (as traditional methods are) to the location in which the tests is developed while the use of a low number of sensors and simple excitation devices helps to reduce dramatically the cost of implementation.

The general objective of the thesis consists on the demonstration of the usefulness of dynamic assessment on building components (such as masonry walls, stone piers or RC beams and slabs) using a simple-layout experiment but based intensively in numerical simulation.

The methodology to achieve the objective include tasks such as:

- The study the influence of different parameters on dynamic behavior of structures. This process -also known as parametrical study- recognizes the influence of the variables when performing a model updating.

- A series of laboratory campaigns to identify the influence of different structural damages on dynamic parameters. Studied damage-influence include: Stiffness deterioration by cracking on supported or suspended beams, carbonation of concrete, sulfate attack on concrete and rebars, chloride attack on concrete and axial load on masonry walls and piers.

- The application of a simple-layout method of dynamic assessment in real-life buildings. In some of those cases, static load test (direct identification method) is also developed to compare the reliability of the dynamic approach.

Experimental works and field studies carried out in this investigation have permitted to conclude that a combined implementation of a simple dynamic testing and numerical modeling is able to characterize the current structural conditions of a building component. The proposed dynamic assessment layout has conduced to the identification of characteristics such as boundary conditions, cracking levels, geometry properties or levels of axial loading. By comparing systematically the experimental and the numerical frequencies, it can also be concluded that a detailed model is able to predict the dynamic behavior of a building component. This prediction was accurate not only for undamaged conditions, but also for different damage scenarios. The present research has contributed to ascertain that dynamic testing is a valuable tool to assess the structural conditions of single concrete or masonry building elements such as concrete beams, RC or prestressed slabs, masonry walls or stone piers.

Contents

CHAPTER 1.   INTRODUCTION

CHAPTER 2.   *STATE-OF-THE-ART* ON DETERIORATION AND INSPECTION TECHNIQUES

CHAPTER 3. *STATE-OF-THE-ART* ON DAMAGE IDENTIFICATION BY DYNAMIC INSPECTION

CHAPTER 4.   LAY-OUT OF APPLIED DYNAMIC ASSESSMENT

CHAPTER 5.   PARAMETRICAL SENSITIVITY STUDIES

CHAPTER 6.   LABORATORY WORKS

CHAPTER 7. FIELD STUDIES

CHAPTER 8.   CONCLUSIONS AND FINAL REMARKS

one

Introduction

1.1.   Introduction

Dynamic inspection, based on the monitoring of the dynamic response of structures by means of either natural or forced vibration, has deserved growing interest during the last years due to its potential capacity to provide information on the gometrical or mechanical properties of the structure and its possible deterioration at low cost and in a non-destructive way.

A variety of non-destructive techniques are today available to assess damage in structures. Most of these thechniques, such as those based on the emissionand measure of acoustics waves, eddy currents, magnetic fields, X-rays, etc., require the vicinity of the damage to be known a priori and the portion of the structure being inspected to be readily accessible. Subjected to these limitations, these experimental methods can detect damage on or near the surface of the structure.

Dynamic inspection constitutes one of the few monitoring methods that affords the identification of geometrical or mechanical properties of a complete structural member. Usually, the dynamic response of a structure, at any point, is influenced by the general properties of the member, meaning that local measures provided by a limited set of sensors may be significant of the overall behavior of the structural

member. Furthermore, the representativity of the measures may me enhanced by an adequate choosing of the locations of the sensors used.

Inspection by dynamic monitoring has become a practical task probably since only 15 or 20 years. Its applicability to practical engineering taks has been probably allowed by the arrival of powerful personal computers and, in turn, the development of affordable equipment for dynamic acquisition. As presented further in Chapter 3, dynamic inspection is today being increasingly used in different engineering fields. One of the most common and better-studied applications is found in the structural evaluation of bridges (Casas, 1988; Doebling, 1996 or Peeters, 2000).

The interest in developing applications of dynamic assessment is manifested in the efforts carried out by many research groups at the international level, such as the Structural Mechanics Section of the Catholic University of Leuven [KUL], the Department of Civil Engineering of the University of Rome "The Sapienza" or the National Research Laboratory "Los Alamos" in United States or the "Earthquake research institute" of the University of Tokyo. On the other hand, the subject is deserving specific conferences, such as the recent European conference on *"System Identification and Structural Health Monitoring"* (June of 2000), celebrated in Madrid under the frame of *COST committee for structural dynamics* [COST, 2000]. The conference called over a hundred participants who presented applications related all kind of civil, architectural, historical, aeronautical, structures, thus showing the wide field of applications of dynamic testing,

The motivation to extend the applicability of dynamic testing to building components is the pervasive occurrence of damage on this structural typology. Diverse research works addressed on this field have already been developed and are presented further in the *state-of-the-art.*

Structural assessment of buildings is today a complex activity that involves a high interference with the usage of the structure and costly techniques such as core extraction or load testing. The obtained information is restricted only to the location in which the destructive-tests were developed. Nevertheless, dynamic testing can

extend the structural inspection to every structural component, covering the gaps left by other more complex techniques. A simultaneous use of destructive tests (restricted number of core extraction and load testing) and an exhaustive dynamic characterization may provide a complete panorama of the structural condition of the assessed building.

One of the advantages of dynamic testing that can be fully rentabilized when adressing to building components, is its repeatability. Several dozens and even hundreds of dynamic tests can be carried out in few hours. This characteristic becomes the test into an attractive alternative for the evaluation of building structural components with a repetitive pattern such as concrete slabs, masonry or concrete columns, masonry walls or prestressed and RC beams. All this structural components are commonly present in building construction.

This thesis addresses two key issues of a real-life monitoring system. The first issue (the hypotheses) is the option for a simple dynamic test based on the usage of a limited number of sensors and output-*only* measurements. The use of a low number of sensors and shock hammer helps to reduce dramatically the cost of implementation if compared with traditional dynamic techniques. The exclusion of complex excitation devices (such as shakers or shaking tables), the reduction of the number of sensors and the subsequent data acquisition simplification are some of the characteristics of the proposed method. The second issue (validation of the hypotheses) is to probe the effective usability of the defined technique. The method will be applied on real structures and laboratory specimens under controlled conditions to show that it may actually provide, in spite of its simplicity, valuable information about the geometric and material properties and also about the possible deterioration of the structure.

1.2. Objectives

1.2.1. General

The general objective of the thesis consists on the demonstration of the usability of dynamic assessment on building components (such as masonry walls, stone piers or RC beams and slabs) as a combination of a simple lay-out experiment with intensive numerical simulation.

1.2.2. Particular

The following partial objectives are envisaged to attain the above-mentioned general objective:

- To review the previous contributions to the *state-of-the-art* on dynamic identification of structures.

- To define the dynamic testing lay-out in which the present research is to be based. The proposed test must take in account the *state-of-the-art* and other features such as economy, simplicity, versatility and effectiveness.

- To characterize the influence of the main geometrical and mechanical parameters on the dynamic behavior of structural building components. This study includes specific parametrical studies such as:

  o the influence of mass, reinforcement, support conditions, strain modulus, damage and tension stiffening in RC beams

  o the influence of mass, reinforcement, support conditions, strain modulus, damage, tension stiffening, shape and orthotropy in RC slabs.

  o the influence of support conditions, axial load and hardening process in stone piers.

- To characterize the influence of different types of damage (mechanical or chemical) on the dynamic response of reinforced concrete beams.

- To analyze the possibility of correlating the axial load with measured dynamic properties in masonry components (walls and piers).

- To calibrate a numerical model able to simulate accurately the variation of the dynamic properties under different load or damage conditions for all the studied components (beams, slabs, walls and piers).

- To validate the effectiveness of the proposed procedure of dynamic assessment by studying real cases. Field-studies includes:

  o the dynamic identification and model updating of one-way RC slabs

  o the dynamic testing and model updating of a prestressed concrete slab

  o the dynamic assessment of historical construction including different structural masonry components.

- To draw conclusions and recommendations about dynamic testing for different types of building components. This recommendations include considerations on:

  o testing equipment

  o data acquisition and system identification

  o numerical modeling

  o interpretation of the results

- Finally, to point out future research lines related to dynamic testing and identification in building components.

1.3.   Methodology

The methodology to achieve this general objective is divided into a series of tasks. Those tasks are synthesized in the next lines:

- A deep literature review on damage identification, analyzing previous works carried out in topics like: dynamic evaluation of concrete structures, measurements of dynamic properties of structures, concrete durability, damage identification, etc. This state-of-the-art analysis must constitute the background for the new technique proposal.

- To propose a method of dynamic evaluation of concrete beams and slabs based on the actual scientific knowledge. This technique must match the basic criteria of being simple and reasonably effective.

- Study the influence of different parameters on dynamic behavior of structures. This process -also known as parametrical study- recognizes the influence of the variables when performing a model updating. Some of the studied variables are boundary conditions, elasticity modulus, dead loads, participation of pavements on stiffness, tension stiffening, etc.

- A series of laboratory campaigns to identify the influence of different structural damages on dynamic parameters. Studied damage-influence include: Stiffness deterioration by cracking on supported or suspended beams, carbonation of concrete, sulphate attack on concrete and rebars, chloride attack on concrete and axial load on masonry walls and piers. After developing those experimental programs, it will be possible to define which kind of damage can be identified through dynamic test. Experimental laboratory works include:

    - The influence of artificially induced chemical attack on dynamic parameters of concrete beams (Laboratory campaign).

    - The influence of mechanical (cracking) damage on simply supported RC beams (Laboratory campaign).

- The influence of mechanical (cracking) damage on support-isolated RC beams (Laboratory campaign).

- The influence of axial load on dynamic parameters of masonry walls and piers (Laboratory campaign).

- Application of the method in real-life buildings. In some of those cases, static load test (direct identification method) is also developed to compare the reliability of the dynamic approach. Field studies include:

  - Application of the test for dynamic identification of real-building concrete floor slabs (Real case studies).

  - The use of dynamic assessment of masonry walls and piers subjected to axial load in real buildings (Real case studies).

- Finally, to explore some other possibilities such as: the correlation between the stiffness reduction (cracking) and the prediction of the load-caring capacity or the correlation between the identified damping with the real stiffness (influenced by the existence of cracks).

1.4. Organization of the document

Chapter 1

Introduces the thesis, situating the specific contribution into a more general frame. Objectives are also defined and the methodology to achieve them is proposed.

Chapter 2

This research work is supported in certain theoretical background. The chapter situates the reader in to the frame of durability of concrete structures and structural monitoring methods.

Chapter 3

This chapter develops a deep state-of-the-art review on dynamic damage identification. The last advances in dynamic identification of structures are mentioned in this chapter, the previous state-of-the-art reviews on system identification are mentioned and applications to different kinds of structures are also classified.

Chapter 4

In this chapter a lay-out for dynamic testing on building components and its requirements are defined. The goal of the method is to identify damage in members of reinforced concrete elements or masonry walls and piers. The method requires measurement of dynamic parameters on the structure and the adjustment of a numerical model using those parameters. In this chapter, every part of the proposed method (from data acquisition to model updating) is described in full detail.

Chapter 5

When identifying dynamic properties from a real structure, many different parameters can influence the observed data. Those parameters can be boundary conditions, stiffness of architectural elements like pavements or walls, modulus of elasticity, level of cracking, dead load and many others. In this chapter, an investigation of the influence of every of those parameters on the numerical model is developed. Detailed geometry and material behavior is considered, including non-linear phenomena and reinforcement steel.

Chapter 6

This chapter describes several experimental research programs carried out under laboratory conditions. Those campaigns study the influence of different degradation processes on dynamic parameters of concrete beams. The goal of the first of this works is to identify the influence of typical chemical attack (Carbonation, Sulphate and Chloride attack) on the dynamic behavior of concrete beams. Other laboratory campaigns were addressed to investigate the evolution of dynamic parameters after

load/cracking processes. Evaluated parameters were natural frequencies or modal shapes. Two works were developed in this sense, one in a 6 m span suspended concrete beams (University of Leuven, Belgium) and other in a 2.75 m span supported concrete beams (Technical University of Catalonia). Finally, laboratory works developed on masonry walls and piers are also described. In this chapter, those laboratory campaigns are fully described.

Chapter 7

A series of practical applications of the test were developed in real buildings. In this chapter, the development of those dynamic tests is described in detail. Dynamic testing is used on every case in the solution of different engineering field-problems. Several concrete-slabs were evaluated in different buildings in Spain and Belgium. The dynamic test is simultaneously developed with static load-test in some cases. All the practical applications carried out on real structures are described on detail in this chapter. Additionally, a series of applications in historical constructions are presented on this chapter. The pillars of the cloister of Girona's Cathedral were dynamically evaluated to identify material properties and constrain conditions of the Romanesque columns. A load-caring wall in Palau Güell in Barcelona was also tested dynamically several times to identify damage and morphology. The façade of the church of Notre Dame of Laken in Belgium was subject to a study due to atmospheric degradation on the pinnacles of the main tower.

Chapter 8

This final chapter summarizes the conclusions of this work. Some new possibilities are also studied (like the study of damping or the prediction of remaining load caring capacity of the structure based on dynamic testing). Additionally, some unsolved problems and suggestions for future research are mentioned.

two

State-of-the-art on deterioration and inspection techniques

2.1. Introduction

This chapter is objected to present a brief description of the *state-of-the-art* on two different areas of the knowledge that are considered the *start-point* for the development of this thesis. Those areas are the related to deterioration of concrete structures and inspection techniques.

The alteration of the dynamic parameters of a concrete structure is due basically to changes in basic properties related to: Geometry, material or boundary conditions. Typical processes that modify material or geometry characteristics are related with deterioration. On the first part of this chapter, a brief description of the deterioration processes that take place in concrete structures is presented.

A good approach for identifying defects of a mathematical model used in the design or evaluation of structures consists on investigating its behavior by means of field tests. This clear need of interaction with the structure, favored by the development in terms of acquisition and microcomputers has impelled the improvement of *in-situ* structure evaluation techniques. Structural health monitoring is an active field of research, driven by the need to complement subjective visual inspection methods by objective nondestructive evaluation tools based on physical measurements and computer analyses. The objective of the last part of this chapter is to situate the dynamic test as a non-destructive evaluation tool in the context of available

techniques; therefore, a review of the non-destructive methods in general is developed.

2.2.   Durability in concrete structures.

2.2.1.   Generalities on deterioration

Every concrete structure has to sustain its intended service life; this is, to maintain its required strength and serviceability during an expected period. Concrete, under this concept, should withstand the processes of deterioration to which it can be exposed.

Causes of inadequate durability manifest itself by deterioration, which can be due either to external factors or internal causes within the concrete itself. The various actions can be physical, chemical or biological [Regourd, 1983]. Among physical causes, mechanical damage is caused by impact, abrasion, erosion or cavitation. The chemical causes of deterioration include the alkali-silica and alkali-carbonate reactions. External chemical attack occurs mainly trough the action of aggressive ions such as chlorides, sulphates or carbon dioxide, as well as many natural or industrial liquids and gases. Physical causes of deterioration include the effects of high temperatures or differences in thermal expansion in hardened concrete. An important cause of damage is alternative cycles of freezing and thawing and the association of use of de-icing salts.

Rostam [1992] affirms that behind corrosion of steel reinforcement, there are only tree important deterioration processes: alkali-silica reaction, chemical attack and damage due to freezing and thawing cycles. This consideration is frequently founded on literature. These three mechanisms, in addition to abrasion, are also considered by ACI [1991] as the main causes of deterioration.

2.2.2.   Physical deterioration

Cracking is the first visible sign under deterioration process. Many causes can produce cracking in concrete, as presented in section 2.2.5. of this chapter.

Campbell-Allen and Roper [1991] have presented a detailed study on cracking and its consequences.

As temperature of structural concrete in service is lowered, the water held in capillary pores in the hardened cement paste is in a manner similar to the freezing in pores in rock [Neville, 1995], and expansion of concrete takes place. If re-freezing follows subsequent thawing, further expansion takes place, so that repeated cycles of freezing and thawing have an accumulative effect. The process takes place mainly in the cement paste. Studies of freezing and thawing processes on concrete, have also demonstrated degradation of aggregates under cold conditions. The action of freezing was studied by Malhorta [1991]. He has accepted the hypothesis that osmotic pressure is the cause of the observed damage.

Under many circumstances, concrete surfaces are subjected to abrasion. This may be due to attrition by sliding, scrapping or percussion. In the case of hydraulic structures, the action of abrasive materials carried by water leads to erosion. Another cause of damage to concrete in flowing water is cavitation.

Abrasion seems to involve high-intensity stress applied locally so that the strength and hardness of the surface zone of concrete strongly influence the resistance to abrasion.

Erosion of concrete is an important type of damage, which can occur in concrete on contact with flowing water. It is convenient to distinguish erosion due to solid particles carried by the water and damage due to pitting resulting from cavities forming and collapsing in water flowing at high velocities. The rate of erosion depends on the quantity, size, shape and hardness of transported particles. Quality of concrete and velocity of flow are also important factors when erosion is considered.

2.2.3. Chemical attack

There are three fluids, which can enter concrete, that are relevant to durability: water, pure or carrying aggressive ions, carbon dioxide and oxygen. They can move trough concrete in different ways, but all transport depends primary on the structure of the hardened cement paste.

Discussion of the behavior of concrete is generally based on the assumption that ambient medium is air which does not react with hydrated cement paste. However, in reality, air contains CO_2, which, in the presence of moisture, reacts with hydrated cement; the actual agent is carbonic acid, because gaseous CO_2 is not reactive.

Carbonation by it self, does not cause deterioration of concrete but it has an important effect. One of these is the carbonation shrinkage. With respect to durability, the importance of carbonation lies in the fact that it reduces the pH of the pore water in hardened Portland cement paste from between 12.6 to 13.5 to a value of about 9. The significance of this change is that steel embedded in hydrating cement paste rapidly forms a thin passive layer of oxide which strongly adheres to the underlying steel and gives it complete protection for reaction with oxygen and water. This state of steel is known as passivation. Maintenance of passivation is dependant on adequately high pH of the pore water in contact with passivating layer. Thus, when the low pH front reaches the vicinity of the surface of reinforcement steel, the protective oxide film is removed and corrosion can take place.

Carbonation occurs progressively from the outside of concrete exposed to CO_2, but does so at decreasing rate because CO_2 has to diffuse trough the pore system, including the already carbonated surface zone of concrete. Such diffusion is a slow process if the pores in hydrated cement paste are filled with water because diffusion of CO_2 in water is 4 orders of magnitude slower than in air.

The highest rate of carbonation occurs at a relative humidity of 50 to 70 percent. A way of giving a broad picture is to say that, in concrete wit water/cement ratio of 0.60, a depth of carbonation of 15mm would be reached after 15 years, but at a water/cement ratio of 0.45 only after 100 years.

Carbonation can also have some positive consequences, because $CaCo_3$ occupies a greater volume than $Ca(OH)_2$ which it replaces, so the porosity of carbonated concrete is reduced. Also, water released by $Ca(OH)_3$ on carbonation may aid the hidratation of remaining unhydrated cement. This changes result on increased surface hardness, reduced surface permeability, reduced moisture movements and increased resistance to those forms of attack, which are controlled by permeability.

Other important chemical source of deterioration in concrete is the sulfate attack. Solid salts do not attack concrete, but when present in solutions, they can react with hydrated cement paste. Particularly common are sulfates of sodium, potassium, magnesium and calcium, which occur only in soil or groundwater. The significance of this lies in the fact that those other sulfates react not only wit $Ca(OH)_2$ but also with the various product of hidratation.

The consequences of sulfate attack include not only disruptive expansion and cracking, but also loss of strength of concrete due to the loss of cohesion in the hydrated cement paste and the adhesion between it and the aggregate particles. Concrete attacked by sulfates has a characteristic whitish appearance. The damage usually starts at edges and corners and is followed by progressive cracking and spalling which reduce the concrete to a soft state.

Sulfate attack reacts mainly with $Ca(OH)_2$ and C_3A, forming etringite. This reaction forms expansive products and can cause deterioration. Chemical reaction under sulfate attack has been widely studied by Regourd [1983].

An important chemical phenomena suffered by concrete is also the alkali-silica reaction. During the past few years, an increasing number of chemical reactions between the aggregate and the surrounding hydrated cement paste have been observed. The most common reaction is that between the active silica constituents of the aggregate and the alkalis in cement. The reaction starts with the attack of the siliceous minerals in the aggregate by the alkaline hydroxides in pore water derived from alkalis (Na_2O and K_2O) in the cement. As a result, an alkali-silicate gel is formed [Neville, 1995] either in planes of weakness or pores in the aggregate

(where reactive silica is present) or on the surface of the aggregate particles. In the latter case, a characteristic altered surface zone is formed. This may destroy the bond between the aggregate and the hydrated cement paste.

The reaction can be disruptive and manifest itself as cracking. The crack width can range from 0.1 mm to as much as 10 mm in extreme cases [Kropp, 1995]. The cracks are rarely longer than 25 mm. Hence, in most cases, the alkali-silica reaction adversely affects the appearance and serviceability of a structure, rather than its integrity; in particular, the comprehensive strength of the concrete in the direction of the applied stress is not greatly affected.

Chloride attack is different in that the primary action is the corrosion of steel reinforcement, and it is only as a consequence of this that the surrounding concrete is damaged. Corrosion of reinforcement is one of the major causes of deterioration of reinforced concrete structures in many places.

Chloride ions can be present in concrete due to two basic processes: incorporated and introduced:

Incorporated chlorides can be present in concrete after the use of additions, basically hardening accelerators, which can contain $CaCl_2$ [Helene, 1993]. This salt is melted in water with chlorides products. Other way of adding chlorides to concrete is by aggregates or in mixture water, mainly when this material are taken from costal zones. In this case source of chlorides is NaCl [Papadakis et. al, 1996]. In case that mixture water proceeds from a recycling plant or receives treatment before use (against micro organisms), chlorides can also be included.

Introduced chlorides are incorporated to the concrete after hardening process. Normally, this kind of chlorides comes from NaCl or $MgCl_2$, included in de-icing salts. Introduced chlorides can enter to the structure of concrete also, and commonly, by direct contact with seawater. This is more obvious in the semi-covered structures or in the surrounding structures influenced by wind transport.

Helene [1993] mentioned that this introduction could take place also by cleaning products, for example, using HCl solutions in low concentration.

2.2.4.   Corrosion of reinforcement steel

The protective passive layer on the surface of embedded steel was mentioned on section 2.2.3. This layer, which is self-generated soon after the hydration of cement has started, consists on γ-Fe_2O_3 tightly adhering to the steel. As long as the oxide layer is present, the steel remains intact. However, chloride ions destroy the film and, with the presence of water and oxygen, corrosion occurs. Chlorides were described by Verbeck [1975] as "a specific and unique destroyer".

A brief description of the corrosion phenomenon is as follows. When there exists a difference in electrical potential along the steel in concrete, an electrochemical cell is set up. The cell consists on anodic and cathodic regions, connected by the electrolyte in the form of the pore water in the hardened cement paste. The positively charged ferrous ions Fe^{++} at the anode pass into the cathode where they are absorbed by the constituents of the electrolyte and combine with water and oxygen to form hydroxyl ions $(OH)^-$. These travel trough the electrolyte and combine with ferrous ions to form ferric hydroxide, which in converted by further oxidation to rust.

In case of reinforcement steel, there is an electrochemical corrosion process, because steel is embedded in a liquid media, and ions can circulate trough this electrolyte. Typical anodic and cathodic reactions are respectively:

$Fe \Rightarrow Fe^{++} + 2e^-$

$4e^- + O_2 + 2H_2O \Rightarrow 4(OH)^-$.
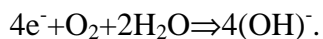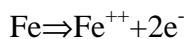
It can be seen that oxygen is consumed and water is regenerated, but it is still needed for the process to continue. Thus, there is no corrosion in dry concrete, probably bellow a relative humidity of 60 per cent; nor is there corrosion in concrete fully immersed in water, except when water can include air, under wave action for example.
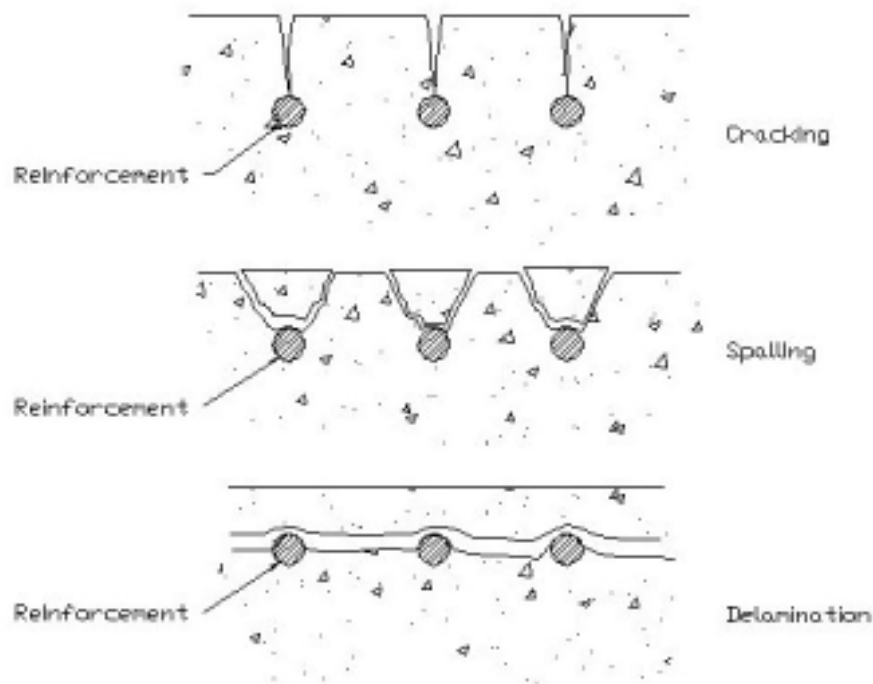
Figure 2.1. Pathology generated in concrete by steel corrosion

2.2.5. Signs and causes of deterioration in concrete structures

The signs of deterioration are either physical or chemical processes, which can cause visible signs of damage. Inspectors should therefore look in particular for the following signs of deterioration [Federation Internationale de la Precontrainte, FIP, 1986]:

Spalling

This is caused for example by:

   (a) the corrosion of steel reinforcement or other embedded metal

(b) the freezing of cracked or porous concrete

(c) chemical attack

(d) poor quality concrete

(e) insufficient reinforcement or overloading

(f) thermal shocks due to fire

(g) accidental mechanical damage

(h) bearing of a concrete element over another with insufficient joint width

Cracking

Cracks in concrete not always jeopardize the safety or bearing capacity of a structure. The possible effects of cracks must be considered in the context of cause. Cracks can be the effect or cause of a fault, or even both. Reinforced concrete is not wholly monolithic.

The design and structural analysis of a reinforced concrete structure are based on the hypothesis that the concrete will crack in the tension zone before the tension bars can take up the tension. Cracks in this part of a member will therefore not affect the immediate load bearing capacity of the member even if the cracks are of considerable width. However cracks in concrete cover will permit the entry of corrosion-accelerating agents to the steel, and thus brake down the corrosion protection of the reinforcement. Consideration should therefore be given to the possible need to seal by injection cracks that are wider than those allowed by the building code.

Consideration may have to be given to the fact that cracks influence the stiffness and dynamic response of a structure, where this has not already been considered in the design. Unforeseen cracks in prestressed concrete may entail a risk of fatigue failure, if they are subjected to repeated loading.

Cracks in the compression zone of a load-bearing member are often indicative of a lack of shear resistance, which could lead to ultimate failure of the structure.

Cracks can be classified in different bases. A simple method is to classify according to the primary cause as follows:

- Cracks in fresh concrete: They can be caused by plastic shrinkage; from movement or heat curing.

- Thermal cracks: These are: cracks across the whole section caused by heat of hidratation; surface cracks caused by heat of hidratation; or cracks across the whole section caused by the influence of ambient temperature.

- Shrinkage cracks: These can be due to: restraint from the surrounding structural elements; drying from one surface; different shrinkage rates or times; or different total shrinkage.

- Durability cracks: These can be caused by: freezing and thawing; corrosion of steel; attack by sulphates; or aggregate reactions (e.g. alkali-silica).

- Cracks caused by loading: These can be due to: bending, tension, shear, torsion, bond failure or concentrated load.

- Other cracks: These can be due to: fire damage; overloading; settlement; incorrect prestressing; impact; or secondary effects of tendon curvature.

Before a repair method is selected the cause of the cracks must be determined. It is also necessary to determinate whether the cracks are active or dormant. The behavior of a crack is checked by means of periodic observations using tell-tales.

Debonding of joints.

This is a particular liable to occur where there is a large change in cross sectional area or whether dissimilar materials are bonded to concrete, for example:

(a) at epoxy resins expansion joints.

(b) where mastic asphalt water proofing material is used.

(c) where there is a topping layer such as granolithic flooring.

(d) where sealants are used.

Erosion

Mechanical action due to usage, weather and water leads to abrasive wear caused by sliding, scraping or percussion.

Corrosion of concrete due to chemical attack

The high alkaline cement paste formed by hidratation is subjected to chemical attack, which can only act trough dissolution in the pore water of the cement-paste. The resistance of concrete to chemical attack depends therefore on the water permeability of concrete, on the type and size of pore, and on the type of cement used. (See section 2.2.3. of this chapter).

2.3.   Methods for Structural Identification

2.3.1. Introduction

Maintenance comprises any work, including inspection, necessary for a structure to continue functioning as intended. Preventive maintenance consist of any work necessary to prevent a structure to deteriorate in such a way that is not functioning properly. Inspection of structures is the process by which any deterioration in the structure is observed and recorded.

2.3.2. The Importance of the Inspection and its Implementation

In general, concrete structures require very low maintenance other than inspection and minor repairs. However, in some cases cleaning is necessary because of

environment pollution, plant growth, nests, etc. and is particularly important when the accumulation of dirt might restrict the movements of expansion joints.

Defects on maintenance of structure can produce one or more of the following consequences:

- Deterioration of the appearance of the structure.

- The appearance of cracking or deformations, causing concern to the users.

- Expensive repairs derived from the absence of simple maintenance.

- Reduction of the load carrying capacity of the structure.

- The structure may become unsafe.

- The structure may be reduced in value or useful life.

The main reasons for maintenance and regular inspection are:

- To control the functional requirements and provide assurance that the structure is safe and fits for its designed use.

- To identify actual and potential sources of trouble and misuse at the earliest possible stage.

- To monitor the influence of the environment since there is a relation between the aggressiveness of the environment and the durability of concrete structures.

- To provide information on which decisions on maintenance and repair works can be made.

During the inspection it should be remembered that any deterioration has a cause, and it should be the aim of the engineer to find the cause. If the cause is ignored, the deterioration will be repeated. The as-built working drawings, design calculations,

soil reports, etc. should be available to assist in the assessment and diagnosis of faults and reassessment of the load carrying capacity.

Inspection classes

Inspection can be categorized in 3 classes: routine, extended and spatial inspection. Besides categorized inspections there are casual observations made by users of the structure. These are unlikely to happen in a regular basis, but can be of major importance.

Routine inspection

A routine inspection should be carried out methodically at regular intervals. The inspector should work trough a checklist that has been prepared for the particular type of structure by the engineers responsible for both design and maintenance. The inspection should be carried out by a trained inspector under the general supervision of an engineer and results compared with the results of previous inspections. A written report should be made of the condition of the structure and its various parts. The routine inspection is primary a visual inspection and, in general, special access or equipment is not required.

Extended Inspection

Normally, an extended inspection should be carried out in place of every second routine inspection. The aim of an extended inspection should be to carry out a close and more intensive examination of all elements of the structure, and thus special access, remote viewing techniques, underwater equipment, and so on may be required. If this is unacceptable, representative sections of the structure should be closely inspected. In addition to the checklist of the routine inspection, special instructions applicable to the structure in question should be considered. A full written report containing photographs and drawings should be prepared, when necessary.

It is recommended that the same person would carry out routine and extended inspections.

Special Inspection

A special inspection is made when unusual circumstances where for example:

- A specific condition is discovered by casual or cursory observation or by a routine or extended inspection.

- Specific conditions are found for similar materials or similar structures, e.g. concern over the condition of concrete containing high-alumina cement in certain structures resulted in the close inspection of many structures.

- Structures are subjected to critical stresses or are known to have weakness, e.g. a highway bridge before, during and after the passage of an exceptional load.

- Settlement may become larger than that allowed for in the design

- Exceptional events (e.g. flood, fire, collision, earthquake, etc.) occur.

- There is a change of use of the structure.

The special inspection may require a great deal of supplementary testing and structural analysis and may even include research.

Inspection intervals

Inspection intervals are a matter for engineering judgment and must be decided for each situation. They depend on many factors including:

- The type and importance of the structure

- The loading conditions and severity of loading

- The consequence of failure

- The influence of an aggressive atmosphere that influences the speed of deterioration

Table No. 2.1 gives a general indication of the intervals that might be applicable for routine and extended inspection. Structures are classified as follows:

Class 1: where the possible failure would have catastrophic consequences and/or the serviceability of the structure is of vital importance for the community.

Class 2: where possible failure might cost lives and/or where the serviceability of the structure is of considerable importance.

Class 3: were it is unlikely that possible failure of the structure have fatal consequences and/or when a period with the structure out of service can be tolerated.

Environmental and loading conditions are defined as follows:

(a) Very severe: the environment is aggressive and there is cyclic of fatigue loading

(b) Severe: The environment is aggressive, with static loading, or the environment is normal, with cyclic or fatigue loading

(c) Normal: the environment is normal, with static loading.

It is possible that consequences of failure may vary from one part of the structure to another; in this case one part of the structure should be classified differently from another. Similarly, the environment or loading conditions are likely to vary within the structure. Here, different parts of the structure may need to be inspected at different intervals [table 2.1].

Environmental and loading conditions	Classes of the structures					
	1		2		3	
	Routine inspection	Extensive inspection	Routine inspection	Extensive inspection	Routine inspection	Extensive inspection
Very severe	2*	2	6*	6	10*	10
Severe	6*	6	10*	10	10	-
Normal	10*	10	10	-	Only superficial inspections	

Table 2.1 Recommended intervals for routine and extended inspections

2.3.3. Inspection techniques

There is a wide variety of methods available for the inspection and identification of damage in structures. A schematic classification of them [table 2.1] was developed by Poston et. Al [1995].

Test/Method	Basic Reference	Application	Examined property	Comments
Structural Integrity and overview				
Visual exam including:				
Crack mapping	Bridge Inspection Panel [1984]			
Endoscope's survey	ACI. [1968]			
Photographs	Manning and Bye. [1983]	All structural elements	Condition of the structure	Simplest but most important inspection method.
Stereo pairs	Cement and concrete association [1988]			

Test/Method	Basic Reference	Application	Examined property	Comments
Hammer testing Chain drags, etc.	Moore et al. [1973] Savage [1985] Manning and Bye [1983] Cantor [1984]	All structural elements	Presence of cracks, spalls and delaminations	Hammer test or chain drags can detect surface laminations to 75-100mm deep.
Covermeter surveys to locate reinforcement, prestressing ties, etc.	BSI [1988B]	All structural elements	Location of bars and their diameter, cover deep.	Influenced by magnetic aggregates and difficulties with lapped or closely spaced bars or layers of bars.
Thermography	BSI [1986ª] Manning [1985] BSI [1986ª] Manning and Holt [1980] Kunz and Eales [1985]	Mainly bridge decks [with asphalt and plain concrete] and other elements	Presence of lamination	Influenced by water on deck, rapid scan system.
Radar	Manning [1985] Cantor [1984] BSI [1986ª] Kunz and Eales [1985] Mkalar et to the [1984]	Mainly bridge decks	voidage on large scale, including reinforcement, ducts, etc.	Bulky equipment; signals can be difficult to interpret
Acoustic emission	Hendry and Royles [1985] Manning [1985] BSI [1986ª]	All structures during load testing	Determination of initiation and the origin of cracks	Specialized inspection equipment and interpretation
Dynamic response e.g. Sonic-echo, continuous vibration	Stain [1982] Manning [1985]	Pile testing	Pile integrity	Specialized inspection equipment and interpretation
Load tests	BSI [1986ª] BSI [1986C] Menzies [1978] Jones and Oliver [1978] ACI [1985ª]	Structural elements	Defection under loads against structural analysis	Expensive but informative

Test/Method	Basic Reference	Application	Examined property	Comments
Determination of concrete quality and composition				
Core samples	Concrete society [1987]	All structural elements	Used in physical, chemical and petrographic analysis of quality	Required for almost all laboratory testing, restricted by access of certain members; can be expensive
Power drilled samples	BSI [1981] ASTM [1987ª] Building Research Establishment [1977]	All elements and structures	Chlorides, sulphates and moisture content of concrete	Simple, but subject to errors of contamination
Partially non-destructive assessment of strength, e.g. Windsor probe, pull-out testing, Schmidt Hammer, etc.	BSI [1981] Keiller [1982]	All structures and elements	Strength, usually converted to equivalent compressive	Variation in simplicity; common errors in precision [15-30%], Information only on concrete cover; often sensitive to operator and equipment; they can damage the concrete
Ultrasonic pulse velocity	BSI [1986C]	All structures and elements	concrete quality, uniformity, presence of cracks, voids, etc.	Quick scan in all the thickness, it can be correlated with the strength
In-situ permeability test	ASTM [1987C] Concrete society[1988] Lawrence [1981] Montgomery and Adams [1985]	All structures and elements	Concrete quality and permeability, generally restricted to cover.	Can be difficult to use in-situ, it can be affected by moisture of the concrete, surface conditions, etc.
Condition and serviceability of the steel				
Half-Cell, potential mapping	ASTM [1987F] Figg and Mardsen [1985] ASTM [1983] Baker [1986]	All structures and elements	Detects corrosion in the steel [and its possible level]	The methods single-cell and double-cell used with copper and silver electrodes requires in-situ calibration.

Test/Method	Basic Reference	Application	Examined property	Comments
Resistivity of cover	Manning [1985] Vassie [1980] Figg and Marsden [1985] Wenner [1915]	All structures and elements	Electrical resistance of concrete cover	Method of four tests using superficial or absorbed electrodes.

Table 2.2 Classification of non-destructive techniques.

2.3.4. Non-destructive methods for the evaluation of concrete structures

Prior to undertaking repairs on concrete structures, a condition assessment to determine the existing conditions and the nature and causes of observed distress must be conducted. Absence of this information can lead to a highly inefficient repair.

Traditionally, condition assessment has generally meant a visual examination of the structure along with select-coring of various concrete elements for compressive strength testing, perhaps petrographic analysis, and chain drag sounding. Although these techniques are still helpful and largely necessary, during recent years, other very valuable and practical NDE methods have been developed. The new generation of methods greatly improves the efficiency of the condition assessment process. Some of this recently developed non-destructive evaluation technologies allow for relatively rapid inspection of damage and deterioration in concrete structures.

Poston et. All. [1995] define NDE as any test or method that yields information regarding the quality of a structure (or portion of it) that does not impair the serviceability of the element or structure. Therefore, destructive testing in the sense of removing samples from a structure or element (as coring), is considered a non-destructive test. Although the common application of these tests is concrete bridges, the techniques and methods discussed in this section are also applicable to all kinds of concrete and masonry structures.

Olson et al. [1990] consider non-destructive testing and evaluation (NDTE) as techniques based on the measurement of wave propagation. These authors define NDTE as data-providers of dynamic properties and directly or indirectly related to physical conditions of the system under test. This, provide engineers with critical data that cannot be economically obtained with traditional destructive tests. Three NDTE methods, applicable to deep foundations are fundamentally considered in their article:

- Seismic echo (SE). The test is conducted from the surface. Typical test equipment consists in impulse hammer, accelerometers and geophone receivers, and a signal analyzer.

- Impulse Response (IR). Similar to SE. Also measures the dynamic stiffness at the head of a shaft, as indication of soil-foundation interaction conditions.

- Crosshole Sonic Logging (CSL). Is a downhole method for quality assurance testing of drilled shaft foundations. Access tubes, typically PVC plastic or steel, must be cast-in-place during construction to permit logging.

2.4. Discussion

Reduction of the stiffness is one of the clear signs of a damage process that occurs in a civil structure. Cracking, steel corrosion, chemical degradation, differential settlements and many other damages produce changes in global stiffness of the structure. Therefore, measurements of the stiffness can be correlated to appearance of damage. Unfortunately, there is not available standard-tools for measuring global stiffness.

Several newer generation NDT techniques, such as impact-echo testing and infrared thermography, allow for relatively rapid inspection of local damage and deterioration of structures. NDT has become an integral part of condition assessment and is of considerable value to engineers involved in the repair of structures.

The type of NDE chosen must be carefully studied to meet project objectives. NDE can be a valuable tool, but a given technique may not be practical or yield applicable results in all cases. The practical and most effective approach to condition assessment utilizes a variety of NDT techniques to contrast complementary information.

A NDE technique for global evaluation of structures is still needed. State-of-the-art techniques are effective only when applied near to the damage. Dynamic identification techniques can identify a global modification of the stiffness of the structure. If the deterioration process modify the stiffness of the structure, dynamic tools can be helpful to measure those variations. Dynamic testing procedures are not normalized by the codes yet, and therefore are not systematically used.

three

State-of-the-art on Damage Identification by Dynamic Inspection

3.1. Introduction

An important issue when dealing with vibrating structures is the numerical simulation. Thus, the basic concepts, and a brief introduction of the theory of vibrating systems are described in this chapter. Fundamental theory of single degree of freedom (SDF) and multy-degrees of freedom (MDF) system is presented. Some work developed by diverse authors on the dynamic modulus of elasticity and its comparison with static ones are also presented. The damage model used to include stiffness degradation in FEM of concrete structures is explained and discussed.

Secondly, the chapter contains a review of the technical literature concerning the detection, location, and characterization of structural damage via techniques that examine changes in measured structural vibration response. Dynamic identification methods are categorized according to required measured data and analysis technique. The analysis categories include changes in modal frequencies, changes in measured mode shapes (and their derivatives) and changes in measured flexibility coefficients. Methods that use property (stiffness, mass, damping) matrix updating, detection of nonlinear response, and damage detection via neural networks are also summarized. The applications of the various methods to different types of engineering problems are categorized by type of structure and are summarized. The types of structures include beams, trusses, plates, shells, frames, bridges, masonry and other large civil structures. The chapter describes as well, the development of

the damage-identification methods and its applications and summarizes the current state-of-the-art of this technology.

3.2. Previous reports on the *state-of-the-art*

The promising perspective of vibration-based health monitoring inspired many researchers all over the world. A detailed survey of the technical literature and interviews of selected experts to determine the state of the art of the damage-detection field (using modal analysis procedures) was presented by Richardson [1980]. The survey focused on structural integrity monitoring for nuclear power plants, large structures, rotating machinery, and offshore platforms, with by far the largest amount of literature associated with rotating machinery. Doebling *et al.* surveyed and classified the literature in a complete report published by Los Alamos National Laboratory [1996]. Several doctoral dissertations that address damage detection and related issues have been published. Each dissertation contains a literature survey and a development of the theory relevant to its scope. These dissertations include Casas [1988], Rytter [1993], Hemez [1993], Kaouk [1993], Doebling [1995] and Peeters [2000]. Mottershead and Friswell [1993] present a survey of the literature related to dynamic finite element model (FEM) updating, which has been used extensively for structural damage detection. Their review contains a list of references on the topic of model updating. This chapter summarizes and compares the literature generated during the last few years. A resume of previous reviews developed by Casas [1988], Doebling et al. [1996] and Peeters [2000] is also included.

3.3. Vibrating systems

3.3.1. Introduction

The aim of this section is to introduce some concepts and definitions used furthermore in the thesis. Dynamic identification of structures is supported on that theory of structural dynamics. A basic review of this theory is condensed in this

section. The objective of this review is to define some concepts, language and terminology used in upcoming chapters.

A mode of vibration can be defined as a way of vibrating, or a pattern of vibration, applied to a system or structure that has several degrees of freedom with different amplitudes of deflections. A mode of vibration comprises two distinct elements: first, a time variation in the vibration and, second, a spatial variation of amplitude of the motion across the structure. The time variation defines the frequency of oscillations together with any associated rate of decay or growth. The spatial variation defines the different vibration amplitudes from one point on the structure to the next. Systems can be discrete, described by a finite number of specific degrees of freedom or continuous, whose motion is defined by a continuous function of position. It is convenient to focus the discussion on the former of those two forms, the discrete type, as this is the more widespread type in use. However, it should be noted that all properties are common to both discrete and continuous versions [Canet and Barbat, 1988].

There are basically two types of vibration mode:

- Free vibration modes and

- Forced vibration modes

Modes of the first category, by far the more common, are sometimes called "normal" or "natural" modes (both names are equivalent), and those of the second category are sometimes referred to as "operating deflection shapes". As the name imply, these two types of mode relate to fundamentally different types of vibration. Free vibration modes describe the motion that takes place in a system that is free of any external excitation or forcing. They are therefore completely determined by the properties of the system of structure itself. Forced vibration modes are strongly influenced by the nature of the external excitation that generates the motion (when shakers are used) and are thus a reflection of both, the system's parameters and the external forces.

3.3.2. Dynamic properties of structures

Two fundamental aspects distinguish static and dynamic structural problems: the variation on time (in a dynamic problem, applied loads and structure's answer vary in the time) and the determination of reactions and internal tensions [Clough and Pienzen, 1993].

In a dynamic problem, the resulting displacements of the structure are associated to the accelerations that take place due to inertia forces; the internal moments and shears are obtained by balancing static and inertia forces. The relationship between actions and response is expressed quantitatively by means of a mathematical model. The physical characteristics to consider in model's definition are the mass and the stiffness reduction of the structure. The evaluation of the dynamic behavior of a structure requires solving numerically the differential equations that describe the vibrations that take place.

Equations of movement

The mathematical expressions that govern the dynamic answer of the structures are the equations of the movement [Clough and Pienzen, 1975]. They can be obtained starting from three principles of the classic mechanics: d'Alembert principle, the principle of the virtual works and the principle of Hamilton.

D'Alembert formulation of the principle is as follows [Clough and Pienzen, 1975; Biggs, 1964]: a dynamic system is balanced when all the forces, included inertia, fit static equilibrium equations for every instant of time. In accordance with this principle, in a model with several degrees of freedom, equations of the movement can be deduced establishing the dynamic balance of each mass. For the mass m_r this balance condition is expressed according to the formula [3.1].

$$F_{i_r}(t) - F_{e_r}(t) - F_{a_r}(t) = 0 \qquad\qquad\qquad [3.1]$$

The full dynamic model is in balance when every one of its masses also is. Considering balance for every mass of the system and expressing it in a matrix form, the equation [3.2] is obtained.

$$\mathbf{F}_i(t) - \mathbf{F}_e(t) - \mathbf{F}_a(t) = \mathbf{0} \qquad\qquad [3.2]$$

In [3.2] static forces, inertia and damping correspond to the follow matrix expressions: $\mathbf{F}_e(t) = \mathbf{K} \cdot \mathbf{X}(t)$, $\mathbf{F}_i(t) = -\mathbf{M} \cdot \ddot{\mathbf{X}}(t) + \mathbf{J}a(t)$ y $\mathbf{F}_a = \mathbf{C} \cdot \dot{\mathbf{X}}(t)$, where $\mathbf{K}$ is stiffness matrix, $\mathbf{M}$ mass matrix and $\mathbf{C}$ damping matrix.

Substituting the expressions of acting forces in the expression of global equilibrium [3.2] the equations of movement of the model are obtained.

$$\mathbf{M} \cdot \ddot{\mathbf{X}}(t) + \mathbf{C} \cdot \dot{\mathbf{X}}(t) + \mathbf{K} \cdot \mathbf{X}(t) = -\mathbf{M} \cdot \mathbf{J} \cdot \mathbf{a}(t) \qquad\qquad [3.3]$$

Damped free vibrations in the dynamic model are expressed according to [3.4] and if damping is not taken in account, expression [3.5] describes the free vibrations with not damping in the model.

$$\mathbf{M} \cdot \ddot{\mathbf{D}} + \mathbf{C} \cdot \dot{\mathbf{D}} + \mathbf{K} \cdot \mathbf{D} = \mathbf{0} \qquad\qquad [3.4]$$

$$\mathbf{M} \cdot \ddot{\mathbf{D}} + \mathbf{K} \cdot \mathbf{D} = \mathbf{0} \qquad\qquad [3.5]$$

Undamped models with a single degree of freedom

The dynamic characteristics of the models with a single degree of freedom are defined studying the un-damped free vibrations. This belongs to the conservative model of the figure 3.1 whose movement is governed by the equation [3.6].

$$m \cdot \ddot{x}(t) + k \cdot x(t) = 0 \qquad\qquad [3.6]$$

The system of the figure 3.2. vibrate due to an initial condition of displacement, velocity or acceleration and it is not subjected to any interference during its vibration.
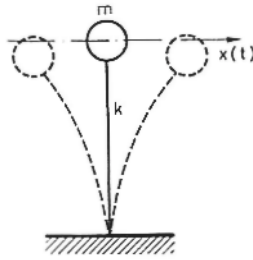
Figure 3.2. Preservative Model with a single degree of freedom.

Dividing equation [3.6] by m, and using notation $\omega^2 = \dfrac{k}{m}$, this is transformed in equation [3.7].

$$\ddot{x}(t) + \omega^2 \cdot x(t) = 0 \qquad\qquad [3.7]$$

The magnitude ω is a dynamic characteristic of the system; is the vibration frequency and is expressed in radians per second (rad/s). Other dynamic characteristics are natural period $T = \dfrac{2 \cdot \pi}{\omega}$ and cyclic frequency f defined by

$$f = \frac{1}{T} = \frac{\omega}{2 \cdot \pi} \ .$$

Systems with several degrees of freedom

In a system with several degrees of freedom and not damping, free vibration is expressed as system [3.5]. This differential equation system has to define particular solutions as $\mathbf{D}(t) = \mathbf{A} \cdot e^{i\omega t}$ or $\mathbf{D}(t) = \mathbf{A} \cdot sen(\omega t + \Psi)$, where vector $\mathbf{A}$ contains vibration amplitudes, ω is pulsation and Ψ is the angle of face. Substituting in [3.5] expressions of particular solutions, the next system of equations is obtained:

$$(\mathbf{K} - \omega^2 \cdot \mathbf{M}) \cdot \mathbf{A} = \mathbf{0} \qquad\qquad [3.8]$$

This algebraic homogeneous lineal equations system creates an auto-value problem. The system has different solutions from the trivial (vibrating system) only if equation [3.9] has a solution; this conditioning can be expressed in a polynomial

form ($\omega^{2n}+\alpha_1\omega^{2n-2}+\alpha_2\omega^{2n-4}+\ldots+\alpha_{n-1}\omega^2+\alpha_n=0$), obtaining by this way the characteristic equation.

$$|\mathbf{K}-\omega^2\cdot\mathbf{M}|=0 \qquad\qquad [3.9]$$

The solutions that are obtained from the characteristic equation are the auto-values of the system; this is the natural frequencies of the system with several degrees of freedom. The frequencies can be ordered in a matrix form [3.10].

Natural periods of the system are defined by $T_i=\dfrac{2\pi}{\omega_i}$.

$$\mathbf{\Omega}=\begin{bmatrix} \omega_1 & & & & & 0 \\ & \omega_2 & & & & \\ & & \ddots & & & \\ & & & \omega_i & & \\ & & & & \ddots & \\ 0 & & & & & \omega_n \end{bmatrix} \qquad\qquad [3.10]$$

System with proportional damping

Damping forces in a structure are produced by diverse causes; some of them are sensitized in the next paragraphs:

- Friction between surfaces. Damping force, according wit Coulomb's theory, is proportional to normal force in contact surface, which is considered constant and independent to displacements and velocities.

- Damping owed to vibrations of the structure situated in an external media.

- Damping owed to internal friction of the material, basically due to imperfect elasticity. In this case damping is proportional to recuperation force and is known as structural damping.

Damped systems with a single degree of freedom

Damping can be defined studying the vibrations of a dynamic model as the one of the figure 3.3.
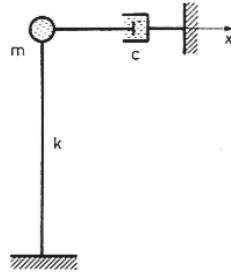
Figure 3.3 Damped system wit a single degree of freedom.

Damped free vibration model is described by equation [3.11].

$$m \cdot \ddot{x}(t) + c \cdot \dot{x}(t) + k \cdot x(t) = 0 \qquad\qquad [3.11]$$

Dividing [3.11] by m and introducing notation $\dfrac{c}{m} = 2\beta$, results in equation [3.12] which solution is obtained substituting expression $x(t) = e^{rt}$, this proportionate characteristic equation [3.13] which has a solution $r_{1,2} = -\beta \pm \sqrt{\beta^2 - \omega^2}$.

$$\ddot{x}(t) + 2 \cdot \beta \cdot \dot{x}(t) + \omega^2 \cdot x(t) = 0 \qquad\qquad [3.12]$$

$$r^2 + 2\beta r + \omega^2 = 0 \qquad\qquad [3.13]$$

Critical damping, described by coefficient c_c, can be defined by [3.14], where results in $c_c = 2m\beta = 2m\omega$.

$$\beta_c^2 - \omega^2 = 0 \qquad\qquad [3.14]$$

When damping is higher than critical value, $c > c_c$, is the case of a super-damped system. This situation cannot be found in civil engineering structures, under these conditions, the structure would not vibrate, and it would only go back to the original position.

The case with damping inferior to the critical value, $c < c_c$, is common on structures subjected to dynamic actions. This kind of damping can be defined introducing the damping coefficient υ, which is the percentage of the critical damping, and is expressed with $\upsilon = \dfrac{c}{c_c} = \dfrac{c}{2m\omega}$.

When the case of infra-critical damping is achieved, solution of [3.13], r_1 y r_2, is complex, as general solution can be written as: $x(t) = c_1 e^{r_1 t} + c_2 e^{r_2 t}$.

Evaluation of damping in a structure is a basic problem of dynamics. In general, is solved by the use of identification techniques that can estimate structural characteristics trough excitation-response measurements.

Identification of vibration systems is in a sense the inverse of the analysis problem. In the analysis, a response is predicted based on the knowledge of the system's properties and excitation. The identification, in contraposition, extracts a model based on knowledge of an excitation and the response. It is usually based on experimental acquired data, and measurement aspects have to be considered when performing such tasks. Identification of vibrating structures is the basic field of this dissertation, and is treated on detail in the next chapter.

3.3.3. Dynamic modulus of elasticity

The non-linear stress-strain curve of concrete creates a difficulty in establishing a unique value for the modulus of deformation (E_c). It depends on stress level, rate of loading, and strength of concrete, as well as concrete ingredients. The secant strain modulus is the slope of a straight line passing from the origin to any point on the stress-strain curve. It is the most common measurement of the modulus of elasticity

in concrete. In practice the value given by ACI code 318-83 is used. This value of E_c is usually defined by codes as a secant modulus under static loads up to the working stress level.

When the dynamics of the structure is studied, is more appropriate to use the modulus of deformation of concrete measured by dynamic systems, where dynamic loadings are involved. It is usual to describe the values obtained from dynamic methods as *dynamic elastic modulus (E_d)*. This notation is intended to differentiate it from the static method of finding the modulus of elasticity, from load deflection curve.
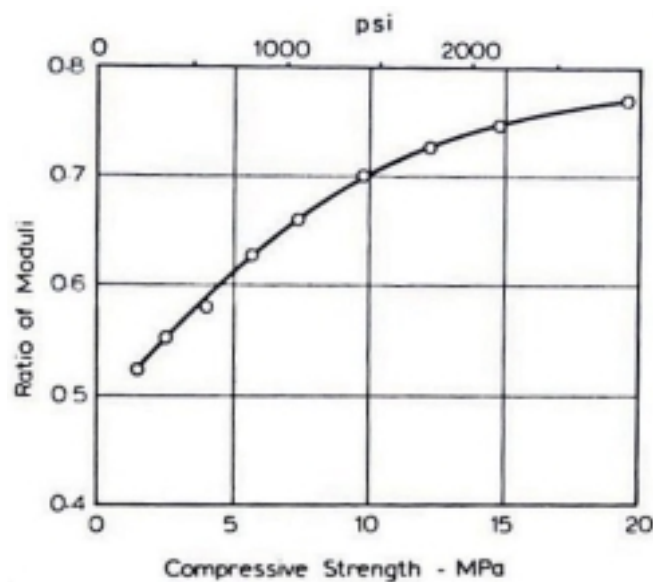
Figure 3.4. Relation between static and dynamic modulus of concrete for different strengths.

Sukhvarash and Milard [1984] studied how well the static modulus of elasticity of concrete calculated by using ACI 318-83 correlates with the values obtained from vibrational methods. Dynamic elastic modulus was measured with non-destructive test by means of generating transverse and longitudinal vibrations. The authors conclude that E_d is more accurately obtained from transverse vibration tests.
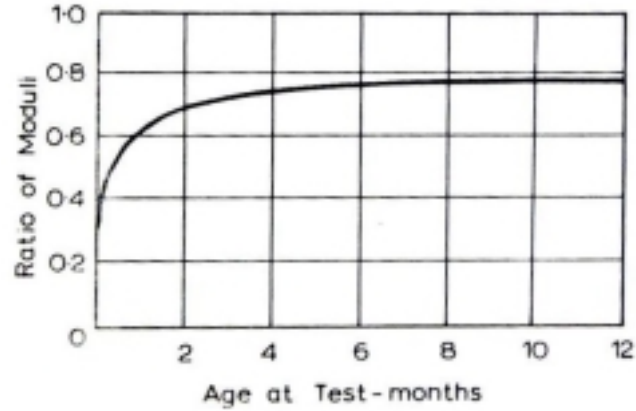
Figure 3.5. Ratio of static and dynamic moduli at different ages.

The procedure for determining the dynamic modulus of elasticity is fully described in chapter six. Since during vibration of the specimen, only a negligible stress is applied, the dynamic modulus refers to almost purely elastic effects and is unaffected by creep or other phenomena. For this reason, the dynamic modulus is approximately equal to the initial tangent modulus determined in the static test and is therefore appreciably higher than the secant (static) modulus. The difference between the dynamic and static moduli is also due to the fact that the heterogeneity of concrete affects the two moduli in different ways [Sukhvarash and Milard, 1984]. Fig 3.4 shows that the ratio of the static to dynamic moduli is higher the higher the strength of concrete. For a given mix the ratio increases also with age. [Fig 3.5]. According to the British Code CP 110:1972, the moduli, expressed in GPa, are related by the expression:

$$E_c = 1.25E_d - 19$$

Where E_c and E_d are the static and dynamic module respectively. The relation does not apply for concretes containing more than 500 kg of cement per cubic meter of concrete or to lightweight aggregate concrete. For the latter, the expression

$$E_s = 1.04E_d - 4.1$$

is suggested.

For both lightweight and normal concrete, it has been suggested that the relation between the static and dynamic moduli is a function of density of concrete, just as is the case with the relation between the static modulus and the strength. Popovics et. al [1990] founded a linear relation between E_c and E_d defined by:

$E_c = E_d{}^{1.4} D^{-1}$,

where D is the density of concrete.

Jerath and Shibanni [1984] defined the dynamic modulus of concrete by testing transverse oscillations of a reinforced concrete beam. For a rectangular beam under transverse vibration, the relationship between the natural frequency, *f*, and the dynamic elasticity modulus, E_d, is expressed as:

$$E_d = (Wl^3 f^2) / (k\, b\, h^3)$$

In which *W*=weight of the reinforced concrete beam; *l* = span of the beam;

b = width of the beam; and *h* = depth of the beam. The constant *k* has a theoretical value of 79.3 in / sec^2 for a simply supported beam and the first model of vibration.

3.3.4. Numerical modeling of reinforced concrete structures

3.3.4.1. Introduction

When modeling reinforced concrete structures, an important phenomenon related to stiffness deterioration is the cracking of the concrete under tensile stress. To take this mechanism in account, the concrete behavior must be considered independently of the rebar. Effects associated with the rebar/concrete interface, such as bond slip and dowel action, are modeled approximately by introducing some "tension stiffening" into the concrete modeling to simulate load transfer across cracks through the rebar. The post-failure behavior for direct straining across cracks is modeled with the tension stiffening option, which allows defining the strain-softening behavior for cracked concrete. The introduction of tension stiffening in the model also allows for the effects of the reinforcement interaction with concrete

to be simulated in a simple manner. The tension stiffening option is required in the concrete model, therefore a brief introduction and references to the available literature is presented in the next paragraphs.

3.3.4.2. Tension Stiffening

The stress-strain characteristics of concrete under tension in cracked reinforced concrete structures are different from the stress strain characteristics of plain concrete, primarily due to the bond with steel. Last century Morsch [1909] showed that a block of concrete between two consecutive cracks is capable of carrying tensile stresses and that the stiffness of the cracked reinforced concrete between the cracks is higher than the stiffness of the reinforcing steel alone. This property is defined as *Tension Stiffening*. Several approaches have been proposed for assessing tension stiffening based on experimental results [Gilbert and Warner, 1978; Damjanic and Owen, 1984; Schnobrich, 1985; Cope, 1986] or based on fracture mechanics principles [Hilleborg, 1982; Bazant and Oh, 1984].
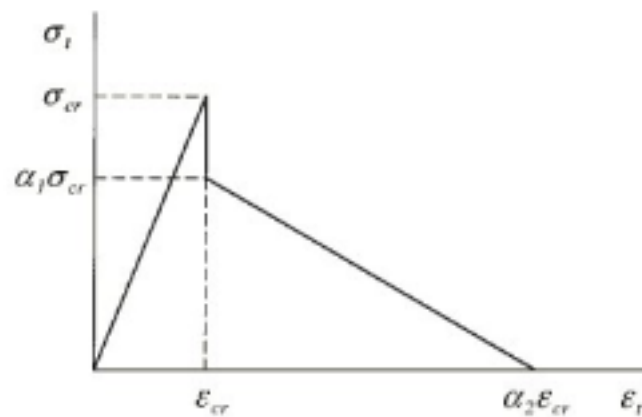
Figure 3.6. Tension Stiffening parameters.
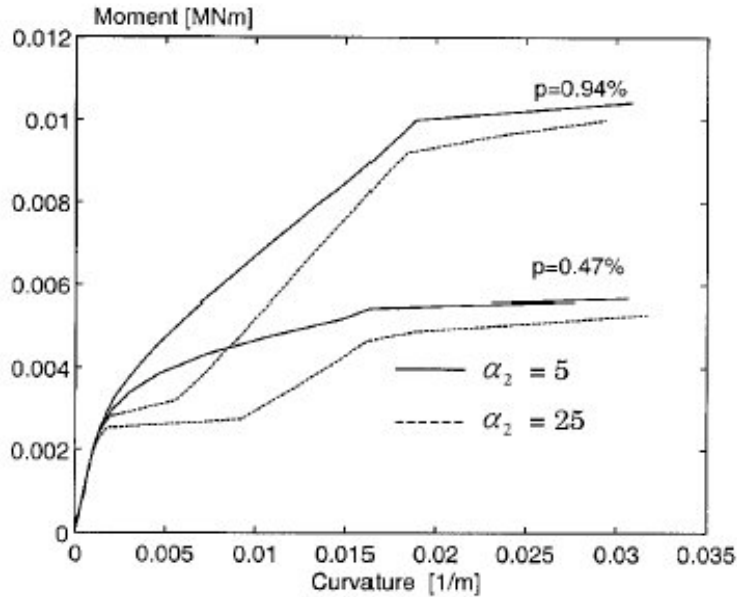
Figure 3.7. Influence of "α" on curvature.

In the smeared crack approach, *tension stiffening* effect is often modeled by the descending branch of a stress strain relationship for tensile concrete. The relationship is characterized by parameters α_1 and α_2 [Fig. 3.6.], which are related to the cracking stress σ_{cr} and cracking strain ε_{cr}, respectively. Values of α_2 proposed by different authors [Schnobrich 1985; Prakhya and Morley 1990] range from 5 to 25. Two moment curvature diagrams, computed for an actual experimental beam [Jokubatis 1967] for two values of α_2 equal to 5 and 25 are shown in Fig. 3.7. ($\alpha_1 = 1$). Two values of reinforcement ratio were assumed: the actual one ($p = 0.94\%$) and the twice decreased ($p = 0.47\%$). The value of the parameter α_2, that controls the tension stiffening, significantly affects the moment-curvature diagrams [Fig.3.7.], particularly at the initial cracking stages of the section with the lower reinforcement ratio.

Experimental investigation of tensile [Williams 1986] and flexural [Clark and Speirs 1978; Clark and Cranston 1979] members has shown that the tension stiffening effect is mostly dependent on the diameter of reinforcement bars,

reinforcement ratio, and the distribution of reinforcement. An attempt was made by Prakhya and Morley [1990] to include several parameters affecting the tension stiffening into the stress-strain curves. On the basis of simplified assumptions and by using some experimental data of Williams [1986], Clarkand Speirs [1978], and Clark and Cranston [1979], modified an equation of the stress-strain curve proposed by Carreira and Chu [1986]. However, Kaklauskas and Ghaboussi [2001] considered that the experimental data did not cover cases of small reinforcement ratios and the model proposed by Prakhya and Morley [1990] lacked statistical justification.

Even at early ages of concrete, shrinkage may lead to significant tensile stresses in concrete, particularly for members with higher reinforcement ratios. However, most researchers studying tension stiffening effect and the shape of the stress-strain relationship for tensile concrete have disregarded shrinkage effects [Kaklauskas and Ghaboussi, 2001]. Unfortunately, determination of stresses in reinforced concrete structures caused by shrinkage is hampered by uncertainty in prediction of the free concrete shrinkage strain. Different methods for the assessment of the free concrete shrinkage give widely varying estimates [Gilbert 1988].

Average stress-strain curves for tensile concrete can be obtained form tension tests of reinforced concrete members [Williams, 1986]. However, analysis has shown that these curves do not necessarily assure accurate results for bending problems. Recently a method [Kaklauskas et al. 1997; Kaklauskas, 1998] has been developed for determining the average concrete stress-strain relations in tension and compression from experimental moment-strain (curvature) diagrams of reinforced concrete beams subjected to short term loading. The stress-strain relations are computed incrementally from equilibrium equations for the extreme surface fibers. The computation is based on an idea similar to that described by Prentis [1951] of using the previously computed portions of the stress-strain relations at each load increment to compute the current increments of the stress-strain relations. This methodology will lead to a large number of average stress-strain curves of concrete in tension for a wide range of values of parameters, such as the beam dimensions,

reinforcement ratios, rebar diameter, reinforcement arrangement, and concrete strength.

Neural network material models that were first generated by Ghaboussi et al. [1991] are ideal tools for the modeling of such complex material behavior as the tensile branch of concrete in a reinforced concrete beam and its dependence on a number of parameters. Ghaboussi and his coworkers have successfully used neural networks in modeling the constitutive behavior of a number of materials, including plain and reinforced concrete, geo-materials, and fiber-reinforced composites [Ghaboussi et al. 1996; Ghaboussi and Sidarta 1998].

3.4. Dynamic testing of structures.

3.4.1. Excitation techniques.

Different authors have compared and classified the sources of excitation for dynamic testing on structures. Salawu and Williams [1995] provide a review of full-scale dynamic testing of bridges where methods of excitation are examined. Farrar et al. [1999] summarized the various methods that have been used to excite bridge structures during dynamic testing. Peeters et al. [2000] evaluated the various sources of excitation that have been applied on bridge Z24, in Switzerland. These authors evaluated both forced artificial sources such as shakers and drop weight and ambient, natural sources such as wind and traffic. The exhaustive use of testing in evaluation of bridges has resulted in the American Society of Civil Engineers [ASCE] Committee on Bridge Safety publishing a guide for field-testing of bridges in 1980 [ASCE 1980]. RILEM committee 20-TSB also proposed a standard for in-situ testing of bridges [1983]. Both of the previous documents include details on excitation procedures.

The methods of exciting a bridge for dynamic testing fall into two general categories: 1) Measured-input tests; and 2) Ambient test. In general, test with measured inputs are conducted on smaller bridges. For larger truss, suspension and

cable stayed bridges; ambient tests become the only practical means of exciting the structure [Farrar et al, 1999].

Methods for determining the modal characteristics (resonant frequencies, mode shapes and modal damping ratios) of structures subjected to measured inputs are well established, particularly when the input forcing function is well characterized. In the measured-input excitation testing of bridges, a wide variety of forcing techniques are used including various types of shakers, step relaxation, and various methods of measured impact. The methods of measured input excitation are summarized on detail in Farrar et al. [1999].

Ambient excitation is defined as the excitation experienced by the structure under its normal operating conditions. All structures are subjected to ambient excitation from sources as traffic, wind or seismic actions. This type of excitation has been largely used for both small and large bridge structures. Normally, ambient excitation cannot be measured during the test. For larger bridge structures, this is the only practical means of exciting the structure. Ambient excitation is also used with smaller bridges when other constraints prevent the bridge from been taken out of service during the test [Farrar et al. 1999]. Casas [1995] reported the results of ambient vibration test on several bridges. Ambient vibration was measured under traffic conditions.

3.4.2. Equipment.

The data acquisition portion of the structural health monitoring process involves selecting the types of sensors to be used, selecting the location where the sensors should be placed, determining the number of sensors to be used, and defining the data acquisition and storage hardware. Economic considerations play a major role in these decisions. Another consideration is how often the data should be collected. In some cases it is adequate to collect data immediately before and at periodic intervals after a severe event.

Data acquisition issues for structure-applications include the sensor type and the number of sensors, sensor location, sensor mounting, environmental effects on the sensors, signals recording, and record duration. Averaging, windowing and similar data processing parameters must also be determined. Another issue is determining the steps that could be taken to make the data acquisition as repeatable as possible.

The primary sensors used for bridge health monitoring are piezoelectric accelerometers. Force-balance accelerometers, electric resistance and vibrating-wire stain gages are also widely used. More recently, fiber–optic sensors utilizing Bragg grating [Todd, et al., 1999] have been studied as a means of increasing channel counts for bridge monitoring in a cost-effective manner. In addition to the motion measuring devices, anemometers and temperature sensors such as thermocouples are used to characterize the environmental variability. Data transmission and recording are done in manners similar to most mechanical vibration applications as summarized in [McConnell, 1995]. Recent developments in wireless data acquisition systems have shown promise for large civil engineering structures. When ambient excitation sources are used, all channels of data are typically recorded simultaneously. The damage to be monitored and the number of available sensors typically dictate sensor placement.

3.5. Dynamic identification of structures

As mentioned previously, the field of structural identification is very wide and encompasses both local and global methods. This survey will be limited to methods that are used to infer damage from changes in vibration characteristics of the structure.

Many different issues are critical to the success of using the mechanical vibration characteristics of a structure for damage identification and health monitoring. Among the important issues are excitation and measurement considerations, including the selection of the type and location of sensors, and the type and location of the excitations.

Another important topic is signal processing, which includes such methods as Fourier analysis, time-frequency analysis and wavelet analysis.

In this section, these peripheral issues will not be directly addressed. The scope of this chapter will be limited to the methods that use changes in modal properties (i.e. modal frequencies, modal damping ratios, and mode shapes) to infer changes in mechanical properties, and the application of these methods to engineering problems. The literature related to damage identification in rotating machinery has not been included.

A system of classification for damage-identification methods, as presented by Rytter [1993], defines four levels of damage identification, as follows:

• Level 1: Determination that damage is present in the structure

• Level 2: Determination of the geometric location of the damage

• Level 3: Quantification of the severity of the damage

• Level 4: Prediction of the remaining service life of the structure

The literature in this chapter can be classified mostly as Level 1, Level 2, or Level 3 methods because these levels are most often related directly to structural dynamics testing and modeling issues. Level 4 –prediction- is generally categorized with the fields of fracture mechanics, fatigue life analysis, or structural design assessment and, as such, is not addressed in the structural vibration or modal analysis literature.

This section is organized as follows: First, the literature relevant to the methods used to detect and locate damage is reviewed. Next, the applications of these techniques to specific structures and engineering problems are reviewed.

A summary of the literature pertaining to the various methods for damage identification and health monitoring of structures based on changes in their measured dynamic properties is presented in this section. The methods are

categorized based on the type of measured data used, and/or the technique used to identify the damage from the measured data.

3.5.1. Changes in frequencies

Available literature related to damage detection using shifts in natural frequencies is quite large. The observation that changes in structural properties cause changes in vibration frequencies was the impetus for using modal methods for damage identification and health monitoring. Because of the large amount of literature, all papers on this subject are not included. An effort has been made to include the early work on the subject, some papers representative of the different types of work done in this area, and papers that are considered by other authors to be significant contributions in this area. Also, many papers are included only in Section two as they present only applications of these methods to different structures, rather than new theoretical work on the use of frequency shifts in damage detection.

It should be noted that frequency shifts have significant practical limitations for applications to the type of structures considered in this chapter, although ongoing and future work may help resolve these difficulties. The somewhat low sensitivity of frequency shifts to damage requires either very precise measurements or large levels of damage.

For example, in offshore platforms damage-induced frequency shifts are difficult to distinguish from shifts resulting from increased mass from marine growth. Tests conducted on the I40 bridge [Farrar, et al., 1994] also demonstrate this point. When the cross-sectional stiffness at the center of a main plate girder had been reduced 96.4%, reducing the bending stiffness of the overall bridge cross-section by 21%, no significant reductions in the modal frequencies were observed. Currently, using frequency shifts to detect damage appears to be more practical in applications where such shifts can be measured very precisely in a controlled environment, such as for quality control in manufacturing. As an example, a method known as "resonant ultrasound spectroscopy", which uses homodyne detectors to make

precise sine-sweep frequency measurements, has been used to determine out-of-roundness of ball bearings [Migliori, et al., 1993]. Also, because modal frequencies are a global property of the structure, it is not clear that shifts in this parameter can be used to identify more than the mere existence of damage. In other words, the frequencies generally cannot provide spatial information about structural changes. An exception to this limitation occurs at higher modal frequencies, where the modes are associated with local responses. However, the practical limitations involved with the excitation and extraction of these local modes, caused in part by high modal density, can make them difficult to identify. Multiple frequency shifts can provide spatial information about structural damage because changes in the structure at different locations will cause different combinations of changes in the modal frequencies. However, as pointed out by several authors, there are often an insufficient number of frequencies with significant enough changes to determine the location of the damage uniquely.

The forward problem, which usually falls into the category of Level 1 damage identification, consists of calculating frequency shifts from a known type of damage. Typically, the damage is modeled mathematically, and then the measured frequencies are compared to the predicted frequencies to determine the damage.

Lifshitz and Rotem [1969] present what may be the first journal article to propose damage detection via vibration measurements. They look at the change in the dynamic module, which can be related to the frequency shift, as indicating damage in particle-filled elastomers. The dynamic module, which are the slopes of the extensional and rotational stress-train curves under dynamic loading, are computed for the test articles from a curve fit of the measured stress strain relationships at various levels of filling.

Adams, et al. [1978] examine a method whereby damage in a structure that can be represented as one-dimensional can be identified from changes in the resonant frequencies associated with two modes. The change in the frequencies associated with the first two bending modes and first torsional mode of an offshore light

station tower to identify damage were examined by Vandiver [1975, 1977]. Based on numerical simulations, the author concludes that changes in the effective mass of the tower resulting from sloshing of fluid in tanks mounted on the deck will produce only 1% change in the frequencies of the three modes being considered. By systematically removing members from a numerical model the authors demonstrated that failure of most members produces changes in resonant frequencies greater than 1%, and, thus, that damage in most of the members will be detectable. A numerical simulation of rust formation (reduction in wall thickness of the structural tubes by 1.27 mm, actual wall thicknesses varied from 8.18 mm to 25.4 mm) showed a 3.71% reduction in the bending mode frequencies.

Begg, et al. [1976] note that severance of members in a scale model offshore structure produced 5% to 30% change in resonant frequencies. When an extra bracing member was added to a North Sea platform, frequency increases of 10% were observed. When power spectra were examined for changes in resonant frequencies, it was noted that the lower-frequency peaks were associated with the spectral content of the input rather than resonance of the structure. Cracks were found to have little influence on the axial stiffness of members and, hence, did not reveal themselves when the global modes were examined. In these modes the members behaved primarily as truss elements. The authors suggest that monitoring local high-frequency bending modes of the individual members provides a better indication of cracking as both the crack and the associated water fill have more influence on these modes. Locating the damage from changes in frequencies alone was considered impractical.

Loland and Dodds [1976] use changes in the resonant frequencies, mode shapes, and response spectra to identify damage in offshore oil platforms. The mode shapes are necessary to ensure that the changes in modal frequencies are properly tracked. Changes in resonant frequencies of 3% were caused by changes to the mass on the decks and by changes in tide level. Frequency changes of 10% to 15% were observed when a structural modification was implemented that resembled a structural failure near the waterline. Thus, the authors conclude that changes in the

response spectrum can be used to monitor structural integrity. Wojnarowski, et al. [1977] examine the effects of eleven different parameters on the dynamic properties of an offshore lighthouse platform using finite element analysis. Foundation modeling assumptions, entrained water, marine growth, corrosion, variation in deck loads, and failed structural members are some of the parameters that were examined. The largest changes in frequencies were the result of changes in soil foundation properties. Cawley and Adams [1979a] give a formulation to detect damage in composite materials from frequency shifts. They start with the ratio between frequency shifts for modes *i* and *j*. A grid of possible damage points is considered, and an error term is constructed that relates the measured frequency shifts to those predicted by a model based on a local stiffness reduction. A number of mode pairs is considered for each potential damage location, and the pair giving the lowest error indicates the location of the damage. The formulation does not account for possible multiple-damage locations.

Results of a numerical study on damage in an offshore platform were reported by Coppolino and Rubin [1980]. The authors compared a FEM of a platform against measured modal data, and then the effect of severance of various members on the structural response was modeled numerically. Depending on the location of the damage, changes in resonant frequencies on the order of 1% to 2% were found to be indicative of damage. Other damage locations were not detected by changes in the resonant frequencies. Duggan, et al. [1980] study the use of ambient, above-waterline vibration measurements on offshore platforms as a means of structural integrity monitoring. The program was aimed at determining the stability of vibration behavior under varying environmental and operating conditions, as well as the changes associated with structural modification. Three platforms in the Gulf of Mexico were monitored. On one platform, repairs and replacements of legs and braces took place during the study. The conclusion of this study was that changes in frequencies caused by removal of a bracing member could not be distinguished from shifts caused by normal operating changes. Because damage caused changes

in the order of the modes, the authors state that it is essential to identify the mode shapes associated with the resonant frequencies to track the changes accurately.

Kenley and Dodds [1980] examine changes in resonant frequencies to detect damage in a decommissioned offshore platform. The authors find that only complete severance of a diagonal member can be detected by changes in the global modal frequencies. They state that damage has to produce a 5% change in the overall stiffness before it can be detected. For global modes, the resonant frequency can be detected to within 1%, but for local modes the error increases to 2% to 3% because peaks in the power dwi dwj spectrum are not as well defined. Flooding and half-severance of diagonal members were detected from local below-water measurements. The authors again point out that it is important to associate a resonant frequency with a mode shape when trying to track changes in frequency as an indicator of damage.

Crohas and Lepert [1982] describe a "vibro-detection device" that was mounted on structural members of an offshore oil platform. The device applies an input to the member and measures its response. Frequency response functions (FRFs) are then determined for the members by measuring the acceleration response that results from the excitation. Flooding of a test brace produced a 10% decrease in the resonant frequency, while the frequencies of neigh-boring braces were unaffected. A 30% through-crack located near the end of the test brace could also be detected.

Gudmundson [1982] proposes a technique for modeling cracks in a beam cross section using a static flexibility matrix. This flexibility matrix is determined using two different approaches. The first approach uses static stress-intensity factors, and the second approach uses a static FEM. The author compares numerical simulations of the beam modal frequencies using these two crack models for various crack lengths and crack positions. The results demonstrate that this method provides accurate predictions of the beam modal frequencies. The author also demonstrates that the modal frequencies decrease more slowly with a fatigue crack that opens and closes than with a crack that stays open.

Nataraja [1983] reports on a program designed to monitor North Sea platforms over a two-year period and to demonstrate the feasibility of such a system for structural damage detection. Results showed that only the lowest natural frequencies could be identified with certainty and that these frequencies were stable throughout the monitoring period. Changes in deck mass could be detected in the vibration signatures, and, hence, the author states that it is imperative to monitor the deck mass in order to distinguish changes in mass from structural damage. The author concludes that the measured accelerations can only be used to detect global changes in the structure and not localized damage.

Results from a project where the response of British Petroleum's Alpha Forties platform was monitored on a regular basis over 2.5 years was reported by Whittome and Dodds [1983]. This study was undertaken to examine the feasibility of using changes in resonant frequencies to monitor the structural condition of offshore platforms. It was found that there was less than a 1.5% change in the resonant frequencies over the monitored time. Significant drops in frequencies were noticed when drilling operations were ongoing. These changes resulted from added mass on the deck. Damage was introduced in a numerical model of the structure that had been benchmarked against the measured response. It was concluded that changes in the resonant frequencies produced by damage or foundation deterioration were greater than the observed variations in resonant frequencies of the undamaged platform over time.

Tracy and Pardoen [1989] present an analytical solution for the vibrational frequencies and mode shapes for a composite (orthotropic) beam with a midplane delamination. They divide the beam into four sections: above, below, and on either side of the delamination. The transverse bending and axial vibration differential equations are considered for each section. The model allows for independent extensional and bending stiffnesses. The transverse deflections of the sections above and below the delamination are constrained to vibrate together, which restricts the analysis to midplane delaminations. After all simplifications and

boundary conditions are applied, 14 unknown constants are left. The characteristic equation is solved numerically to give frequencies and mode shapes.

Ismail, et al. [1990] demonstrate that the frequency drop caused by an opening and closing crack is less than that caused by an open crack. This property is a potentially large source of error that is considered by few of the researchers using frequency changes. It implies that the frequency drop is affected by factors such as preload and residual stress, not just crack size and location. It also serves to decrease the already low sensitivity of the method.

A project that examines changes in the dynamic properties of a scale model offshore platform was reported by Osegueda, et al. [1992]. Resonant frequencies were found to decrease with damage, and this decrease was an order of magnitude greater than the standard deviation of the measurement. These authors noted that to track the changes in resonant frequencies properly, the mode shape associated with these frequencies must be identified. The results of modal tests performed on both reinforced and plain concrete beams were reported by Chowdhury and Ramirez [1992]. Qualitative observations of the changes in resonant frequencies and power spectra resulting from simulated damage, changes in strength, and changes in applied load were made. Although changes in the spectra were observed, no attempt to correlate these changes with the damage or other conditions was made.

Fox [1992] shows, using numerical and experimental data from a beam, that changes in the resonant frequencies are a poor indicator of damage in a beam with a saw cut. In the experimental data, resonant frequencies were actually observed to increase slightly for some modes after the damage had been introduced. These increases were attributed to inaccuracies in the methods used to estimate the resonant frequencies.

An experimental study of the sensitivity of the measured modal parameters of a shell structure to damage in the form of a notch was conducted by Srinivasan and Kot [1992]. The authors found that the resonant frequencies of the shell structure

were insensitive to damage, with measured changes not exceeding the frequency resolution of the measurements.

A technique to identify damaged parts using statistical methods and measured natural frequencies was proposed by Pape [1993]. By looking for resonances outside of the mean standard deviations, he detected parts with gross defects. The ability to resolve smaller defects was not yet realized. It was hoped that this technique would replace the more expensive and time-consuming mechanical testing already done on these parts.

Penny, et al. [1993] present a method for locating the "most likely" damage case by simulating the frequency shifts that would occur for all damage cases under consideration. The measured frequencies are then fit to the simulated frequencies for each simulated damage case in a least-squares sense. The "true" damage case is indicated by the minimal error in this fit.

A method for using frequency-shift measurements to detect damage in a smart structure was presented by Slater and Shelley [1993]. They described the theory of modal filters used to track the frequency changes over time. They also described how the system deals with sensor failures or sensor calibration drift over time.

Friswell, et al. [1994] present the results of an attempt to identify damage based on a known catalog of likely damage scenarios. The authors presume that the prior model of the structure is highly accurate. Using this model, they computed frequency shifts of the first n modes for both the undamaged structure and all the considered types of damage. Then ratios of all the frequency shifts were taken, resulting in numbers. For the candidate structure, the same numbers were computed, and a power-law relation was fit to these two sets of numbers. When the body of data is noise-free, and when the candidate structure lies in the class of assumed damages, the correct type of damage should produce a fit that is a line with unity slope. For all other types of damage the fit will be inexact. The likelihood of damage was keyed on the quality of the fit to each pattern of known damage. Two measures of fit were used: the first was related to the correlation coefficient; the

second was a measure of how closes the exponent and coefficient were to unity. Both measures were defined on a scale from 0 to 100. It was hypothesized that damage was present when both measures were near 100.

Meneghetti and Maggiore [1994] derive a sensitivity formulation for locating a crack in a beam from frequency shifts. Using an analytical result, the local stiffness change required to produce a given frequency shift was plotted as a function of crack position. Such a curve was plotted based on measured frequency shifts for several modes. The intersection of the curves was used as an indicator of the crack location.

A detailed closed-form solution for the frequencies of a beam containing a slot was presented by Man, et al. [1994]. They investigated how the minimum detectable crack size can be determined from the frequency shifts predicted by the model of the slotted beam. The authors concluded that the minimum slot size that is detectable using the techniques of this paper is 10% of the beam depth. The inverse problem, which is typically Level 2 or Level 3 damage identification, consisted of calculating the damage parameters, e.g., crack length and/or location, from the frequency shifts. In this section, summaries of some of the key works describing the inverse problem are presented.

Wang and Zhang [1987] estimate the sensitivity of modal frequencies and cross-spectral densities to changes in the structural stiffness parameters. The hypothesis is that modal characteristics themselves are not sensitive to damage, but that certain frequency ranges in the structural frequency response are sensitive to damage.

Stubbs, et al. [1990] and Stubbs and Osegueda [1990a, 1990b], discuss a method for damage identification that relates changes in the resonant frequencies to changes in member stiffnesses using a sensitivity relation. Stubbs and Osegueda [1990a, 1990b] developed another damage detection method using the sensitivity of modal frequency changes that is based on work by Cawley and Adams [1979a]. This method is demonstrated to produce more accurate results than the previous method

in the case where the number of members is much greater than the number of measured modes.

Sanders, et al. [1992] use the frequency sensitivity method of Stubbs and Osegueda [1990a] combined with an internal-state-variable theory to detect damage in composites. The damage theory includes parameters which indicate two possible types of damage: extensional stiffness changes caused by matrix micro-cracking and changes in bending stiffness caused by transverse cracks in the 90degree plies. The technique is applicable in general to any internal variable theory that can predict stiffness changes resulting from changes in the measured parameters.

Balis Crema, et al. [1995] use the modal parameter sensitivity equations presented by Stubbs and Osegueda [1990a] to locate damage. The authors examine the effects of the location of the damage on successful damage detection, as well as the relationship between the modes used in the analysis and the position of the damage.

3.5.2. Changes in modal shapes

The use of modal shapes instead of natural frequencies to detect damage in structures has been addressed in recent years by many researchers. West [1984] presented what is possibly the first systematic use of mode shape information for the location of structural damage without the use of a prior FEM. Osegueda, et al. [1992] report on a project that examines changes in the dynamic properties of a scale model of an offshore platform subjected to damage. Mode shape changes could not be correlated with damage in this study. Fox [1992] shows that single-number measures of mode shape changes such as the MAC are relatively insensitive to damage in a beam with a saw cut. Mayes [1992] presents a method for model error localization based on mode shape changes known as structural translational and rotational error checking (STRECH). Srinivasan and Kot [1992] found that changes in mode shapes were a more sensitive indicator of damage than changes in resonant frequencies for a shell structure.

Ko, et al. [1994] present a method that uses a combination of MAC, COMAC and sensitivity analysis to detect damage in steel framed structures. Salawu and Williams [1994] compare the results of using mode shape relative change and mode shape curvature change to detect damage. Salawu and Williams [1995] show that the MAC values can be used to indicate which modes are being affected most by the damage. Lam, et al. [1995] define a mode shape normalized by the change in natural frequency of another mode as a "damage signature." Salawu [1995] proposes a global damage integrity index that is based on a weighted ratio of the damaged natural frequency to the undamaged natural frequency.

3.5.3. Changes in mode shape curvature / strain mode shape changes

An alternative to using mode shapes to obtain spatial information about vibration changes is using mode shape derivatives, such as curvature. It is first noted that for beams, curvature and bending strain are directly related as:

$$\varepsilon = \frac{y}{R} = ky \qquad [1]$$

where e is strain, *R* is radius of curvature, and k is curvature or 1/R. The practical issues of measuring strain directly or computing it from displacements or accelerations are discussed by some researchers.

Chance, et al. [1994] found that numerically calculating curvature from mode shapes resulted in unacceptable errors. Chen and Swamidas [1994] found that strain mode shapes facilitated the location of a crack in a cantilever plate using FEM simulation. Strain changes with the introduction of a crack in a tubular were evaluated by Tjoint Nwosu, et al. [1995]. In general, it was found that measurements in strains instead of measurements in curvature directly, dramatically improved results. The authors found changes in strain to be much greater than any frequency shifts and to be measurable even at a relatively large distance from the crack.

3.5.4. Dynamic flexibility measuring method

Another class of damage identification methods uses the dynamically measured flexibility matrix to estimate changes in the static behavior of the structure. Because the flexibility matrix is defined as the inverse of the static stiffness matrix, the flexibility matrix relates the applied static force and resulting structural displacement. The use of measured flexibility as a "condition index" to indicate the relative integrity of a bridge was proposed by professor Aktan, et al. [1994]. They apply this technique to two bridges and compare the measured flexibility to the static deflections induced by a set of truckload tests. Pandey and Biswas [1994] present a damage-detection and location method based on changes in the measured flexibility of the structure. Toksoy and Aktan [1994] compute the measured flexibility of a bridge and examine the cross-sectional deflection profiles with and without a baseline data set. Mayes [1995] uses measured flexibility to locate damage from the results of a modal test on a bridge. A method for decomposing the measured flexibility matrix into elemental stiffness parameters for an assumed structural connectivity was proposed by Peterson, et al. [1995].

Lin [1990] proposes the unity check method for locating modeling errors and uses the location of the entry with maximum magnitude in each column to determine the error location. Lin [1994] extends the unity check method to the problem of damage detection. Gysin [1986] demonstrates the dependency of this method on the type of matrix reduction used and on the number of modes used to form the flexibility matrices. A weighted error matrix, where the entries are divided by the variance in natural frequency resulting from damage in each member was presented by Park, et al. [1988]. The authors applied their formulation to both beam models and plate models.

A variation on the use of the dynamically measured flexibility matrix is the use of the dynamically measured stiffness matrix, defined as the pseudo-inverse of the dynamically measured flexibility matrix. Similarly, the dynamically measured mass and damping matrices can be computed. Salawu and Williams [1993] use direct

comparison of these measured parameter matrices to estimate the location of damage.Peterson, et al. [1993] propose a method to use the measured stiffness and mass matrices to locate damage by solving an "inverse connectivity" problem, which evaluates the change in impedance between two structural DOF to estimate the level of damage in the connecting members.

3.5.5. Matrix update methods

Another class of damage identification methods is based on the modification of structural model matrices such as mass, stiffness, and damping to reproduce as closely as possible the measured static or dynamic response from the data. These methods solve for the updated matrices (or perturbations to the nominal model that produce the updated matrices) by forming a constrained optimization problem based on the structural equations of motion, the nominal model, and the measured data. Comparisons of the updated matrices to the original correlated matrices provide an indication of damage and can be used to quantify the location and extent of damage. Methods that use a closed-form, direct solution to compute the damaged model matrices or the perturbation matrices are commonly referred to as optimal matrix update methods. Reviews of these methods have been published by Smith and Beattie [1991a], Zimmerman and Smith [1992], Hemez [1993], and Kaouk [1993].

Baruch and Bar Itzhack [1978], Kabe [1985], and Berman and Nagy [1983] have a common formulation of the optimal update problem that is essentially minimization of the Frobenius norm of global parameter matrix perturbations using zero modal force error and property matrix symmetry as constraints. Chen and Garba [1988a, 1988b] present a method for minimizing the norm of the property perturbations with a zero modal force error constraint. Another approach to this problem used by Kammer [1988] and Brock [1968] can be formulated as minimization of modal force error with a property matrix symmetry constraint. McGowan, et al. [1990] report ongoing research that examines stiffness matrix adjustment algorithms for application to damage identification. Zimmerman and

Kaouk [1992] implement such an eigenstructure assignment technique for damage detection.

3.5.6. Non-linear methods

Actis and Dimarogonas [1989] develop a FEM for a beam with an opening and closing crack. Shen and Chu [1992] and Chu and Shen [1992] develop a closed form solution for the vibration of a beam with an opening and closing crack subjected to lower frequency harmonic forcing. Krawczuk and Ostachowicz [1992] develop a model for transverse vibration of a Bernoulli Euler beam with an opening and closing crack. They model the beam as two sections on either side of the crack connected by a torsional spring.

3.5.7. Neural network-based methods

In recent years there has been increasing interest in using neural networks to estimate and predict the extent and location of damage in complex structures. Neural networks have been promoted as universal function approximators for functions of arbitrary complexity. A general overview of neural networks can be found in Bishop [1994]. The most common neural network in use is the multilayer perceptron (MLP) trained by back propagation. In Doebling et al. [1996], a general terminology was defined consistent with common usage by calling a MLP trained by back propagation a "backprop neural network.".

Kudva, et al. [1991] used a backprop neural network to identify damage in a plate stiffened with a 4 x 4 array of bays. The authors found that the neural network was able to predict the location of the damaged bay without an error but that predicting hole size was more difficult with sometimes erratic results. Wu, et al. [1992] used a backprop neural network to identify damage in a three-story building modeled by a two-dimensional "shear building" driven by earthquake excitation. On test data, the neural network was only able to identify third-floor data with any accuracy.

Elkordy, et al. [1993] used back-propagation neural networks to identify damage in five-story buildings. The predictions of damage were generally correct to within 10%. Elkordy, et al. [1994] is a slightly modified version of this paper. Manning [1994] used backprop neural networks to identify damage in a 10-bar truss structure and a 25-bar transmission tower with active members.

3.6. Applications to specific structures

3.6.1. Beams

In Gudmundson [1983], the author discusses the dynamic behavior of cracked beams. The idea is that the loss of stiffness resulting from the crack can be represented by an equivalent flexibility matrix. The flexibility matrix is determined by an energy balance equation where the elastic energy of the flexibility matrix is balanced with the strain energy near the crack. The method is used to compute frequency shifts for a cantilevered beam with edge cracks. The results agree well with experimental data.

Yuen [1985] performed FEM modeling on cantilevered beams where damage was modeled using an element with reduced stiffness. He found his mode-shape-based eigen-parameters to be slightly more sensitive to the damage than frequency shifts.

Ju and Mimovich [1986] model damage in cantilevered beams by a "fracture hinge," a concept developed by the authors. The beams were aluminum with dimensions 9.5 mm x 63.5 mm x 457 mm. The authors made twenty beams, introducing damage at five positions along the length by milling slots at two depths and two widths. The slots were wide enough to never close on the compressive part of the bending cycle. The frequencies of the first four bending modes were measured before and after the cracks were machined. The authors used the frequency shifts of the first four bending modes to estimate the location and extent of damage in the beams. Damage was modeled by introducing a fracture hinge at the location of the crack. The fracture hinge is a torsional spring whose

stiffness depends on the crack geometry. The strength of the fracture hinge could be measured experimentally, and when incorporated into the subsequent analysis, could be used to predict frequency shifts resulting from the cracks to within 0.3%. Using the frequency shifts, the authors were able to locate the crack damage to within 3% on average, provided the crack occurred at a position in the beam with high bending moment. The authors were much less successful at estimating crack intensity.

Sanders, et al. [1989] present a method, also based on the measurement of modal parameters, to detect the location and extent of damage in structures. The work was based on the use of modal sensitivity equations, and is applied to fiber-reinforced composite beams.

Ismail, et al. [1990] investigated the effect of fatigue crack closure on the frequency changes of cracked cantilever beams. Based upon a combined experimental-numerical program, the authors conclude that the drops in resonant frequencies alone, especially for the higher modes, are insufficient measures of crack severity. The reliability of the vibration testing method for detecting the presence and nature of the crack was, however, demonstrated.

Lin and Ewins [1990] applied their nonlinearity localization technique to a specially designed nonlinear structure. A rectangular frame, suspended by springs, was driven by a shaker with a feedback loop such that the force applied was proportional to the cube of the displacement. The measured matrix describing the nonlinearity, based on measured modes at two response levels, indicated the region of the nonlinearity but also showed false indications in other regions.

Rizos, et al. [1990] performed tests on 300mm x 20mm x 20mm steel cantilever beams. Saw cuts of 2mm (0.078 in.) to 14mm (0.55 in.) depth were introduced at locations throughout the length of the beam. The beam was excited at a resonance, and the amplitude of vibration was measured at several points along the length. From these amplitude measurements, the crack location and length were calculated. The values given were within 8% of the actual values in all cases.

Kam and Lee [1992] applied their crack-detection and location algorithm to the same data set and also reported good results while Silva and Gomes [1990] present detailed experimental results on natural frequencies in slotted free-free beams. They give tables of all the frequencies they measured so that other investigators can use the results. The beam considered was steel, 0.72m long, with a 32 mm x 16 mm cross section. A slot was introduced into the beams with a 0.5 mm wide milling cutter. Slots ranged in depth from 1/8 to 1/2 of the beam thickness, and were introduced in both dimensions *(x* and y) of the cross section. For each of the 32 beams, the first four frequencies were measured both before and after damage.

Stubbs and Osegueda [1990a] apply their sensitivity method of damage identification to numerical examples of a 10 m long by 200 mm wide by 600 mm deep, simply-supported concrete beam with various damage scenarios. Stiffness reductions for bending modes are modeled by reducing the moment of inertia over finite lengths at one or more locations along the beam. For axial modes, the stiffness reductions are modeled by reducing the area of the beam over finite lengths. For single damage locations, the sensitivity method accurately predicted the extent and location of the damage, while occasionally identifying additional low-level damage at locations adjacent to the actual damage location. Results for multiple damage locations are similar to those obtained for the single damage location, but with one failure to locate the second damage location. The authors conclude by posing four questions that must be asked of this damage-identification method:

- What is the smallest defect that can be detected?

- Can small frequency changes associated with damage scenarios studied actually be measured accurately?

- How will nonlinear behavior affect the accuracy of the method?

- How accurately can an analyst develop the sensitivity matrices for an existing structure?

Their response is that general answers to these questions are not available, and they must be studied with regard to the particular application being investigated.

Subsequently, Stubbs and Osegueda [1990b] apply the same techniques to a series of 1 m long by 25 mm wide by 12.7 mm deep aluminum cantilevered beams. Damage was simulated by reducing the cross-section area of the beam over finite length intervals. Impact excitation was used to excite the structure. Resonant frequencies were computed by fitting a parabola to peaks in the Fourier spectrum of the frequency response signal. Practical aspects to the testing, such as removing and replacing the beam in its support fixture, are discussed. Results of the damage identification procedure are similar to those obtained from numerical examples reported in Stubbs and Osegueda [1990a] and show that this method can accurately locate the damage and accurately predict the extent of the damage.

Hop [1991] presents an experimental program of dynamic investigations to determine the effect of the degree of prestressing on the natural frequency and the logarithmic decrement of free vibration damping in concrete beams. The author has determined a relation between degree of prestressing and damping.

Fox [1992] performed impact modal tests on a 1 m long by 12 mm deep beam with saw cuts 1 mm, 3 mm and 6 mm deep located 200 mm from one end. Soft springs were use to simulate free boundary conditions during the tests. Modal analyses of the test specimens were also performed numerically with finite element analysis. Although the resonant frequencies and MAC values showed little change, damage could be located by examining relative changes in the mode shapes whose frequencies were found to shift as a result of damage.

Huang and Gu [1993] studied a finite element simulation of a cantilever beam 400 mm long with a cross-section of 6 mm x 35 mm. The authors used a single displacement node and calculated an ARMA model to fit the response. The residual was the quantity whose cumulant was estimated. The authors showed that in numerical studies both with and without noise the cumulant was very near zero

for the un-cracked beam, but nonzero for the cracked beam because a non-linearity was present.

A numerical trade study using a 40 DOF simply supported aluminum beam was conducted by Kim and Bartkowicz [1993]. The authors showed how the number of sensors and modes affects the ability to locate structural damage.

Salawu and Williams [1993] apply the error matrix method to a beam FEM and compare the results to some other criteria, such as changes in mass-normalized mode shapes and changes in the measured stiffness matrix. They also introduce the matrix cursor method, which uses vector space theory to identify the nonzero rows and columns of a dynamic error matrix. They use measured parameter matrices in all of these methods.

Budipriyanto and Swamidas [1994] measured the modal parameters of a notched cantilevered beam in air and both partially and fully submerged in water. The beam was notched symmetrically on both top and bottom surfaces. Measurements were taken with accelerometers and strain gages. Results presented include natural frequencies, damping ratios, and peak response magnitudes for all combinations of sensor type and degree of submergence.

Chance, et al. [1994] tested a beam containing a "bilinear crack device." A groove was machined into the beam, and two pieces were inserted into the groove. The two pieces were designed to open and close like a fatigue crack. FRFs from stepped-sine excitation clearly showed nonlinear behavior. Mode shapes from accelerometers were not able to locate the crack. Curvature shapes from measured strains clearly located the damage, provided that the strain gages were located close enough to the crack.

Dong, et al. [1994] measured their strain-mode-shape-based parameter on a beam containing a fatigue-induced crack. They were easily able to locate the crack, and the results agreed with FEM predictions. They gave no details on the beam material or dimensions or how deep the crack was.

Kaouk and Zimmerman [1994a] apply the MRPT matrix update technique to a cantilevered beam with a discrete lumped mass. The beam was tested with the lumped mass in place, and then the mass was removed and the beam retested. The technique was able to locate this damage case uniquely using the first four measured modes.

Ko, et al. [1994] apply a MAC/COMAC-based damage identification technique to data acquired from a 2 m square steel portal frame. The frame was instrumented at eleven locations. An impact hammer test was performed to estimate mode shapes and frequencies, then a shaker test was performed to obtain accurate identification of the mode shapes. Tests were conducted with the joints in both rigid and pinned conditions, and then damage was simulated by removing bolts at 2 locations—one at a column-beam connection, and one at a column-base connection.

Meneghetti and Maggiore [1994] apply a sensitivity-based damage-detection method to experimentally measured results on a steel beam 600 mm long with a 15 mm square cross section. Slots 0.3 mm wide were milled into several beams. They were able to locate a slot only 2 mm deep by measuring the pre and post-damage frequencies.

Perchard and Swamidas [1994] obtained measurements with accelerometers and strain gages on a cantilever beam with a machined notch. Frequency shifts did not match FEM predictions. Changes in damping and residues did not correlate well with the damage, but changes in off-peak amplitudes in FRFs did correlate well with the damage. Strain-based FRFs were also very sensitive to damage, provided that the strain gages were near enough to the damage location.

Silva and Gomes [1994] applied a frequency shift method to data collected experimentally from fatigue-cracked steel beams. They used a cantilever beam 600 mm long with a 18 mm x 32 mm cross section. Fatigue cracks 8 mm to 16 mm long were introduced into the beam at locations ranging from the fixed end to 75 mm from the free end. The authors do not specify the directions of the cracks. In all cases they were able to determine the crack location to within 12 mm and the length

to within 1 mm. The best results were obtained when the first four frequencies were used.

Chen, et al. [1995] tested two C 3 x 4.1 channel sections that were 3.6 m long. Damage was introduced by successively cutting away portions of the flange. The step-relaxation method (quick release of a suspended weight) was used to excite the beams. Acceleration response measurements were made along the length of the beam. The authors found that relatively severe damage (damage that under the original design load produced the onset of a plastic hinge) caused less than 5% changes in the resonant frequencies of the beams. Mode shapes identified from the free vibration decay of the structure were not found to be useful in locating the damage.

Fritzen, et al. [1995] applied a Kalman filtering technique to FEM-generated time histories of a pinned-pinned beam with an opening and closing crack. They were able to precisely detect, locate, and quantify the crack. They also applied the technique experimentally to a T-frame consisting of two solid aluminum beams welded together. A non-closing notch with depth of 30% of the beam thickness was machined using a procedure known as wire electric discharge machining. The technique successfully located and quantified the notch.

Prime and Shevitz [1996] present experimental results from the vibration of a cantilever polycarbonate beam containing an opening and closing crack. The beam is 61cm long, 5.1 cm wide and 1.21 cm thick with a crack penetrating to half of the thickness. The crack was made by bonding together 3 pieces of polycarbonate. The excitation was step relaxation, i.e., pull and release. A variety of techniques was used to examine the nonlinear response.

Zimmerman, et al. [1996] describe the development of an integrated structural damage detection system. The system includes data acquisition hardware and software, damage-identification software, and a damage-identification demonstration test article consisting of a cantilevered beam with various damage scenarios. The authors explain the details of the test article design, the operation of

the software, and particular difficulties that were encountered during the development. The primary difficulty encountered was the systematic extraction of the modal parameters from the measured frequency response data.

Chowdhury and Ramirez [1992] performed impact modal tests on 27 reinforced and un-reinforced concrete beams 762 mm long by 89 mm wide by 152 mm. deep. Some of the beams had defects cast into them to simulate delaminations and cracks. Free boundary conditions were simulated by suspending the beam with plastic belts during these tests. The authors also examined changes in frequency and power spectra caused by changes in strength, applied loads, and incremental loads.

Slastan and Pietrzko [1993] measured frequencies and mode shapes on reinforced concrete beams before and after damage. The beams were 6 m long, had a T-shaped cross-section, and were tested with both simply supported and cantilevered boundary conditions. Damage was introduced incrementally by static loading to three levels. Results were considered for both hammer and shaker excitation. They found the frequency shifts to be measurable but small. These authors found that the mode shapes and damping values contained little useful information.

Allbright, et al. [1994] measured mode shapes on a deteriorated, prestressed concrete beam. The beam, taken from a bridge, was a 23.3 m long box section, 910 mm wide, 840 mm high with 127 mm thick walls. The beam had eighteen 13 mm diameter prestressing steel tendons. Three tendons in one corner of the beam had corroded along the length of the beam except for a 1 m length at each end. An impact hammer and accelerometers were used to measure a FRF for the beam. The damage in the beam manifested itself as torsional coupling in the bending modes of the beam. The flexibility matrix measured from the modal tests agreed well with the flexibility matrix obtained using static tests.

Casas [1994] and Casas and Aparicio [1994] report the testing of four pairs of beams. Each pair consisted of an undamaged beam and a beam with cracks introduced by the form work at various locations along the length. Impact excitation

was applied to the top of the beam without a driving point response measurement. Two acceleration responses were measured at the center point and quarter point. Based on the measured resonant frequencies and the two measured modal amplitudes, a nonlinear least-squares algorithm was employed to determine equivalent moments of inertia for beam elements of a FEM in the damaged region. Static testing was then performed to assess the accuracy of the identified damage model. The damage conditions as well as the end boundary conditions were successfully identified by this method.

Damage identification in reinforced concrete structures by dynamic stiffness determination was investigated by Maeck et al. [1999a]. The authors developed a comparative study between two different techniques to calculate the stiffness degradation of a concrete beam. Studied methods include frequency-only measurements and modal shapes monitoring.

A study on prestressed concrete beams and damage determination by dynamic testing was developed by Ambrosini et. al [1999]. An experimental campaign was developed cutting prestressed bars until 50% of the total section. Frequencies and modal shapes were measured under different load steps. A correlation between the damage and the dynamic parameters was formulated. A numerical model was also developed to simulate the full process.

3.6.2. Trusses

Smith and McGowan [1989] and McGowan, et al. [1990] present the results of experimental and analytical modal analyses on a 10-bay aluminum truss structure, where each bay was 0.5 m square. In general, damage was more apparent in the resonant frequency changes than in changes associated with mode shapes as quantified by MAC values. Stubbs, et al. [1990] applied a sensitivity-based method of damage identification to a numerical simulation of a cantilevered, 20-bay plane truss, where each bay was 1m square. The authors point out that false predictions may be made near the support or free end of the structure. For the multiple damage cases, the magnitude of the damage was predicted accurately and, in most cases, the

damage locations were also accurately predicted. Kashangaki [1991] proposes the use of the DSMT test-bed at NASA-Langley Research Center for damage detection research. Kashangaki, et al. [1992) use the DSMT data in their examination of some issues inherent in the use of modal data for detecting damage in truss structures. A relationship is drawn between the accuracy of the measured modes and frequencies and the feasibility of detecting damage in the truss members.

Doebling, et al. [1993a, 1993b] apply a sensitivity-based FEM update scheme to an 8 bay suspended truss with asymmetrically placed lumped masses, the so-called "MUDDE" truss. The results demonstrated that modes whose selection is based on highest overall strain energy content in the damaged structural configuration provide the most information about the damage and thus are the best modes to use in the model update. Kaouk and Zimmerman [1993] apply the MRPT matrix update technique to the DSMT 8-bay truss data. The result provides a good example of the difficulty of locating damage when the modes do not store a high level of strain energy in the members which undergo damage.

Peterson, et al. [1993] use an inverse-connectivity technique to locate the damage in the MUDDE truss from the measured mass and stiffness matrices. The results demonstrate that the ability of the measurements to distinguish rotational DOF is crucial when structural changes are manifested primarily in bending behavior. Slater and Shelley [1993] apply an adaptive modal filtering scheme to a 9-bay, 4.5 m suspended truss. They demonstrated the ability of the system to detect frequency shifts over time by adding and removing constraints. They also showed the ability of the system to handle faulty sensors by disconnecting sensors during the test. Kaouk and Zimmerman [1994c] use the MRPT matrix update technique to perform damage detection when a baseline data set is available in lieu of an analytical model. The results were shown to be successful overall, although the algorithm still performed better with a correlated baseline FEM.

Hemez and Farhat [1995] apply their element-by-element sensitivity update method to the DSMT 10-bay truss data. They examine some specific issues

surrounding the location of damage in this structure, including the selection of the type and number of finite elements, the modeling of the cantilever boundary condition, the selection of the modes used in the update, and the limitations of the sensitivity-based technique. Hinkle, et al. [1995] examine the effects of gravity preloading on the joints of a precision deployable truss structure. Directional dependencies consistent with the orientation of the deployment joints were discovered in the measured flexibility. Doebling [1996] applies a parameter-level minimum-rank update procedure to the data from the 8-bay DSMT truss. Results of a simple modes election procedure confirmed the conclusions of other authors regarding a deficiency in minimum-rank update techniques that constrain the rank of the solution to be equal to the number of modes used in the matrix update. Dos Santos and Zimmerman [1996b] apply a hybrid stiffness matrix update algorithm to the data from the 8-bay DSMT truss. The authors also point out that the quality of the results from the hybrid method is strongly dependent on the accuracy of the estimated stiffness matrix perturbation from the MRPT algorithm.

3.6.3. Plates and shells

Wolff and Richardson [1989] examine the changes in modal parameters after several damage cases are simulated on an aluminum plate with a centerline rib stiffener. The first damage case is the removal of a bolt at the center of the plate. The second damage case is the removal of a bolt at the end of the plate. The first damage case was clearly observed in frequency changes of the first several modes, while the second was not. The local effects of the second case vs. the global effects of the first case are cited as the explanation for these results.

Richardson and Mannan [1992] applied a stiffness sensitivity method to a 500 mm x 190 mm x 8 mm aluminum plate. A 25 mm saw cut was made in the edge of the plate to simulate damage. Mode shapes and resonant frequencies of the plate were measured before damage using an impact excitation method. Boundary conditions for the test are not described. After damage, the sensitivity method required only the measurement of resonant frequencies. Damage was successfully

located using a pseudo-inverse search technique to locate the largest negative changes in stiffness.

Chen and Swamidas [1994] and Swamidas and Chen [1995] present FEM results for a cantilever plate containing a crack. Their best data for locating damage were determined to be strain mode shapes. Chance, et al. [1994] present FEM results for a cantilevered plate containing a hole. Mode shape curvatures are shown to be better indicators of damage location than mode shape displacements.

Chen and Swamidas [1996] performed swept-sine modal tests of a T-plate joint. Modal parameters that were examined include resonant frequencies, acceleration FRFs, and strain FRFs. Resonant frequencies showed less than a 4% change for a crack halfway through the thickness of the plate. Changes in magnitude of the strain FRFs obtained relatively close to the cracked region gave better indications of the damage.

Saitoh and Takei [1996] have applied the modal sensitivity method developed by Richardson and Mannan [1992] to a plate with a crack in it. The results showed small decreases in frequencies associated with the damaged plate. Changes in damping were inconsistent, and MAC values showed no change when the damaged plate was compared to the undamaged plate.

Srinivasan and Kot [1992] tested a 305 mm diameter by 686 mm long cylindrical structure with 2.5 mm wall thickness, which had a circumferential notch machined in it at mid-height. Impact excitation was applied to the cylinder, which was suspended by relatively soft springs to simulate free boundary conditions. No specific damage identification method was employed. Instead, the authors examined changes in the resonant frequencies and changes in the mode shapes. Resonant frequencies were found to be insensitive to the damage with changes not exceeding the frequency resolution of the measurements. Mode shapes were found to be a more sensitive indicator of damage as quantified by the MAC values between the damaged and undamaged mode shapes.

Nwosu, et al. [1995] performed FEM analyses on a tubular T-joint using shell elements for the tubes and line spring elements for a crack. They modeled one cracked and one un-cracked configuration. Their results showed large changes in bending moment with the introduction of the crack. These could presumably be measured with strain gages. Significantly, these changes were quite noticeable even in regions relatively distant from the crack.

3.6.4. Frames

Friswell, et al. [1994] applied their method to two structures: a frame structure and a cantilevered plate. Both were made of steel, and the length of both was approximately 0.5 m. Damage was simulated by saw cuts in the structures. The algorithm was applied and found to be reasonably successful. The algorithm was able to correctly find the damage but gave some false positive responses when the actual structure was intact.

Choudhury and He [1996] apply their method for detecting damage using FRF changes and FEM mass and stiffness matrices to data from a planar frame structure with dimensions of approximately 900 mm by 420 mm. The damage consisted of two cuts, each 5 mm wide, made on opposite sides of one of the beam members at the same cross section. They were able to locate the damage successfully using their method in conjunction with a dynamic expansion procedure (used to estimate the values for the FRFs at unmeasured FEM DOF).

Saitoh and Takei [1996] have applied the modal sensitivity method developed by Richardson and Mannan [1992] to forty automobile car doors with over 100 spot welds. When applied to the car doors, the data obtained from damaged structures appears to be in the scatter of the data from the undamaged structures

3.6.5. Bridges

Although vibration-based structural health monitoring is applicable to a large range of structures, bridges are considered as important applications. The main bridge-

building boom in the USA was situated in the sixties when the interstate system was constructed. The situation in Europe is similar with the construction of the highways in the same era. Most of these bridges are reaching their critical age and it is expected that the budget demands for maintenance will peak in 2010. Vibration-based monitoring is certainly a helpful tool in assessing the condition of these bridges and in making maintenance schedules. More recent long-span cable-stayed and suspension bridges are equipped with an embedded monitoring system consisting of sensors such as: accelerometers, nemometers, displacement transducers, inclinometers, strain gauges, temperature sensors, ... Examples of instrumented bridges exist all over the world. As reported in Farrar [1999], one of the best-equipped bridges is probably the Tsing Ma Bridge in Hong Kong. The bridge was built in 1997, has a main span of 1377 m and is monitored by nearly 600 sensors.

Bridge monitoring systems are not only used to detect damage. Reported applications and objectives of existing monitoring systems include: quality control during the construction of the bridge; verifying design parameters of a newly constructed bridge; serving as a warning system for traffic closure when the bridge is subjected to excessive wind loading; and condition assessment about its serviceability and ultimate limit state. However, generally speaking, there is some vagueness in how the measurement data are currently interpreted in terms of condition assessment and apparently a lot of "engineering judgement" comes into play

A recent extensive survey of bridge failures in the United States since 1950 is presented by Shirole and Holt [1991]. These authors point out that recent responses of engineers to bridge failures have been reactive. Bridge design modifications and inspection program changes are often made only in response to catastrophic failures.

The collapse of the Tacoma Narrows Bridge a half century ago is a classic example of this reactive attitude because it led to the inspection and modification of other

suspension bridges. The widespread introduction of systematic bridge inspection programs was directly attributed by Shirole and Holt to the catastrophic bridge collapse at Point Pleasant, WV, in 1967 1 . Design modifications for seismic response of bridges have been made as a direct consequence of the 1971 San Fernando Earthquake [Gates, 1976].

At present in USA, bridges are generally rated and monitored during biennial inspections, largely with the use of visual inspection techniques. There is the possibility that damage could go undetected at inspection or that cracks in load-carrying members could grow to critical levels between inspection intervals [see Gorlov, 1984]. Sudden damage leading to bridge collapse also occurs as a result of collision. For example, the AMTRAK railroad bridge collapse in the Southeastern US in 1993 involved the collision of a barge with the bridge. [According to statistics presented by Shirole and Holt, more than 13% of identified failures of US bridges since 1950 are attributed to collisions.] Based on the above information, a quantitative, possibly continuous, mechanism of bridge damage detection may be appropriate for certain types of bridges; specifically, those bridges with non-redundant structural members. Additionally, the use of an active damage-detection system may be appropriate in some cases. For example, such a system could detect sudden significant damage to the bridge structure resulting from collision and trigger a system to close the bridge to traffic.

Since 1979, numerous studies involving the development and application of damage detection techniques for bridge structures have been reported. Salane, et al. [1981] use changes in the dynamic properties of a three-span highway bridge during a fatigue test as a possible means of detecting structural deterioration resulting from fatigue cracks in the bridge girders. The authors found that changes in bridge stiffness and vibration signatures (mechanical impedance plots) can be used as indicators of structural deterioration resulting from fatigue. Stiffness coefficients were calculated from experimentally-determined mode shapes. Excitation was provided by an electro-hydraulic actuator.

Kato and Shimada [1986] perform vibration measurements on an existing prestressed concrete bridge during a failure test. A reduction in natural frequencies could be detected as the statically applied load approached the ultimate load; however, damping values were largely unaffected.

Turner and Pretlove [1988] perform a numerical vibration analysis on a simple beam representation of a bridge subjected to random traffic loading. The motivation for the work was the development of a structural condition monitoring system that did not require a measured excitation force. Biswas, et al. [1990] discuss the state of degradation of bridges in the US, emphasizing that the current 24-month inspection interval for highway bridges has two major drawbacks. They performed modal tests on a 2-span continuous composite bridge in both undamaged and damaged conditions.

In a work by [Samman, et al., 1991], a scale model of a typical highway bridge was used to investigate the change in FRF signals caused by the development of girder cracks. The authors used a procedure from the field of pattern recognition to accentuate the differences in the FRFs between cracked and un-cracked bridges. The method also provided some crack location information. Spyrakos, et al. [1990] performed a series of experiments on a set of beams designed to have dynamic responses similar to actual bridges. Each beam was given different damage scenarios (type, location, degree), and low-level free vibration tests were performed. The authors found a definite correlation between the level of damage and the dynamic characteristics of the structure. It was found that frequency change might be an insufficient indicator of structural safety (less than 5% change in frequency was associated with critical damage). However, the study suggests that the method may be applicable to more severely damaged structures to provide an indication of remaining serviceability.

Mazurek and DeWolf [1990] present strong arguments in favor of a continuous automated vibration monitoring system for highway bridges, citing several unexpected collapses and near collapses of bridges. (The collapse of one Rhode

Island Bridge was prevented when a passerby observed severe cracking of a primary girder at mid-span). The authors found that major structural degradation can cause significant changes to both resonant frequencies and mode shapes. Tang and Leu [1991] performed experiments on a defective prestressed concrete girder bridge. They found that mode shape changes might be a more effective indicator of damage in bridges than frequency shifts (for damage detection, they state a frequency shift on the order of 0.01 Hz must be detectable). The step relaxation method was used to excite the bridge. Law, et al. [1992] performed vibration tests on a one-fifth scale model of a reinforced concrete beam-slab bridge deck. The results based on the FRF or its magnitude appear to be superior to those based on the phase of the FRF.

Raghavendrachar and Aktan [1992] performed impact tests on a three-span reinforced concrete bridge with a goal of detecting local or obscure damage, as opposed to severe, global damage. The authors concluded that modal parameters may not be reliable as damage indicators if only the first few modes are measured. For this type of damage, modal information for higher modes would be required. An extensive survey and analysis of structural damage detection has been completed by Kim and Stubbs [1993]. The authors assessed the relative impact of model uncertainty on the accuracy of nondestructive damage detection in structures. The authors applied their approach to a plate-girder bridge and a 3-dimensional truss-type bridge.

Aktan, et al. [1994] assess the reliability of modal flexibility as an indicator of bridge condition by comparing the measured flexibility to the flexibility obtained using a static-load truck test. They estimated that the error in measured flexibility resulting from modal truncation was about 2% after 18 modes had been included. In Biswas, et al. [1994] the authors study crack detection in a scale model of a bridge structure. The method was also applied to data with noise added and still found to be sensitive to crack lengths as small as 13 mm. Farrar, et al. [1994] present the results of a damage-detection experiment performed on the I40 bridge over the Rio Grande river in Albuquerque, NM. This bridge was designed so that

the two main plate girders carry all the loads of the bridge. Such a design is called "fracture critical," since failure of either of the main girders is assumed to produce catastrophic failure of the bridge. In general, the results indicate that modal frequency is not a sensitive indicator of damage, as it took a large reduction in the bridge bending stiffness to see any changes in the measured modal frequencies. However, the mode shapes were shown to be more sensitive indicators of damage.

Samman and Biswas [1994] tested a scale model bridge consisting of a concrete slab bonded to three steel girders. Vibration tests were performed on the damaged structure as well as the undamaged structure and the repaired structure. Toksoy and Aktan [1994] use the measured flexibility matrix to assign a condition index to a bridge. When a baseline data set is available, the deflection profiles are compared directly. Alampalli, et al. [1995] repeatedly tested a single span, steel girder bridge with an integral concrete deck in an undamaged condition to examine the variability in resonant frequencies, modal damping, and mode shape data caused by random test variations and environmental effects. The authors concluded that changes in resonant frequencies can be used to indicate damage as these changes were beyond the statistical variations caused by random test variations and environmental effects, but that changes in mode shapes as measured by MAC or COMAC values are not sensitive enough to locate damage.

Farrar and Cone [1995] present further analysis of the I40 bridge damage detection data set described by Farrar, et al. [1994]. The results imply that modal frequencies, modal damping ratios, and mode shapes may not be sensitive enough indicators to detect damage at an early enough stage to be practical. James, et al. [1995] present the results of two damage-location techniques applied to the body of data from the I40 bridge damage detection test described by Farrar, et al. [1994]. The results of this test indicate that the STRECH technique provides a better global indication of damage, but that the MAXCON technique appears to be more robust to measurement errors and more applicable to measured dynamic data. Simmermacher, et al. [1995] examine the effects of FEM mesh density on successful application of the MRPT matrix update algorithm. This research

examines the tradeoffs between large and small FEMs for application of the MRPT to the I40 bridge data. Stubbs, et al. [1995] present the application of a previously developed damage identification technique to the I40 bridge damage-detection data. It is noted that an advantage of this algorithm is the ability to locate damage without knowledge of the structure's material properties.

Liang, et al. [1995] apply their ETR damage-identification method to data obtained on the steel Peace Bridge over the Niagara River near Buffalo, NY. Since no damage could be added to the bridge, the authors used the test as an opportunity to study the repeatability of the necessary parameters and to observe the changes in the structure resulting from construction repair work. The impact hammer tests yielded better overall results than the ambient input tests. Salawu [1995] and Salawu and Williams [1995] apply the global damage integrity index and local integrity index method to a voided-slab reinforced concrete bridge that was being repaired. The MAC matrix gave some indication of the modes that were affected by the damage, and the COMAC values indicated the location of the damage, but these parameters also indicated changes at locations that did not correspond to damage. Sibbald, et al. [1995] used plots of the dynamic stiffness to identify damage in scale-model masonry arch bridges. The authors were able to detect spandrel wall separation and different levels of fill by examining changes in the plots of the dynamic stiffness.

Zhang and Aktan [1995] use changes in curvatures of the uniform load surface (the deformed shape of the structure when subjected to a uniform load), calculated using the uniform load flexibilities, to identify damage in a numerical simulation of the Cross County highway bridge near Cincinnati, OH. The change in curvature was shown to be a sensitive indicator of this local damage. Changes in other modal parameters (resonant frequencies and mode shapes) were shown be insensitive to the damage.

Kong, et al. [1996] performed ambient vibration studies on a scale-model steel-girder bridge in both undamaged and damaged conditions. Damage was imposed by

removing a roller support under the girder. Resonant frequencies, damping ratios, and modal ETRs were measured before and after the damage. The ETR was observed to be the most sensitive indicator of damage. The resonant frequencies and damping were found to be inconsistent indicators of damage. Villemure, et al. [1996] report the tests on reinforced concrete bridge piers after damage had been introduced by quasi-static lateral loads. No consistent trends were observed for the viscous damping, but the hysteretic damping was shown to increase with increasing damage levels.

To summarize, it appears that over the past 15 years there has been repeated application of modal properties of bridges to the fields of damage detection and structural monitoring. The work has been motivated to a great extent by several catastrophic bridge failures. Earlier work utilized primarily modal frequency changes to detect damage, but more recent work has shown that frequency changes are insufficient. Changes in mode shapes are more sensitive indicators and might be more useful for detection of the defect location. Damping changes have not generally been found to be useful for damage detection in bridges. Finally, other more sensitive methods of computing damage from modal properties are being developed.

3.6.6. Masonry

Ellis [1998] developed some non-destructive test, which was used to evaluate the integrity of 534 stone pinnacles of the Palace of Westminster in London. The objective of the test was to measure the fundamental natural frequency of the individual pinnacles so that the frequency of each pinnacle could be compared with the frequencies of similar pinnacles, thereby identifying any pinnacle, which was significantly different from the norm. Two types of test were established: an impact test for the smaller pinnacles, which involved attaching a transducer to a pinnacle; and a laser test for the larger pinnacles, which involved monitoring their ambient (wind) response.

Genovese and Vestroni [1998] developed experimental investigations of an old masonry building taking in account its non-linear behavior. Frequency response functions from small amplitude forced oscillations were used as experimental data to identify modal parameters. They found that the response is sensitive to the characteristics of the excitation and that the evolution of the dynamic behavior of the structure subjected to increasing levels of force is characterized by the decrease of the modal stiffness.

Koh, et al. [1995] apply a condensation method for local damage detection of multistory frame buildings to a numerical simulation of a 12-story plane-frame structure and a 6-story steel frame structure. Damage, ranging from 10% to 45.6% reductions in the story stiffness, was successfully identified without false indications in the undamaged floors. The method was found to be insensitive to reasonable assumed damping values for the structures.

Dynamic evaluation technique was used to asses the mechanical behavior with the objective of redesign and rehabilitate panel buildings in Prage [Gattermayerova and Bayer, 1998]. Stress and strains were also determined by means of dynamic test in the base of a eight-storey panel building.

Forced vibration test carried out on an old masonry house using a vibrodyne and on a 1:5 scale model in laboratory were presented in 1996 [Vestroni et al.]. On this research project, professor Vestroni and his co-workers induced in a first step small amplitude oscillation to determinate the dynamic characteristics of the structure. The evolution after large amplitude oscillations furnishes a correlation between modal quantities and structural damage. The found forced vibration test as a very affective tool for an understanding of the dynamic of the dynamic behavior of masonry buildings. The role of identification techniques in processing experimental data is shown to be fundamental to a correct interpretation of test results and to extend their meaning beyond the studied cases.

Some examples of dynamic testing of historical masonry constructions are presented by Sigmund and Herman [1998]. Different sources of excitation are

compared in this paper. Dynamic data is used to setup numerical models and to simulate extreme loading conditions. The authors conclude that dynamic testing can be a valuable tool on model updating of ancient structures.

Ambient vibration tests have a number of features, which make them particularly attractive over other methods. A study of the use of ambient vibration for evaluation of masonry buildings was presented by Slastan and Foissner [1995]. The authors developed different experiment in high and low-rise masonry buildings. The use of dynamic testing under ambient vibration was found helpful in the model updating process.

Bensalem et al. [1995] developed experiments on a laboratory brickwork bridge under dynamic excitation and measurements. The proposed method was used to characterize dynamic behavior of masonry bridges. A linear dynamic finite element model was also developed to predict the arch's behavior at each load step. Not only hammer excitation but also mass shakers were used on the test. The hammer was found superior to the steady state or shaker methods.

Roca and Molins [1997] applied dynamic testing on the inspection of three different masonry bridges in Spain. The analysis of experimental data and its comparison with numerical simulations were used to adjust the proposed numerical model. The models were used afterwards to estimate the ultimate capacity of the structure. The authors conclude that dynamic testing can be successfully used as an inspection tool on the masonry bridges presented.

3.6.7. Other civil structures

Petroski and Glazik [1980] present a simple model for a cracked cylindrical shell, which is used to model cracks in nuclear reactor components such as vessels and piping. The results indicate that cracks can have a large influence on both the bending deformations and the stress intensity factors in the cylinder walls.

Hearn and Testa [1991] formed fatigue cracks in a welded steel frame. The changes in the natural frequency of the wire rope were relatively insensitive to damage and could be observed only at the higher tension levels.

Salawu [1994] gives an overview on applying vibration testing to the non-destructive evaluation of civil engineering structures. This summary discusses many of the practicalities associated with this type of testing including the influence of environmental factors and the need for an accurate baseline measurement.

James, et al. [1995] apply two damage identification techniques to a horizontal axis wind turbine (HAWT) blade. A field test capability that uses non-contact sensing apparatus such as a laser doppler vibrometer is proposed to monitor the health of HAWTs.

Lam, et al. [1995] applied a mode-shape-based detection routine to a steel frame. The authors' method was able to select the correct damage state from six possible states, which were defined to be loose connections at the four beam-column joints and the two column-ground joints.

Prion, et al. [1996] performed impact and ambient vibration tests on a four-story steel frame with steel shear walls. Changes in viscous damping did not show a consistent trend, and it was concluded that this parameter is a poor damage indicator.

Skjaerbaek, et al. [1996] developed a procedure to locate and quantify damage in a multistory reinforced concrete frame structure from a single response measurement made at the top of the structure. The method correctly located the damage in the structures at higher levels of excitation but identified undamaged areas as damaged when very low levels of excitation were studied.

A study on damage assessment of jacketed RC columns using vibration test was presented by Feng and Bahng [1999]. A neural-network technique was found

effective to estimate changes in the stiffness based on the measured dynamic characteristics.

3.7. Discussion

From reviewed literature, it is conclude that vibration-based damage detection relies upon the fact that a local stiffness change affects the global dynamic characteristics of the structure. The main advantage of this method was that measurements at one location were sufficient to assess the condition of the whole structure. The measurement location may differ from the location of the damage. Vibration-based methods were applied intermittently and implying a temporarily deployment of the sensors and the acquisition system and/or continuously, implying the embedment of the sensors in the structure. In the continuous setting, a shift from a preventive time-based to a predictive condition-based maintenance strategy was achieved. This shift reduced both the risk of a serious failure of the structure and the overall maintenance costs by excluding unnecessary inspection activities.

The interest in the ability to monitor a structure and detect damage at the earliest possible stage was pervasive throughout the civil, mechanical and aerospace engineering communities. Current damage-detection methods are either visual or localized experimental methods such as acoustic or ultrasonic methods, magnet field methods, radiographs, eddy-current methods and thermal field methods. All of these experimental techniques require that the vicinity of the damage is known a priori and that the portion of the structure being inspected is readily accessible. Subjected to these limitations these experimental methods can detect damage on or near the surface of the structure. The need for additional global damage detection methods that can be applied to complex structures has led to the development of methods that examine changes in the vibration characteristics of the structure. Damage or fault detection, as determined by changes in the dynamic properties or response of structures, is a subject that has received considerable attention in the literature. The basic idea is that modal parameters (notably frequencies, mode shapes, and modal damping) are functions of the physical properties of the structure

(mass, damping, and stiffness). Therefore, changes in the physical properties will cause changes in the modal properties.

Ideally, a robust damage detection scheme will be able to identify that damage has occurred at a very early stage, locate the damage within the sensor resolution being used, provide some estimate of the severity of the damage, and predict the remaining useful life of the structure. The method should also be well-suited to automation. To the greatest extent possible, the method should not rely on the engineering judgment of the user or an analytical model of the structure. A less ambitious, but more attainable, goal would be to develop a method that has the features listed above, but that uses an initial measurement of an undamaged structure as the baseline for future comparisons of measured response. Also, the methods should be able to take into account operational constraints. For example, a common assumption with most damage identification methods reported in the technical literature to date is that the mass of the structure does not change appreciably as a result of the damage. However, there are certain types of structures such as offshore oil platforms where this assumption is not valid. Another important feature of damage-identification methods, and specifically those methods which use prior models, is their ability to discriminate between the model/data discrepancies caused by modeling errors and the discrepancies that are a result of structural damage.

The effects of damage on a structure could be classified in literature as linear or nonlinear. A linear damage situation was defined as the case when the initially linear-elastic structure remained linear-elastic after damage. The changes in modal properties were a result of changes in the geometry and/or the material properties of the structure, but the structural response could still be modeled using a linear equation of motion. Nonlinear damage was defined as the case when the initially linear-elastic structure behaves in a nonlinear manner after the damage has been introduced. One example of nonlinear damage was the formation of a fatigue crack that subsequently opens and closes under the normal operating vibration environment. Other examples included loose connections that rattle and nonlinear

material behavior. A robust damage-detection method would be applicable to both of these general types of damage. The majority of the papers summarized in this chapter address only the problem of linear damage detection. Most of the damage identification methods reviewed in this chapter relied on linear structural models. Further development of methods that have an enhanced ability to account for the effects of nonlinear structural response has the potential to enhance this technology significantly. An example of such a response would be the opening and closing of a fatigue crack during cyclic loading, in either an operational situation or in the case of a forced vibration test. Many methods are inherently limited to linear model forms and, therefore, cannot account for the nonlinear effects of such a damage scenario.

A topic of primary importance is the dependence on prior analytical models and/or prior test data for the detection and location of damage. Many algorithms presumed access to a detailed FEM of the structure, while others presumed that a data set from the undamaged structure was available. Often, the lack of availability of this type of data can make a method impractical for certain applications. While it is doubtful that all dependence on prior models and data can be eliminated, certainly steps can and should be taken to minimize the dependence on such information.

Measurement sensors number and location is another important issue that has not been addressed to any significant extent in the current literature. Many techniques that appear to work well in example cases actually perform poorly when subjected to the measurement constraints imposed by actual testing. Techniques that are to be seriously considered for implementation in the field should demonstrate that they can perform well under the limitations of a small number of measurement locations, and under the constraint that these locations be selected a priori.

A topic that is a point of controversy among many researchers is the general level of sensitivity that modal parameters have to small flaws in a structure. Much of the evidence on both sides of this disagreement is anecdotal because it is only demonstrated for specific structures or systems and not proven in a fundamental

sense. This issue is important for the development of health monitoring techniques because the user of such methods needs to have confidence that the damage will be recognized while the structure still has sufficient integrity to allow repair. A related issue is the discernment of changes in the modal properties resulting from damage from those resulting from statistical variations in the measurements: a high level of uncertainty in the measurements will prevent the detection of small levels of damage.

Regarding long-term health monitoring of structures such as bridges and offshore platforms, the need to reduce the dependence upon measurable excitation forces is noted by many researchers. The ability to use vibrations induced by ambient environmental or operating loads for the assessment of structural integrity is an area that merits further investigation.

Available literature also has presented studies where different health-monitoring procedures are compared directly by application to a common data set. Some data sets, such as I40 Bridge data set, have been analyzed by many different authors using different methods, but the relative merits of these methods and their success in locating the damage have not been directly compared in a sufficiently objective manner.

Three necessary components for the success of a dynamic test in a structure were detected in literature: Pre-define of the objectives of the test; all test's details must be carefully organized; and finally, the results must be presented in a manful fashion. From the reviewed literature experiences, it can be extracted that redundancy in instrumentation was always helpful and that best instrumentation give the best ratio between accuracy and cost. To summarize, it appears that over the past 15 years there has been repeated application of modal properties of structures to the fields of damage detection and structural monitoring. In the civil engineering field, the work has been motivated basically by several catastrophic bridge or building failures in one hand, and by dramatic reduction of equipment's costs, in the other. Earlier work utilized primarily modal frequency changes to

detect damage, but more recent work has shown that frequency changes are insufficient. Changes in mode shapes are more sensitive indicators and might be more useful for detection of the defect location. Damping changes have not generally been found to be useful for damage detection in bridges. Finally, is worth considering some other methods of computing damage from modal properties that are being developed, such as dynamic flexibility measuring; strain mode shapes changes or neural network-based methods.

In general terms, it was the opinion of the authors of previous literature reviews that sufficient evidence exists to promote the use of measured vibration data for the detection of damage in structures, using both forced response testing and long-term monitoring of ambient signals. It is clear, though, that the literature in general needs to be more focused on the specific applications and industries that would benefit from this technology, such as health monitoring of bridges, offshore oil platforms, airframes, and other structures with long design life. Additionally, research should be focused more on testing of real structures in their operating environment, rather than laboratory tests of representative structures. Because of the magnitude of such projects, more cooperation will be required between academia, industry, and government organizations. If specific techniques can be developed to quantify and extend the life of structures, the investment made in this technology will clearly be worthwhile. Obviously, those conclusions motivated the present doctoral dissertation and serve as starting point of the next chapter: A new proposal for dynamic assessment of concrete elements and masonry walls and piers.

four

Lay-out of applied dynamic assessment

4.1. Introduction

Vibration testing is now a mature and widely used tool in the analysis of structural systems. The actual *state-of-the-art* shows development on dynamic identification of much kind of structures. Actually the tools are already available for dynamic performance testing, but the field of practical applications has not achieved the desired level of simplicity. In this chapter a simple and affordable layout for dynamic assessment of structural building components is proposed.

The basic sequence of system identification applied to civil structures involves tree basic entities [Ljung, 1987]: the acquisition of data, the set of models and the determination of the better model approach, guided by the data. In the present research work, those steps are defined as follows:

The *data acquisition*: consists on excitation of the structure by artificial means (impact hammer) and the record of its *output-only* dynamic response trough attached sensors.

The *set of models*: is a theoretical approach using a FEM simulation, where the system (structure) is fully represented, particularly the full load history and geometric/material non-linearity.

Finally, the *determination of the best model*: is where identification methods are used. The assessment of model accuracy is typically based on how the model performs when it attempts to reproduce the observed data.

Furthermore, the available literature classifies damage identification in the following stages:

- level 1 *detection*: Is the structure damaged or not?

- level 2 *localization*: Where is the damaged area located?

- level 3 *quantification*: What is the extent of damage?

- level 4 *prediction*: What is the remaining service life of the structure?

A typical approach to extend vibration-based methods beyond level 1 is the use of a large number of sensors, allowing the location of damage based on detecting a local mode-shape change. Accuracy on localizing the damage is typically limited to the spatial resolution of the sensor network [Friswell, 1995]. Another approach (level 1) requires fewer sensors, but needs an analytical model of the structure. Parameters of the model that are related to damage are *updated* so that the dynamic characteristics of the model correspond to the measurements. The method proposed for the assessment of structural building components falls into this category.

The proposed layout consists in creating an analytical model and updating it by using static and dynamic testing. The initial finite element model is validated by comparing the numerical eigendata (natural frequencies) with the eigendata acquired from the modal tests. The aim of the experimental layout is to recover the system's modal characteristics from experimental data. The method consists basically on the use of simple technical resources, and procedures of low complexity. Frequency-only measurements are developed with a low number of sensors. The advantages of the method are related with its high repeatability, low cost and easy implementation.

4.2. Basic requirements

Ideally, a robust damage detection scheme will be able to identify that damage has occurred at a very early stage, locate the damage within the sensor resolution being used, provide some estimate of the severity of the damage, and predict the remaining useful life of the structure. The method should also be well-suited to automation. While possible, the method should not rely on the engineering judgment of the user or an analytical model of the structure. A less ambitious, but more attainable, goal would be to develop a simpler method that uses a low number of sensors, reducing dramatically the implementation set-up and therefore reducing the resolution and accuracy. A numerical model of the structure should be used as the baseline for comparisons of measured response. The method should be able to discriminate between the model/data discrepancies caused by modeling errors and the discrepancies that are a result of structural damage.

The proposed technique consists basically in the use of simple measurement hardware. Simultaneously, a numerical model must be developed and updated using the observed dynamic parameters.

The measurement hardware consists basically on four components: the mounting system; impact hammer for excitation; 3 or 4 acceleration transducers to measure the response of the structure; and a signal amplifier and portable computer to modulate and record the signals [see Appendix A for more details].

The requirements of the proposed approach are:

- Cost: Advantageous when compared to other NDT alternatives. Simple equipment and non-specialized personal are required for the implementation of the test.

- Portability: Light and portable equipment is used. Low number of sensors is needed.

- Non- interference: The tests has to keep the structure in normal operation with not of very little interference to the inhabitants and users.

- Repeatability: Multiple measurements permit statistical treatment of the observed data. The development of multiple tests should not represent an important increment of the costs.

- Predictive capacity. The method is strongly supported in a numerical model, and its main objective is the optimization of the model. When the model is updated, it must be able to predict the behavior of the structure under different loading conditions.

- Effectiveness: A clear conclusion about the structural condition of the studied member should be generated.

4.3. Detailed aspects

4.3.1. Generation of impulsive force

There are two methods to artificially excite a structure. Either a shaker is connected to the structure, which provides a force proportional to a specific input voltage, or the structure is hit, usually with a normalized hammer. A third method, which is sometimes useful is to preload the structure with a static force, which is the released to produce a step relaxation in force input to the structure. Typical examples of the latter include releasing weights from bridges and severing tensioned cables connecting towers to the ground. The structure can also be excited by natural means such as traffic, wind, or micro-seismic forces. Different authors have compared and classified the sources of excitation for dynamic testing on bridges. Salawu and Williams [1995] provide a review of full-scale dynamic testing of bridges where methods of excitation are examined. Farrar et al. [1999] summarized the various methods that have been used to excite bridge structures during dynamic testing. Peeters et al. [2000] evaluated the various sources of excitation that have been applied on bridge Z24, in Switzerland.

From the theoretical standpoint, there is not difference between a shaker test and an impact test. If pure forces can be applied, without any interaction between the applied force and the structure, and if mass-less transducers cause not effect on the structure, then we can achieve the theoretical behavior.

From the practical standpoint, shakers and response transducers generally do have an effect on the structure during the modal test. The main item to keep in mind is that the structure under test is not only the structure for which modal data is to be collected, but also everything involved in the acquisition of the data –the structure suspension, the mass of the transducers, the potential stiffness of the shaker arrangement, etc. So while theory demonstrates that there should not be any difference between the impact and the shaker tests, often there will be differences due to the practical aspects of collecting data [Avitabile, 1998]

Basically, the most important difference is due to the shaker mass and stiffness. Impact tests do not suffer of these limitations. Therefore, impact test is selected as the source of excitation for the proposed methodology. Obviously, impact test represent many other advantages versus shaker –economy, simplicity, versatility- are few of them. The advantages of shaker excitation show out when evaluating larger structures, which are not considered on this research work.

Is commonly said that the impact-hammer input spectrum should be flat over the whole frequency range of interest when performing an impact test. It would be better to say that the input spectrum should be "reasonably flat" over all frequencies with "no significant drop off to zero" in the frequency spectrum.

The input spectrum is expected to have sufficient fairly excitation over the frequency range of concern. If the input spectrum were to completely drop to zero, then the structure would not be exited at the frequency, which is desirable.

The cut-off frequency (until where the force level is relatively constant) can be changed by using tips (hammer cover) of different stiffness and hammers of different mass. When choosing tip is important to keep in mind some facts. The

input force spectrum exerted on the structure is a combination of the stiffness of the hammer/tip as well of as the stiffness of the structure. Basically the input power spectrum is controlled by the length of time of the impact pulse. A long pulse in the time domain, results in a short narrow frequency spectrum. A short pulse in the time domain, results in a wide frequency spectrum. The choice of cut-off frequency is critical to the accurate measurement of the modes of interest, as hammer will not excite the structure with any great energy at frequencies above the cut-off frequency. Therefore, the frequency range of interest must be less than this frequency. The cut-off frequency should not be too high, otherwise energy is expended in exciting the structure at higher frequencies which are not of interest, leaving less energy to excite the structure at the frequencies of real interest. [Avitabile, 1998].

4.3.2. Instrumentation

Piezoelectric transducers are used to measure both the force used to excite the structure and its response. Strain in these piezoelectric materials generates an electrical charge that, with the appropriate signal conditioning, may be converted into a voltage in a suitable range. Accelerometers essentially consist of a mass that is connected to the structure via piezoelectric material, which acts as a very soft spring. This mass spring system has its own resonant frequency, which should be well above the frequency range of interest. Acceleration in the structure then produces an inertial force in the piezoelectric material, which at frequencies well below the accelerometer resonance will be proportional to the acceleration. The signal conditioning usually includes facilities to enter the calibration constants for the transducer, so that the output from these conditioners is, for example, one volt per g acceleration. Other type of transducers may be used. Strain gauges may be more suitable for low frequency response where the acceleration will be very small. Non-contact devices such as optical, capacitive or inductive transducers may also be used.

Accelerometers may be mounted to the structure by a variety of methods, for example using glue, magnets, bolts or beeswax. Magnets and beeswax have the advantage of allowing the easy moving of accelerometers. There are two classical methods to obtain the measurements at the locations of interest. With sufficient resources in transducers and analyzer capability, transducers may be placed at every location. This provides simultaneous measurement of the response at every point and provides more consistent data. The proposed method intends to use as low transducers as possible, with the aim of simplifying to the maximum the resources. The transducers must be light and not add significant mass to the structure. The alternative is to have only one accelerometer and to place it an each location in turn. Data measured in this way will not be consistent, because the structure changes between measurements due to the repositioning of the accelerometer.

4.3.3. Data processing

The majority of the analysis of vibration data is performed digitally. Thus the analogue signals from the transducer are converted to digital signals via analogue to digital converters (ADCs). The sampling rate is chosen to be at least twice, and preferably slightly higher, the maximum frequency in the analogue signal. This is called *Shannon's sampling theorem* and allows the analogue signal to be reconstructed from the digital signal. One major problem with sampled data is called *aliasing*. Two sinusoidal signals of different frequencies can produce identical digital signals. Figure 4.1. shows an example of this phenomenon, where the crosses represent the sampled data points. The problem is caused by a sampling rate that is too slow, so that high frequencies appear as low frequencies. The solution is to prevent any frequencies above half the sampling rate appearing in the analogue signal by using a low pass filter with a sharp cut-of, calling anti aliasing filter. Most analysis system incorporate anti-aliasing filters whose cut-off frequency is varied as the sampling rate and frequency range of interest varies. The accuracy of the digital signal depends on the number of binary digits used to represent the analogue signal relative to the maximum allowed by the ADC. In most modern analysis systems, al least 16 bit ADCs are used, which gives a minimum resolution

of 0.3 mV on an ADC with a range of +/- 10 V. Choosing the correct range for the ADC during testing, either manually or automatically, solves the problem of inadequate resolution due to the analogue signal being too small [Avitabile, 1998].
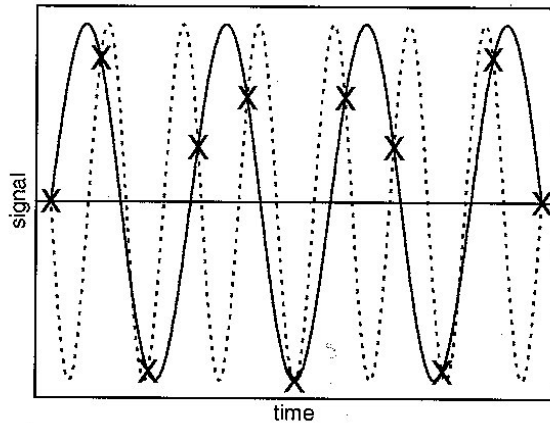
Figure 4.1. Aliasing phenomena

Once the measured data is converted to a digital signal it may be processed by computer hardware. The signal at this stage is in the time domain and represents the force input to the structure, and its response is a function of time, but measured at discrete sampling instants. Although parameter identification is possible using time domain data, and is common in control system analysis, the quantity of measured data and computation required make time domain data impractical for typical structural systems. Also time domain data is very difficult to interpret and most experimental vibration engineers prefer to work in the frequency domain. In the frequency domain, the signal is described by its constituent frequencies. In particular, for periodic signals, which are sampled at discrete time instants, a finite length Fourier series may be used to describe the signal. For a sampled signal $\{x_k\}$, consisting on N samples over a time period of T seconds, this is defined by

$$x_k = x(t_k) = \frac{a_0}{2} + \sum_{k=1}^{N/2} \{a_j \cos\frac{2\pi j t_k}{T} + b_j \sin\frac{2\pi j t_k}{T}\} \qquad [4.1.]$$

where

$$a_0 = \frac{1}{N}\sum_{k=1}^{N} x_k$$

$$a_j = \frac{1}{N}\sum_{k=1}^{N} x_k \cos\frac{2\pi jk}{N}$$

$$b_j = \frac{1}{N}\sum_{k=1}^{N} x_k \sin\frac{2\pi jk}{N}$$

A Fourier series may be caused because the signal is periodic, and the series is of finite length because the signal is sampled. The set of spectral coefficients a_j and b_j are called the discrete Fourier transform of the signal x. In practice, the discrete Fourier transform is efficiently calculated by variations to the method given by Cooley and Turkey [1965], which is generally called the Fast Fourier Transform (FFT) [Avitabile, 1998].
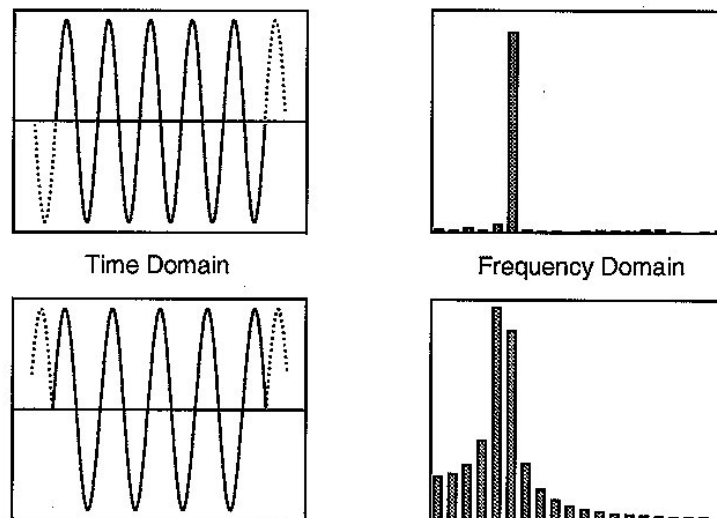
Figure 4.2. Leakage phenomena.

One major problem with the analysis of vibration data is that the signal is assumed to be periodic over the sampling interval chosen. In general this will not be true, and leads to a problem known as *Leakage*. Figure 4.2. illustrates the problem showing a sinusoidal signal with one sampling interval equal to an integer multiple of the signal period, and a second different sampling interval. As the signal is sinusoidal, the Fourier transform should only be non-zero at one frequency. In the second case,

leakage has caused some of the power contained in the frequency of the sinusoidal to "leak" into adjacent frequencies. Leakage is corrected to some extents by multiplying the signal by a window function. This window function is zero at the beginning and end of the sampling interval and so forces the sampled signal to be periodic. A good window function will produce a Fourier transform that is close to that which would be produced if the signal were sampled for an infinite time [Avitabile, 1998].
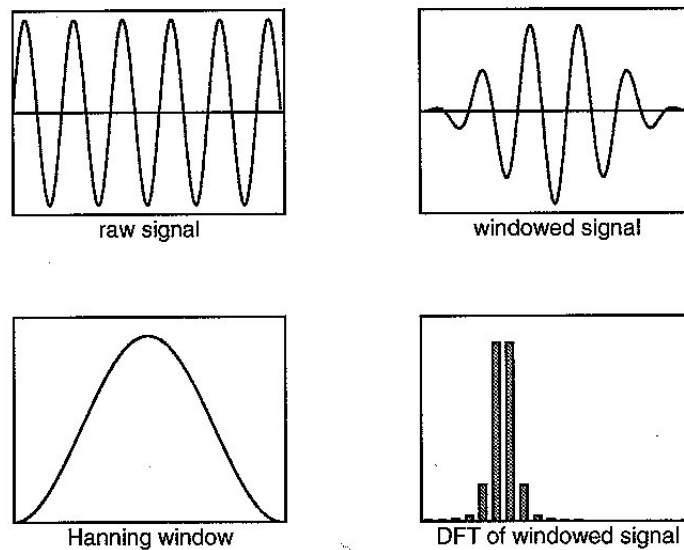
Figure 4.3. Common windowing processes.

Figure 4.3. shows the effect of applying a commonly used window function called the *Hanning Window* to the second example of figure 4.2. The improvement on the Fourier transform is obvious. The Hanning window is not suitable for impact excitation, where an *exponential window* is generally used. Figure 4.4. illustrates the use of the exponential window on the response of a structure excited with a hammer. The window increases the apparent damping in the measured data, so that the measured response is approximately zero at the end of the sampling interval. This artificial increase in damping may be easily removed after the natural frequencies and damping ratios have been computed. Most analysis systems have the ability to apply the common window functions to the measured data.
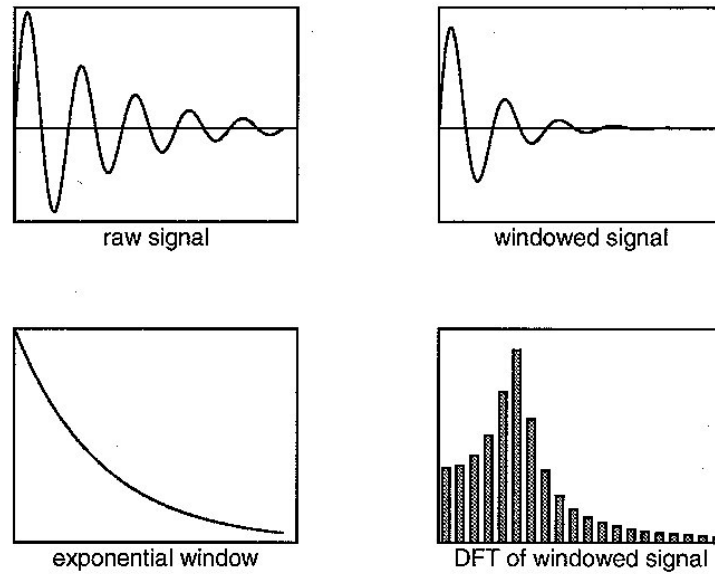
Figure 4.4. Exponential windowing process.

4.3.4. Noise, errors and incomplete data

The data obtained from the structure under test will be used to update the parameters on an analytical model. It is therefore vital to predict and if possible, eliminate the likely errors in the measurements. Errors may be either random or systematic. Any signal corrupted by random noise is, by its nature, unpredictable. Although individual noise values are random, the noise may be described by a statistical distribution. Two important statistical parameters are the mean, which relates to the average value of the noise, and the variance, which indicates the variability of the noise. The most commonly used statistical distribution to represent noise [Avitabile, 1998] is the *Gaussian* distribution. The distribution is totally specified by the mean and variance, given by μ and σ^2 respectively; the probability that a noise signal x is between x_1 and x_2 is given by:

$$P(X_1 \leq X \leq X_2) = \int_{X1}^{X2} p(x)dx$$

where p(x)=$\dfrac{1}{\sqrt{2\pi}\sigma}exp\left(\dfrac{(x-\mu)^2}{2\sigma^2}\right)$is called the probability density function.

Figure 4.5. shows the probability density function for the Gaussian distribution and also shows the mean, μ, and the standard deviation σ. It is evident that the levels close to the mean are more likely to occur. This distribution is far more important than it may appear. As random signals with equal distributions are added together, the Central Limit Theorem [Hogg and Craig, 1978] sates that the summed signal will have a distribution which converges to the Gaussian distribution, irrespective of the form of distribution of the original signal.

Random errors may be reduced by careful experimental technique, choice of excitation method and by averaging the data. Averaging the data reduces the variance of the noise on the averaged data and so reduces the effect of the noise.

Systematic errors are difficult to remove from the data and are a serious problem in this technique. The most typical errors are reviewed in this section, starting with the structure itself. The mounting of the structure should allow accurate modeling of the system. For example, if a section is to be rigidly clamped, then every effort must be made to ensure that the mounting is stiff relative to the structure, in the frequency range of interest. Similarly, if the structure is to be tested free-free, then the mounting springs must be very flexible so that the rigid body modes of the structure are considerably lower than its first flexible modes. Significant errors will arise in the measurement data, compared to an otherwise accurate analytical mode, if, say, the structure is assumed to be clamped, but in reality the connection is relatively flexible. If it is possible to measure the stiffness associated with the mounting system, then this may be incorporated to the model. Significant unknown mounting stiffness should be avoided because they must be identified, with detracts from the identification of the primary unknown parameters in the model.

Attaching transducers to the structure may also introduce significant systematic errors [Avitabile, 1998], as mentioned previously. Mass loading or local stiffness due to the attachment system will change the structure. Accelerometers can also

produce mass loading and local stiffness problems, particularly with scaled or light structures.
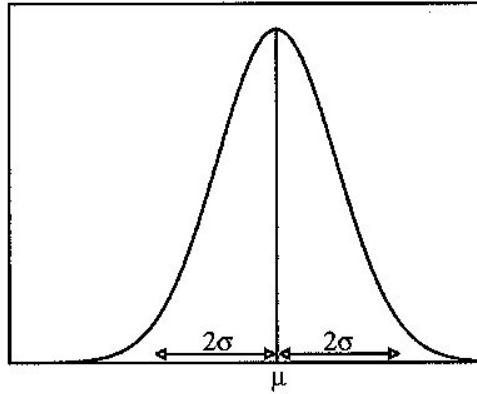
Figure 4.5. Gaussian distribution of noise.

The processing of the data may also produce systematic errors. Leakage has been mentioned in the previous section and leads to an overestimating of the damping. Processing data can convert random noise with zero mean into noise with non-zero mean. The modal extraction methods can produce statistically biased estimates or computational modes, which are not properties of the structure.

All structures encountered in practice are non-linear to some degrees. The effects of non-linearity depend upon many factors, such as the excitation type and level, the boundary conditions and environmental factors. Methods, such as those based on the Hilbert transform or higher order FRFs, exists to detect whether or not a structure is behaving in a non-linear manner. Tomlinson [1994] provided a summary of these methods. Model updating in this thesis is concerned with linear analytical models, although the identification of the parameters of non-linear model is possible.

Errors in measured data can never be eliminated. The estimate of the natural frequencies are usually very good, whereas mode shape and damping estimates usually contain relatively high levels of noise. The object is to reduce the effect of these errors by good experimental technique. This is another reason to develop

frequency-only measurements: a more simple but more reliable information from the analyzed structure.

The data obtained from vibration testing can contain not only error but also be incomplete in two different ways: not all the modes will be measured, and the FRFs will be measured at a subset of the analytical degrees of freedom.

In theory it should be possible to measure as many mode shapes as we require. In practice, this is not possible because the limitations on the frequency range of available transducers and data acquisition hardware. Also, as the frequency increases so does the modal density, causing considerable difficulty for the modal extraction algorithms. Even if these difficulties could be overcome it would still be impossible to accurately measure all the modes of a structure. A finite element model can only accurately predict the lower third or so of the natural frequencies and mode shapes. Therefore the structure could not be expected to reproduce all the modes predicted by the model.

Finite element models can be very large, extending in some cases to several thousand degrees of freedom. Experimental modal analysis rarely uses more than a couple of hundred transducers. Consequently not all degrees of freedom in the analytical model will be measured. There are often internal nodes, which cannot be measured. Rotational degrees of freedom are very difficult to measure with accuracy. There are ways of overcoming this difficulty, for example reducing the analytical model order.

4.3.5. Numerical simulation

4.3.5.1. Concrete members

The concrete structures behavior is typically provided by means of rebars, which are one-dimensional strain theory elements (rods) that can be defined singly or embedded in oriented surfaces. Rebars are typically used with metal plasticity models to describe the behavior of the rebar material and are superposed on a mesh of standard element types used to model the concrete.

With this modeling approach, the concrete behavior is considered independently of the rebar. Effects associated with the rebar/concrete interface, such as bond slip and dowel action, are modeled approximately by introducing some "tension stiffening" into the concrete modeling to simulate load transfer across cracks through the rebar. Details regarding tension stiffening are provided below.

The post failure behavior for direct straining across cracks is modeled with a *tension stiffening* model, which allows to define the strain softening behavior for cracked concrete. This model also allows for the effects of the reinforcement interaction with concrete to be simulated in a simple manner. The *tension stiffening* model is required in the concrete model, used to specify tension stiffening by means of a post-failure stress−strain relation or by applying a fracture energy-cracking criterion.

Specification of strain softening behavior in reinforced concrete generally means specifying the post failure stress as a function of strain across the crack. In cases with little or no reinforcement this specification often introduces mesh sensitivity in the analysis results in the sense that the finite element predictions do not converge to a unique solution [Hibbit et. al, 1995], as the mesh is refined because mesh refinement leads to narrower crack bands. This problem typically occurs if only a few discrete cracks form in the structure, and mesh refinement does not result in formation of additional cracks. If cracks are evenly distributed (either due to the effect of rebar or due to the presence of stabilizing elastic material, as in the case of plate bending), mesh sensitivity is less of a concern.
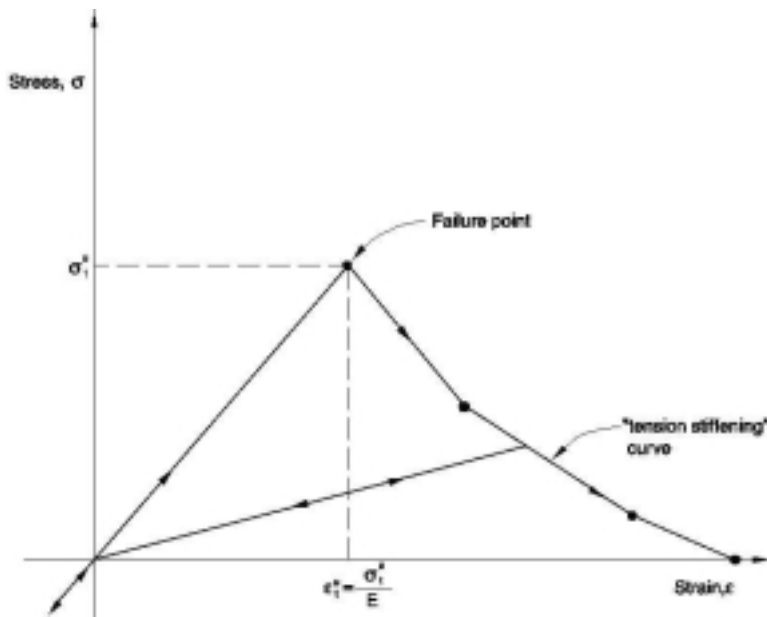
Figure 4.6. "Tension stiffening" model.

In practical calculations for reinforced concrete, the mesh is usually such that each element contains rebars. The interaction between the rebars and the concrete tends to reduce the mesh sensitivity, provided that a reasonable amount of tension stiffening is introduced in the concrete model to simulate this interaction [Figure 4.6.]. The tension stiffening effect must be estimated; it depends on such factors as the density of reinforcement, the quality of the bond between the rebar and the concrete, the relative size of the concrete aggregate compared to the rebar diameter, and the mesh. A reasonable starting point for relatively heavily reinforced concrete modeled with a fairly detailed mesh is to assume that the strain softening after failure reduces the stress linearly to zero at a total strain of about 10 times the strain at failure [Van Greunen, 1979; Kang, 1977; Berzegar-Jimshidi, 1980]. The strain at failure in standard concretes is typically 0,0001, which suggests that tension stiffening that reduces the stress to zero at a total strain of about 0,001 is reasonable. This parameter should be calibrated to a particular case.

The choice of tension stiffening parameters is important since, generally, more tension stiffening makes it easier to obtain numerical solutions. Too little tension stiffening will cause the local cracking failure in the concrete to introduce

temporarily unstable behavior in the overall response of the model. Few practical designs exhibit such behavior, so that the presence of this type of response in the analysis model usually indicates that the tension stiffening is unreasonably low.

When the principal stress components are dominantly compressive, the response of the concrete is modeled by an elastic-plastic theory using a simple form of yield surface written in terms of the equivalent pressure stress, and the Mises equivalent deviatoric stress. Associated flow and isotropic hardening are used. This model significantly simplifies the actual behavior. The associated flow assumption generally over-predicts the inelastic volume strain. The yield surface cannot be matched accurately to data in triaxial tension and triaxial compression tests because of the omission of third stress invariant dependence. When the concrete is strained beyond the ultimate stress point, the assumption that the elastic response is not affected by the inelastic deformation is not realistic. In addition, when concrete is subjected to very high-pressure stress, it exhibits inelastic response: no attempt has been made to build this behavior into the model.

The simplifications associated with compressive behavior are introduced for the sake of computational efficiency. In particular, while the assumption of associated flow is not justified by experimental data, it can provide results that are acceptably close to measurements, provided that the range of pressure stress in the problem is not large. From a computational viewpoint, the associated flow assumption leads to enough symmetry in the Jacobian matrix of the integrated constitutive model (the "material stiffness matrix") such that the overall equilibrium equation solution usually does not require unsymmetric equation solution. All of these limitations could be removed at some sacrifice in computational cost.

The option used to define the stress-strain behavior of plain concrete in uniaxial compression outside the elastic ranges is included in Abaqus. Compressive stress data are provided as a tabular function of plastic strain and, if desired, temperature and field variables. Positive (absolute) values should be given for the compressive

stress and strain. The stress-strain curve can be defined beyond the ultimate stress, into the strain-softening regime [Figure 4.7].
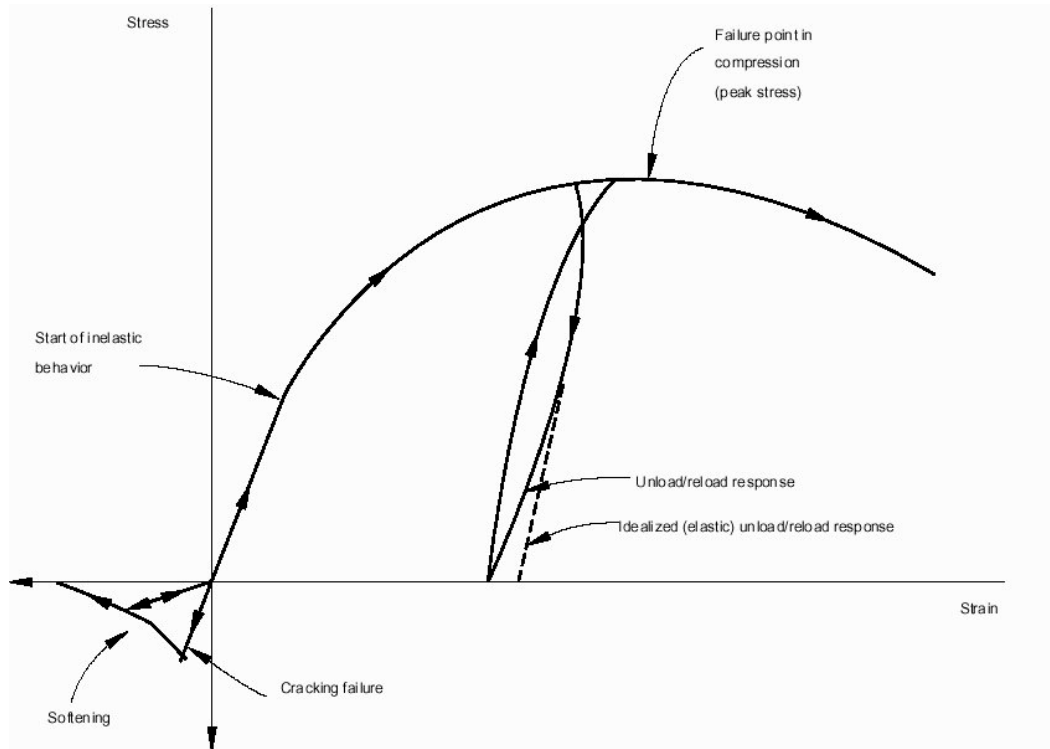
Figure 4.7. Uniaxial concrete model.

When concrete is loaded in compression, it initially exhibits elastic response. As the stress is increased, some non-recoverable (inelastic) straining occurs and the response of the material softens. An ultimate stress is reached, after which the material loses strength until it can no longer carry any stress. If the load is removed at some point after inelastic straining has occurred, the unloading response is softer than the initial elastic response: the elasticity has been damaged. This effect is ignored in the model, since we assume that the applications involve primarily monotonic straining, with only occasional, minor unloadings. When a uniaxial concrete specimen is loaded in tension, it responds elastically until, at a stress that is typically 7%-10% of the ultimate compressive stress, cracks form. Cracks form so quickly that, even in the stiffest testing machines available, it is very difficult to observe the actual behavior. The model assumes that cracking causes damage, in the

sense that open cracks can be represented by a loss of elastic stiffness. It is also assumed that there is no permanent strain associated with cracking. This will allow cracks to close completely if the stress across them becomes compressive.
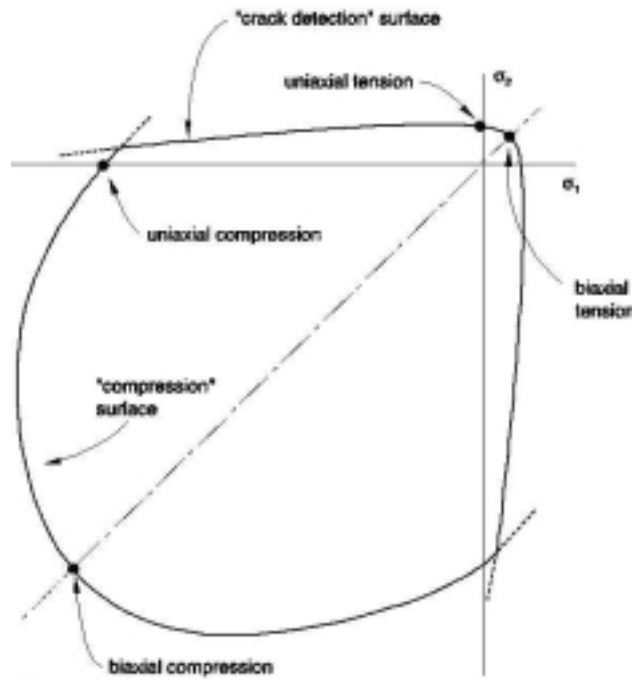
Figure 4.8. Multiaxial concrete model.

In multiaxial stress states these observations are generalized through the concept of surfaces of failure and flow in stress space. These surfaces are fitted to experimental data. The surfaces used are shown in Figure 4.8.

The numerical modeling technique adopted for the present work is based on the following assumptions on the behavior of flexural reinforced concrete members:

(1) The hypothesis of plane sections of beam bending and the resulting linear distribution of strain within the depth of the beam section is adopted;

(2) Perfect bond between reinforcement and concrete is assumed. Reinforcement slippage occurring at advanced stress-strain states is included into the stress-strain diagram of tensile concrete;

(3) The constitutive model is based on the smeared crack approach, i.e., stresses and strains are averaged over representative lengths to span several cracks; and

(4) All fibers in the tensile concrete zone follow the same stress-strain law. This is also applied to the fibers of the compressive zone.

The last assumption is less accurate for tensile concrete. As Gilbert and Warner [1978] showed, for the given constant strain in the cracked concrete, fibers close to the reinforcement carry larger average stresses than fibers more distant from that reinforcement.

4.3.5.2. Masonry members

A hardening process is defined as an increase of strain modulus after certain levels of axial loading. Load-induced hardening has been observed in masonry elements subjected to moderate axial loading [Oliveira, 2003]. A variation of the natural frequencies of masonry members subjected to axial loading can appear due to two facts: modification of the boundary conditions or a load-induced hardening process. Figure 4.9. represents an hypothetical constitutive equation of a material with a strong hardening process.

As mentioned in previous sections, the dynamic behavior of the structure is highly-dependent on the deformation modulus and if that modulus is changing under different load scenarios, the dynamic properties of the structure can also be dependent on the load level.
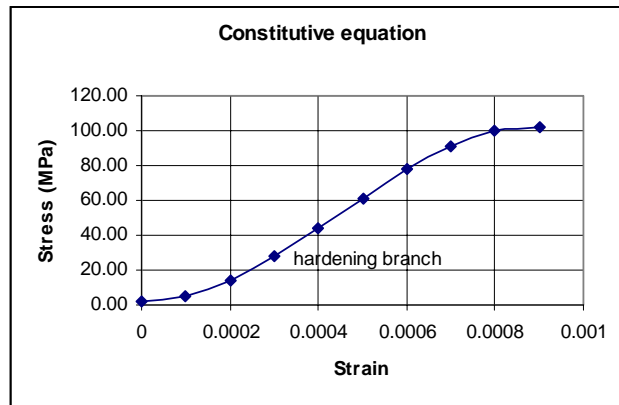
Figure 4.9. Constitutive equation of an hypothetical material with a high hardening ratio

Therefore, if the load scenario is unknown, dynamic identification can also be a valuable tool to define load-levels. If an element made of the hypothetical material described above is loaded until failure, the natural frequencies will suffer modifications trough the loading process The variation of the first natural frequency is dependent of the load, and for a same frequency two different load-values can be determined [Figure 4.10].
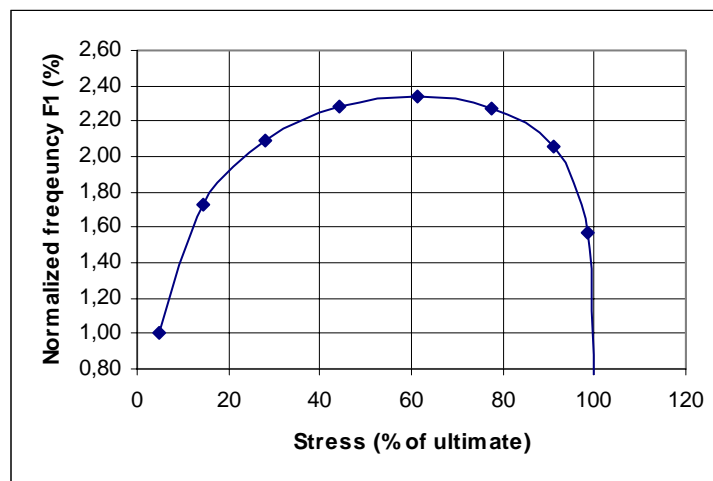
Figure 4.10. Variation of first natural frequency versus applied stress in a hardening-type material.

4.3.6. Model updating

Finite-element model updating has become a viable approach to increase the cor-relation between the dynamic response of a structure and the predictions from a model. In model updating, parameters of the model are adjusted to reduce a penalty function based on residuals between a measurement set and the corresponding model predictions. Typical measurements include the modal model (natural frequencies and mode shapes) and the frequency response functions. The choice of penalty function, and also the optimization approach, has been the subject of much research and is well covered in literature [Mottershead and Friswell 1993, 1995, 1998].

The updating procedure of numerical Finite Element models of civil engineering structures using experimental modal parameters (eigenfrequencies, modeshapes) can be regarded as an optimization problem. The objective function consists of the (weighted) sum of the differences between the numerically calculated and the corresponding experimentally measured modal parameters of the structure. The uncertain structural and physical variables of the model (connections, boundary conditions, material properties...) are changed locally until the differences, and thus the objective function, are minimized. In this way a physically more correct model is obtained on which further analysis can be made.

A critical phase in the updating procedure is the selection of the appropriate updating parameters (uncertain variables of the model), the relevant measurement data (modal parameters) and their relative weight. A finite element model, which will be updated, requires in its preparation the consideration of factors not normally taken into account in regular model construction. Of these, the choice of updating parameters is the most important. The analyst should attempt to assess the confidence, which can be attributed to various features of the model. For example, the main span of a beam, away from the boundaries, might be considered to be model with a high level of confidence. Joints and constraints could be considered to be less accurately modeled, and therefore in greater need of updating. The parameterization of the inaccurate parts of the model is important.

A typical technique to solve the optimization problem is the gradient-based. The modal parameters are expressed as linear functions of the updating parameters using the modal sensitivities. Expressing the differences between the analytical and the experimental modal parameters -eigenfrequencies and/or modeshapes- results in a system of linear equations in terms of the updating parameters. The system can be completed with additional orthogonality conditions. Since the number of equations exceeds the number of updating parameters, the system is over-determined and no exact solution exists. The Least Squares-solution minimizes the norm of the residual vector. An iterative solution process is required because in reality the modal parameters are non-linear with respect to the updating parameters.

However, another and better approach to solve the optimization problem is the use of global optimizers (genetic algorithms, evolutionary strategies,…) instead of local optimizers (hill-climbing strategies). Global optimizers are more suitable to solve updating problems because they are more robust, they do not get trapped in local minima and they are less sensitive to the initial values of the updating parameters. Furthermore, no modal sensitivities have to be calculated. But a disadvantage of the global optimisers is the need of many function evaluations.

Both of the previously described techniques are very robust and require a high deployment of resources. Obviously, the robustness of these techniques converts them into a more complete and reliable methods, but also set important limitations for its practical implementation.

The proposed approach to optimize the model is the use of frequency-only data. A vector of natural frequencies is extracted from the FFT of every measurement, and treated numerically to reduce noise and errors. A final and unique vector of natural frequencies is obtained, representing the whole structure. This vector is used as the objective function and does not suffer any modification during the parameter identification process.

4.3.7. Comparing numerical and test data

An important requirement in design is to be able to compare experimental results from prototype structures with predicted results from a corresponding finite element model. In finite element model updating the experimental and analytical databases should be compared to assess the improvement in the modeled response. In this comparison, major problems arise because of the large number of degrees of freedom in the analytical model; the limited number of transducers used to measure the response of the structure; and modeling inaccuracies, in particular the omission of damping in the numerical model.

However, the proposed methodology has achieved very reasonable levels of accuracy (as described in cases study, furthermore). And the simplicity of the technique makes it affordable for practical applications.

The definition of a finite element model is fundamental. The model must be simple and with a reasonable number of DOF. Refining of the mesh, and consequently increment of nodes, does not increase the accuracy of the model. It is important to consider that only few of the lower frequencies can be identified under normal circumstances. The model must include some damage model (tension stiffening in the case of reinforced concrete, for example) and logically must include also the eigenproblem solution (dynamic properties evaluation).

At this level, it is possible to evaluate the firs few natural frequencies in the model, which are dependent of the level of damage and some other unknown parameters. In the model updating, parameters of the model are adjusted to reduce a penalty function based on the residuals between a measurement set and the corresponding model predictions.

4.4. Concluding Remarks

The intention of this work is to contribute to the sate-of-the-art with the development of a damage identification technique. This technique must include two

different processes. First, the observation of the structure, known as system identification (observation of phenomena) and secondly the model updating (hypotheses). To reach this objective it is necessary to follow a methodology, applying scientific method into a series of observations and then establishing certain hypotheses. This process is described by the following stages:

- A first stage consists on the optimization of data acquisition network. Multiple possibilities on the location and kind of sensors, types of acquired signals, resolution of the sign, number of sensors or duration of the test are considered.

- After acquiring dynamic signals, a post-processing is needed. This process consists on the identification of modal parameters from the time domain response. Experience has shown that Fast Fourier Transformation (FFT) is an effective procedure. This process translates the dynamic-signal from the time to the frequency domain. Once frequency domain is reached, a typical method for identifying dynamic parameters is the *pick picking* technique. This technique presents some disadvantages in complex systems that are discussed further on. The occurrence of dynamic contamination (like traffic, heavy machinery, etc.) has also to be treated in this signal post-processing. Therefore, it is necessary to implement a process of System identification (SI) like subspace identification method (SIM) to recognize objectively the natural parameters of the structure and to discard the noise. This SI process must then extract, clearly and with no doubt, modal parameters from the observed structure.

- After obtaining reliable dynamic information from the structure, a process of model updating is needed. It was decided to use a non-linear finite element platform [Hibbit, 1995] for this mean. The model must consider the different load stages suffered by the structure. It is important to simulate every stage of the structure's life that affects dynamic parameters. The goal of this

process is to simulate a non-linear evolution of natural frequencies, supported on a finite element model.

- When the real behavior of the structure and the prediction of the model reach certain approach, it is necessary to optimize this correlation. This is the process of parameter identification. Here, the finite element analysis is used as a subroutine of a more global technique. This technique performs multiple solutions of the model carrying out small variations in the parameters. Those parameters can be constitutive equations, damage degree, contour conditions or even maximum load-level ever reached. Parameter identification is defined as the statistical process where the variables of the model are combined to the best fit.

Modern computers, which are capable of processing large matrix problems at high speed, have enabled the construction of large and sophisticated numerical models, and the rapid processing of digitalized data obtained from analogue measurements. The most widespread approach for numerical modeling in engineering design is the finite element method. It would be superficial to imagine that updating is straightforward or easy: it is beset with problems of imprecision and incompleteness in the measurements and inaccuracy in the finite element model.

The extent to which a numerical model can be improved by updating depends upon the richness of information on the test structure contained in measurements. In general, the measurements will be both imprecise and incomplete. The imprecision takes the form of random and systematic noise. Electronic noise from instruments can be largely eliminated by the use of high quality transducers, amplifiers and analogue to digital conversion hardware. Signal processing errors, such as aliasing and leakage, may be reduced by the correct choice of filters and excitation signals. Systematic errors can occur when, for example, the suspension system fails to replicate free-free conditions, or when the mass of a roving accelerometer causes changes in measured natural frequencies. Rigidly clamped boundary conditions are usually very difficult to obtain in a physical test. Extreme care is necessary to either

eliminate systematic errors, or to obtain an assessment of them, which can be used in subsequent processing.

The proposed method is aimed to explode the best capabilities of available technology on dynamic identification. However, the applied resources are drastically minimized. It is considered that simple equipment is more likely to be used it real cases than other complex alternatives. A sacrifice on quantity and quality of acquired data is definitely done, but a big save on implementation and technicians time is also achieved. To find the equilibrium between those two different factors is one of the objectives of this doctoral dissertation.

five

Parametrical Sensitivity Studies

5.1. Introduction

As mentioned in the previous chapter, model updating is used to adjust numerical Finite Element Models (FEM) to modal test results. Model updating can also be described as a parameter identification technique.

The procedure of updating numerical FEM using experimental modal parameters (natural frequencies) can also be regarded also as an optimization problem, since the objective of the process is to minimize the (weighted) sum of the differences between the numerically calculated and the corresponding experimentally measured modal parameters of the structure. The uncertain structural and physical variables of the model (connections, boundary conditions, material properties,...) are changed locally until the differences, and thus the objective function, are minimized. In this way a physically more correct model is obtained in which further analysis and simulation can be done.

A critical phase in the updating procedure is the selection of the appropriate updating parameters (uncertain variables of the model), the relevant measurement data (modal parameters) and their relative weight. In this chapter, a parametrical study is developed to understand the influences of different parameters on the dynamic behavior of the FEM. Three different models are evaluated under different parametric variation. First, a beam-type non-linear finite element model is created in a commercial FEM platform [Hibbit, 1995], secondly a bi-dimensional plate-type with combination of shell and linear elements is developed under the same platform

and finally a masonry column is also modeled as a linear structure under a different platform (SAP2000).

Studied parameters include: Mass, reinforcement ratio, corrosion of rebars, support conditions, strain modulus, stiffness modification due to cracking, hardening properties and *tension stiffening* parameters.

When possible, the use of dimensions is avoided. A *normalized frequency* is used in most of the cases and is defined as the calculated frequency up to a reference constant value. The reference constant value has in all the cases an abscise value of 100%. For example, in figure 5.5. a 100% of the normalized frequency has a correspondence with a 100% of the self-weight. A 50% of the self-weight corresponds to a normalized frequency of 130% or an increment of 30% from the reference value.

The intention of avoiding the use of dimension is to give to all the graphs a more general perspective. By this way the plots can be used not only for the evaluated particular case but also for other purposes.

5.2.   Method

The applied method consists of defining a Finite Element Model, which must include dynamic properties evaluation (eigenvalue solution). The first approach of the model is fixed and then all parameters are changed gradually and independently. The aim of this parameter variation is to identify the influence of the studied parameter on the natural frequencies of the model. Several hundreds of numerical models have been evaluated (one for each case), for this purpose results are presented graphically and in some important cases also in a table.

5.3.   Concrete beams

The model used is known in *ABAQUS* as *spatial linear* with stiffness associated with deformation of the beam's "axis". These deformations consist of axial deformation, curvature change (bending); and, in space, torsion. The model offers additional flexibility associated with transverse shear deformation between the beam's axis and its cross-section directions. The model assumes that the transverse

shear behavior of Timoshenko beams is linear elastic with a fixed modulus and, thus, independent of the response of the beam section to axial stretch and bending. The beam can be subjected to large axial strains. The axial strains due to torsion are assumed to be small. In combined axial−torsion loading, torsional shear strains are calculated accurately only when the axial strain is not large. The beam elements use a lumped mass formulation.

The main advantage of beam elements is that they are geometrically simple and have few degrees of freedom. This simplicity is achieved by assuming that the member's deformation can be estimated entirely from variables that are functions of position along the beam axis only.

The fundamental assumption used is that the beam section (the intersection of the beam with a plane that is perpendicular to the beam axis) cannot deform in its own plane (except for a constant change in cross-sectional area, which may be introduced in geometrically nonlinear analysis and causes a strain that is the same in all directions in the plane of the section).

Rotary inertia effects are usually insignificant for slender beam structures. For thicker beams the rotary inertia plays a role in dynamic analysis, but to a lesser extent than shear deformation effects.
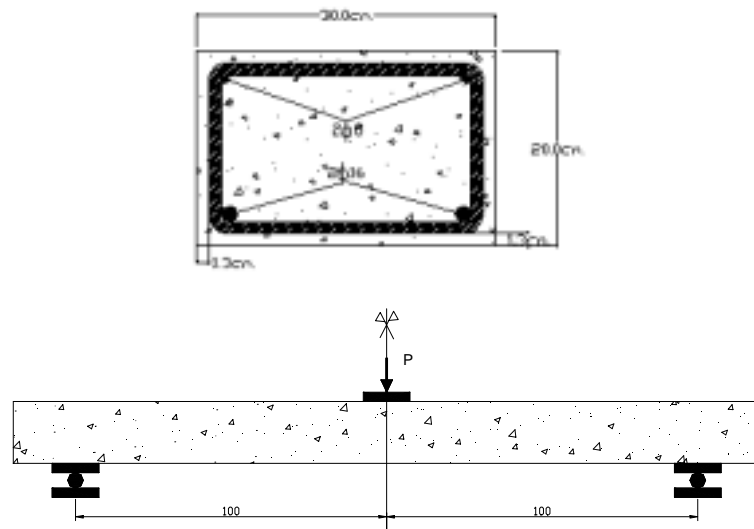
Figure 5.4. Scheme of the modeled beam.

The modeled beam was 2,40 m long of rectangular cross section (300 × 200 mm). To avoid any coupling effect between horizontal and vertical bending modes, the width (300 mm) was chosen to be different from the height (200 mm). The beam had 4 reinforcement bars, two of 16 mm diameter in the low layer and two of 8 mm in the high layer, corresponding to a reinforcement ratio of about 0.83 % [Figure 5.4]. Shear reinforcement consists of vertical stirrups of diameter 12 mm, every 150 mm. This beam was not only modeled but also constructed and tested, this chapter regards only with modeling, but the experimental campaign is presented in section 6.1 of the next chapter.

5.3.1. Mass influence

In section 3.3.2. the *vibration frequency* ω was defined as a dynamic characteristic of the system dependent of stiffness (k) and mass (m).

Other properties of the system are natural period $T = \dfrac{2 \cdot \pi}{\omega}$ and cyclic frequency $f = \dfrac{1}{T} = \dfrac{\omega}{2 \cdot \pi}$. The relation between mass and cyclic frequency is dependent of the mass, and can be observed on those equations.

In this example, the stiffness of the beam was kept, but a different density of the material is used to obtain different masses. In other words, the gravity is modified from a factor of four to 0.25 [table B.1. appendix B]. The model shows a strong influence of the mass in natural frequencies as expected. [Figure 5.5.]
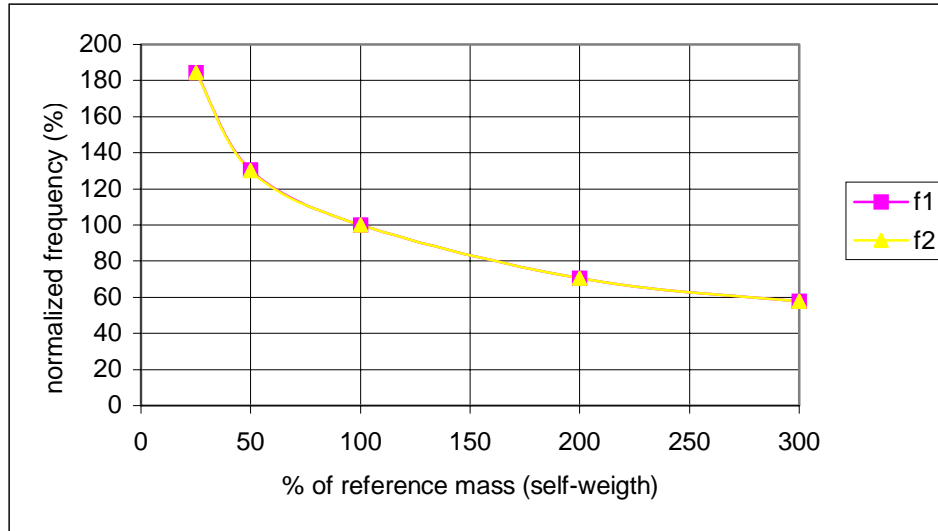
Figure 5.5. Influence of mass on first two natural frequencies.

5.3.2. Reinforcement ratio

There is an important influence of the reinforcement steel bars on the dynamic behavior of the modeled beam. On one hand, the reinforcement area is modified and thus a direct increment on the stiffness of the reinforced section is observed. Secondly, and more evident is the influence of the tensile reinforcement area after load processes. In this section, both phenomena are numerically simulated on the beam described in 5.3.

For the present study, effects associated with the rebar/concrete interface, such as bond slip and dowel action, are modeled approximately by introducing some *tension stiffening* into the concrete model to simulate load transfer across cracks through the rebar [as described in section 5.2. of this chapter]. For a higher tensile reinforcement area, the stiffness after cracking remains higher. For this study, the reinforcement area varied from 2 6-mm bars to 2 24-mm bars [Table B.2. appendix B]. Four different load scenarios were simulated: Unloaded, 20 kN mid-span load, 40 kN mid-span load and 60 kN mid-span load.

An important variation of the first two natural frequencies was observed on different damage scenarios [figures 5.6. and 5.7.]. The first two lines (unloaded and 20 kN load) are less sensitive to the reinforcement, the other two cases (40 and 60

kN load) are much more sensitive to the reinforcement. Non-plotted points did not converge in the simulation and therefore represent failure of the beam. Elasticity modulus for concrete was 28,8 GPa and for steel was 200 GPa
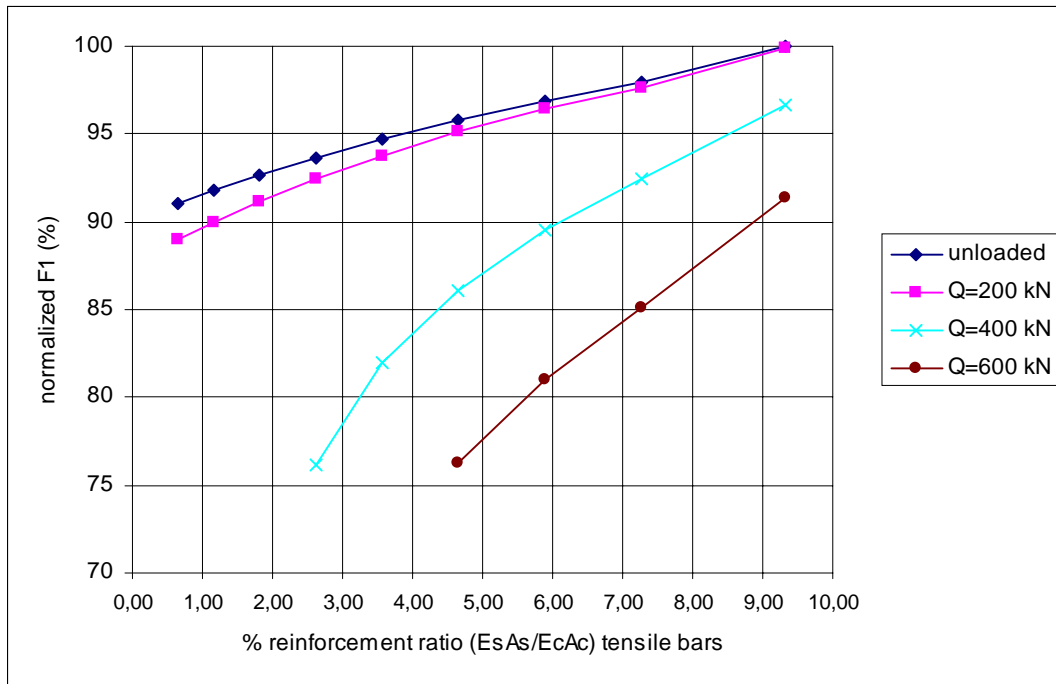
Figure 5.6. Variation of first natural frequency due to tensile reinforcement level
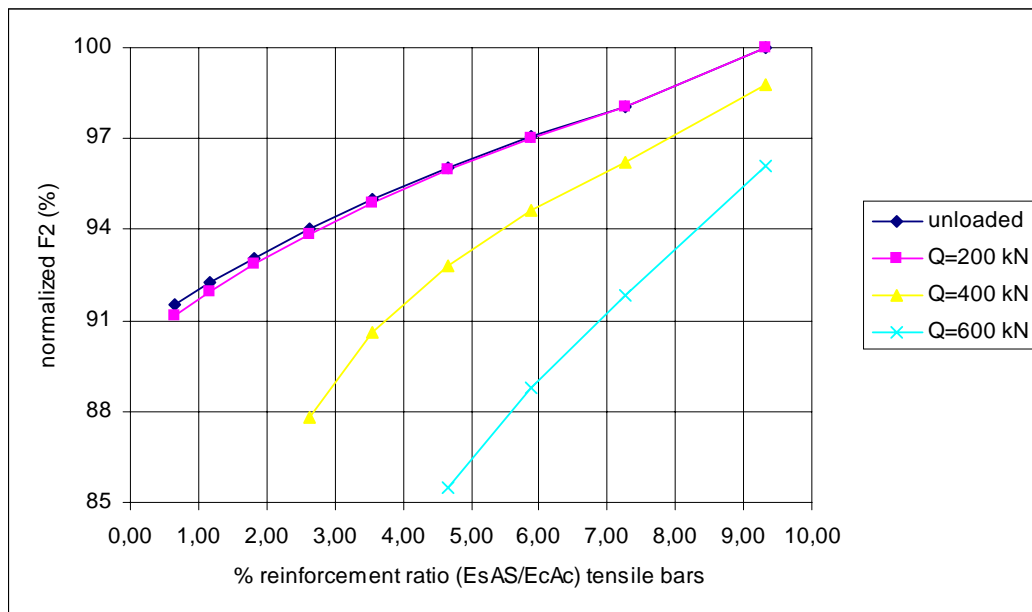
Figure 5.7. Variation of second natural frequency due to tensile reinforcement level

Figure 5.8. represents the evolution of the first natural frequency versus loading, for four different reinforcement levels.
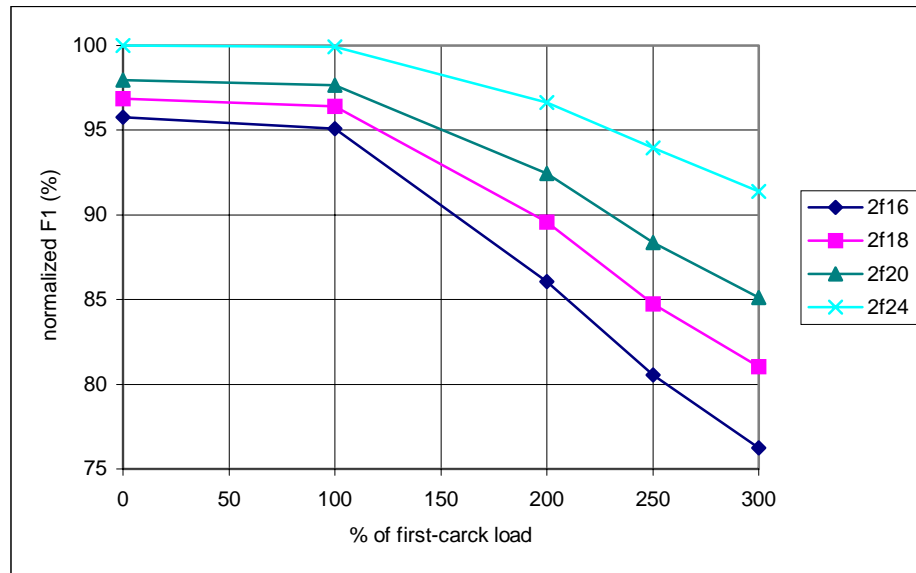
Figure 5.8. Variation of first natural frequency due to loading process

The same simulation was developed for compressive steel reinforcement under different load scenarios [table B.3. appendix B]. Compressive steel reinforcement did not show any modification on the dynamic behavior of the beam. Natural frequencies showed a slightly increment only due to the inertia modification. Under load processes, the influence of compressive steel is almost null (the slope of the different lines is similar). This phenomenon is described for first natural frequency in figure 5.9. and for second natural frequency in figure 5.10. If a successive incremental load process is applied to the beam, the dynamic behavior remains flat until the appearance of the first crack ant falls linearly until complete failure. The addition of compressive rebars does not represent a substantial improvement of the stiffness or ultimate load [figure 5.11.].
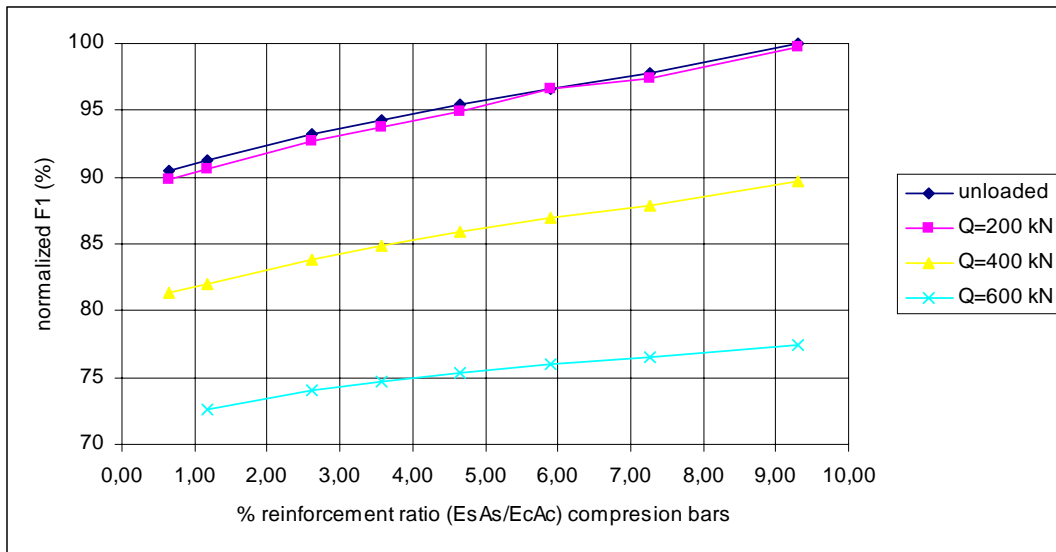
Figure 5.9. Variation of first natural frequency due to compressive reinforcement level
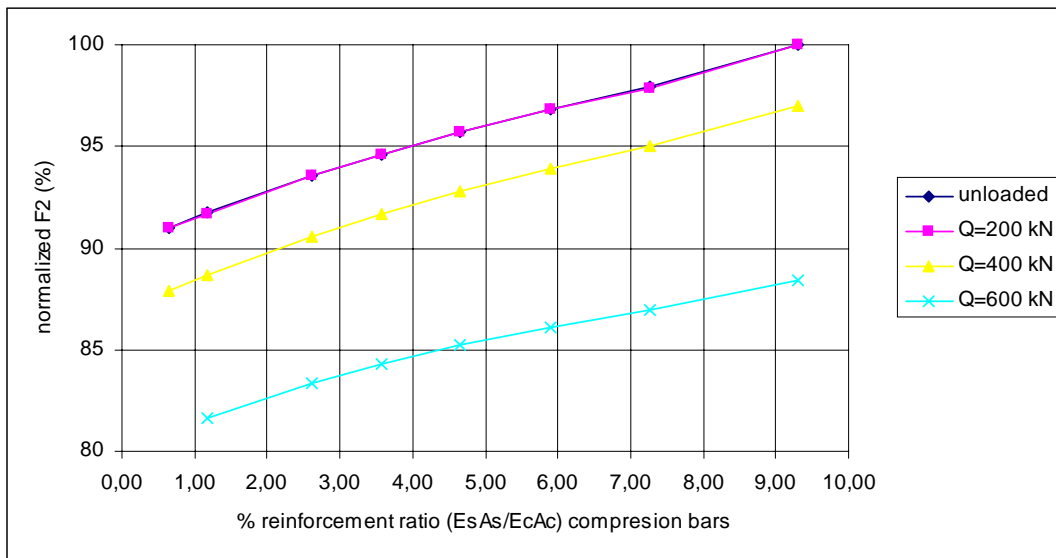
Figure 5.10. Variation of second natural frequency due to compressive reinforcement level
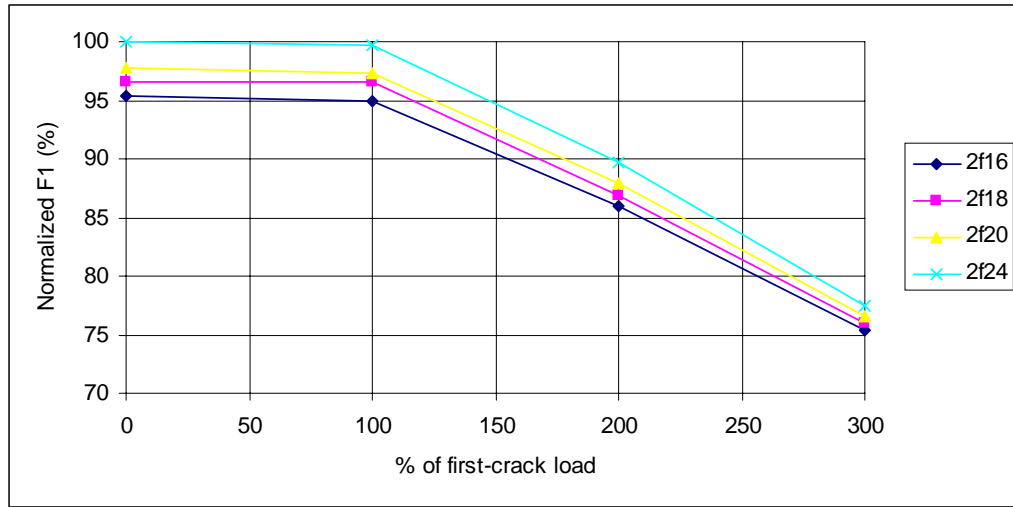
Figure 5.11. Variation of first natural frequency due to loading process

5.3.3. Support conditions

It is possible to evaluate natural frequencies with the equation: $\omega_n = \left(\dfrac{\varphi_n}{l}\right)^2 \cdot \sqrt{\dfrac{E \cdot I}{\mu}}$,

were φ_n is a function of support conditions and the number of natural frequency.

The ratio between first and second natural frequency, obtained as $\dfrac{f_2}{f_1} = \left(\dfrac{\varphi_2}{\varphi_1}\right)^2$,

depends only of support conditions and not of mechanical properties of the beam. In a free-free supported beam, the second natural frequency is four times the first ($f_2 / f_1 = 4$); when the beam is double-clamped, this ratio decreases to: $f_2 / f_1 = 2.75$.

If first and second natural frequencies are known, it is possible to determinate the support conditions of the beam.

 On this case, the support condition of the beam was changed from a free-free to a double clamped condition. Natural frequencies showed an important modification, and the proportion between the second and the first natural frequencies also observed important changes [table B.4. appendix B].
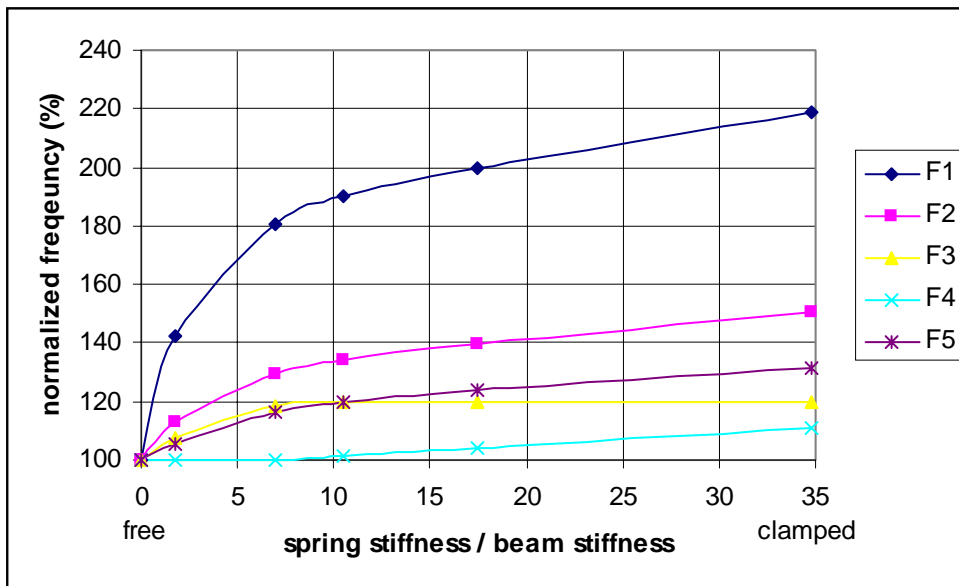
Figure 5.12. Influence of clamping on natural frequencies.

Figure 5.12. shows the variation of the first five natural frequencies when the support conditions are modified. The values of the frequencies are normalized dividing by the free-free condition reference-value. The support condition is defined as the coefficient p = spring stiffness/beam stiffness. The beam stiffness is a constant value defined as EI/L. The variation is more important for the first and second frequencies. In this case the 4_{th} frequency showed almost not sensitive to boundary conditions.

The proportion between the second and the firs natural frequencies is very helpful when support conditions are unknown. If the first two natural frequencies can be identified, the proportion between them can be a clear indicator of support conditions. The value fluctuates from 2, 55 –free condition- to 3,75 –clamped condition- [figure 5.13.].

A slightly difference on the evolution of the first natural frequency under different support conditions was observed between damaged and undamaged beams. The damage was generated applying a 550 kN concentrated load at midspan of the beam. This load represents approximately 85% of the ultimate load. This difference is more important under free-free support conditions [figure 5.14.].
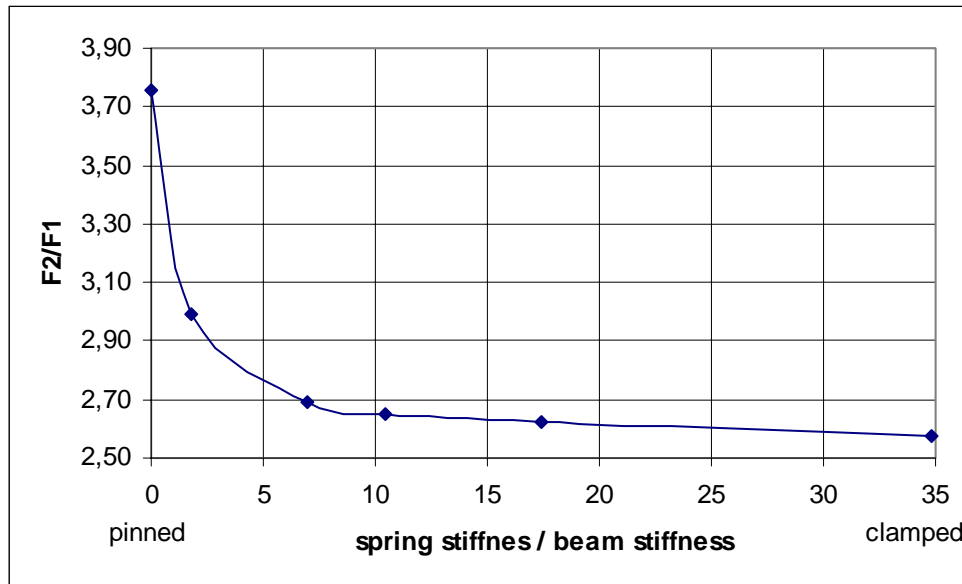
Figure 5.13. First and second frequency ratio under different clamping levels
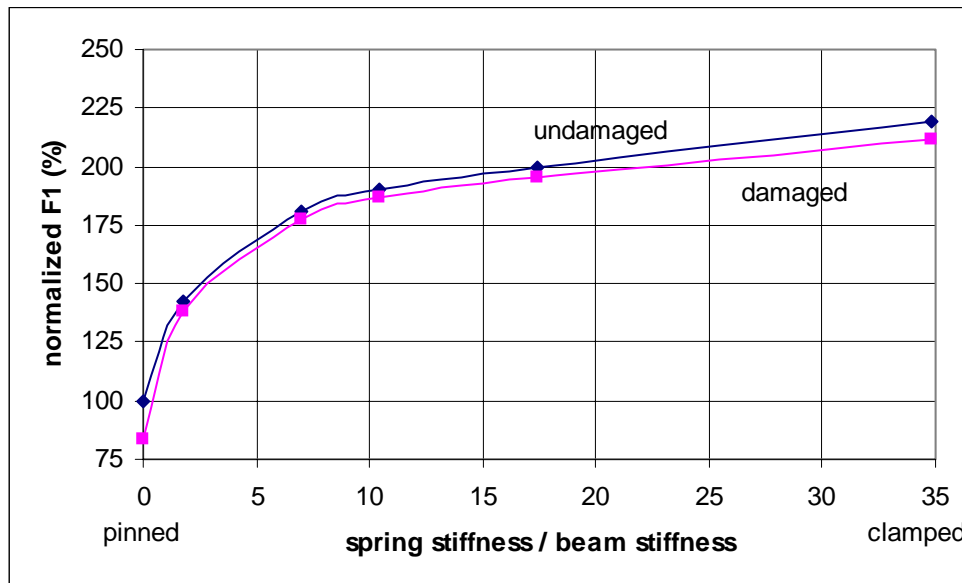
Figure 5.14. Behavior of first natural frequency under different support conditions

5.3.4. Strain modulus

It exists a direct relationship between the modulus and the stiffness of the structure and thus, its dynamic behavior. In this example, the strain modulus of the beam is gradually modified and the dynamic parameters of the beam are calculated for every

value. The resultant frequencies resulted influenced for the different values for the strain modulus under different load scenarios [table B.5. appendix B].
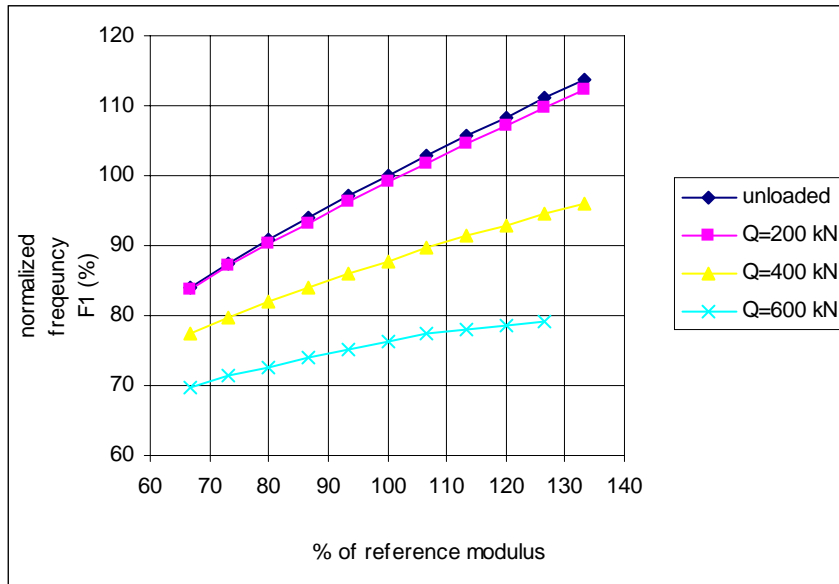
Figure 5.15. First natural frequency vs. strain modulus

The variation on the first natural frequency of the beam when strain modulus is modified can be observed in figure 5.15. The system was analyzed for different values of elasticity modulus (x axis) and for different load-cracking stages. The load and cracking process is generated in all the cases by means of applying a concentrated load at the mid-span of the beam. Q defines the magnitude of the load.

The variation of both first and second natural frequencies due to modifications on stain modulus is strictly linear. Other important phenomenon is that the slope of the lines decreases for a mayor damage [figures 5.15 and 5.16]. In other words, undamaged beams are subjected to a higher influence of modification in strain modulus and damaged beams are influenced also for other parameters like reinforcement or tension stiffening variables (studied further on).
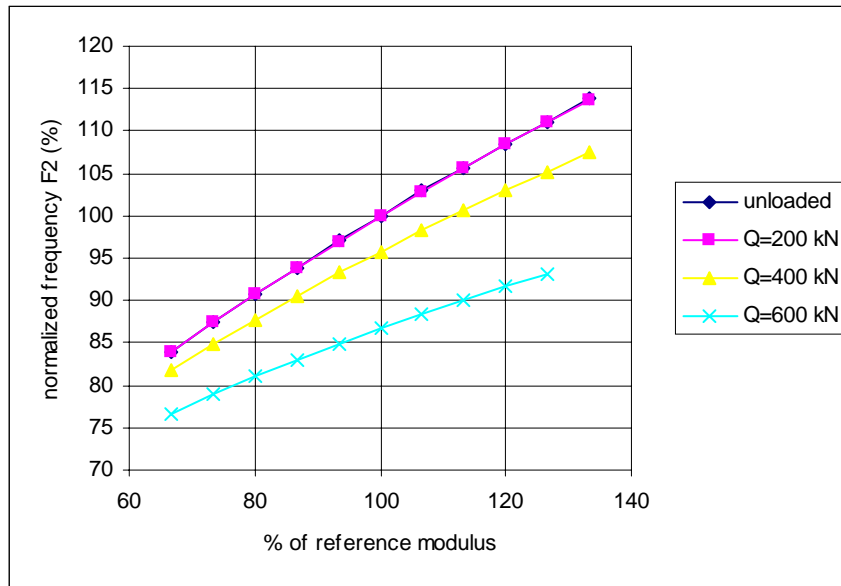
Figure 5.16. Second natural frequency vs. strain modulus

The second natural frequency was studied under the same conditions and is represented in figure 5.16. It is worth to mention that under a low-level of damage (20 kN) the values of the frequencies are equal to the undamaged case. First natural frequency (previous case) presented a slightly difference [figure 5.15].
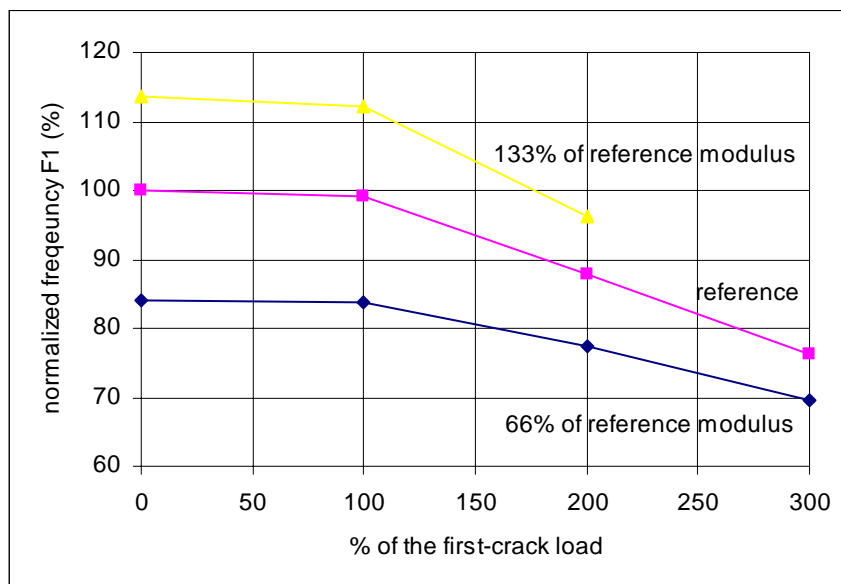
Figure 5.17. Influence of strain modulus on the first natural frequency after the loading process

Figure 5.17. represents the variation of the first natural frequency under a load-cracking process. Three different elasticity modulus were used, and for every case an important variation on the frequency is observed after the appearance of the first crack (at about 200 kN).

In figure 5.18., the relative evolution (the frequency up to the initial value) of first three natural frequencies is represented versus different elasticity modulus. First and second frequencies share the same sensibility under different elasticity modulus. Third frequency is less sensitive to this parameter.
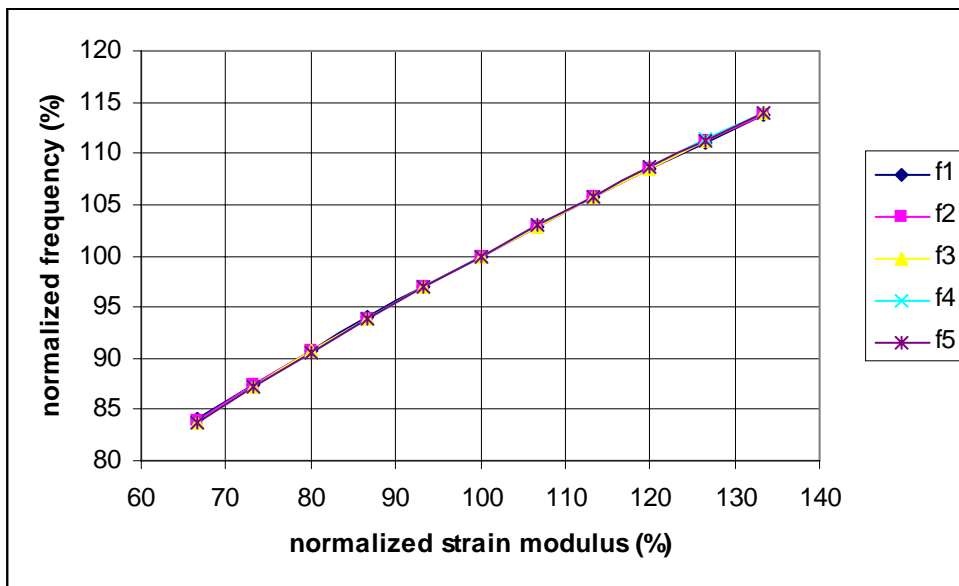
Figure 5.18. Relative variation of first tree natural frequencies for different strain modulus

5.3.5. Influence of cracking

After an occurrence of cracking the inertia of the beam and therefore its stiffness are reduced. The magnitude of this reduction is different for every case and depends of many factors like geometry, support conditions, reinforcement steel, etc. In this exercise, the beam was subjected to a growing load applied on the mid-span. The first two frequencies were calculated for every step and the numerical evolution of them can be observed in table B.5. appendix B.

First crack did not occur until 20 kN. After first crack the frequencies drop continuously until the failure of the structure. When the model did not include tension stiffening, the maximum load carried out by the beam was only 15 kN. In figure 5.19 the evolution of the first natural frequency can be observed. Figure 5.20. represents the relative evolution (using initial value as a reference) or the natural frequencies two to five. Under concentrate loading, frequency five ($f5$) is less sensitive to changes then other frequencies.
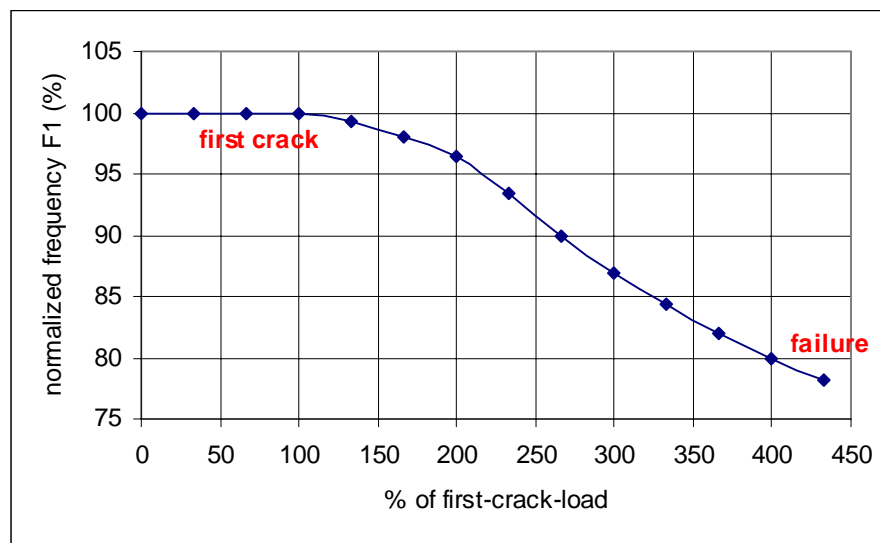
Figure 5.19. First natural frequency variation thorough the loading process
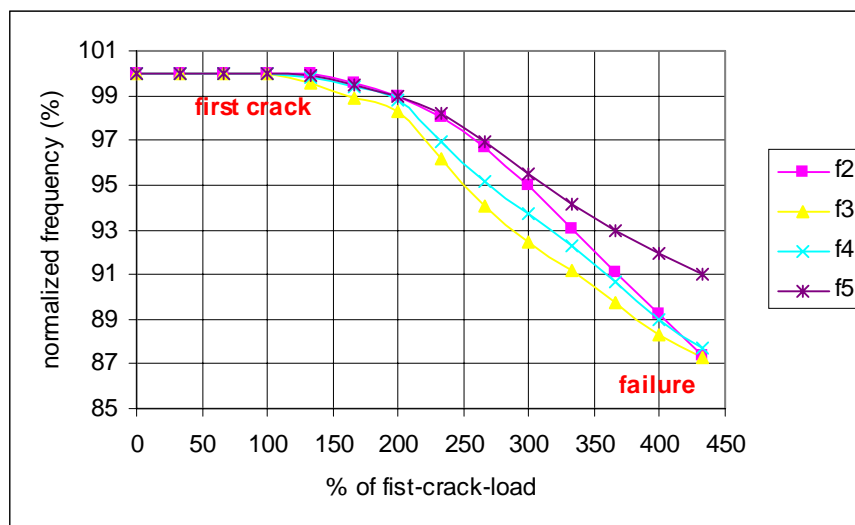
Figure 5.20. Relative variation frequencies two to five thorough the loading process

In the next example, the beam was subjected to a growing distributed load. The first two frequencies were calculated for every step and the evolution of them can be observed in table 5.7. First crack did not occur until 100 kN/m. After first crack the frequencies drop continuously until the failure of the structure.

If the model does not include tension stiffening, the maximum load carried out by the beam would be only 100 kN/m. In other words, the appearance of the first crack would mean the failure of the beam.

For the first natural frequency, the loading procedure caused a flat behavior of the values for the elastic interval. After the occurrence of the first crack a reduction of the stiffness, and therefore, the magnitude of the frequency is noticed [figure 5.21.]. From the figure is advertised that the behavior of the first natural frequency has a strong non-linear component. This is due to the non-linear constitutive equations of the materials and the tensile capacity of concrete between cracks (tension stiffening).
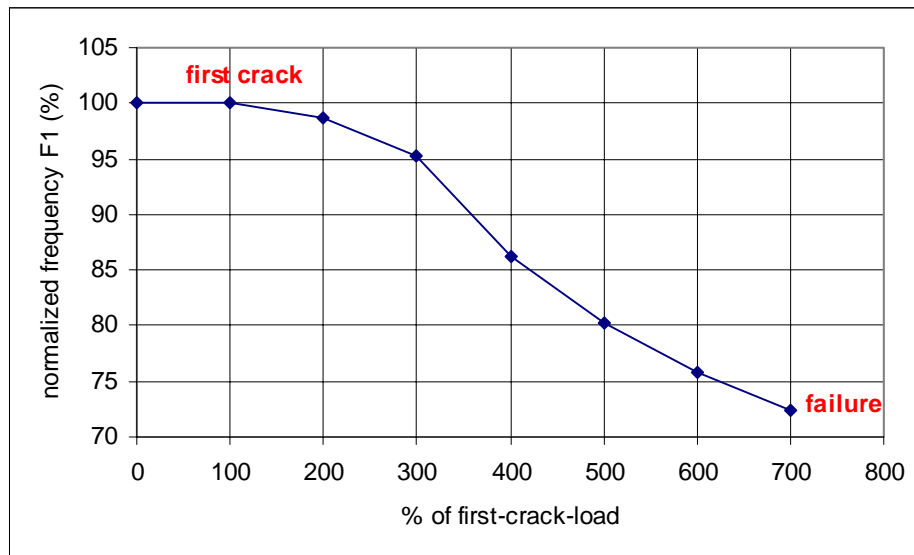
Figure 5.21. First natural frequency variation due to distributed load.

The frequencies two to five were also evaluated for an increasing distributed load. The behavior of those frequencies is analogue to the previous case (*f*1) and the influence of cracking presents slightly differences between the different frequencies [figure 5.22.]
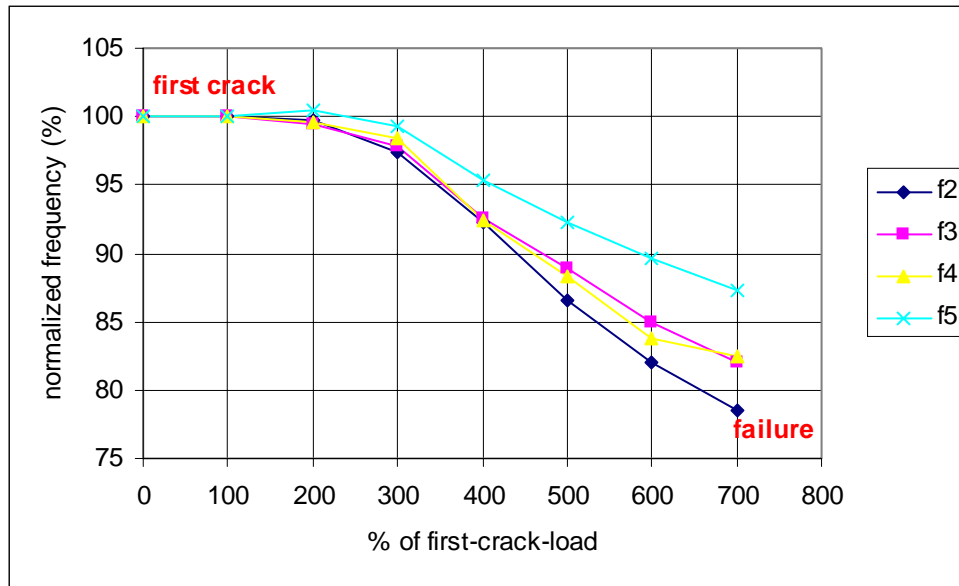
Figure 5.22. Relative variation due to distributed loading on natural frequencies two to four.

In figure 5.23. a comparison of the reduction of the first natural frequency versus maximum applied bending moment is plotted. The dynamic behavior of the beam under the same moment but different loading scheme (concentrated or distributed) showed not an important influence on the first natural frequency (f1).
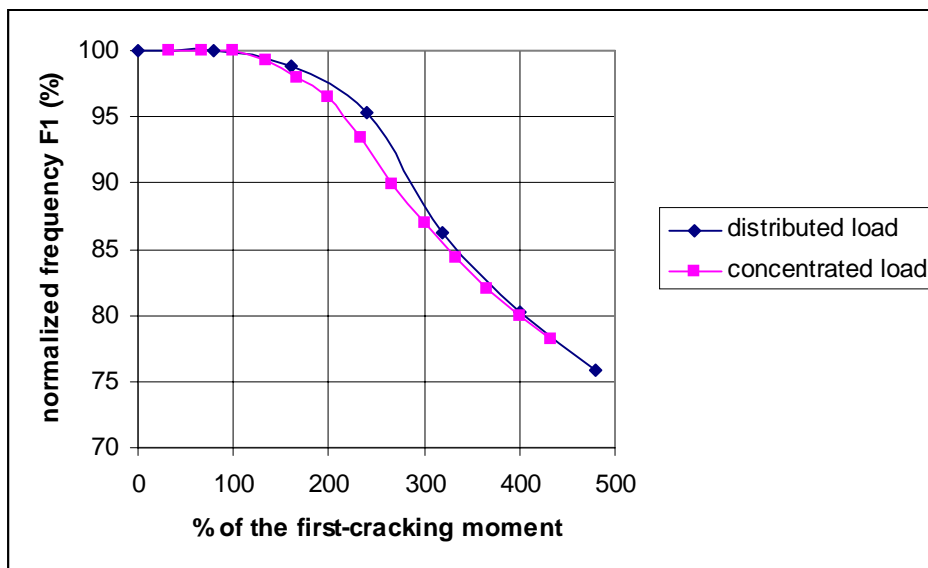
Figure 5.23. Comparative evolution of first natural frequency after distributed or concentrated loading processes.

5.3.6.   Influence of the *Tension Stiffening* parameters

Available literature present two ways to work with tension stiffening in concrete:

- Models with reference to the concrete [Van Greunen, 1979; Kang, 1977; Berzegar-Jimshidi, 1980]

- Models with reference to steel [Gilbert, 1978]

In the present dissertation, the model with reference to concrete is used in all the cases. The reason to use this model is the simplicity on the implementation in the FEM.

The tension stiffening parameters in the applied model are basically two: the maximum tensile capacity of concrete (f_{ct}) and the tension stiffening branch amplitude (ts_a). The tensile capacity of concrete defines the appearance of the first crack and thus the stiffness reduction. The tension stiffening branch amplitude defines the stiffness of the section for the range between the first crack and the failure. To represent the importance of this parameter, a damage process is necessary, otherwise the concrete section still undamaged and the tensile stresses are not achieved. Therefore, three load cases are studied with 20, 40 and 60 kN of concentrated load applied at mid-span [Table B.8. appendix B].

Figure 5.24 represents the first natural frequency for different tensile capacities of the concrete subjected to three different damage scenarios. For a high damage level (60 kN) the relationship between the capacity of tensile concrete and the frequency is linear. This is due to the variation of the position of the neutral fiber of the section and thus the combined inertia of the section (concrete plus steel). For non-damaged sections, the tensile capacity of the concrete does not interfere with natural frequencies because non-cracking phenomena has been achieved.
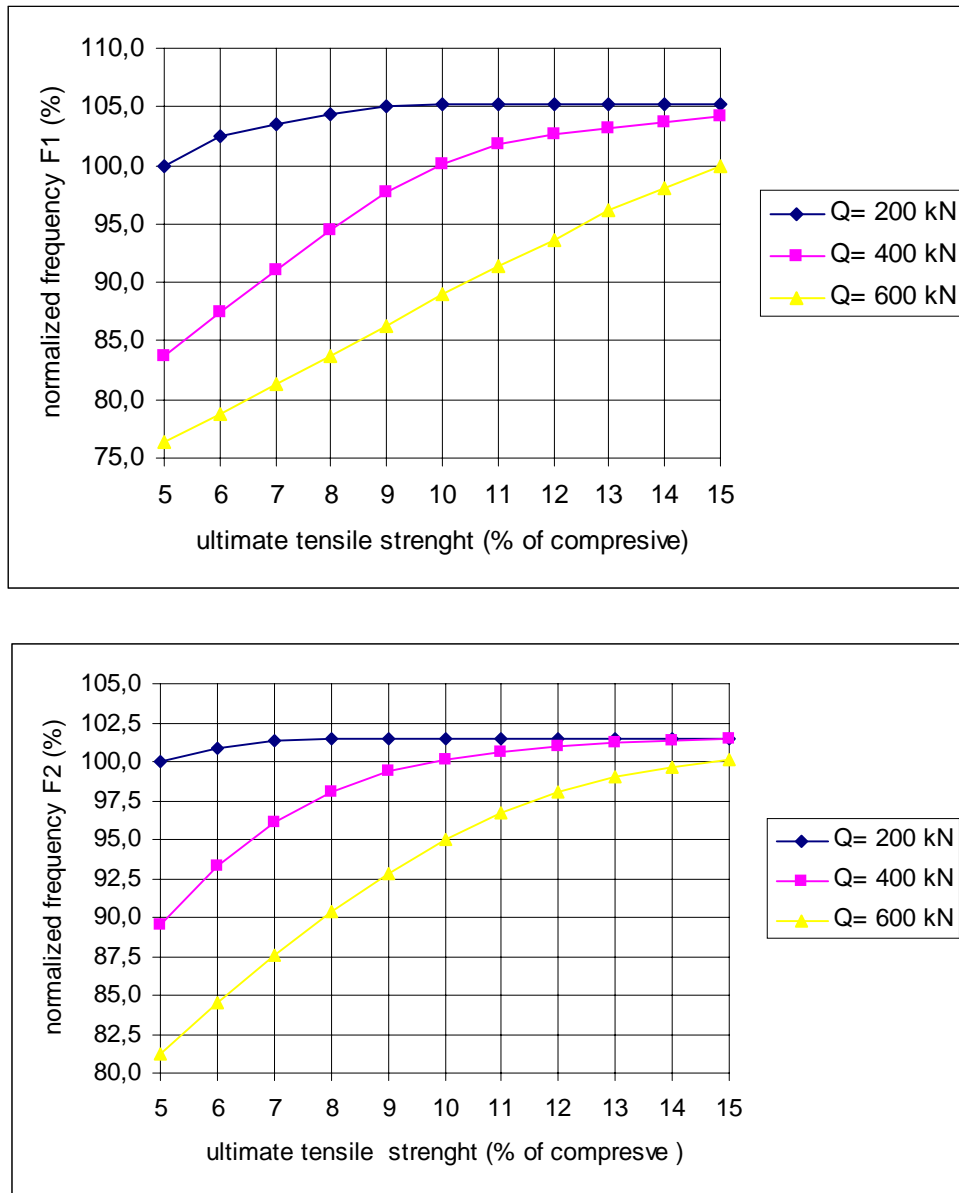
Figure 5.24. Comparative evolution of first (above) and second (below) natural frequencies for different tension capacity of concrete and different mid-span concentrated load (Q)

On the next example, the stain interval where the concrete between cracks contributes to the total stiffness of the section is changed gradually. The first two frequencies under three load scenarios were calculated [table B.9., appendix B]. When the tension stiffening branch amplitude (*TSBA*) is large [figure 5.25] the loose of stiffness takes place gradually and softer than the opposite case: where the

branch is short. [figure 5.25]. The choice of the *TSBA* is an important factor when updating a model to setup not only dynamic parameters but also deformations and curvature.
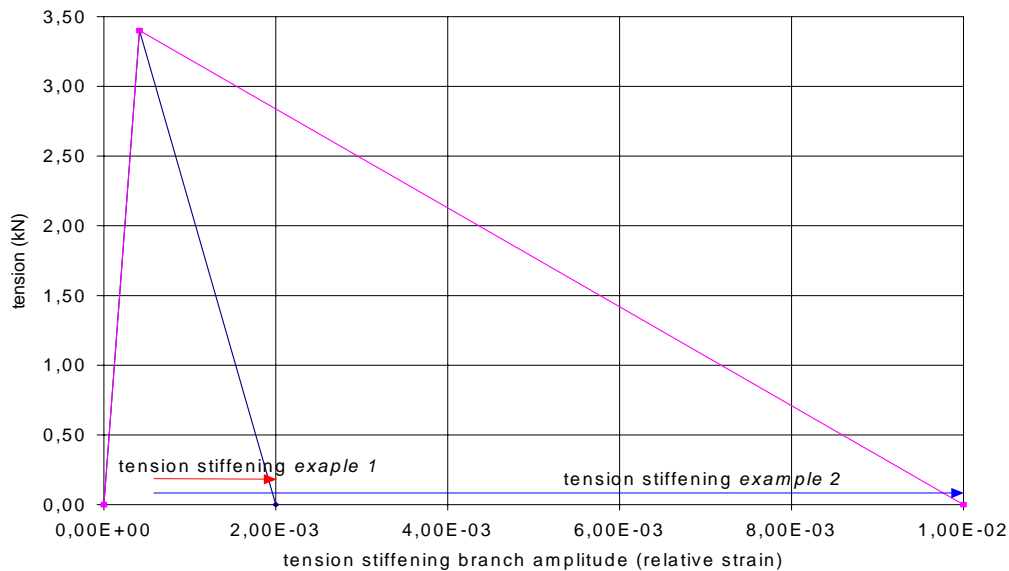
*Figure 5.25. Tension stiffening branch amplitude **TSBA** (2 examples)*

The tension stiffening parameters are fundamental to define the post-cracking behavior of a concrete structure. After the appearance of the first crack, the inertia of the beam becomes a hybrid value, product of the addition of the concrete in compression, the steel in tension and the concrete in tension between cracks. The last of those values is dependent of the tension stiffening parameters. For a short *TSBA* the lost of stiffness after the first crack is radically faster if compared with a long *TSBA*. The dependency of dynamic parameters (natural frequencies in this case) to post-cracking variables like *TSBA* is observed in figure 5.26. The behavior of the first two natural frequencies is plotted versus a modification in the *TSBA*. For a low value of *TSBA,* the lost of stiffness, and therefore the reduction of the frequency value, is evident. It is also noticed that the influence of *TSBA* is higher for a high-damage cases. Beams with null or low damage present a horizontal shape that means no influence to the studied parameter.
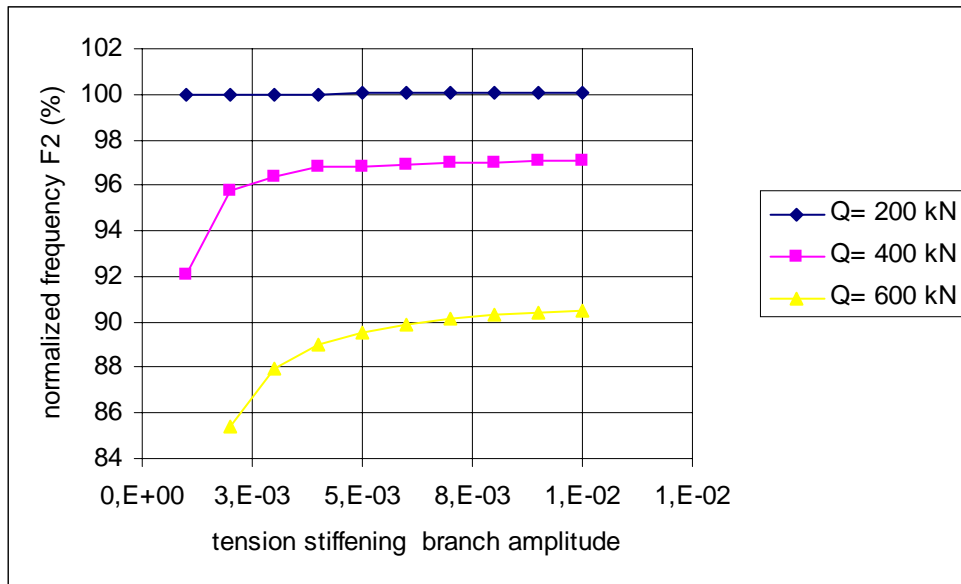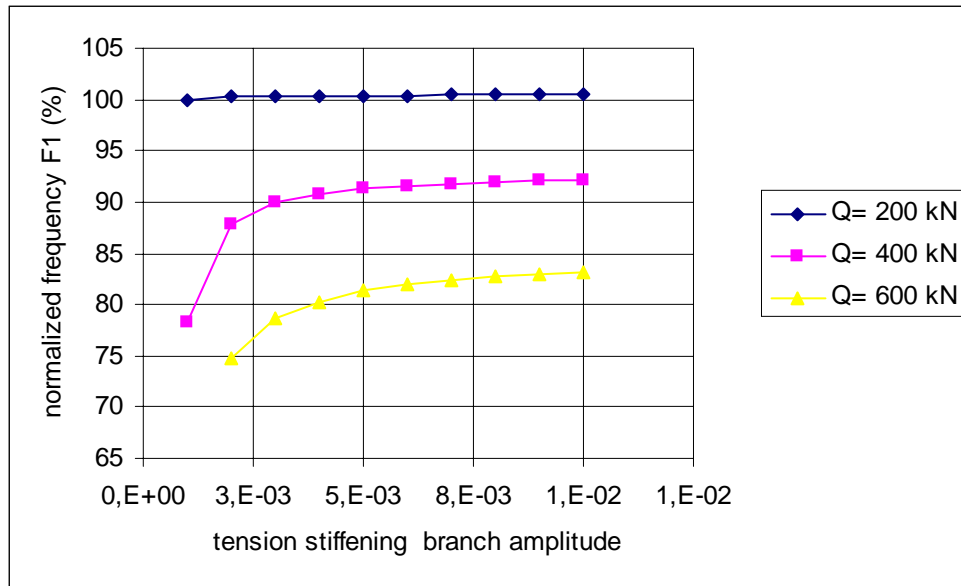
Figure 5.26. Comparative evolution of first (above) and second (below) natural frequencies for different TSBA and different mid-span concentrated load (Q)

5.4.   Two-way slabs

This problem examines the use of cracking models for the dynamic analysis of a 1.75-in thick reinforced concrete slab. The geometry of the problem is defined in Figure 5.27. A square slab is supported in the transverse direction at its four corners and loaded by a point load at its center. The slab is reinforced in two directions at

75% of its depth. The reinforcement ratio (volume of steel/volume of concrete) is 8.5×10^{-3} in each direction. The slab was tested experimentally by McNeice [1967] and has been analyzed by a number of workers, including Hand et al. [1973], Lin and Scordelis [1975], Gilbert and Warner [1978], Hinton et al. [1981], and Crisfield [1982].
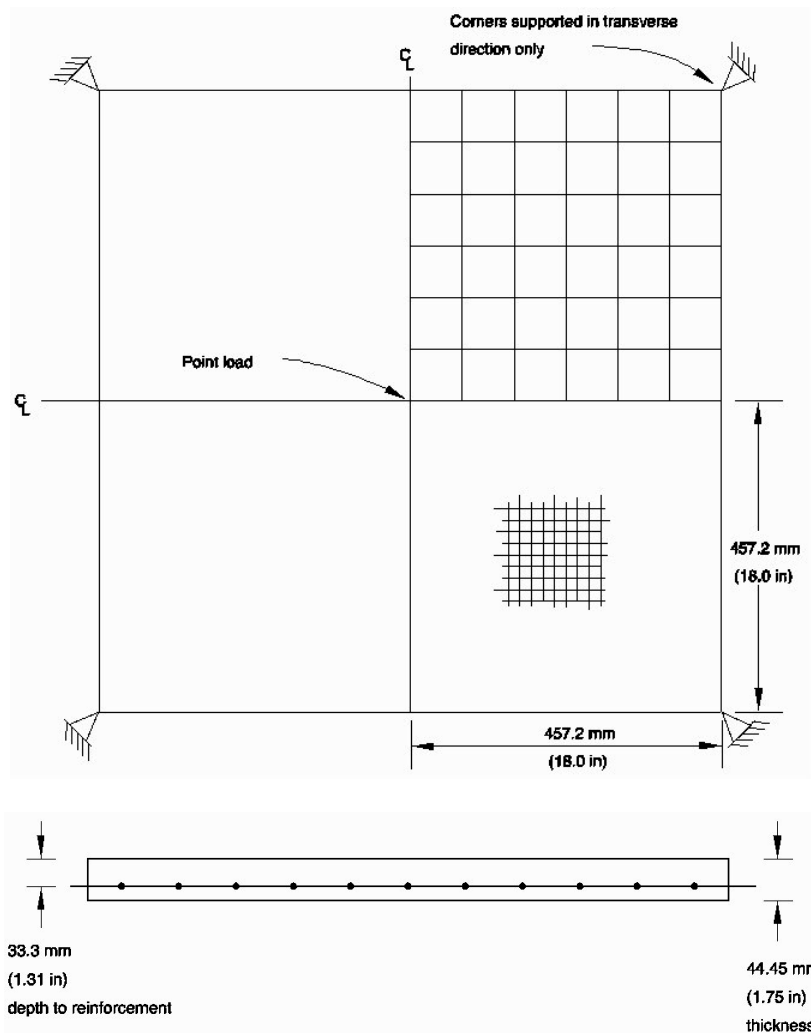
Figure 5.27. Analyzed concrete slab

Symmetry conditions allow us to model one-quarter of the slab. A 3 × 3 mesh of 8-node shell elements is used for the FEM analysis. No mesh convergence studies have been performed, but the reasonable agreement between the analysis results and the experimental data suggests that the mesh is adequate to predict overall response parameters with usable accuracy. Nine integration points are used through the

thickness of the concrete to ensure that the development of plasticity and failure are modeled adequately. The two-way reinforcement is modeled. Symmetry boundary conditions are applied on the two edges of the mesh, and the corner point is restrained in the transverse direction.

The material data is given in Table 5.10. The material properties of concrete are taken from Gilbert and Warner [1978]. Some of these data are assumed values, because they are not available for the concrete used in the experiment. The assumed values are taken from typical concrete data. The compressive behavior of concrete in the cracking model used in the simulation is assumed to be linear-elastic. This is a reasonable assumption for a case such as this problem, where the behavior of the structure is dominated by cracking resulting from tension in the slab under bending.

The modeling of the concrete-reinforcement interaction and the energy release at cracking are of critical importance to the response of a structure such as this once the concrete starts to crack. These effects are modeled in an indirect way by adding "tension stiffening" to the plain concrete model. The simplest tension-stiffening model defines a linear loss of strength beyond the cracking failure of the concrete. In the static example three different values for the strain beyond failure at which all strength is lost (5×10^{-4}, 1×10^{-3}, and 2×10^{-3}) are used to illustrate the effect of the tension stiffening parameters on the response. In the dynamic approach, several values of tension stiffening are evaluated.

Since the response is dominated by bending, it is controlled by the material behavior normal to the crack planes. The material's shear behavior in the plane of the cracks is not important. Consequently, the choice of shear retention has no significant influence on the results. In Abaqus full shear retention is used because it provides a more efficient numerical solution.

Since considerable no linearity is expected in the response, including the possibility of unstable regimes as the concrete cracks, the modified *Riks* method is used with automatic step-increment in the analysis. With the *Riks* method the load data and solution parameters serve only to give an estimate of the initial increment of load. In this case it seems reasonable to apply an initial load of 1112 N (250 lb) on the

quarter-model for a total initial load on the structure of 4448 N (1000 lb). This can be accomplished by specifying a load of 22241 N (5000 lb) and an initial time increment of 0.05 out of a total time period of 1.0. The analysis is terminated when the central displacement reaches 25.4 mm (1 in).

Since the used FEM code (Abaqus) is a dynamic analysis program and in this case we are interested in static solutions, the slab must be loaded slowly enough to eliminate any significant inertia effects. The slab is loaded in its center by applying a velocity that increases linearly from 0 to 2.0 in/second such that the center displaces a total of 1 inch in 1 second. This very slow loading rate ensures quasi-static solutions; however, it is computationally expensive. There is a possibility to reduce the CPU time required for this analysis: the loading rate can be increased incrementally until it is judged that any further increase in loading rate would no longer result in a quasi-static solution.

Concrete properties	
Properties are taken from Gilbert and Warner [1978]	
Properties marked with a * are not available, and are assumed values.	
Young's modulus	28.6 GPa (4.15....10E 6 lb/in 2)
Poisson's ratio	0.15
Uniaxial compression values:	
Yield stress	20.68 MPa (3000 lb/in 2)*
Failure stress	37.92 MPa (5500 lb/in 2)
Plastic strain at failure	1.5E-3 *
Ratio of uniaxial tension to compression failure stress	8.36....10 -2
Ratio of biaxial to uniaxial compression failure stress	1.16*
Cracking failure stress	459.8 lb/in 2 (3.17 MPa)
Density	2.246 × 10 -4 lb s2 /in 4 (2400 kg/m3)

Table 5.10. Material properties for McNeice slab.

The numerical and experimental results are compared in Figure 5.27. on the basis of load versus deflection at the center of the slab. The strong effect of the tension stiffening assumption is very clear in that plot. The analysis with tension stiffening,

such that the tensile strength is lost at a strain of 10 E–3 beyond failure, shows the best agreement with the experiment. This analysis provides useful information from a design viewpoint.
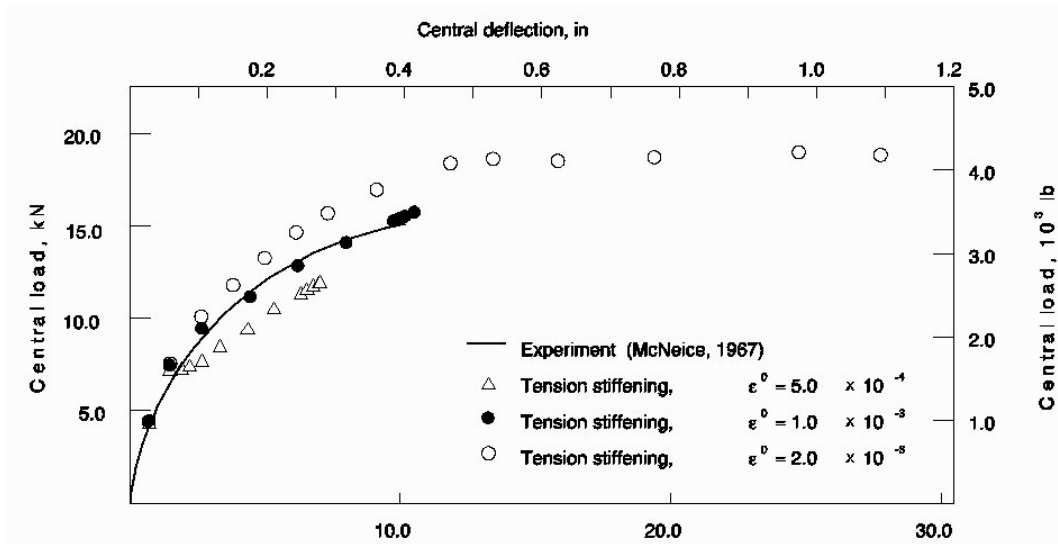
Figure 5.27. Experimental and numerical comparison

5.4.1. Mass influence

The influence of the mass on the natural frequencies is studied by modifying the density of the material. The results are analog to the beam-case; the evolution of the first five natural frequencies is described in table B.10, appendix B.

The relationship between the calculated value of the frequencies and the reference value (initial) is linear [figure 5.28.] and decreases for mass increments.
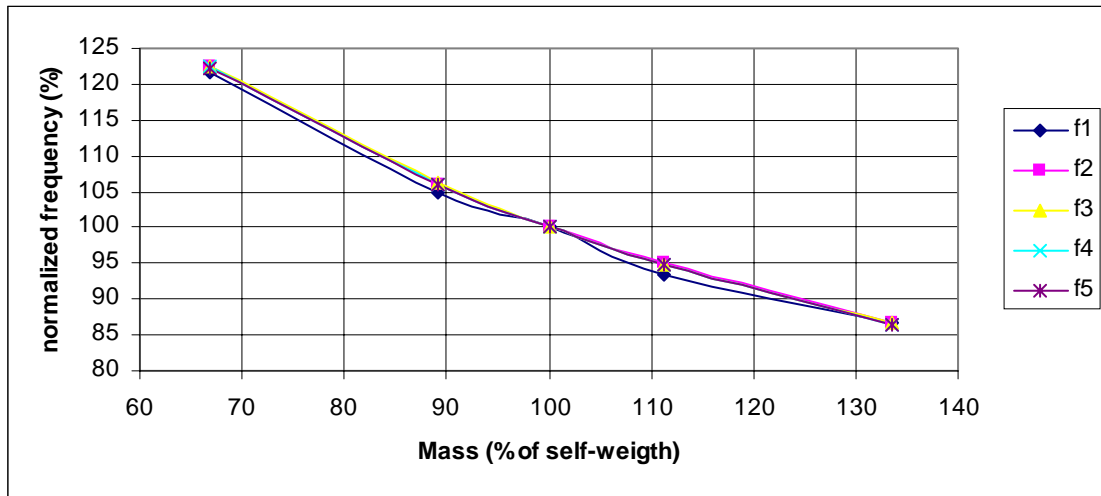
Figure 5.28. Mass influence of first five natural frequencies.

5.4.2. Reinforcement ratio influence

Undamaged state

Only a slightly difference on first five natural frequencies can be observed if the reinforcement ratio is modified [table B.11, appendix B]. The case of slabs is analogue to the case of beams [section 5.3.2]: the variation of the frequencies is only due to variation of the composite inertia of the section [figure 5.29].
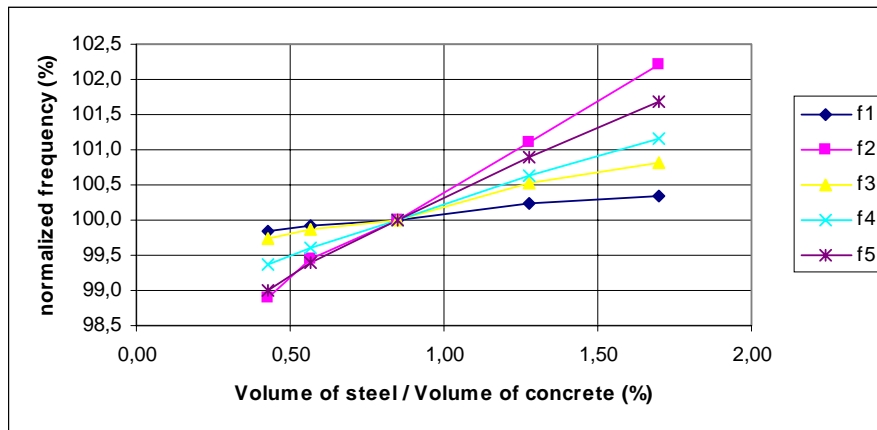
Figure 5.29. First five natural frequencies vs. reinforcement ratio (undamaged condition).
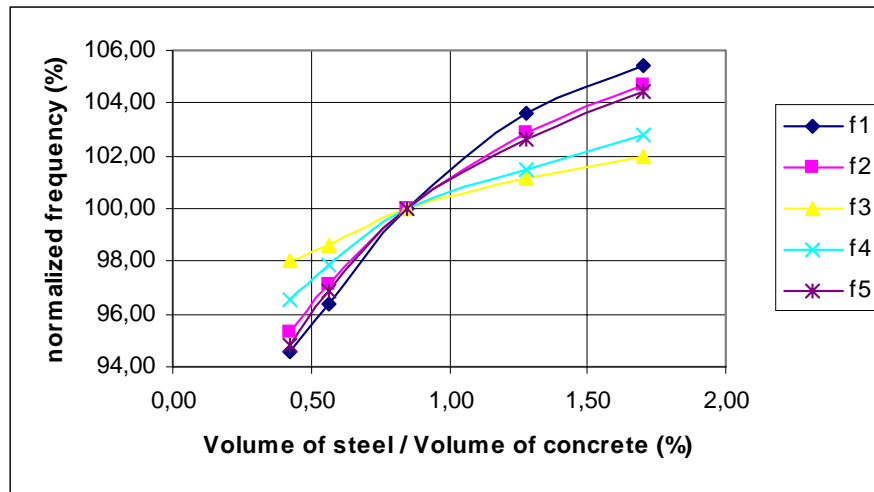
Figure 5.30. First five natural frequencies vs. reinforcement ratio (after loading process).

The variation of the frequencies versus reinforcement ratio seems to be more relevant under certain damage scenario (if compared to previous case). Variations near to 6% are observed [figure 5.30] on the first natural frequency. The analysis was developed applying a concentrated load of 22,7 kN (500 Lb) at mid-span. Under this load certain level of damage is achieved and cracking reduces the stiffness of the slab. The influence of steel is denoted by reducing strain on tensioned fibers and therefore sustaining a higher level of tension stiffening.

5.4.3. Support conditions influence

One of the most important parameters related to dynamic behavior of slabs is definitely support condition. Figures 5.32. and 5.33. show the first and second natural frequencies of the studied slab. The only variation between those two cases is the support condition on the four corners. First case is a free-supported slab; second case changes these conditions to clamp. The modal-shapes remain the same while the values of natural frequencies are substantially modified.
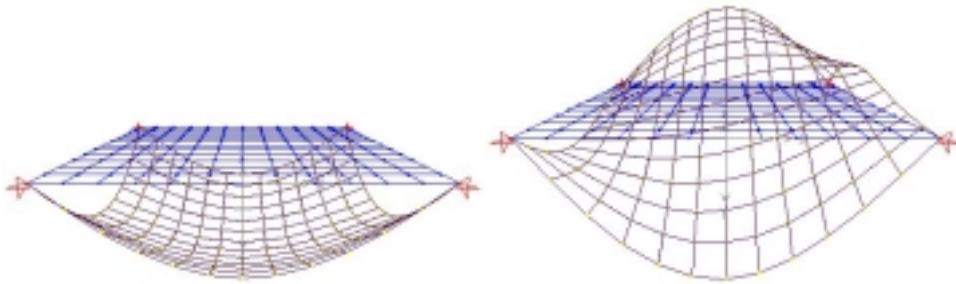
Figure 5.32. First (60 Hz) and second (141 Hz) natural frequencies for corner-pinned support condition.
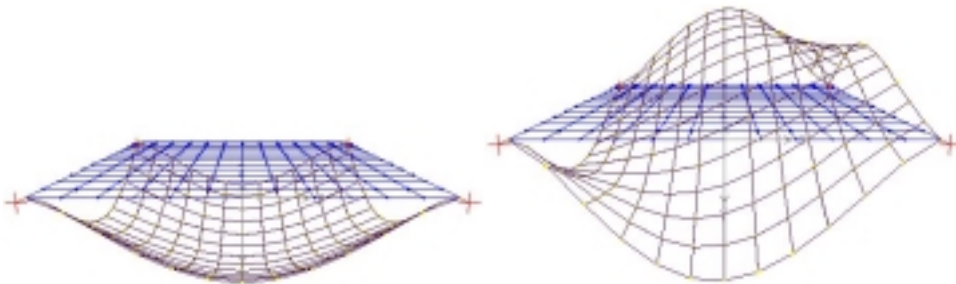
Figure 5.31. First (81 Hz) and second (172 Hz) natural frequencies for corner-clamped support condition.

The second case represents a support-supported condition. Figures 5.33. and 5.34. represent the first and second natural frequencies for support-pinned and support-clamped conditions respectively. Once again the modal shapes remain equal and the variations on the frequencies values are spectacular. It is worth to mention that the only modified parameter is the restriction of degrees of freedom on the support.
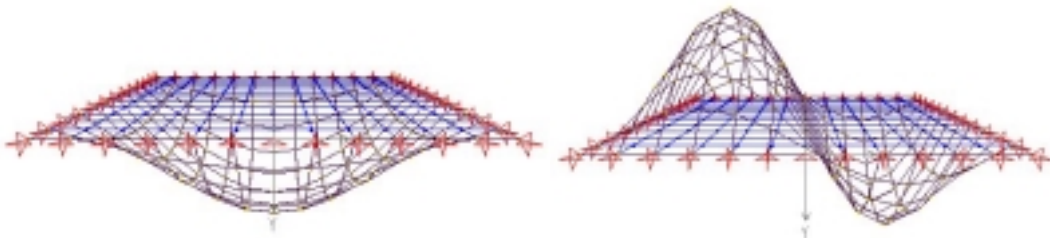
Figure 5.33. First (166 Hz) and second (416 Hz) natural frequencies for support-pinned support condition.
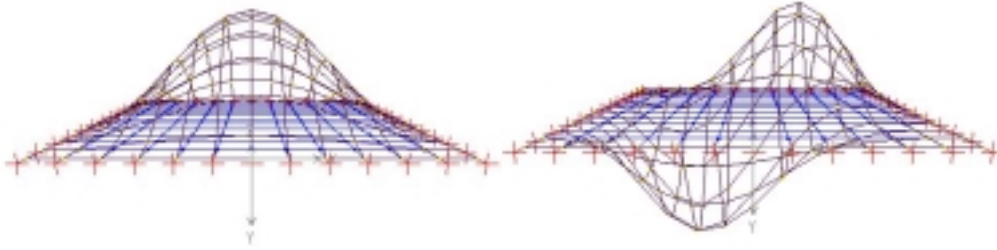
Figure 5.34. First (300 Hz) and second (625 Hz) natural frequencies for support-clamped support condition.

5.4.4. Strain modulus influence

Strain modulus is -as in the case of beams- a parameter with strong influence on dynamic properties of slabs. In this example, the strain modulus of the slab is gradually changed and the first five natural frequencies are evaluated [table B.13., appendix B]. Any of the five frequencies is modified in the same proportion [figure 5.35].
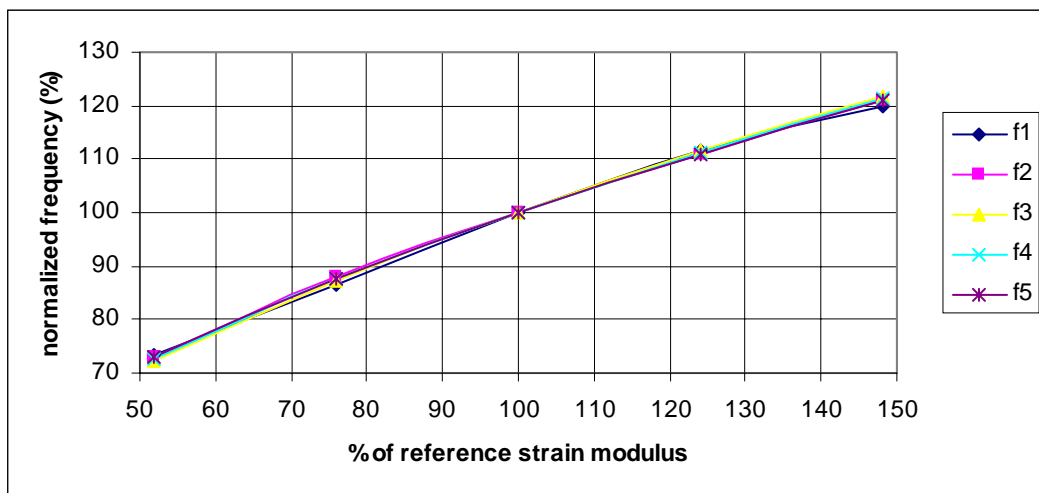
Figure 5.35. First five natural frequencies vs. strain modulus.

5.4.4 Influence of cracking

When cracking occurs after a load process, the dynamics of the slab is modified. On this case an increasing concentrated load was applied al the center of the slab. The variation of the frequencies one to five is presented on table B.14., appendix B.

The influence of cracking is not the same for all frequencies, actually is highly dependent of the modal-shape. In this case the most-affected frequency was $f1$. Frequency three was affected only slightly. Other frequencies were affected by cracking a middle term.
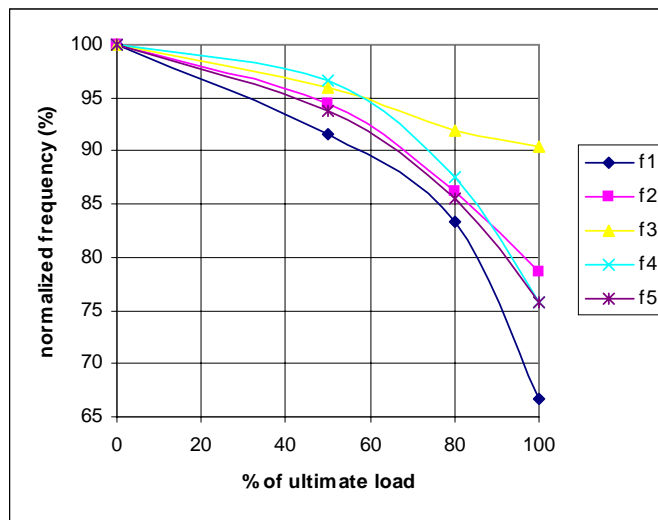
Figure 5.36. First five natural frequencies vs. applied load and damage.

5.4.5.   Tension stiffening amplitude influence

The tension stiffening was fundamental to consider when studying the reduction of stiffness due to cracking. As presented in section 5.4, the best fit for McNeice slab was obtained wit a tension stiffening branch amplitude of 1E-3. On this example this branch is modified and dynamic properties of the slab are evaluated. Table B.15. [Aappendix B] present the tension stiffening values and the frequency list.

The influence of the tension stiffening branch amplitude starts only after the appearance of the first crack; in this example a concentrated load of 22,7 kN (500 Lb) was applied at the center of the slab. This load caused important cracking (and

therefore modification on frequencies) only in the cases with a tension stiffening less than 2E-3.
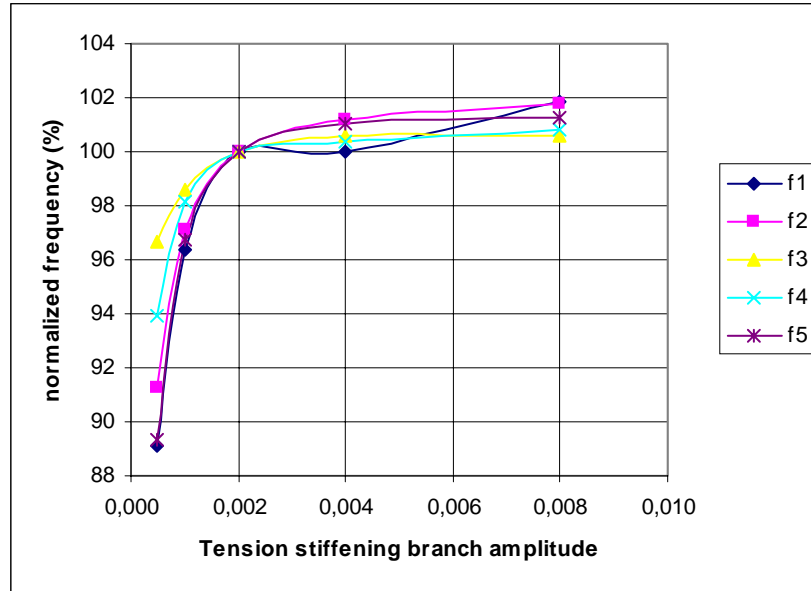
Figure 5.37. First five natural frequencies vs. tension stiffening branch amplitude.

5.4.6. Shape and orthotropy

When two-dimensional structures are modeled dynamically, many factors take a roll. The factors are related to the geometry of the slab. In this example, a study of the influence of those parameters in the dynamics of the slab is developed. Some parameters like thickness, elasticity modulus, material properties were kept. The variation of parameters is more related to support and stiffening by nerves inclusion. Every one of the following tables represents a different case. First, the support conditions are described and then, the first four natural frequencies and modal shapes are plotted. It is important to remark that the slab is the same for all cases; only support conditions are modified in the first six cases.
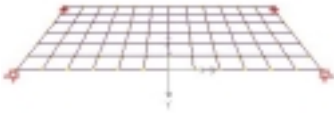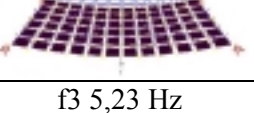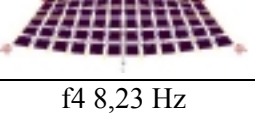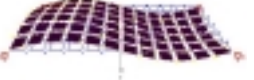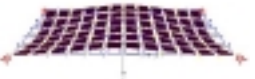
Support conditions	f1 1,48 Hz	f2 4,48 Hz
	f3 5,23 Hz	f4 8,23 Hz
Pinned on the corners		

Table 5.17. First four natural frequencies and modal shapes under a corner-pinned support condition.
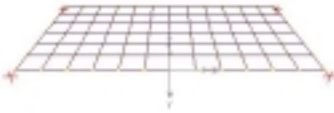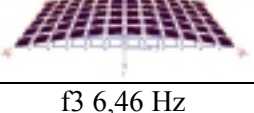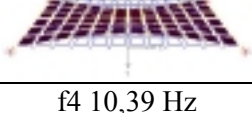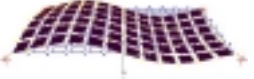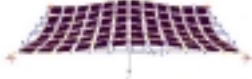
Support conditions	f1 2,17 Hz	f2 5,14 Hz
	f3 6,46 Hz	f4 10,39 Hz
Clamped on the corners		

Table 5.18. First four natural frequencies and modal shapes under a corner-clamped support condition.
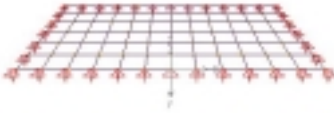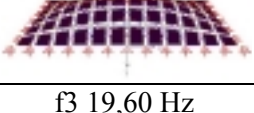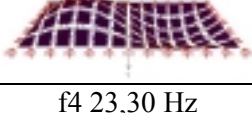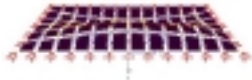
Support conditions	f1 7,68 Hz	f2 12,15 Hz
	f3 19,60 Hz	f4 23,30 Hz
Punned-support		

Table 5.19. First four natural frequencies and modal shapes under a support-pinned condition.
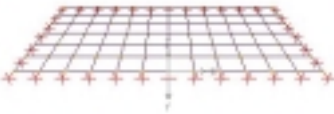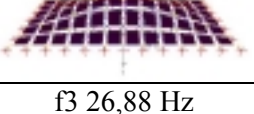
Support conditions	f1 15,24 Hz	f2 19,37 Hz
	f3 26,88 Hz	f4 38,16 Hz
Clamped support		

Table 5.20. First four natural frequencies and modal shapes under a support-clamped condition.
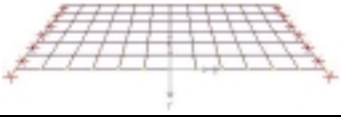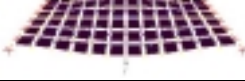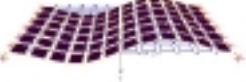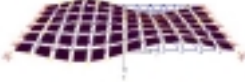
Support conditions	f1 3,49 Hz	f2 5,69 Hz
	f3 9,63 Hz	f4 13,17 Hz
Two-sides clamped (y axis)		

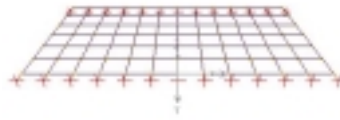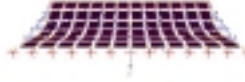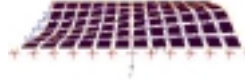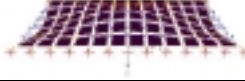*Table 5.21. First four natural frequencies and modal shapes under a support-clamped condition in y direction.*
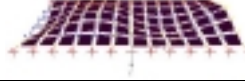
Support conditions	f1 14,02Hz	f2 14,66 Hz
	f3 17,09 Hz	f4 21,41 Hz
Two-sides clamped (x axis)		

Table 5.22. First four natural frequencies and modal shapes under a support-clamped condition in x direction.

The influence of anisotropy on slab stiffness by the inclusion of nerves is studied in the next example. Three different slabs were modeled with 1:1, 1:2 and 1:3 side-ratio [Figure 5.38.]. Those slabs were modified gradually by inclusion of transversal nerves. The inclusion of nerves causes variation of the inertia of the slab from 1 to 38 using as a reference the inertia with no-nerves [Figure 5.39.]. Relative inertia is

defined as: $\sigma = \dfrac{I_{fs}}{I_{ns}}$;

where I_{fs} = Inertia of the flat slab and

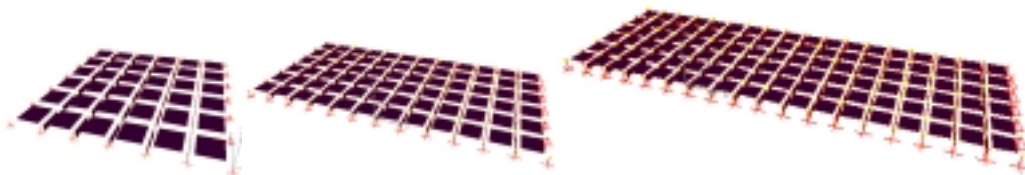 I_{ns} = Inertia of the slab including nerves

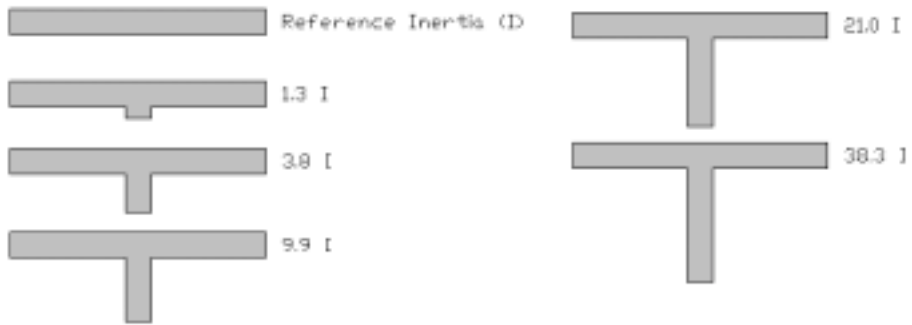*Figure 5.38. Modeled slabs, side-ratio 1:1, 1:2 and 1:3.*

Figure 5.39. Stiffness modification by adding nerves

First of all, a mesh sensibility study was developed to define the number of DOF used in the model. From figure 5.40. it is observed that a simple mesh (546 DOF) reproduces the dynamic behavior of a complex mesh (7350 DOF) with less than 1% error [Figure 5.38]. This error is considered acceptable and therefore the 546-DOF mesh is assumed (6x12 shell elements).
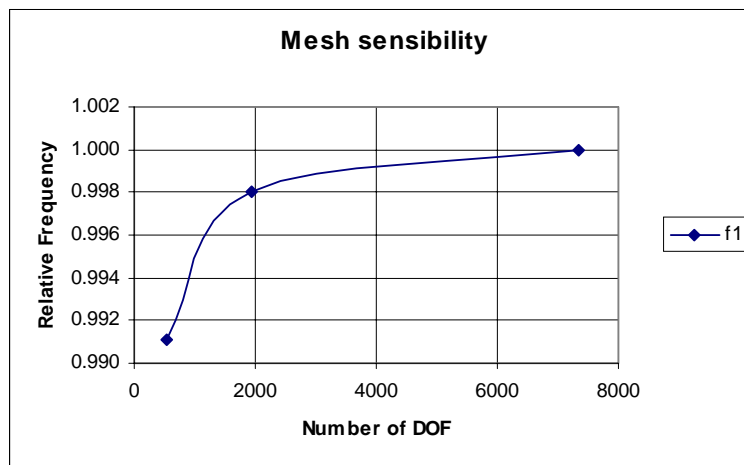

Figure 5.40. Mesh sensibility of first natural frequency.

Number of DOF	546	1,950	7,350
FEM			
First Natural Frequency	9.88 Hz	9.95 Hz	9.97 Hz

Table 5.23. Mesh sensibility of the first natural frequency versus number of DOF's.

In the following figures, the influence of stiffness addition by the construction of nerves is studied.   The inclusion of nerves generates variation of stiffness as described in figure 5.39. In table 5.24 including nerves in one direction gradually modifies a slab with proportions 1x1. Variation on frequencies and modal shapes is observed. In figure 5.41. the variations on the first five natural frequencies (normalized, using f1 as a reference) are plotted. Frequencies one and two present a clear trend, when the nerves are stiffer, the proportion between f1 and f2 seems to decrease in a logarithmic rate. The variation of frequencies 3 to 5 (using always f1 as a reference) present oscillations and do not show any clear pattern.
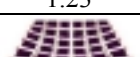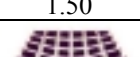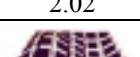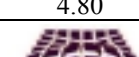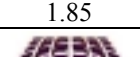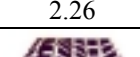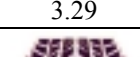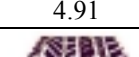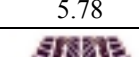
Relative Inertia Slab 1x1	f1	f2	f3	f4	f5
1	1.00	1.85	2.37	3.05	3.44
1.3	1.04	1.82	2.54	3.14	3.32
3.8	1.23	1.88	3.24	3.31	3.74
9.9	1.50	2.02	3.24	4.45	4.80
21.0	1.85	2.26	3.29	4.91	5.78
38.3	2.25	2.56	3.41	4.80	6.44

Table 5.24. First five natural frequencies and modal shapes of a 1x1-sided slab for different σ values.
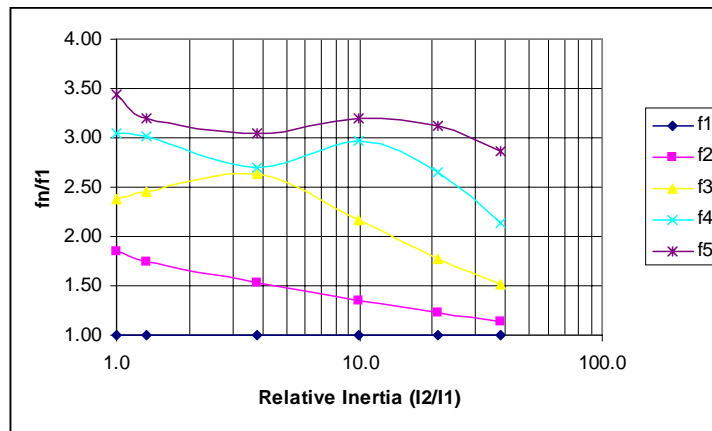
Figure 5.41. Relative variation of first five natural frequencies of a 1x1-sided slab
for different σ values.

In the case of a 2x1-sided slab, the same process was applied: first five natural frequencies and modal shapes were evaluated for different relative inertia values (σ). In table 5.25 the variations of these parameters are plotted. In figure 5.42. the variations on the first five natural frequencies (normalized, using f1 as a reference) are also plotted. Frequencies one to four present a clear trend, when the nerves are stiffer, the proportion between f1 and f_n seems to decrease in a logarithmic rate. The variation of frequency f5 (using always f1 as a reference) presents a slightly oscillation and do not show a clear pattern for low relative inertia values.
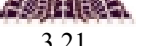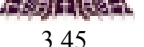
Relative Inertia Slab 1x2	f1	f2	f3	f4	f5
1	1.00	1.19	1.58	2.20	2.66
1.3	1.07	1.24	1.59	2.17	2.88
3.8	1.34	1.46	1.75	2.24	2.95
9.9	1.70	1.79	2.01	2.42	3.04
21.0	2.14	2.20	2.37	2.69	3.21
38.3	2.63	2.67	2.80	3.04	3.45

Table 5.25. First five natural frequencies and modal shapes of a 2x1-sided slab for
different σ values.
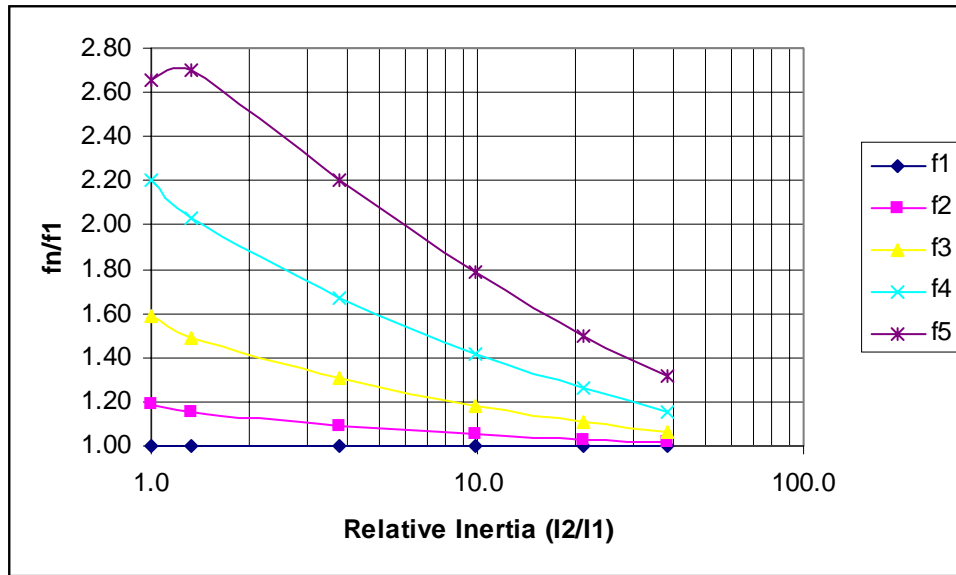
Figure 5.42. Relative variation of first five natural frequencies of a 2x1-sided slab for different σ values.

A 3x1-sided slab was also modeled under the same conditions. First five natural frequencies and modal shapes were also evaluated for different relative inertia values *(σ)*. In table 5.26 the variations of these parameters are plotted. In figure 5.43. the variations on the first five natural frequencies (normalized, using f1 as a reference) are also plotted. All frequencies present a clear trend: when the nerves are stiffer, the proportion between f1 and f_n seems to decrease in a logarithmic rate.
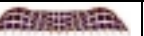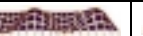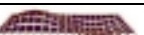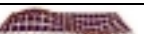
Relative Inertia	f1	f2	f3	f4	f5
1	1.00	1.08	1.23	1.47	1.82
1.3	1.08	1.14	1.28	1.50	1.81
3.8	1.36	1.41	1.51	1.68	1.95
9.9	1.74	1.77	1.85	1.98	2.19
21.0	2.20	2.22	2.27	2.37	2.54
38.3	2.70	2.72	2.76	2.83	2.95

Table 5.26. First five natural frequencies and modal shapes of a 3x1-sided slab for different σ values.
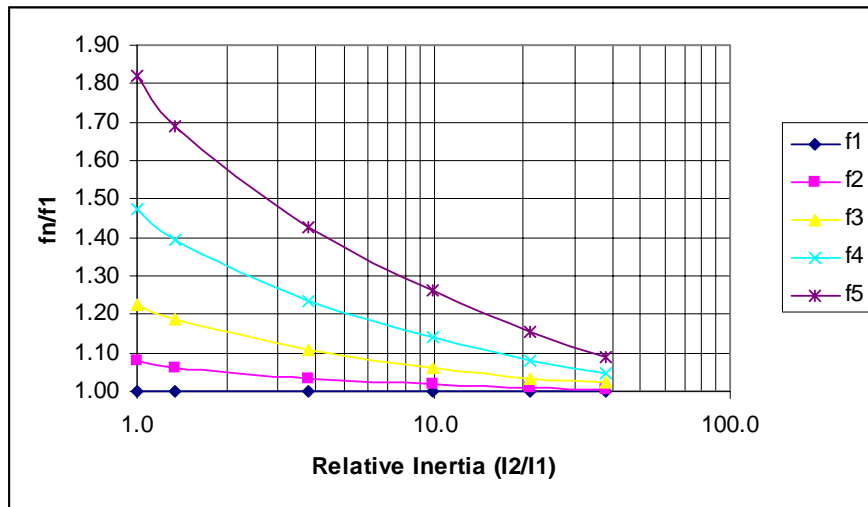
Figure 5.43. Relative variation of first five natural frequencies of a 3x1-sided slab for different σ values.

When relative inertia (σ) is identified from natural frequencies, other parameters of the slab can also be determined. For example: the relative displacements at midspan on every nerve. In figure 5.44, the deformation of the nerve at mid span is plotted versus relative inertia. It can be observed that for a low values of σ, the proportional displacements of adjacent beams is higher than those generated for high values of σ. The proportional displacement of adjacent beams in 1x1-sided slabs [Figure 5.44] present a very similar behavior to 2x1 or 3x1-sided slabs [Figure 5.45]
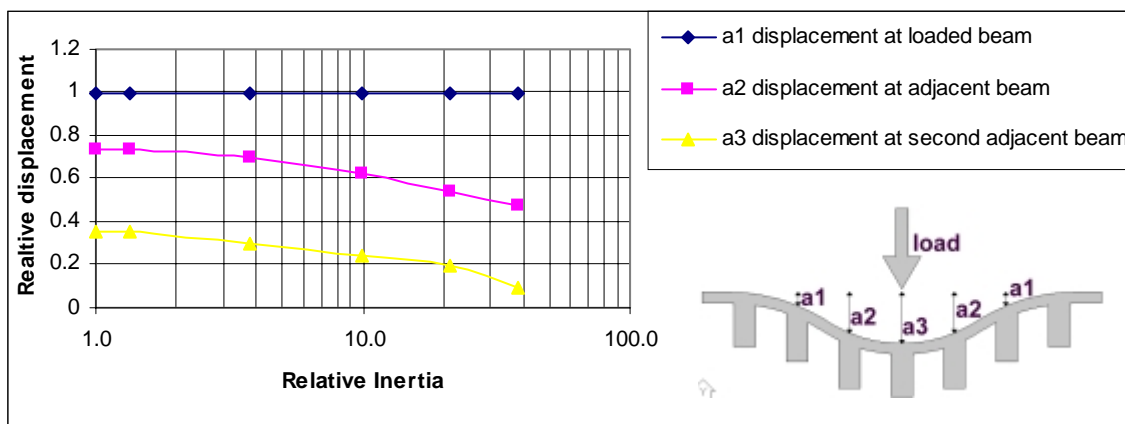
Figure 5.44. Mid-span relative deformation on loaded and adjacent beams of a 1x1-sided slab for different relative inertia factors (σ).
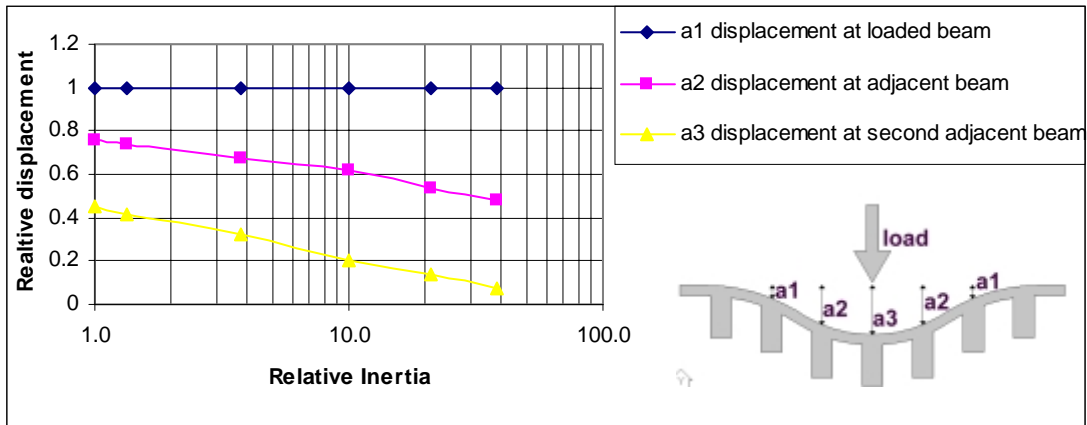
Figure 5.45. Mid-span relative deformation on loaded and adjacent beams of 2x1 and 3x1-sided slab for different relative inertia factors (σ).

Comparatively, reaction on supports can be calculated for different values of σ. When the stiffness of the nerve is increased, the loaded nerve assumes a higher load level and adjacent nerves suffer an unloading process [Figure 5.46.]. One more time, the sides-ratio of the slab (1x1, 2x1 and 3x1) presents a similar behavior [Figures 5.46 and 5.47].
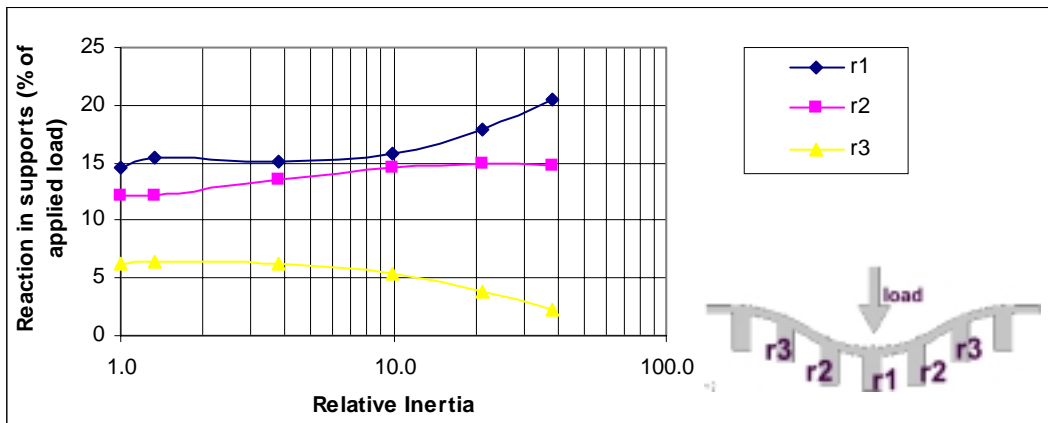
Figure 5.46. Reaction on supports of loaded and adjacent beams of a 1x1-sided slab for different relative inertia factors (σ).
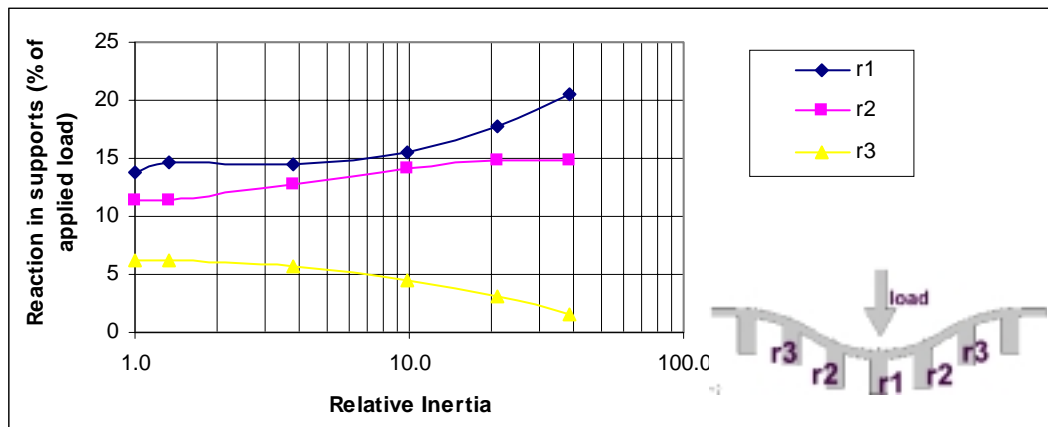
Figure 5.47. Reaction on supports of loaded and adjacent beams of 2x1 and 3x1-sided slab for different relative inertia factors (σ).

5.5. Masonry columns

5.5.1. Introduction

Dynamical behavior of masonry structures made of stone or bricks is dependent on certain parameters like mass, support conditions, damage and many others. This dependency is analog to other structures studied above, but certain phenomena that affects dynamic behavior is inherent to masonry structures: a hardening process in its constitutive equation.

5.5.5. Load-Hardening phenomena

There is not much available information on literature about the hardening process in masonry materials. Therefore some assumptions are made to approach this study:

- The load interval of the structure subject of dynamic identification present a constitutive equation with a single-curvature-shape [Figure 5.50]
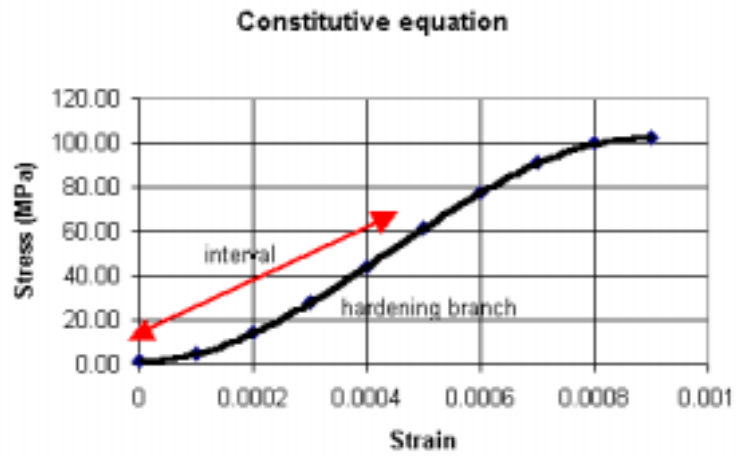
Figure 5.50. Interval of interest in a constitutive equation of a hypothetical material with a high hardening ratio

Therefore, a series of different constitutive equations (CE) are defined in the model and dynamic parameters are evaluated for every different case. These CE share the same mean value of strain modulus, and also share the starting and ending points. The basic difference is that the ratio between starting and ending modulus is gradually changed in an interval from 1 to 2.5 [Figure 5.51]. In other words, the hardening phenomenon is increased gradually from a linear elastic case (ratio =1, no hardening) to the opposite non-linear case (ratio=2.5, high-hardening level).
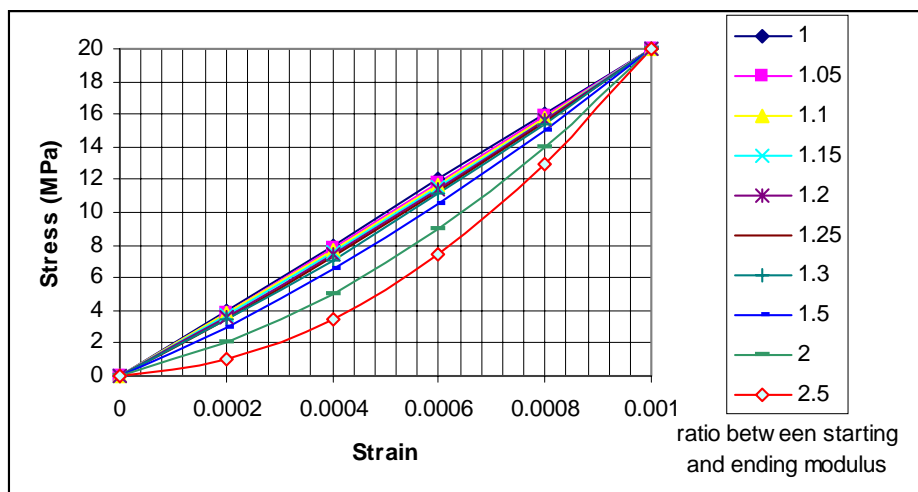
Figure 5.51. Different constitutive equations with a varying hardening level
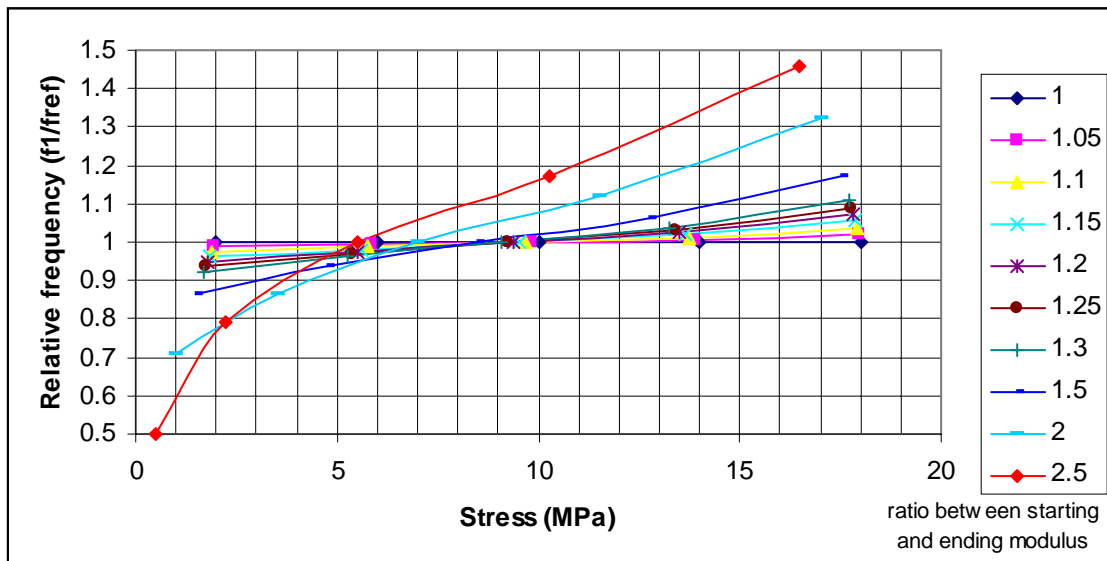
Figure 5.52. Influence of hardening phenomena on first natural frequency

An important influence of the hardening phenomena is observed [Figure 5.52]. For a higher ratio between starting and ending modulus a stronger variation between starting and ending frequencies is observed. In the case of a material that presents a variation of 50% between starting and ending modulus, an approximate variation of 30% between initial and ending frequencies is observed.

5.6. Discussion

When preparing a finite element model that is subjected to parameterization, the consideration of factors not normally taken into account in regular model construction is basic. Of these, the choice of updating parameters is the most important. The analyst should attempt to assess the confidence, which can be attributed to various features of the model. For example, the main span of a beam, away from the boundaries, might be considered to model with a high level of confidence. Joints and constraints could be considered to be less accurately modeled, and therefore in greater need of updating.

The numerical predictions (e.g. natural frequencies and mode shapes) should be sensitive to small changes in the parameters. But it can be very difficult to find joint parameters to which the numerical predictions are sensitive. If the numerical data is insensitive to a chosen parameter, then updating will result in a change to the

parameter of uncertain value, because the difference between predictions and results has been reconciled by changes to other (more sensitive) parameters that might be less in need of updating. The result, in that case, will be an updated model, which replicates the measurements but lacks physical meaning. In this chapter a review of the most important parameters when modeling concrete or masonry structures was developed. The author considers that non-linear parameters, like tension stiffening or constitutive equation of materials, are fundamental when damage models are studied. Also the support condition resulted to be fundamental when modeling two-dimensional structures like concrete slabs. Finally, the hardening phenomena in masonry structures were a key issue when attempting to model such king of structures.

six

Laboratory Works

6.1. Introduction

This chapter describes a series of experimental works developed under laboratory conditions, with the aim at studying the correlation between the occurrence of damage and the variation of the dynamic response of different structural members. Five different campaigns were developed, all them on structural members commonly used in building construction. A brief description of those experimental campaigns is condensed in the following points:

1. Characterization of mechanical damage due to a load-cracking process in simply supported RC beams.

2. Influence of mechanical damage due to a load-cracking process in suspended supported RC beams.

3. Effect of simultaneous mechanical and chemical damage by carbonation, sulphates and chlorides in simply supported RC beams.

4. Influence of axial load on the dynamic behavior of masonry walls

5. Characterization of axial load in the dynamic behavior of stone columns

6.2. Stiffness degradation in supported RC beams

6.2.1. Introduction

An experimental program is set up to establish the relation between damage and changes of the dynamic system characteristics. The objectives in this campaign are:

- To study the influence of different damage levels (reduction of stiffness by cracking) on the first few natural frequencies of concrete beams.

- To calibrate the *tension-stiffening* model proposed in chapter 4.

- To study the influence of carbon fiber laminates (used as a reinforcement) on the dynamic behavior of RC beams.

The beams are simply supported and therefore are subjected not only to forced vibration but also to environmental pollution. The dynamic behavior of the beams is exposed to (and polluted by) the environmental vibration of the laboratory. Identification is therefore more complex but also the support condition of the beams is more similar to real structures.

The methodology used to assess the dynamic parameters of the beams is in Chapter 4. A set of 10 reinforced concrete beams in two different configurations (Beams type I and II, described in the *following* section) was subjected to an increasing static load to introduce cracks. After each load step, an experimental modal analysis is performed on the beam.

In this section, the experimental setup is described, both for the static and dynamic test. The finite element model developed to simulate the damage influence on dynamic properties of the beam is also described. Finally, the results of the evolution of dynamic parameters through the different damage states (both numerical and experimental) are presented, compared and discussed. The experimental campaign was developed on the Structural technology Laboratory in the technical University of Catalonia and was developed in cooperation with Professor Toni Marí and his team. Further details of the experimental works (but not related with dynamic identification) can be found in Oller [2001].

6.2.2. Materials and experimental method

Beams type I

The elements tested were 2,40 m length beams of rectangular cross section (300 × 200 mm). To avoid any coupling effect between horizontal and vertical bending

modes, the width (300 mm) was chosen to be different from the height (200 mm). The beams were reinforced with four bars, two of 16 mm diameter in the bottom layer and two of 8 mm in the top layer, corresponding to a reinforcement ratio of 0.83 % [Figure 6.2.1]. Shear reinforcement consisted in vertical stirrups of 12 mm of diameter, every 150 mm.
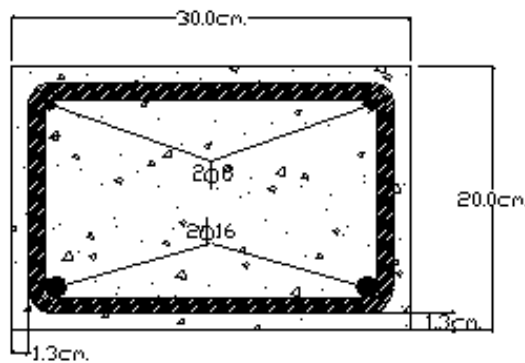
Figure 6.2.1. Cross section of beam type I.

Beams type II

The elements tested were 2,50 m length of rectangular cross section (300 × 200 mm). As for *beams type I*, the width (300 mm) was again chosen to be different from the height (200 mm). The beams were reinforced with four bars, two of diameter of 20 mm in the bottom layer and two of 8 mm in the top layer, corresponding to a reinforcement ratio of 1.21 % [Figure 6.2.2]. Shear reinforcement consisted of vertical stirrups of 12 mm of diameter, every 100 mm.
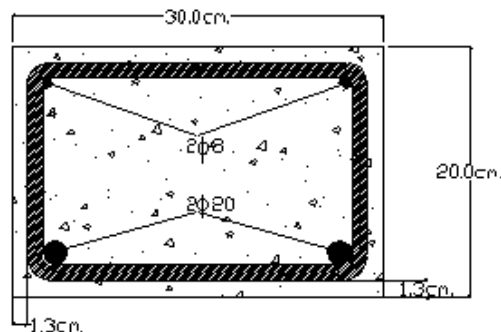
Figure 6.2.2. Cross section of beam type II.

A total beam mass of about 350 kg resulted for a density of the reinforced concrete of 2400 kg/m^3. Both types of beams were tested using the same configuration: pinned supports with a span of 200 cm [figure 6.2.3]. The load was concentrated and applied at midspan, using a 15x40 cm neoprene to ensure a correct distribution.
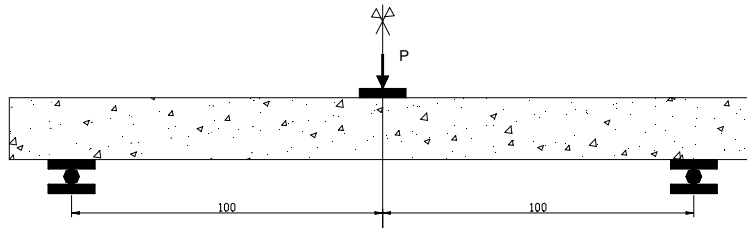
Figure 6.2.3. Lateral view of the beams (both types).

Materials

A concrete with a compressive strength of 25 MPa was designed with an aggregate with a maximum size of 12 mm. A strict control of the strength evolution was developed by testing cylinders after 7, 28 and 126 days of casting concrete. Uni-axial compressive tests and Brazilian test were carried out to obtain maximum compressive and tensile strengths of concrete. Table 6.2.1 presents the obtained results.

Reference	Maximum compressive strength (MPa)	Reference	Maximum tensile strength (MPa)
After 7 days			
Cylinder 01	27,4	Cylinder 04	2,6
Cylinder 02	28,96	Cylinder 05	2,39
Cylinder 03	27,16	Cylinder 06	2,77
average	**27,84**	**average**	**2,59**
After 28 days			
Cylinder 07	34,72	Cylinder 10	3,1
Cylinder 08	32,14	Cylinder 11	2,25
Cylinder 09	38,67	Cylinder 12	3,02
average	**35,17**	**average**	**2,79**
After 126 days			
Cylinder 13	42,32	Cylinder 16	2,93
Cylinder 14	43,74	Cylinder 17	3,44
Cylinder 15	41,64	Cylinder 18	3,02
average	**42,57**	**average**	**3,13**

Table 6.2.1. Tests in concrete cylinders after 7, 28 and 126 days of casting.

Strain controlled tests were also developed after 126 days, to define the complete load-strain relationship of the concrete. The cylinder was instrumented with three strain transducers and the load was servo-controlled by deformation [figure 6.2.4]. The obtained constitutive equation presented a maximum load of about 42 MPa at a 0.21% strain [figure 6.2.5]. The mean value for the identified strain modulus is 28,78 GPa.
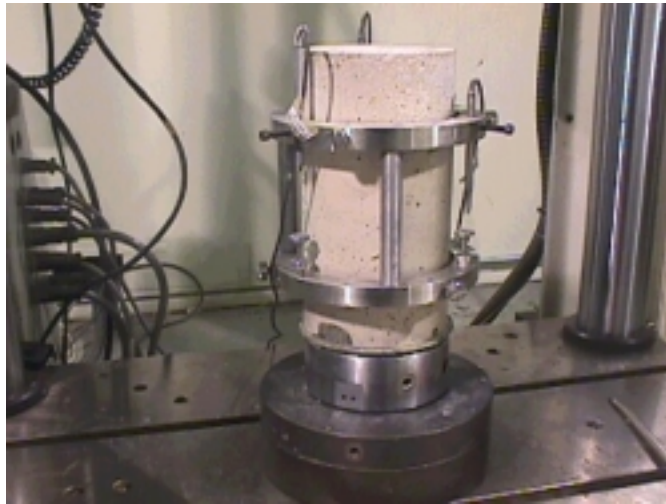
Figure 6.2.4. Instrumentation for strain controlled cylinder tests.
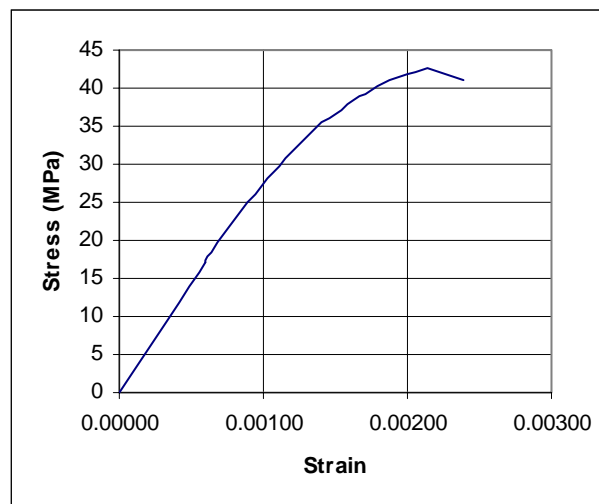
Figure 6.2.5. Experimental stress-strain diagram for concrete.

The dynamic strain modulus was also evaluated following the ASTM C-215 recommendation [figure 6.2.6]. The test consists on the experimental determination

of dynamic strain modulus by measuring dynamic response of a concrete cylinder subjected to dynamic excitation.

The experimentally identified frequencies and calculated modulus are described in table 6.2.2.

cil No.	x mm	y (high) mm	y2 (high) mm	z mm	weith kg	density kg/m3	identified frequency hz	dynamic E modul Gpa
1	149,30	298,20	297,20	149,80	12,00	2.294,77	6.300	32,30
2	150,00	297,50	297,50	149,50	12,00	2.290,19	5.910	28,30
							average	30,30

Table 6.2.2. Dynamic strain modulus calculations.

An increment of 5% is observed between identified Dynamic (30.3 GPa) and Static (28.8 GPa) modulus.

Figure 6.2.6. Identification of the longitudinal frequency in cylinders to calculate dynamic elasticity modulus.

Mechanical properties of steel are detailed in Table 6.2.3.

Elastic limit	543 MPa
Failure Limit	649 MPa
Strain at failure	24.4%

Table 6.2.3. Mechanical properties of reinforcement steel.

After the first cracking process, a strengthening of the beams was performed with carbon fiber laminate (CFL). The applied CFL was of the type S&P 150/2000 of 1.4 mm. Thick and 100 mm. de wide. He CFL was attached to the beam using epoxi-resins as adhesive. The mechanical properties of this material are described in table 6.2.4.

Elasticity Modulus	Tensile maximum stress	Maximum strain
150000 N/mm^2	2500 N/mm^2	1.6%

Table 6.2.4. Mechanical properties of reinforcement carbon fiber laminate.

The beams were loaded in a MTS reaction-frame [figure 6.2.7.] with an actuator having a capacity of 1000 kN and a maximum displacement of 250 mm.

Figure 6.2.7. Static test set-up.

A simply supported condition was obtained by using two hinges [figure 6.2.8]. The hinges were made of a solid 50 mm diameter and 350 mm long cylinder supported in to a plate 350x150x30 mm. The support apparatus were installed above a welded steel structure. The steel structure was designed to be stiffer and therefore has higher frequencies than the concrete beam to avoid coupling effects.
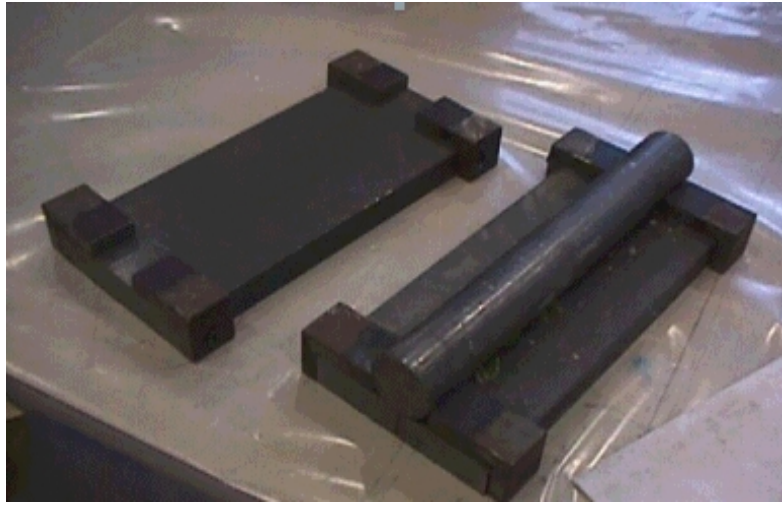
Figure 6.2.8. Used support apparatus.

The load was applied at midspan by controlling the displacement of the actuator (displacement controlled test), independently of the magnitude of the load. The magnitude of the load varied for every specimen. Load is described further on for every particular case. The load was applied trough a 400x200x28 mm neoprene element, to regularize the loaded surface [figure 6.2.9]. Through the loading process, three vertical displacement transducers were attached to the beam, one at mid span ant two at the edges. Horizontal strain gauges were also attached to the beam to measure concrete strain at different distances from the neutral fiber [figure 6.2.10].

Figure 6.2.9. Neoprene element used to regularize the load.

Figure 6.2.10. Attached strain gauges and displacement transducers.

Dynamic testing

The beams were dynamically tested at four different stages of loading process:

- Undamaged beam

- After the application of a service load

- After repairing with carbon fiber laminates

- After ultimate failure

The source of excitation was an impact hammer for all the cases [details of testing equipment are presented in appendix A]. Output only measurements were developed (the input force was not measured). The time-length of the dynamic test was defined as one second in a first approach, but after certain number of tests it was observed that a complete dissipation of the energy took place in less than 0.5 seconds. Therefore, subsequent tests had a time-length of 0.5 seconds.

Two accelerometers were attached to the beam at 15 and 35 cm from mid-span [figure 6.2.11]. To ensure an adequate adhesion, epoxy resin was applied between the accelerometer and the beam. The two attached sensors consisted in:

- a seismic accelerometer of 1 pd. (0.454 kg) with a frequency range of 0.025 to 800 Hz [figure 6.2.12b].

- a quartz accelerometer of 7.4 Oz (0.210 Kg) with a frequency range of 0.5 a 2000 Hz [figure 6.2.12a].

By this combination, the measured range of frequencies achieved 0.025 to 2000 Hz.
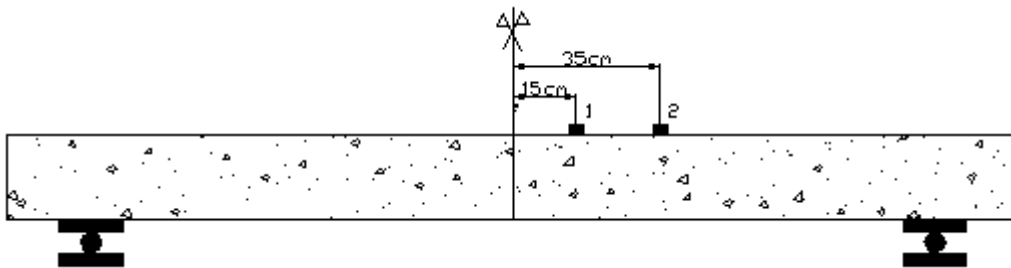
Figure 6.2.11. Dynamic sensors configuration.

(a)   (b)
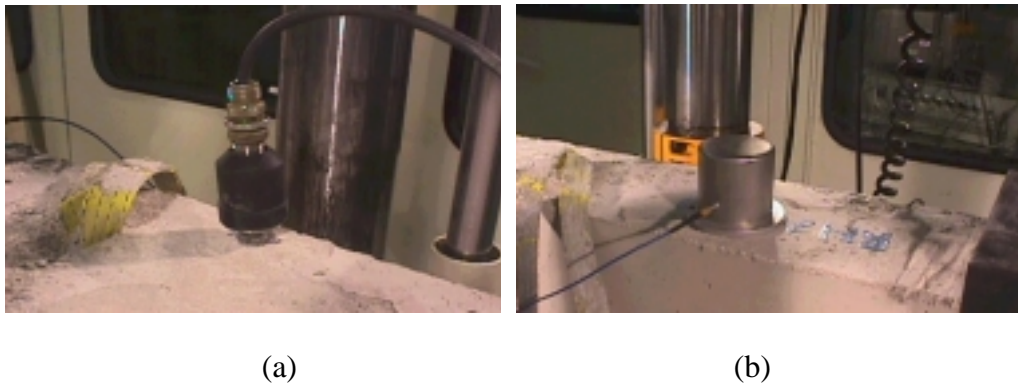
Figure 6.2.12. Dynamic sensors. Quartz (a) and seismic accelerometers (b).

Other electronic equipment was also used to measure dynamic information: a signal conditioner (F482A16 of Piezontronics), connector block (National Instruments CB-40) and a data acquisition card (DAQCard 1200 of National Instruments).

6.2.3. Results

Ten beams were tested, five of each type (*I* or *II*). The first tested beam of each class was used as a reference and it was not reinforced with carbon fiber laminate. Dynamic testing was developed before and after every load process. For all

dynamic tests, the load was retired, so boundary conditions were not modified by the influence of hydraulic actuator and the vibration was completely free.

All the beams showed a clear pattern: the first frequency is highly dominant and easily recognizable.

Some representative diagrams in time and frequency domain are presented in figure 6.2.13.

(a)   *(b)*

(c)   *(d)*
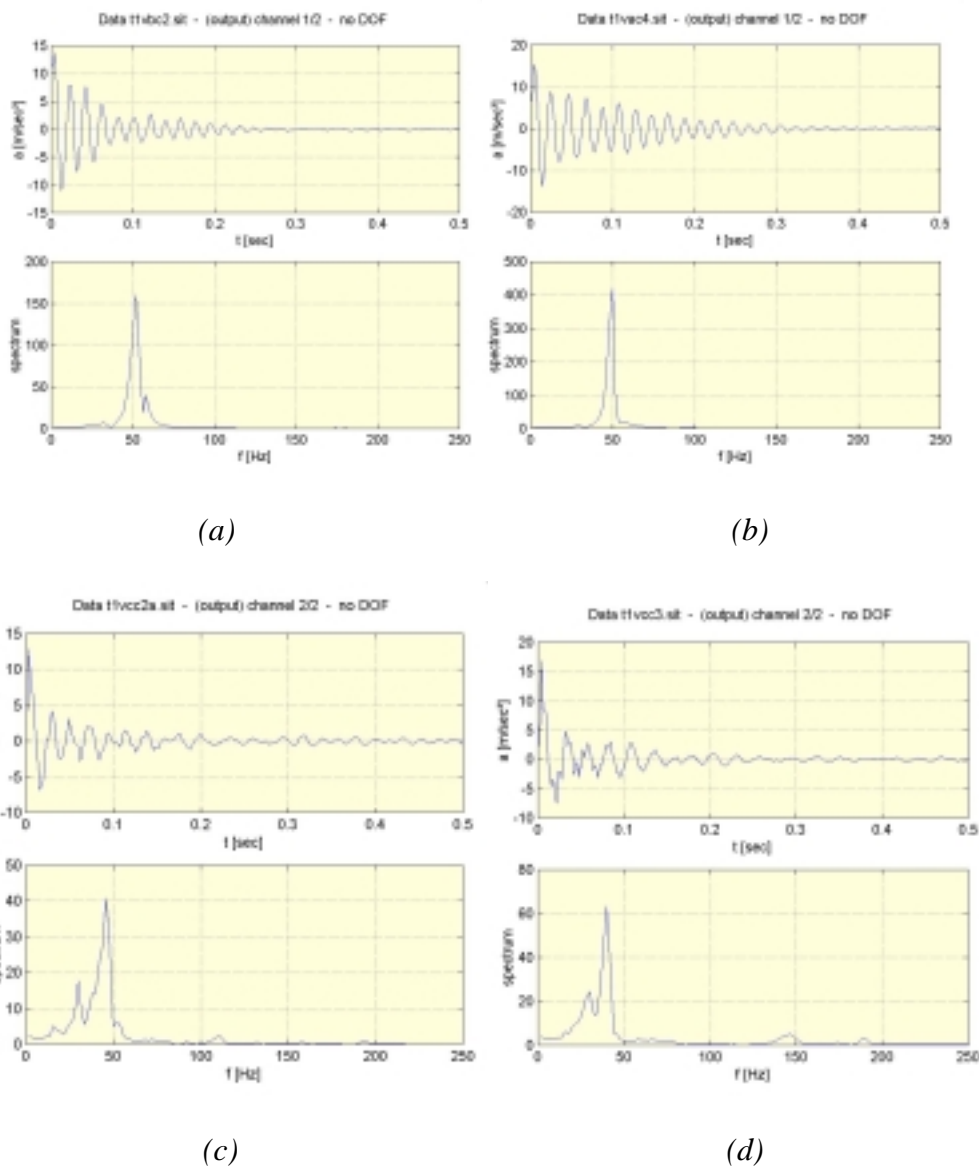
Figure 6.2.13. Dynamic measurements of beam EX1E. Undamaged state (a), after a 50,3 kN load (b), after a 81,15 kN load (c) and after a 82,55 kN load (d).

Beam	applied load (kN)		
	first step	*2d step*	*tird step*
EX1E	50	81	82.55
EX1D	51	74	-
EX1C	49	104	-
EX1B	50	100	-
EX1A	-	-	-

Table 6.2.5. Applied load in beams type I.

Beam	f1 (Hz)					f2 (Hz)				
	undamag	*first step*	*CFL*	*2d step*	*3d step*	*undmgd*	*first step*	*CFL*	*2d step*	*3d step*
EX1E	53	50	-	45	42	163	147	-	131	125
EX1D	59	51	40	40	-	198	163	150	160	-
EX1C	50	45	40	40	-	165	155	145	144	-
EX1B	59	51	45	42	-	234	193	162	154	-
EX1A	-	-	-	50	-	-	-	-	157	-

Table 6.2.6. First and second measured frequencies, beams type I.

Beam	f2/f1				
	undamag	*first step*	*CFL*	*2d step*	*3d step*
EX1E	3,08	2,94	-	2,91	2,98
EX1D	3,36	3,20	3,75	4,00	-
EX1C	3,30	3,44	3,63	3,60	-
EX1B	3,97	3,78	3,60	3,67	-
EX1A	-	-	-	3,17	-

Table 6.2.7. Second / first natural frequencies ratio, experimental results of beams type I.

An increasing load was applied at mid-span; the first step achieved for most of the cases the maximum service load [table 6.2.5 for *beams type I* and table 6.2.8 for *beams type II*]. Natural frequencies were evaluated through all the load process. A clear reduction on the magnitude of the first and second natural frequencies is observed when damage is induced [table 6.2.6 for *beams type I* and table 6.2.9 for *beams type II*]. The ratio between second and first natural frequencies is a good parameter to estimate the support conditions [section 5.3.3.]. For this particular case, this parameter showed small variation for the first three steps of *beams type I* [table 6.2.7] and a higher dispersion for further load steps. *Beams type II* presented a more stable behavior through all load steps [table 6.2.10].

Beam	applied load (kN)	
	first step	2d step
EX2E	50	-
EX2D	74	105
EX2C	66	143
EX2B	71	-
EX2A	72	-

Table 6.2.8. Applied load in beams type II.

Beam	f1 (Hz)				f2 (Hz)			
	undmgd	first step	CFL	2d step	undamag	first step	CFL	2d step
EX2E	44	40	-	-	144	135	-	-
EX2D	58	51	50	50	174	143	146	152
EX2C	54	48	33	30	163	148	103	119
EX2B	43	38	-	-	145	130	-	-
EX2A	55	48	-	-	193	186		

Table 6.2.9. First and second measured frequencies, beams type II.

Beam	f2/f1			
	undmgd	first step	CFL	2d step
EX2E	3,27	3,38	-	-
EX2D	3,00	2,80	2,92	3,04
EX2C	3,02	3,08	3,12	3,97
EX2B	3,37	3,42	-	-
EX2A	3,51	3,88	-	-

Table 6.2.10. Second / first natural frequencies ratio, experimental results of beams
type II.

6.2.4. Numerical and analytical simulation

A numerical simulation of the beams was developed with the objective of complementing the direct-measured data and to simulate the dynamic behavior of the tested elements. The model was able to simulate all the load-unload cycles and the correspondent dynamic evaluation after the appearance of damage. A different model was developed with the objective of following the particular load conditions of every beam. Detailed information of the theoretical background of the model and the considered constitutive equations and tension stiffening simulation has been presented in section 4.3.5.1. and section 5.3.

The discretization of the beams is showed in figure 6.2.14. Beams of Type 1 are modeled with 50 finite elements. Beams of type II with 52 elements.
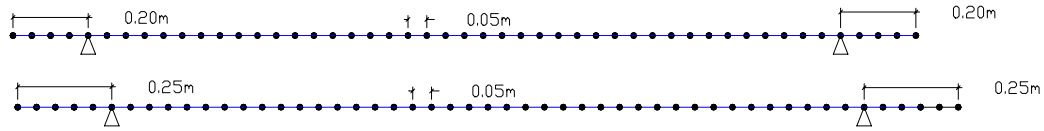
Figure 6.2.14. FEM discretization of the beams. Beam type I (above) and Beam type II (below)

Beam	undamaged		applied	damaged	
	f1 (hz)	*f2 (hz)*	*load (kN)*	*f1 (hz)*	*f2 (hz)*
EX1E	56	212	50	47	179
EX1D	56	212	51	46	175
EX1C	56	212	49	47	179
EX1B	56	212	50	47	179
EX1A	56	212	-	-	-

Table 6.2.11. Evolution of natural frequencies after loading. Numerical model of beams type I.

Beam	undamaged		applied	damaged	
	f1 (hz)	*f2 (hz)*	*load (kN)*	*f1 (hz)*	*f2 (hz)*
EX2E	57	220	116	failure	failure
EX2D	57	220	74	47	179
EX2C	57	220	66	48	182
EX2B	57	220	71	47	179
EX2A	57	220	72	47	179

Table 6.2.12. Evolution of natural frequencies after loading. Numerical model, beams type II.

The ultimate load supported by the beam can be calculated by an analytic way (using typical formulas from concrete desing codes) or by loading the FEM model until failure. Both analytical and FEM ultimate load results are presented in table 6.2.13.

Beams type I		Beams Type II	
Analytic	FEM	Analytic	FEM
68.87 kN	69.025 kN	102.62 kN	94.98 kN

Table 6.2.13. Analytical and FEM ultimate loads

The evolution of the frequencies through the load process can also be calculated using an equivalent cracked inertia [Branson, 1977]. In general, Branson's formula overestimates the influence of cracking, therefore; the calculated frequencies have lower values than the experimental or FEM values. Table 6.2.14 presents the equivalent inertia by using the Branson's formula. If the calculated frequency values are compared to the experimental ones [tables 6.2.11 and 6.2.13], the overestimating results obvious.

Beam	*undamaged* *f1 (hz)*	*applied* *load (kN)*	*Equivalent* *inertia (cm4)*	*damaged* *f1 (hz)*
EX1E	58	50	11.859	40
EX1D	58	51	11.838	40
EX1C	58	49	11.931	40
EX1B	58	50	11.894	40

Beam	*undamaged* *f1 (hz)*	*applied* *load (kN)*	*Equivalent* *inertia (cm4)*	*damaged* *f1 (hz)*
EX2E	60	116	14.979	45
EX2D	60	74	15.073	45
EX2C	60	66	15.125	45
EX2B	60	71	15.089	45
EX2A	60	72	15.085	45

Table 6.2.14. Equivalent inertia method to calculate evolution of frequencies.

6.2.5. Discussion

The results of this experimental campaign allowed some important considerations:

- The method proposed in chapter 4 was successfully applied to identify the dynamic parameters in simply supported RC beams subjected to progressive damage by cracking. First and second natural frequencies were measured; however, higher frequencies were no identified due to the strong interference of pollution from ambient vibration.

- In general, an important reduction of the stiffness -and therefore of the natural frequencies- is observed after a load process. After inducing cracks with a concentrated load (70% of the ultimate), the reduction of the first natural frequency achieves values up to 23%, depending of the magnitude of the load [figure 6.2.15]. The reduction of the frequencies is not the same in all the beams, six beams (1C, 1B, 2D, 2C, 2B and 2A) presented a similar behavior, while the other three (1D, 2E and 1E) are clearly deviated from the average [figure 6.2.15].
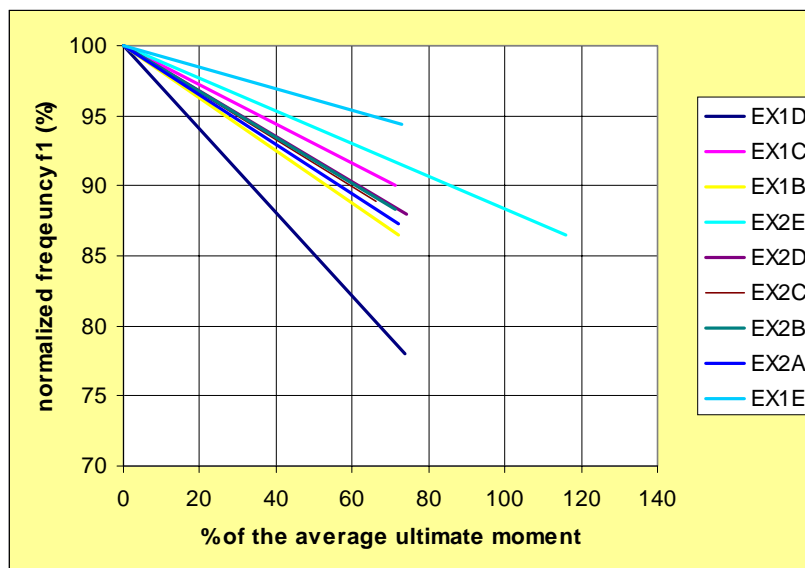
Figure 6.2.15. Evolution of the first natural frequency after the first load step.

- In beams subjected more than one increasing load steps, the first natural frequency decreased continuously for most of the cases [figure 6.2.16]. In the case of beam *EX1D* a slight increment of the frequency is observed after the first load step, this variation is obviously not related to a damage process and is possibly due to uncontrolled experimental factors [figure 6.2.16].
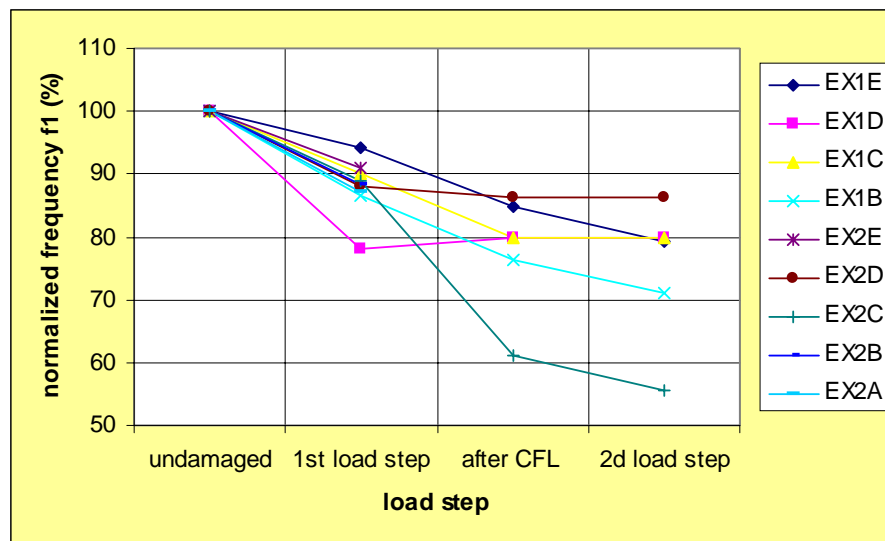
Figure 6.2.16 Evolution of the first natural frequency through all load processes.

- An important dispersion was noticed when comparing first natural frequency of undamaged beams. This variation is possibly due to the age and the curing conditions of the beams. Another possibility is the lost of stiffness of the beams due to curing conditions and shrinkage. It is worth mentioning that some beams presented visible cracks before have been subjected to any load process. Those cracks were produced by uncontrolled construction conditions, such as shrinkage or manipulation of the beams.

- As mentioned before, an important pollution of the dynamic signal was produced by the type of support conditions. The beam was not isolated from the ambient vibration and was simply supported by using a rigid hinge. This connection transmitted ambient vibration from the support to the beam and became a problem when identifying higher frequencies in the FFT diagram, especially after the third frequency.

- Numerical modeling was developed using material characteristics obtained from concrete cylinders. The curing and atmospheric conditions where not exactly the same for cylinders and beams (due to logistics demands). Therefore, if the model is developed using parameters measured in the cylinders, the dynamic behavior of the beam is strongly modified. This behavior does not match to the experimental one. A subject of primary importance is that the use of dynamic strain modulus, measured from concrete cylinders for the numerical simulation generates unrealistic higher values of the stiffness. It seems to be a strong influence of the scale and shape of the structure.

- If a statistical treatment of the data is to be developed, it is fundamental to pay special attention to the construction, curing, and manipulation of the specimens. The same conditions must be kept to all beams to maintain the same characteristics.

- An independent study was developed to investigate if the location of the accelerometer influenced the identified frequencies. The study consisted in evaluating the same beam several times modifying the position of the sensor by 25 cm every time. The accelerometer was attached at 0, 25, 50, 75, 100 and 125 cm from the edge of the beam. (the beam has 250 cm length). The study has demonstrated that any position of the accelerometer is appropriate to identify the first natural frequency (44 Hz) [figure 6.2.17].
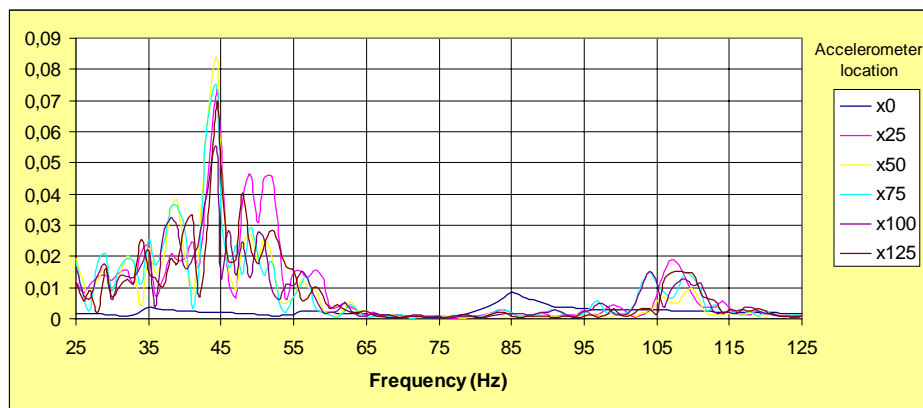
Figure 6.2.16 Frequency spectra for different accelerometer positions.

6.3. Stiffness degradation in suspended RC beams

6.3.1. Introduction

In this section, an experimental program aimed at establishing the relation between damage and changes of the dynamic system characteristics is described. The project consists of a set of five reinforced concrete beam, subjected to an increasing static load to introduce cracks. After each load step, an experimental modal analysis is performed on the beam. In this section, the experimental setup is explained, for both the static and dynamic test. The finite element model developed to simulate the damage influence on dynamic properties of the beam is also described. Finally, the evolution of dynamic parameters through the different damage states (both numerical and experimental) is explained, compared and discussed. The experimental campaign was developed on the Structural Mechanics Laboratory in the Catholic University of Leuven, Belgium. The author of this thesis developed a research stay during 2000 under the direction of professor De Roeck and participated on the tests and numerical modeling described further on. Detailed information of the implementation of the tests can be found in Peeters et al. [1996] and Maeck and De Roeck [1999a, 1999b, 1999c and 2002]

6.3.2. Materials and experimental method

Description of the tested beams

Four objectives were contemplated in designing the test beams:

• The first eigenfrequency should be comparable with the lowest eigenfrequencies encountered in typical civil engineering structures like bridges: 2-10 Hz. Another advantage of a low fundamental eigenfrequency is that within a specific frequency interval (e.g. 0-1000 Hz) a lot of eigenfrequencies will be present. This is important because there is some belief that the higher modes are influenced more by cracking than the lower ones. The eigenfrequencies are proportional to: a height (h) of 0.2 m and a length (L) of 6 m result in a first h/ L 2 eigenfrequency of about 20 Hz.

• Previous test programs [Dieterle and H. Bachmann, 1980 and Rohrmann et al. 1991] have revealed the difficulty of obtaining simple supports for dynamic tests:

ambient vibration interferes with the artificial force input, finite rigidity of the supports can influence mode shapes and eigenfrequencies and radiation will add extra damping to the inherent damping of the (cracked) concrete beam. Therefore, a completely free test setup is adopted which means that the beam is supported by a number of very flexible springs resulting in rigid body eigenfrequencies (around 1 Hz) much lower than the eigenfrequency of the first bending mode (around 20 Hz). A consequence is that the static test configuration will be different from the dynamic one. We should mention the work by Brincker et al. [1995], in which also a free-free dynamic test setup is used. Due to the limited dimensions of the concrete test beam, they could on the one hand suspend the beam vertically, but on the other hand, the eigenfrequencies were quite high (the first eigenfrequency being f1 = 278.8 Hz).

 • To avoid any coupling effect between horizontal and vertical bending modes, the width (0.25 m) is chosen to be different from the height.

 • The reinforcement ratio should be within a realistic range. By a proper choice of the steel quality (yield stress), the interval between onset of cracking and beam failure can be made large enough to allow modal analysis at well separated levels of cracking.

These four conditions result in a 6 m long beam of rectangular cross section (200 × 250 mm). The beams are reinforced with 6 bars of diameter 16 mm, equally distributed over tension and compression side, corresponding to a reinforcement ratio of 1.4 % [figure 6.3.1, left]. Shear reinforcement consists of vertical stirrups of diameter 8 mm, every 200 mm [figure 6.3.2]. The steel stress-strain diagram is experimentally determined. An idealization is shown in figure 6.3.1 [center]. The deformation behavior of the concrete is represented in figure 6.3.1 [right]. A total beam mass of m = 750 kg results from a density of the reinforced concrete of = 2500 kg/m^3. Information of the concrete formula used for all the cases is given in table 6.3.1. The concrete has a 50 kN strength in compression. Tensile strength achieves 5,4 kN.
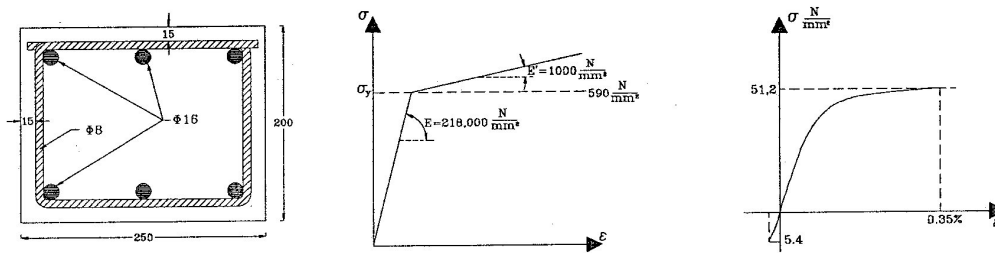
Figure 6.3.1. Cross section [left], stress-strain diagram for steel [center] and stress-strain diagram for concrete [right]
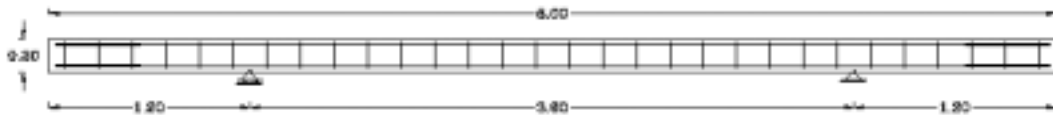
Figure 6.3.2. Beam geometry.

concrete formula		
grain	1120	kg/m3
sand	700	kg/m3
cement	350	kg/m3
water	192.5	kg/m3
w/c ratio	**0.55**	

Table 6.3.1. Formula of the concrete used in all beams.

Three of the beams (number 1, 2 and 5) were simply supported with both sides in a cantilever of 1.2 m to minimize the influence of the own weight. Beam number 3 has the same configuration but using a distance between supports of 6 m (the full beam's span). A static load is applied in the center of the beam [figure 6.3.3]. At each intermediate load step, displacements and crack widths are measured. The other beam (number 4) was tested in with a different support configuration; in this case the damaged was induced in an asymmetrical way. The load and the supports were not symmetrical in a first setup; after a load series, the supports were mirrored to a second setup, as presented in figure 6.3.4.
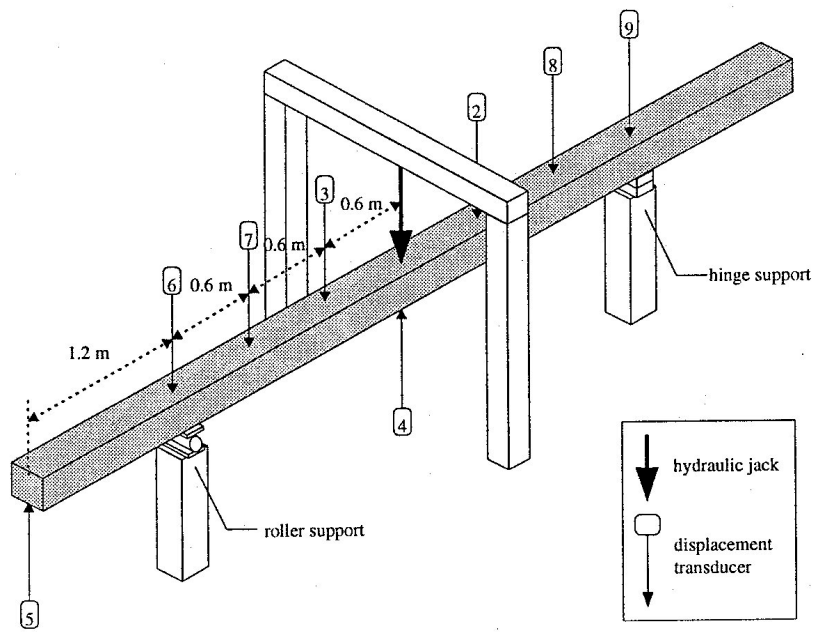
Figure 6.3.3. Static test configuration. Beams 1, 2, 3 and 5.
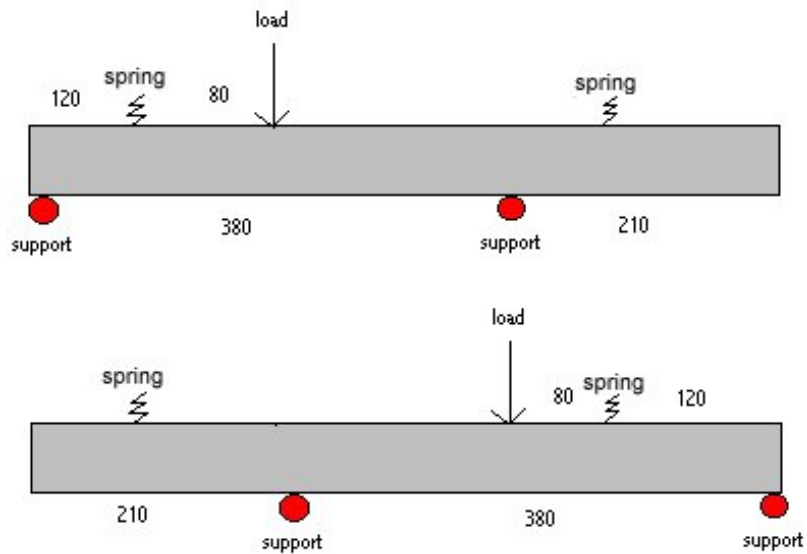
Figure 6.3.4. Static test configuration. First setup (above) and second setup (below). Beam 4.

After every load step, all the beams were unloaded, the supports were removed and the beams were hanged on flexible springs [Figure 6.3.5.], connected to the theoretical nodal points of the first bending mode (distance from the end section). A dynamic force was generated either by an 0.224L electromagnetic exciter (MB MODAL 50A) or an impulse hammer (PCB GK291B20). The vertical force was applied in an outer point of the end section to excite vertical bending and torsional modes.
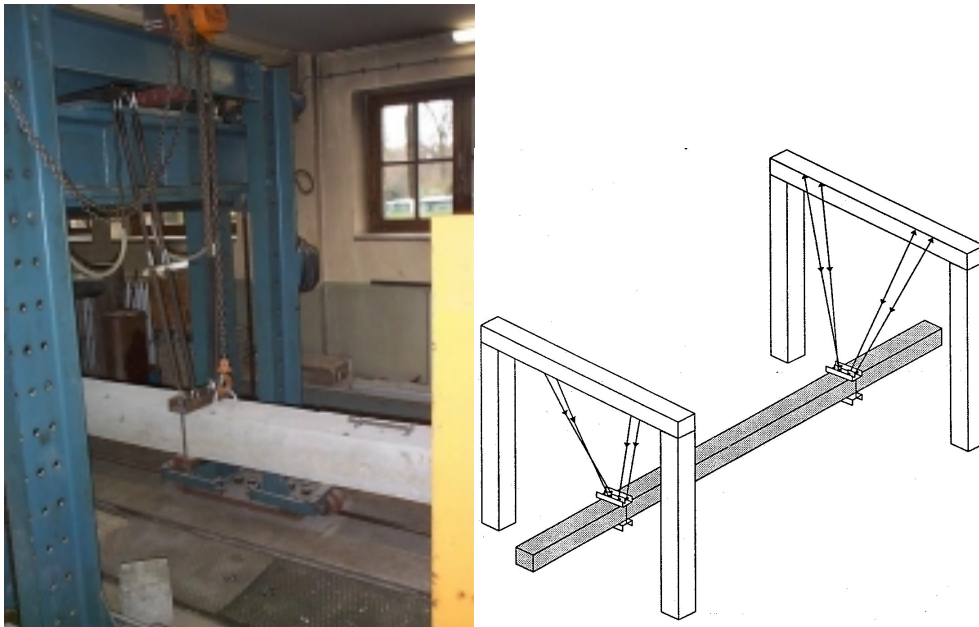
Figure 6.3.5. Dynamic test configuration.

Accelerations were measured at every 0.2 m on both sides of the beam with accelerometers PCB 338A35 and 338B35 [Figure 6.3.6.]. Under this configuration (64 measurement points), it is expected to measure accurately several frequencies and modal shapes. Acquisition system was different for dynamic or static configurations since the tests were independent [Figure 6.3.7.]

Figure 6.3.6. Dynamic instrumentation of the beam.
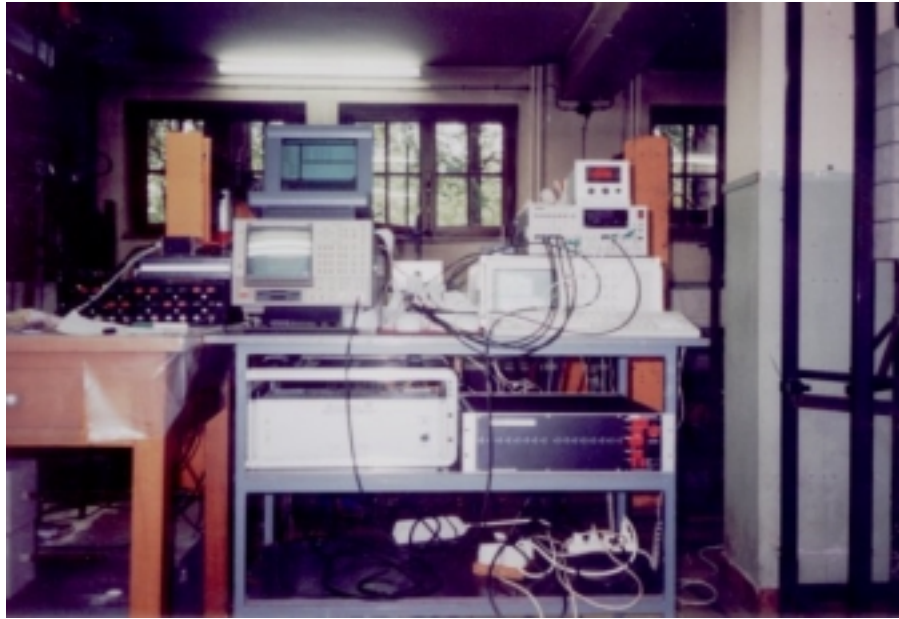
Figure 6.3.7. General view of the dynamic acquisition system.

Materials

At the time of casting, several cylinders are sampled from the concrete used in the beam. The mission of those cylinders is to provide detailed information about the basic constitutive material of the beam. This data is fundamental when performing numerical models of the beam. Tests carried out in cylinders consist on:

- Uniaxial compressive strength

- Brazilian test for tensile strength characterization

- Strain-controlled compressive tests to define strain-stress diagram

- Dynamic modulus test (ASTM C-215)

Uniaxial compressive strength

The same concrete was used for all beams, and the mean value of the compressive strength of this concrete was 51,0 kN. The cylinders were tested several weeks after casting; therefore, this value is used as an asymptotic reference for the age-strength evolution of the concrete.

Brazilian test

The test was developed both in cylinders and cubes taken from the original concrete [figures 6.3.8 and 6.3.9]. After the correction due to the geometry, the mean value of tensile strength resulted in 4,08 kN (8% of the compressive strength).

Figure 6.3.8. Brazilian test, Acquisition and loading systems.

Figure 6.3.9. Brazilian test on cubes to obtain tensile strength of concrete.

Strain-controlled compressive tests

The load was controlled by the mean value of two longitudinal vertical strain transducers, obtaining a post-pick behavior of the concrete [Figure 6.3.10]. The load velocity is 0.001 mm/second between the plates. The maximum strength matched the simple uniaxial tests (51 kN). The maximum load was achieved at a reasonable strain of 0,2% [figure 6.3.11]. A discrete idealization of the results was performed and used furthermore in the numerical simulation [Figure 6.3.12]. Identified average static modulus is 34,0 GPa.

Figure 6.3.10. Strain controlled compressive test on cylinders to obtain static strain modulus.
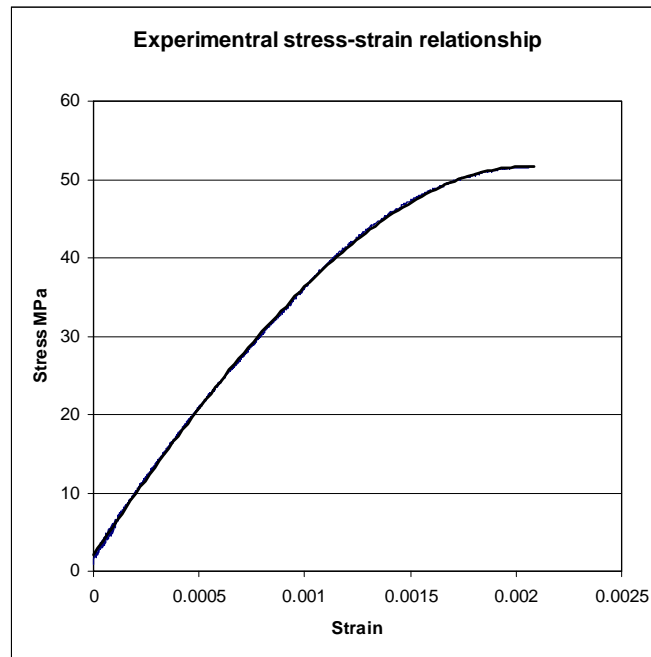
Figure 6.3.11. Experimental stress-strain relationship on cylinders of concrete.
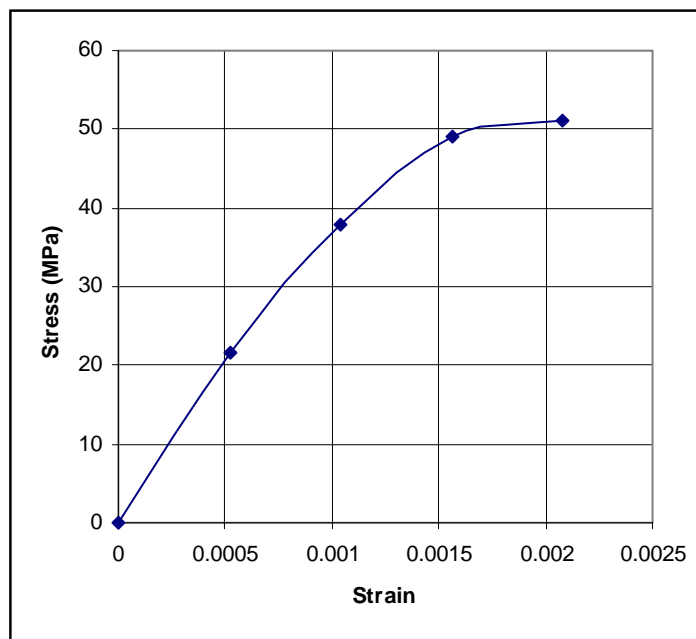
Figure 6.3.12. Discrete constitutive equation of concrete used on the model.

Dynamic modulus test

The test was carried out following the recommendations of ASTM C-215. Six different tests were developed in concrete cylinders and other six in concrete cubes with not significant variation of the results [figures 6.3.13 and 6.3.14]. Identified dynamic modulus is 40,0 GPa. A 17% increment is observed from static (34 GPa) to dynamic modulus, in concordance with available literature and codes (section 3.3.3. of chapter 3).

Figure 6.3.13 ASTM C-215 test to obtain dynamic strain modulus.

Figure 6.3.14. ASTM C215 test to obtain dynamic strain modulus. Acquisition system.

6.3.3. Results

Static test results

The static results of the experimental campaign are not a major subject of this thesis; therefore, full detail in this sense can be obtained from Maeck and De Roeck [1999a, 1999b, 1999c and 2002]. Some results from Beams 1 are presented as an example. Nine points were measured during static loading: applied load and 8 deflection points, location of those measurements is shown in figure 6.19. The first crack was visible at a static load of about 11 kN. At the ultimate load of 60.5 kN, it was impossible to further increase the load, while the displacements increased, meaning that the yield stress of the reinforcement was reached. The force-displacement curve for the mid-section is shown in Figure 6.3.15. At the end of each load step, the beam surface was visually inspected to locate and quantify the cracks [figure 6.3.16]. At load step 2 (24.7 kN), almost all identified cracks were already present. During the following load steps, the individual cracks [figure 6.3.16] were growing but their number did hardly increase.
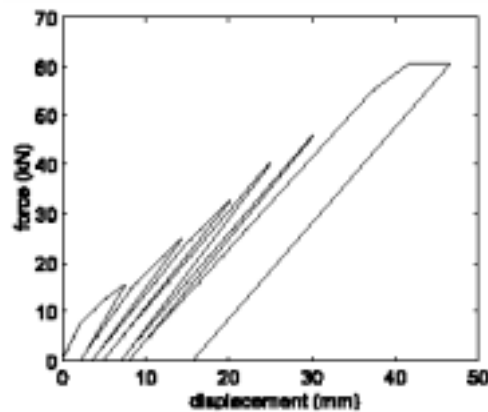
Figure 6.3.15. Results of the three point bending test. Displacements of the mid-section. Beam No. 1.
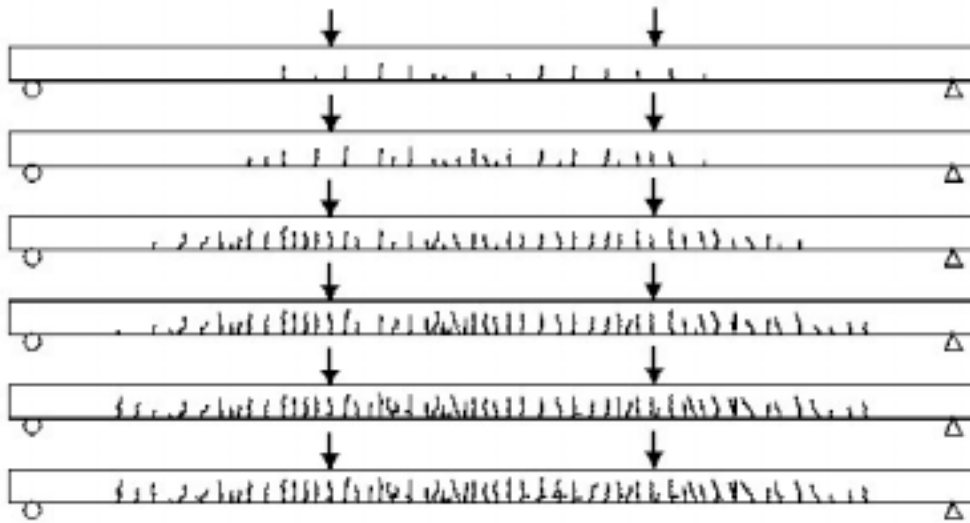
Figure 6.3.16. Evolution of cracks trough the loading process. Beam No. 1.

Dynamic test results

Undamaged state

If the input measurements are not used in the identification procedure, no absolute scaling of the modal amplitudes is possible. To obtain the right relative amplitudes, it is important to carry out simultaneous measurements. For this purpose, 11 Accelerometers were used to simultaneously acquire the response data (IOtech Daqbook /216 acquisition system). A mesh of 58 measurement points was placed on the beam surface at every 20 cm on both sides. 7 Measurement configurations were sufficient to gather all the desired data. At least one reference accelerometer has to be present in every configuration to be able to correlate the different mode shape parts together. A suitable position for this reference accelerometer is one of the end points of the beam: not any mode shape has an inflection at these points. In addition to the common-accelerometer used in every configuration, also the first sensor of a configuration was located at the same position as the last one of the former configuration (leap-frog technique). For each accelerometer configuration a hammer impact test was repeated 3 times. Some typical impact test data are shown in Figure 6.3.17.
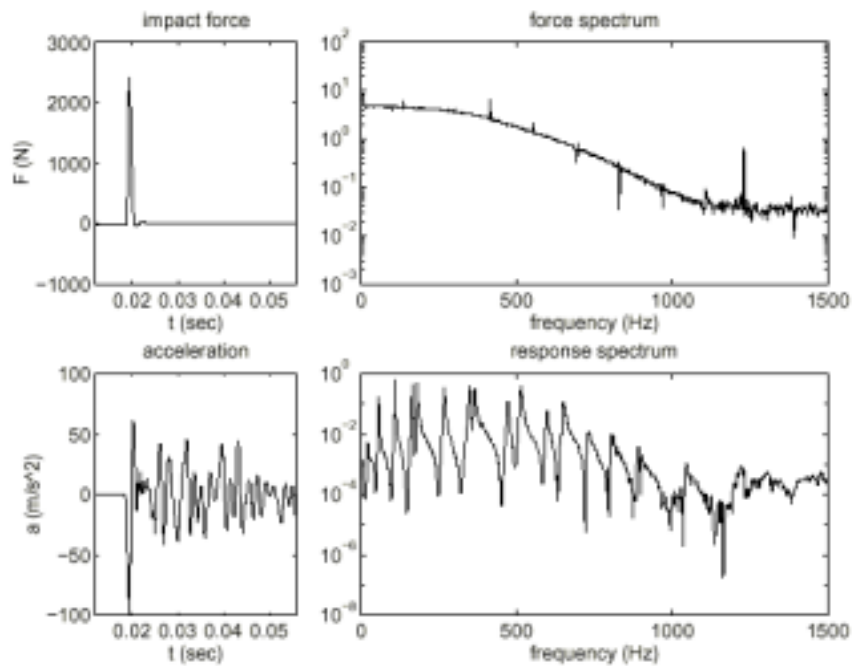
Figure 6.3.17. Time histories and frequency spectra (periodograms) of the impact force and structural response. (fs = 5000 Hz.)
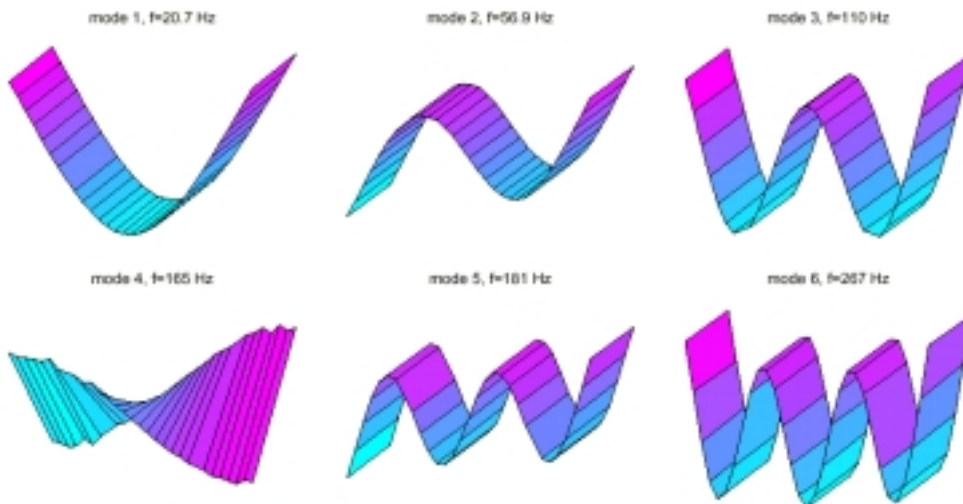
Figure 6.3.18. Experimentally defined modal shapes (mode 1 to 6). Beam No.1.

By a proper choice of the hammer tip, it is possible to generate an adequate response, containing frequency components up to 1000 Hz. For each channel 12288 data points, sampled at 5000 Hz, were collected. The data was preprocessed before

identification: the electrical signals (V) were scaled according to the accelerometer sensitivities to obtain accelerations (m/s ^{2}), the DC- component was removed and the data was filtered by a digital low-pass filter (8th order Chebyshev type I, with a cut-off frequency of 1000 Hz) and re-sampled at a lower rate (2500 Hz). This decimation reduces the amount of data without losing information in the frequency band of interest. The subspace identification method developed by Catholic University of Leuven [Peeters and De Roeck, 2000] was applied to the preprocessed data to obtain the results of figure 6.3.18. Due to the irregular surface of the concrete, the sensitivity axes of the accelerometers were not always perfectly vertical. This fact is clearly reflected in the irregularities observed in the slope of the first torsional mode shape (mode 4, f = 165 Hz, figure 6.3.18).

Damage states

The same procedure as described in the *undamaged state* is repeated after each load step. The beam is dynamically tested after every load step [table 6.3.2]. The evolution of the modal parameters in beam no. 1 is described in Table 6.3.3. and Figure 6.3.19. Due to the rather time-consuming character of the change of the setup between the static and dynamic tests and of the tests themselves, it was impossible to carry out all the intended tests in one day. Before applying the second static load, two weeks after the first, the dynamic test was carried out again. It was observed that the dynamic characteristics of the unloaded beam, hanging on flexible springs, have changed significantly during these two weeks. The almost constant environmental conditions in the lab cannot explain these changes. This "natural" degradation is called load step 1b in the tables and figures.

The first bending (B1) and torsional (T1) eigenfrequencies were most influenced by damage; a decrease of 18 % was observed [figure 6.3.19]. From the second load step to the fifth, the change of eigenfrequencies and damping factors is rather small. As mentioned before, step 2 is also the load step at which almost all the cracks were already present. However, at the ultimate damage state the symmetric bending and antisymmetric torsional modes were decreasing much more spectacularly than in the previous states because of the formation of a plastic hinge at the mid section.

The damping ratio was also calculated using the subspace identification technique [Peeters and De Roeck, 2000]. Although the damping factors were less accurately determined, it is clear that due to damage, they increased in some cases more hat 300% [figure 6.3.20].

Step No.	load (kN)
0	0,0
1	15,5
1b	15,5
2	24,7
3	32,5
4	40,0
5	45,9
6	60,5

Table 6.3.2. Applied load in different steps. Beam No. 1.

Load step	Mode type							
	B1 (s)	B2 (a)	B3 (s)	T1 (a)	B4 (s)	B5 (a)	T2 (s)	B6 (s)
ref	20,67 (0.6)	56,89 (0.6)	109,6 (0.6)	165,1 (0.5)	180,7 (0.6)	267.5 (0.6)	349.7 (0.5)	364.9 (0.6)
1	19,20 (1.1)	55,00 (0.9)	106,1 (0.9)	160,3 (0.8)	174,0 (0.9)	258.9 (0.9)	345.9 (0.6)	353.2 (0.8)
1b	18,23 (2.1)	54,05 (1.1)	103,6 (1.1)	158,3 (0.9)	169,8 (1.1)	253.2 (1.1)	344.7 (0.9)	345.8 (0.5)
2	18,21 (1.8)	52,83 (1.3)	103,3 (1.0)	155,2 (1.0)	168,7 (1.0)	250.5 (1.0)	340.1 (0.8)	343.0 (0.7)
3	18,02 (1.8)	51,66 (1.4)	102,1 (1.0)	152,7 (1.0)	167,5 (1.0)	247.6 (1.1)	336.6 (0.8)	339.8 (0.7)
4	17,69 (1.6)	50,54 (1.5)	100,9 (1.1)	150,6 (0.9)	166,0 (1.1)	244.2 (1.2)	333.2 (1.0)	335.7 (0.6)
5	17,53 (1.7)	49,91 (1.7)	100,0 (1.1)	149,2 (1.0)	165,2 (1.1)	242.2 (1.3)	330.2 (1.0)	333.2 (0.6)
6	16,86 (1.7)	49,71 (1.4)	96,7 (1.1)	135,7 (1.4)	164,5 (1.0)	236.6 (1.2)	327.3 (1.2)	329.5 (0.6)

Table 6.3.3. Variation of the first six bending and first two torsional frequencies (and damping factors between brackets) through the load process. Beam No. 1.

From figure 6.3.19 is evident that the influence of damage in Beam 1, is more important for the first frequency than for further frequencies. Also the damping factor seems to be more affected in the first natural frequency than any other [figure 6.3.20]. This fact represents a benefit when evaluating structures using a low number of sensors, because the first frequency is always easily identifiable.
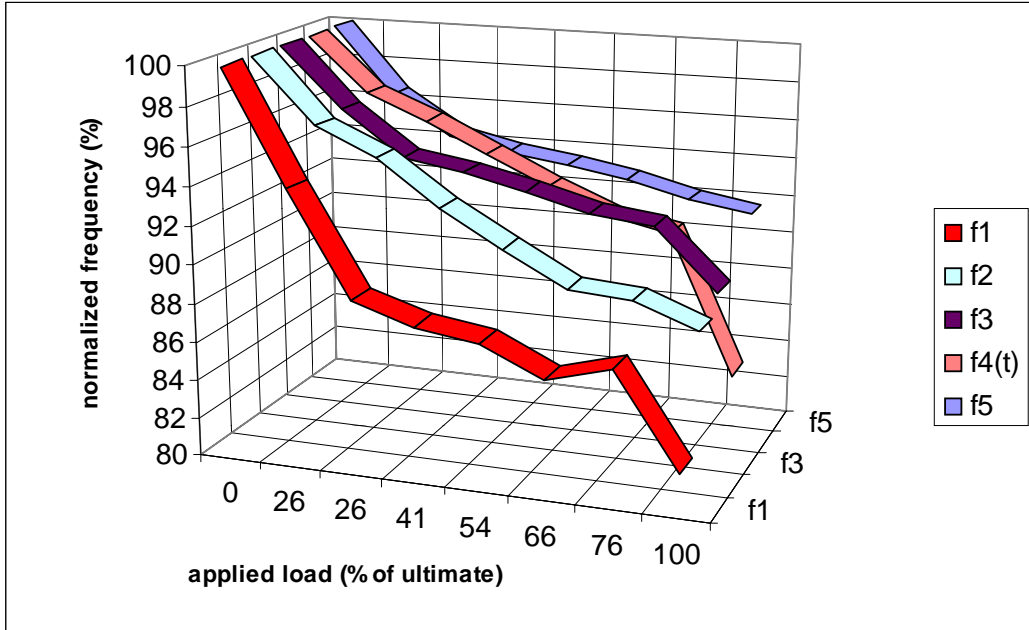
Figure 6.3.19 Relative change of first five natural frequencies through the load

process. Beam No. 1.
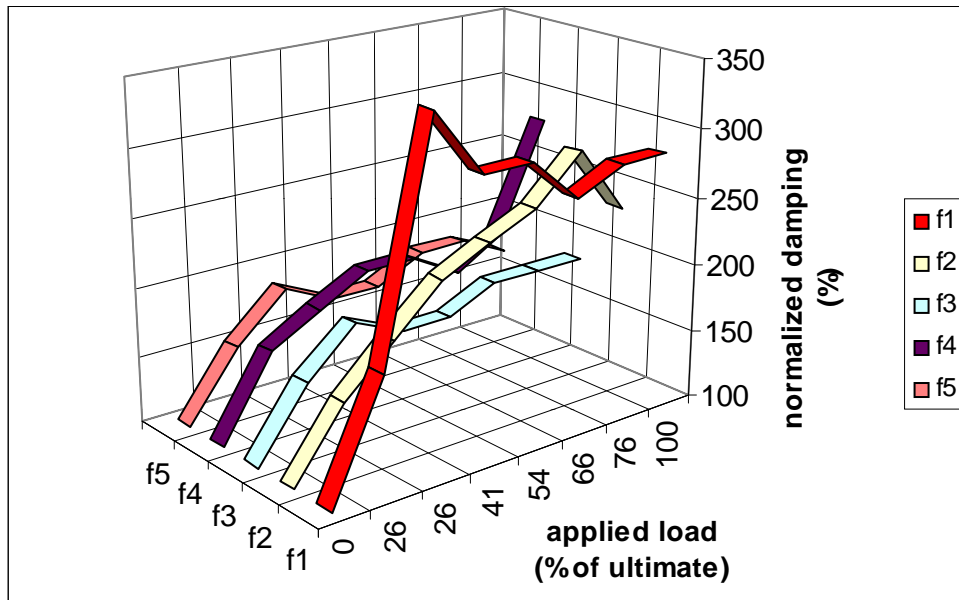
Figure 6.3.20. Relative change of the damping factors of the first five modes.

Beam No. 1.

Beam no. 2 was tested under the same conditions of the first. Once again, a series of load-unload steps where applied to the beam. The magnitude of the applied load was increased in every step [table 6.3.4]. After unloading and hanging the beam, a dynamic test was developed. An important variation of the frequencies is observed [table 6.3.5.], but a clear increment of the frequencies is observed after step five [figure 6.3.21]. Some possible reason to this unexpected change can be related to ageing-effect or uncontrolled change in the support conditions. Obviously, this sudden modification in the trend was not planed in the experiment, and a reasonable explanation of this phenomenon could not be found.

Step No.	load (kN)
0	0,0
1	8,0
2	15,1
3	24,0
4	32,0
5	40,0
6	50,0
7	56,4

Table 6.3.4. Applied load in different steps. Beam No. 2.

laodstep	f1	f2	f3	f4(t)	f5
0	22,4	62,4	119,8	175,1	198,0
1	21,5	61,7	117,4	173,6	195,1
2	18,9	58,5	111,8	166,8	184,2
3	17,5	55,5	107,9	161,4	178,4
4	16,8	53,4	105,3	156,5	174,9
5	18,6	55,6	109,2	160,7	182,1
6	18,7	55,9	108,9	159,7	183,0
7	18,2	55,8	106,3	153,1	182,5

Table 6.3.5. Variation of the first five natural frequencies (Hz) through the load
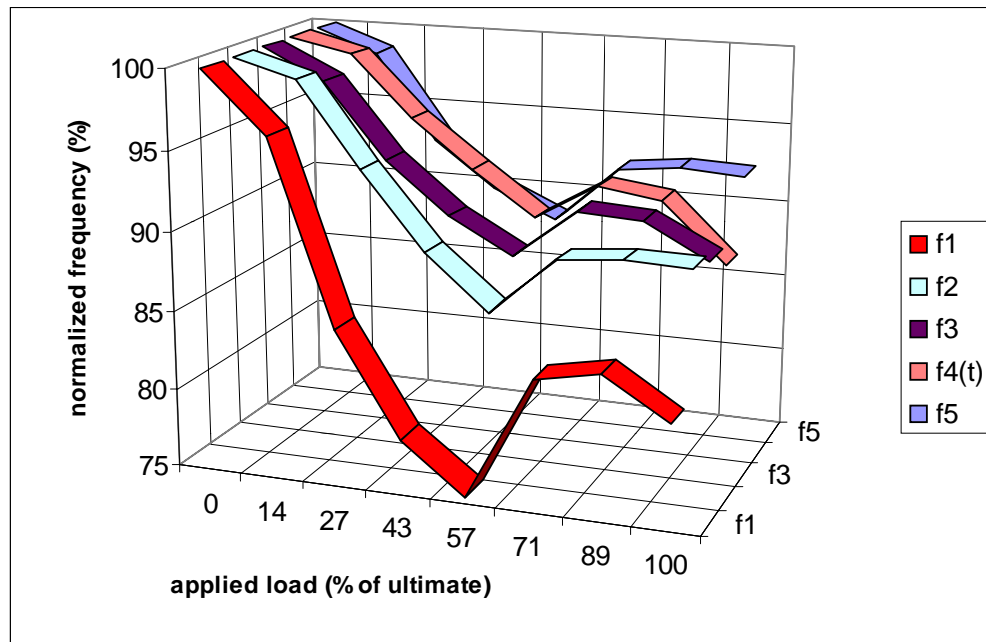
process. Beam No. 2.

Figure 6.3.21 Relative change of first five natural frequencies trough the load

process. Beam No. 2.

Beam no. 3 was subjected again to the same scheme of load-unload and dynamic testing used in the previous beams. In this case, support conditions where modified: the distance between supports was extended to 6 m. (the beam's span). The carried load was obviously reduced [table 6.3.6]. Dynamic test where carried out after every load step and an important reduction of the value of natural frequencies was observed [table 6.3.7.].

Step No.	load (kN)
0	0,0
1	4,0
2	6,0
3	12,0
4	18,0
5	24,0
6	25,3

Table 6.3.6. Applied load in different steps. Beam No. 3.

laodstep	f1	f2	f3	f4(t)	f5
0	21,9	60,3	117,0	175,1	192,1
1	20,0	56,2	110,9	168,6	181,4
2	19,5	54,9	108,6	166,4	178,0
3	19,2	53,2	104,4	162,6	171,7
4	18,7	51,7	101,2	159,4	166,7
5	18,0	50,2	98,2	154,6	161,9
6	16,1	47,5	93,8	139,8	150,9

Table 6.3.7. Variation of the first five natural frequencies (Hz) through the load process. Beam No. 3.

For beam no. 3, the reduction of the natural frequencies presented a continuous reduction through all the lad process [figure 6.3.22]. Is worth to mention that the load increment between steps is not linear, and the almost-linear shape of the lines is a simple coincidence. In an analogue way to beam number 1, the most affected natural frequency is the first one. It presented a reduction of 10% of is original value after applying 16% of the ultimate load (4 of 25 kN). The same frequency was reduced up to 25% before failure.
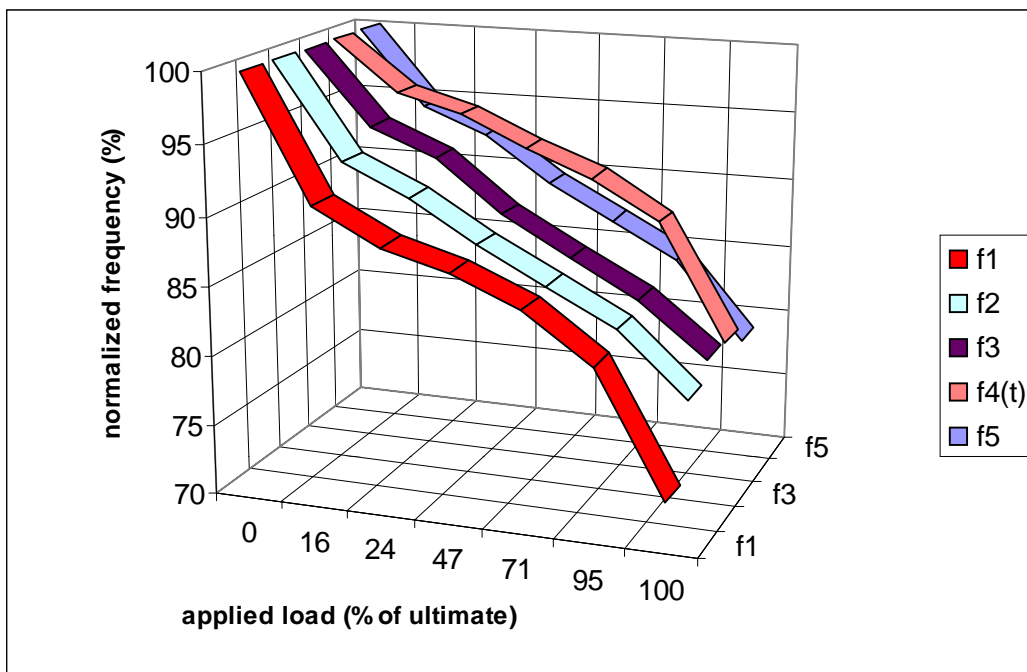
Figure 6.3.22. Relative change of first five natural frequencies trough the load process. Beam No. 3.

The configuration of the supports for beam no. 4 was changed completely: two different setups were used; both setups are symmetrical, according with figure 6.3.4. Six load-steps were carried out in the first support setup and seven load-step for the second setup [table 6.3.8.]. A moderate damage was induced in the first setup, and the beam was taken up to failure in the second setup. The reason to implement this modification in support conditions was basically to study the influence on unsymmetrical damage in the evolution of the natural frequencies. The natural frequencies presented an important reduction through the loading process [table 6.3.9.].

Step No.	setup	load (kN)
1	1	0,0
2	1	8,0
3	1	10,0
4	1	13,0
5	1	19,0
6	1	25,0
7	2	8,0
8	2	10,0
9	2	13,0
10	2	19,0
11	2	25,0
12	2	35,0
13	2	54,0

Table 6.3.8. Applied load in different steps. Beam No. 4.

laodstep	setup	f1	f2	f3	f4	f5
1	1	22,0	63,4	123,3	182,6	201,9
2	1	21,8	62,7	122,4	182,1	200,6
3	1	21,5	61,4	121,0	181,1	198,2
4	1	21,2	60,5	119,8	179,8	196,1
5	1	20,1	57,9	115,2	176,2	189,3
6	1	19,4	56,9	111,6	172,6	185,2
7	2	19,0	54,9	109,2	170,7	181,9
8	2	18,5	52,6	106,3	168,7	177,7
9	2	18,1	51,1	104,1	167,5	174,6
10	2	18,0	50,3	103,1	165,7	171,5
11	2	17,5	49,0	101,0	162,7	166,5
12	2	17,2	48,9	99,4	161,5	165,4
13	2	17,2	48,5	100,2	157,0	165,5

Table 6.3.9. Variation of the first five natural frequencies through the load process.
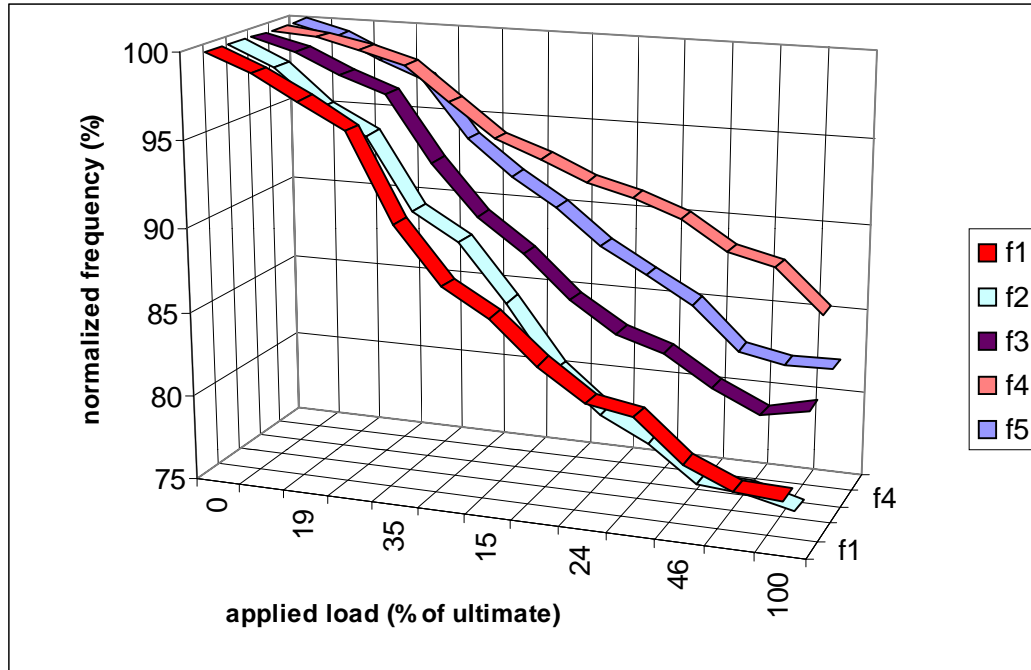
Beam No. 4.

Figure 6.3.23. Relative change of first five natural frequencies trough the load process. Beam No. 4.

A continuous reduction on the value of the frequencies was observed [figure 6.3.23]. The change in the support setup (in step 7) did not influence the continuous reduction of the frequencies. A reduction of 23-24% of the value of the first natural frequency is observed before failure. Once again, the first natural frequency is one of the most affected by cracking (but not the most affected, in this case the second frequency).

Finally, for Beam no. 5. a gradual diminution of the first natural frequencies is observed when generating damage to the beam. The behavior is analogue to the other four beams, and a clear decreasing trend is again identified after a cracking process [figure 6.3.24]. Table 6.3.10 shows the applied loads and table 6.3.11 presents the identified values for the first five natural frequencies.

Step No.	Load (kN)
0	0,0
1	6,0
2	6,8
3	7,5
4	9,0
5	12,0
6	15,0
7	18,0

Table 6.3.10. Applied load in different steps. Beam No. 5.

laodstep	f1	f2	f3	f4	f5
1	20,0	57,9	110,8	171,5	180,9
2	19,1	56,8	108,9	168,5	177,3
3	18,5	56,1	107,2	166,4	173,1
4	18,1	55,2	106,1	164,6	170,8
5	17,8	54,6	105,7	163,4	169,5
6	17,5	53,6	104,6	161,3	167,7
7	17,3	52,7	103,8	159,5	166,8
8	17,1	52,0	103,2	157,8	166,1

Table 6.3.11. Variation of the first five natural frequencies through the load process. Beam No. 5.
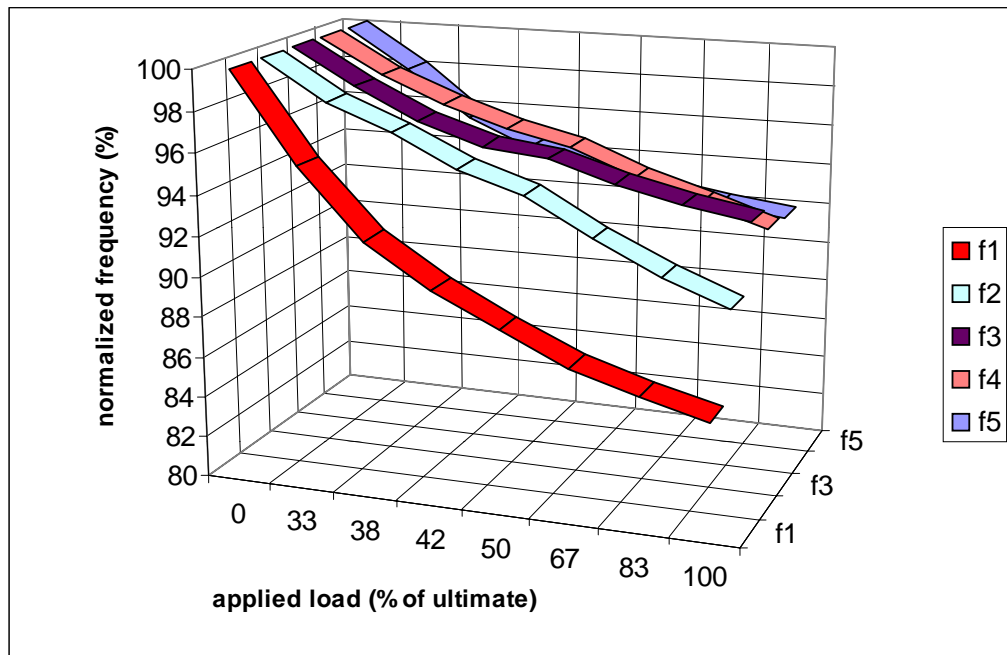
Figure 6.3.24. Relative change of first five natural frequencies trough the load process. Beam No. 5.

6.3.4. Numerical simulation

A finite element model was developed to simulate the full load-unload process and to obtain the natural frequencies after every load step. The complete characteristics of this model are described in 4.3.5.1.

Some data included in the model were directly determined by experimental techniques, and include:

- Strength and constitutive equation of the concrete by a strain-controlled compressive tests.

- Tensile strength of concrete by a Brazilian test.

- Dynamic modulus tests by an ASTM -C215 test.

Because most of the parameters that affect the dynamic behavior of he beams (such as support conditions, strain modulus, geometry and steel reinforcement) were known, the principal goal of this numerical simulation was to study the effect associated with rebar-concrete interface (tension stiffening). The tension stiffening depends on such factors as the density of reinforcement, the quality of the bond between the rebar and the concrete, the relative size of the concrete aggregate compared to the rebar diameter, and the model mesh. A reasonable starting point for relatively heavily reinforced concrete modeled with a fairly detailed mesh is to assume that the strain softening after failure reduces the stress linearly to zero at a total strain of about 10 times the strain at failure. The strain at failure in standard concretes (under tensile stress) is typically 0,0001, which suggests that tension stiffening that reduces the stress to zero at a total strain of about 0,001 is reasonable [Gilbert and Warner, 1978]. This value was used as starting point and updated further on.

Compressive stress data was provided as a tabular function of plastic strain. Positive (absolute) values were given for the compressive stress and strain. The stress-strain curve can be defined beyond the ultimate stress, into the strain-softening regime. The parameters used to define the equation were obtained from experimental strain-controlled uniaxial compressive tests [figure 6.3.12].

Different numerical models are generated with small changes in three parameters: tensile strength of concrete, tension stiffening branch amplitude and strain modulus. The objective function is the experimental data [figure 6.3.25]. A normalized frequency is used to homogenize the plots and to avoid the use of absolute values (Hz). The normalized frequency is defined as the percentage of the initial value with respect to the undamaged condition. By this way, all the frequencies start at 100% and decrease as damage is induced.
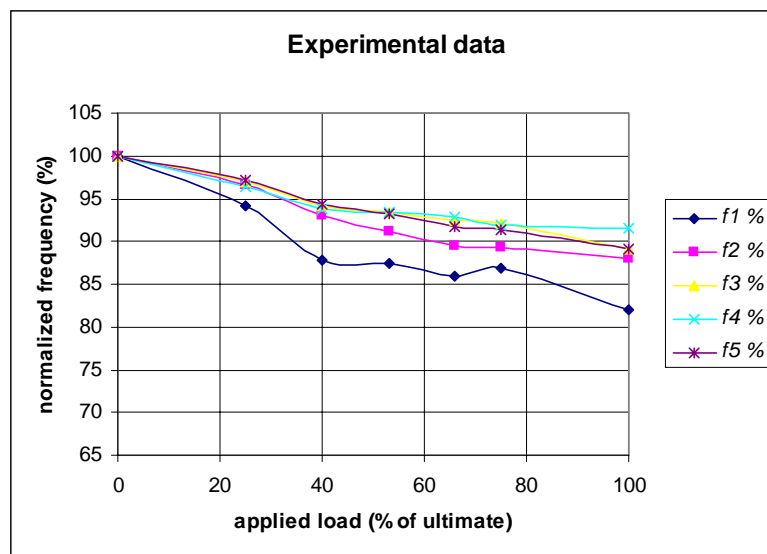
Figure 6.3.25. Objective function defined as the relative change of first five natural frequencies trough the load process from experimental results, Beam No. 1.

Several numerical approaches were developed, and the evolution of the relative frequencies was satisfactory. Figure 6.3.26 shows the frequency evolution diagram for six of this approaches. It is has been shown that for all the cases the first natural frequency is much more sensitive to the damage process, even in a higher ratio than experimental data.

The different models were able to simulate the behavior of the natural frequencies trough the load process in a qualitative manner. However, a quantitative value of this approach is necessary to determinate which FE model is more accurate. Therefore, he use of an error coefficient is proposed to use as a quantitative qualification of every different model.

In a first step, the error is a measure of the deviation from the objective function for an undamaged state. This coefficient is denoted E_u (error for undamaged condition) and is defined by equation 6.3.1:

$$E_u = \sum_{n=1}^{r} \left\| 1 - \frac{fa_{n(numerical)}}{fa_{n(experimental)}} \right\| \qquad\qquad [6.3.1]$$

Secondly, when the objective function is achieved in undamaged condition, other coefficient is used to update de model. This coefficient is related to the evolution of the frequencies through the loading process and denoted E_d (error for damaged condition) and is defined by equation 6.3.2:

$$E_d = \sum_{m=2}^{s} \sum_{n=1}^{r} \left\| 1 - \frac{fr_{mn(numerical)}}{fr_{mn(experimental)}} \right\| \qquad\qquad [6.3.2]$$

where

       s= number of load steps

       r=number of identified frequencies

       fa= absolute frequency value (Hz)

       fr= normalized frequency value (%)
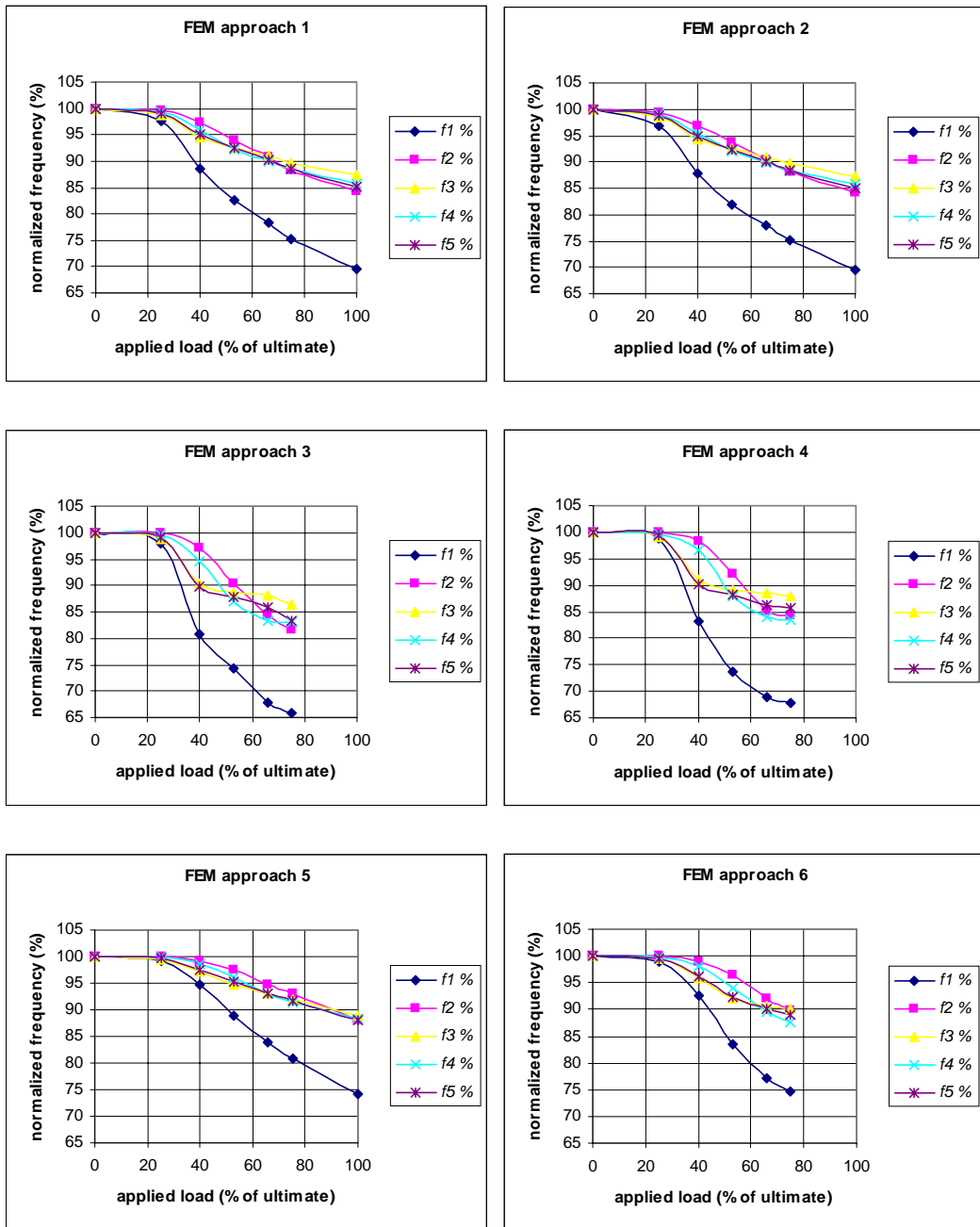
Figure 6.3.26. FEM approaches to the experimental objective function (previous figure), Beam No. 1.

After minimizing E_u changing certain parameters (such as strain modulus or reinforcement ratio) related with undamaged condition, E_d is minimized using a different set of parameters related with damaged condition (such as tensile strength or tension stiffening branch amplitude).

An updating procedure was carried out using the error coefficients defined in eq. 6.3.1 and 6.3.2. The evolution of this process is presented in table no. 6.3.12.

FEM approach	Strain modulus (Mpa)	Tensile strength (% of compresive)	Tension stiffenieng	TSBA	Eu	Ed	ad_u %	ad_d %
1	27.000	7,50	multilinear *	0,04600	0,14	1,07	2,7	3,6
2	26.500	7,25	multilinear *	0,04600	0,10	1,06	2,0	3,5
3	26.500	9,00	multilinear *	0,00730	0,10	1,76	2,0	7,0
4	25.500	10,00	multilinear *	0,00730	0,06	1,62	1,2	6,5
5	25.500	10,00	linear *	0,00730	0,06	0,97	1,2	3,2
6	25.500	10,00	bilinear *	0,00730	0,06	0,94	1,2	3,8

* tension stifening branch amplitude can be defined as a linear of multi-linear function of the strain

Table 6.3.12. Evolution of error coefficients through the updating process of beam

No. 1.

A good image of the accuracy of the proposed model can be obtained by dividing the error parameter (E_u or E_d) by the number of samples (r for E_u or s-1 times r for E_d). For example, for the numerical approach 6, an average deviation (*ad*) of the numerical data from the experimental set is:

ad_u=E_u/r = 0,059 / 5= 0,0118 = 1,18% for undamaged condition

and

ad_d= E_d/ (r * m-1)   = 0,94 (5 * (7-1)) = 0,031 = 3,13% for damaged condition

A different model is developed for beam no. 3. The same model updating process developed for beam no. 1 is carried out. The objective function is again a set of experimental data including the variation of the first five natural frequencies through the load process [figure 6.3.27].
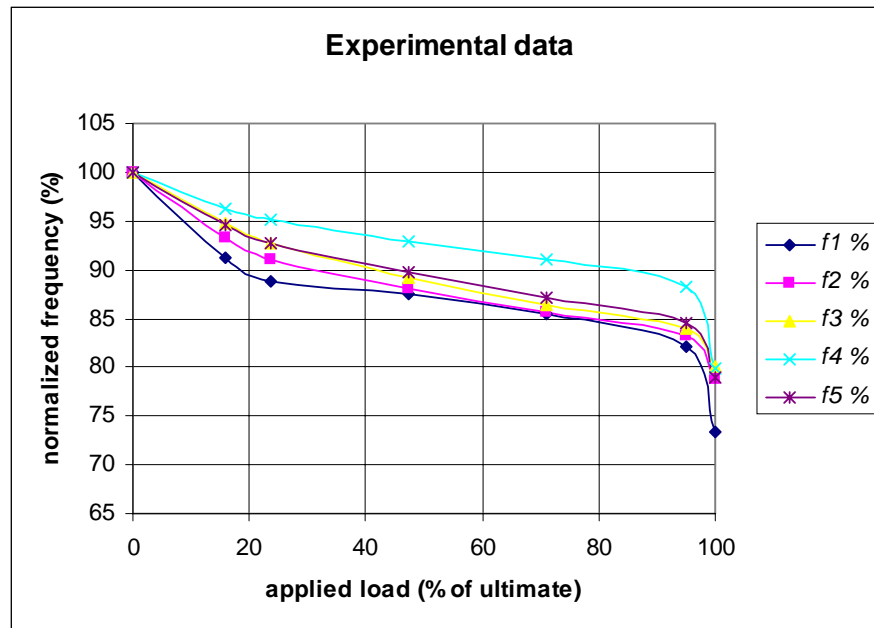
Figure 6.3.27. Objective function defined as the relative change of first five natural frequencies trough the load process from experimental results, Beam No. 3.

Six FEM approaches are developed by changing parameters such as strain modulus of concrete, tension stiffening branch amplitude or tensile strength of concrete. These numerical approximations succeeded in more or less accuracy to reproduce experimental data. The error coefficients defined in eq. 6.3.1 and 6.3.2 are used to quantify the level of approximation to the objective function [table 6.3.13]. Figure 6.3.28 is a graphical representation of the results of six different FEM attempts.
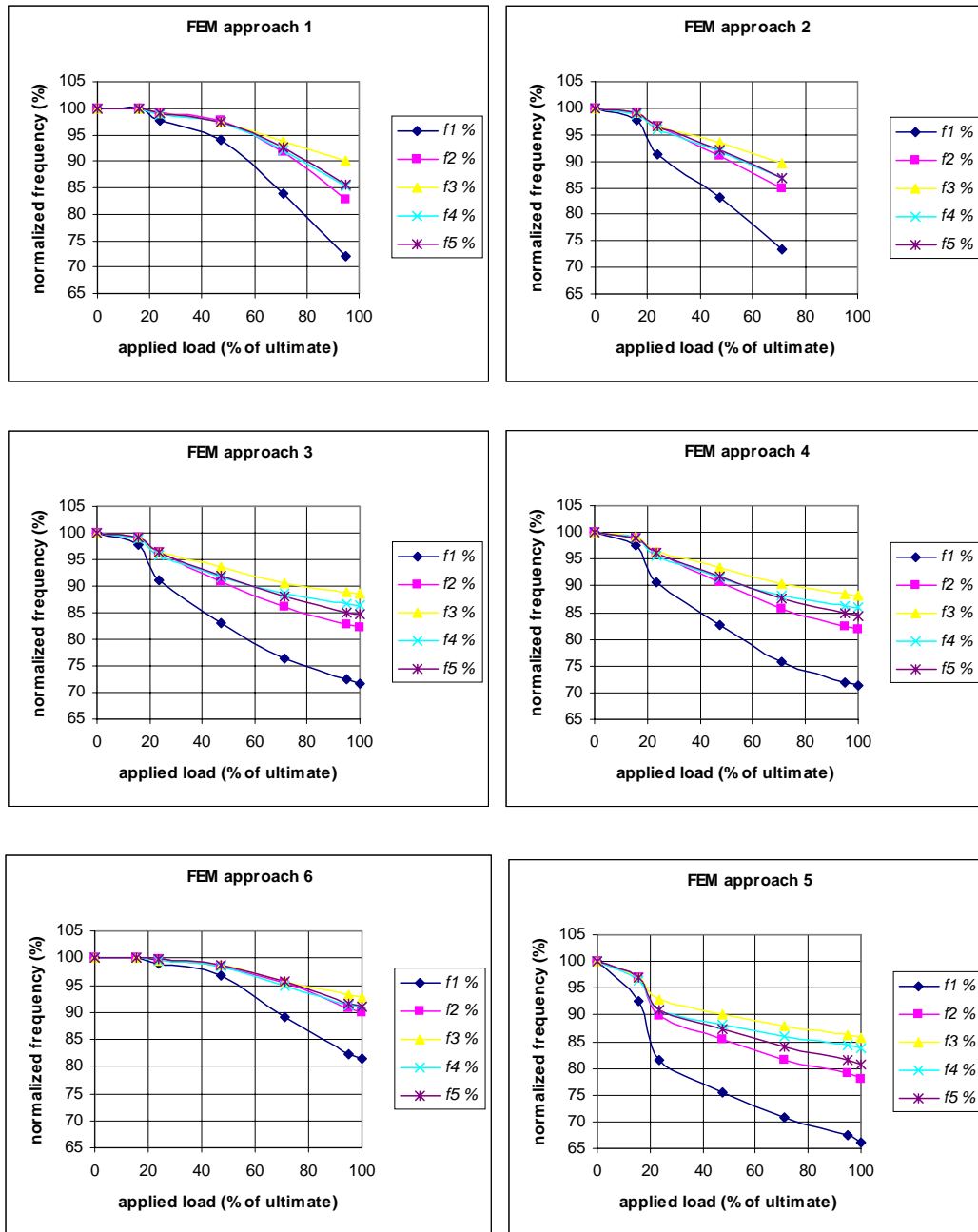
Figure 6.3.28. FEM approaches to the experimental objective function (previous figure), Beam No. 3.

FEM approach	Strain modulus (Mpa)	Tensile strength (% of compresive)	Tension stiffenieng	TSBA	*Eu*	*Ed*	*ad u* %	*ad d* %
1	27.500	10,00	bilinear *	0,0010	0,17	1,58	3,3	5,3
2	27.500	7,00	bilinear *	0,0010	0,17	0,84	3,3	3,4
3	30.000	7,00	bilinear *	0,0100	0,15	0,99	2,9	2,8
4	30.000	7,00	bilinear *	0,0050	0,17	0,99	3,3	2,8
5	30.000	5,00	bilinear *	0,0050	0,17	1,44	3,3	4,1
6	29.500	12,00	bilinear *	0,0050	0,15	2,25	2,9	6,4

* tension stifening branch amplitude can be defined as a linear of multi-linear function of the strain

Table 6.3.13. Evolution of error coefficients through the updating process of beam No. 3.

A similar model was developed for beams 2, 4 and 5, and for all cases, the numerical approach was able to reproduce the complete set of frequencies and their variation through different load and damage scenarios.

6.3.5. Discussion

The results of this experimental campaign allowed some considerations:

- Dynamic testing was successfully applied to identify the dynamic parameters suspended RC beams subjected to progressive damage by cracking. Several natural frequencies were measured by means of a set of 60 accelerometers attached to the beam. The pollution of the ambient vibration was avoided by introducing low-frequency springs between the beam and the supports.

- In an analogue way to section 6.2, the numerical modeling was developed using material characteristics obtained from concrete cylinders. The curing and atmospheric conditions where not exactly the same for cylinders and beams (due to logistics demands). Therefore, if the model is developed using parameters measured in the cylinders, the dynamic behavior of the beam is strongly modified. This behavior does not match to the experimental one. A subject of primary importance is that the use of dynamic strain modulus, measured from concrete cylinders for the numerical simulation generates unrealistic higher values of the stiffness. It seems to be a strong influence of the scale and shape of the structure.

- These experimental works have demonstrated that dynamic properties of concrete beams are modified when damage by cracking is induced. This fact also demonstrates that a measurement of the dynamic properties of the beam could lead to an identification of its properties and its damage level. In figure 6.3.29, the variation of the first natural frequency vs. the damage (defined as the ratio between applied and ultimate moments) is plotted for four different beams and compared with the numerical prediction.
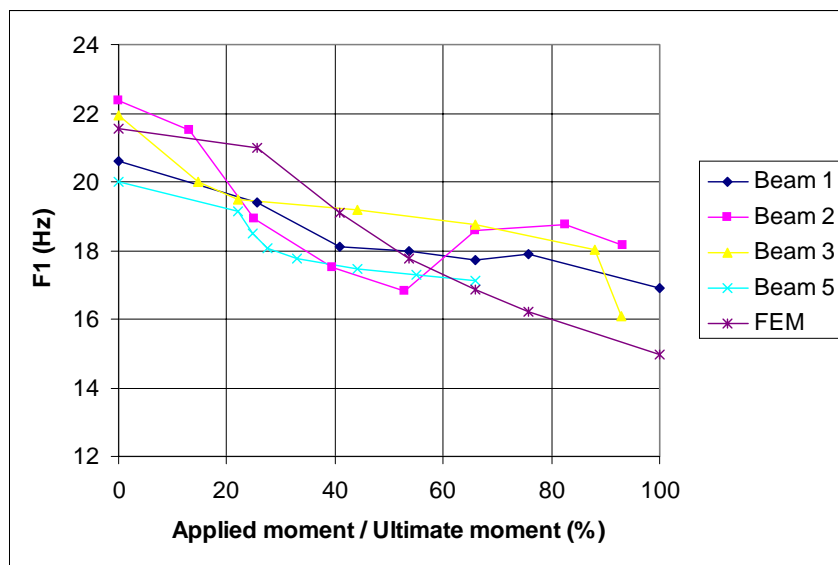
Figure 6.3.29. Comparison between the experimental first natural frequencies of four beams vs. numerical prediction.

- The second natural frequency showed an important modification through the damaging process. An average reduction of 20% of the frequency value is observed [figure 6.3.30] for a maximum applied moment. The numerical prediction is more accurate fo the second natural frequency than for the first one. Nevertheless, the first natural frequency was more sensitive to damage for all the studied cases. The first natural frequency is not only easily recognizable by a simple dynamic test, but also is very sensitive to cracking and it can give valuable information to update a numerical model of the studied beam.
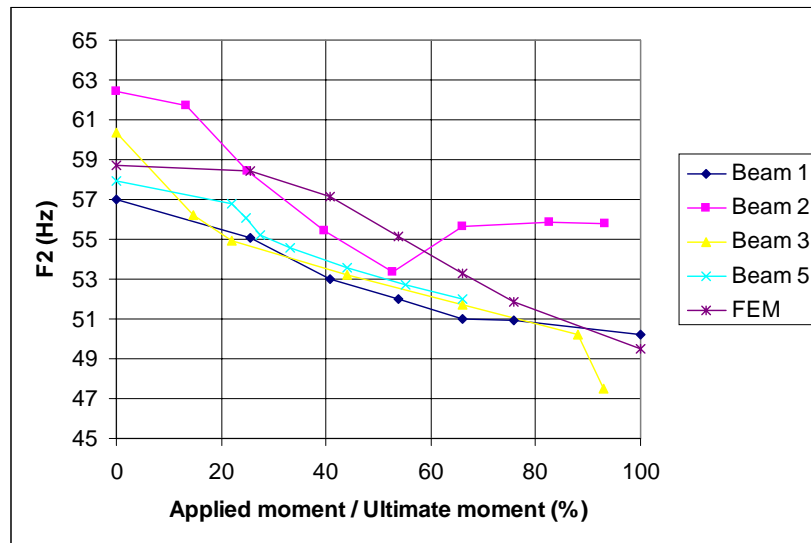
Figure 6.3.30. Comparison between the experimental second natural frequencies of four beams vs. numerical prediction.

- The most important parameter for the optimization of the model was the tension stiffening branch amplitude. In figure 6.3.31 the first six experimental frequencies (blue) and the correspondent numerical ones (red) are plotted. From the figure is observed that the first frequency is affected by cracking in a higher ratio for both cases (numerical and experimental).
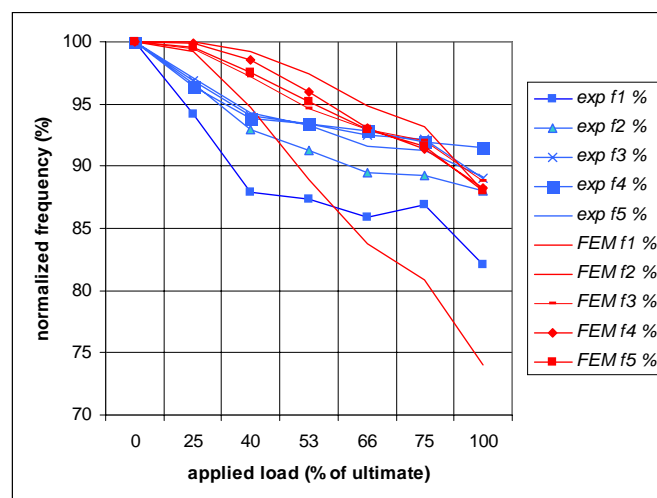
Figure 6.3.31. Comparison between experimental (blue) and numerical (red) results, Beam No. 1.

- The accuracy of the model was different for every evaluated frequency. Figure 6.3.32 presents the evolution of the first three natural frequencies and the comparison with the numerical model.
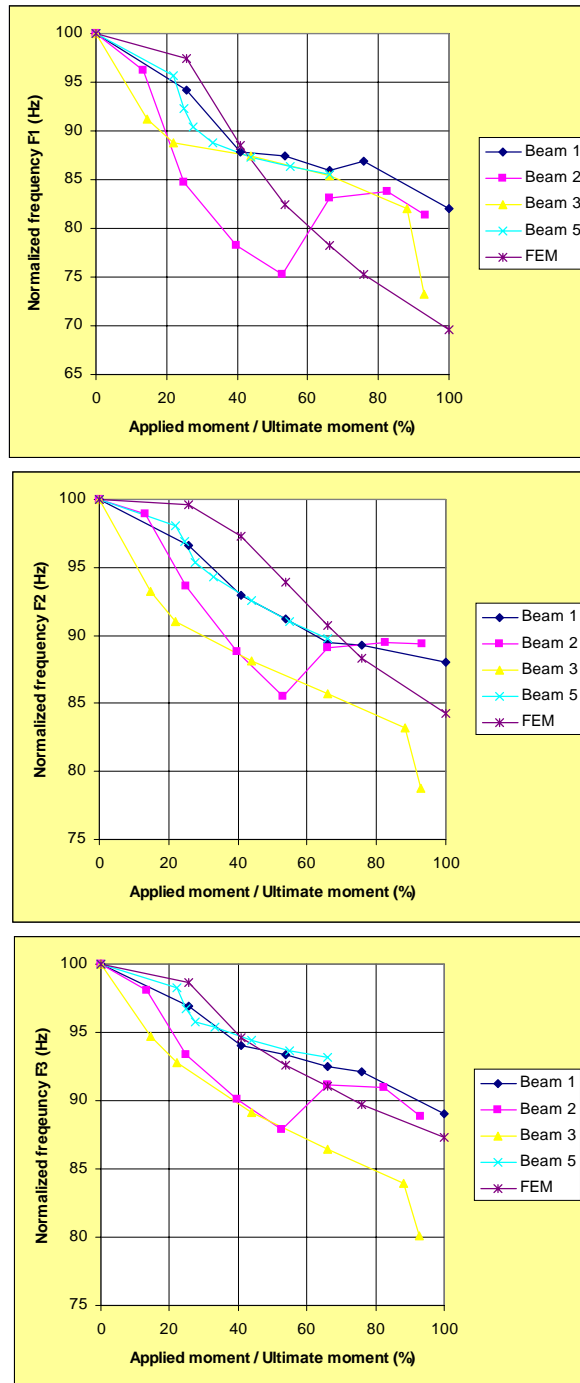
Figure 6.3.32. Evolution of the first three natural frequencies (from above to below) and comparison with the numerical prediction.

- An important factor to adjust numerical and experimental frequencies was the tension stiffening branch amplitude (TSBA). Figure 6.3.33 presents three different models with a variation of the TSBA.
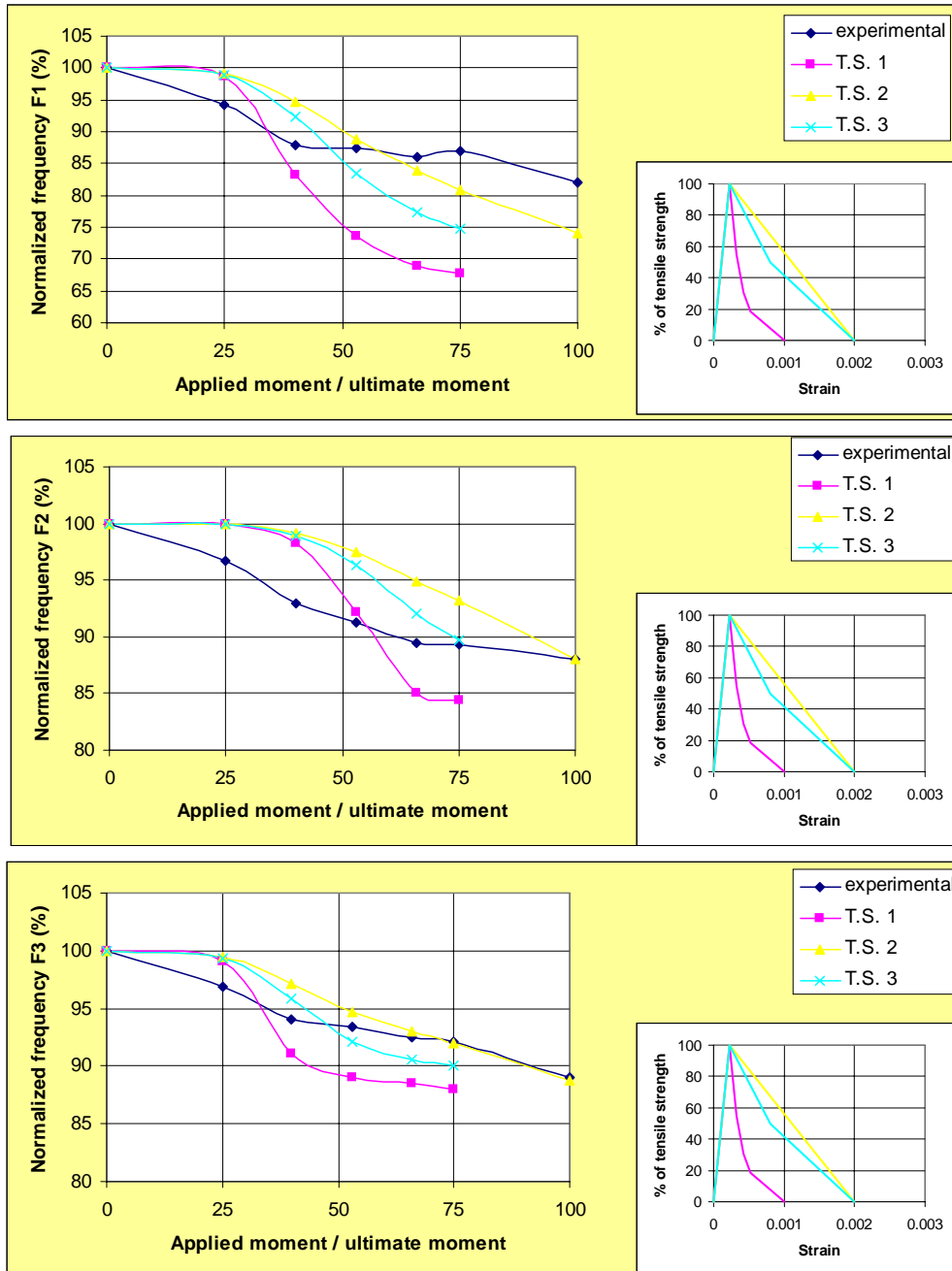
Figure 6.3.33. Evolution of the first three natural frequencies (from above to below) using three different models (varying tension stiffening equations) and comparison with the experimental values.

- Another determinant factor when optimizing the numerical model is the appearance of the first crack; at that point, the frequencies start to decrease. In figure 6.3.34, the first three natural frequencies are numerically determined using three different tensile strength of concrete.
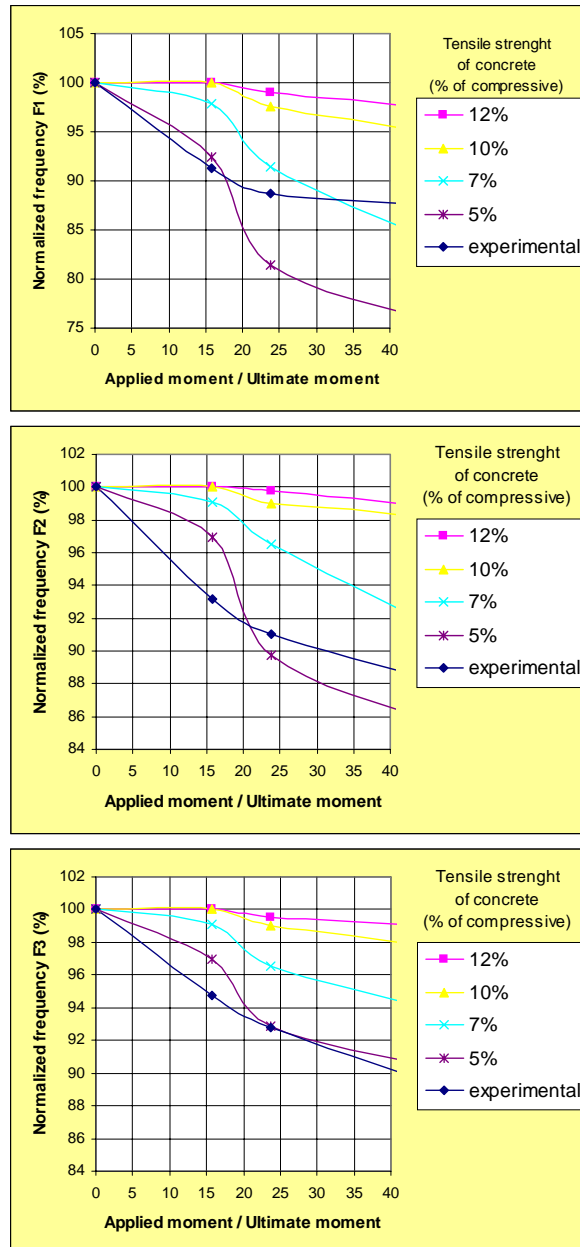
Figure 6.3.34. Evolution of the first three natural frequencies (from above o below) using three different models (varying tensile strength of concrete) and comparison with the experimental values.

6.4. Combined chemical and mechanical damage in simply supported RC beams

6.4.1. Introduction

The objective of the present investigation is to analyze the influence of chemical damage in the dynamic response of simply supported RC beams. The types of deterioration studied in this campaign include carbonation, sulfate and chloride attack.

Chemical degradation can influence dynamic parameters of concrete structures by modifying elasticity modulus, reinforcement section or inducing cracks. Here, the possible usefulness of dynamic testing to identify chemical damage is studied by inducing artificial chemical damage in 26 concrete beams. Three of the most common degradation mechanisms related to atmosphere action are simulated under laboratory conditions.

This campaign is been carried out in the Structures Laboratory of the Technical University of Catalonia. 26 reinforced concrete beams are built with 2 different combination of concrete mixture (20 and 25 MPa). The beams are subjected to chemical attack during 2 years. Reference beams are dynamically tested 28 days, 6, 12 and 24 month after casting. Attacked beams are dynamically tested after 6, 12 and 24 months of chemical attack [table 6.4.1]. This section presents the methodology followed and the results. The dynamic identification process is developed before and after every modification, either chemical (attack) or mechanical (loading) of the beam.

The beams are dynamically tested always in the same configuration: simply supported, with a distance between supports of 1,50 m. The configuration of the dynamic test was selected by its simplicity.

As described further on, the natural frequencies of the chemically attacked beam were altered, presenting an important dispersion.

Concrete type	number of beams	attack type	time from placing of concrete				Total
			1 month	6 months	12 months	24 months	
20 MPa Concrete	13 beams	Carbonatation		1	1	1	3
		Sulfates attack		1	1	1	3
		Chlorides attack		1	1	1	3
		Reference beams	1	1	1	1	4
25 MPa Concrete	13 beams	Carbonatation		1	1	1	3
		Sulfates attack		1	1	1	3
		Chlorides attack		1	1	1	3
		Reference beams	1	1	1	1	4
Total			2	8	8	8	26

Table 6.4.1. Testing schedule of the experimental campaign

6.4.2. Material and experimental method

26 beams were built with the same geometry and the same reinforcement scheme. The section was reinforced with six 10-mm bars; distributed in three layers as indicated [Figure 6.4.1]. Shear reinforcement consisted in 6-mm bars every 90 mm. Mechanical properties of the reinforcement steel are given in table 6.4.2.

Elastic limit f_y	500N/mm²
Ultimate strength f_s	550N/mm²
Failure strain	12%
Ratio f_s/f_y	1.05

Table 6.4.2. Renforcement-steel properties

Half of the beams where constructed with a 20 MPa concrete (w/c ratio= 0.70) and the other half with a 25 MPa concrete (w/c ratio=0.65). The beams where cured with water and covered with a plastic membrane during the first 7 days.
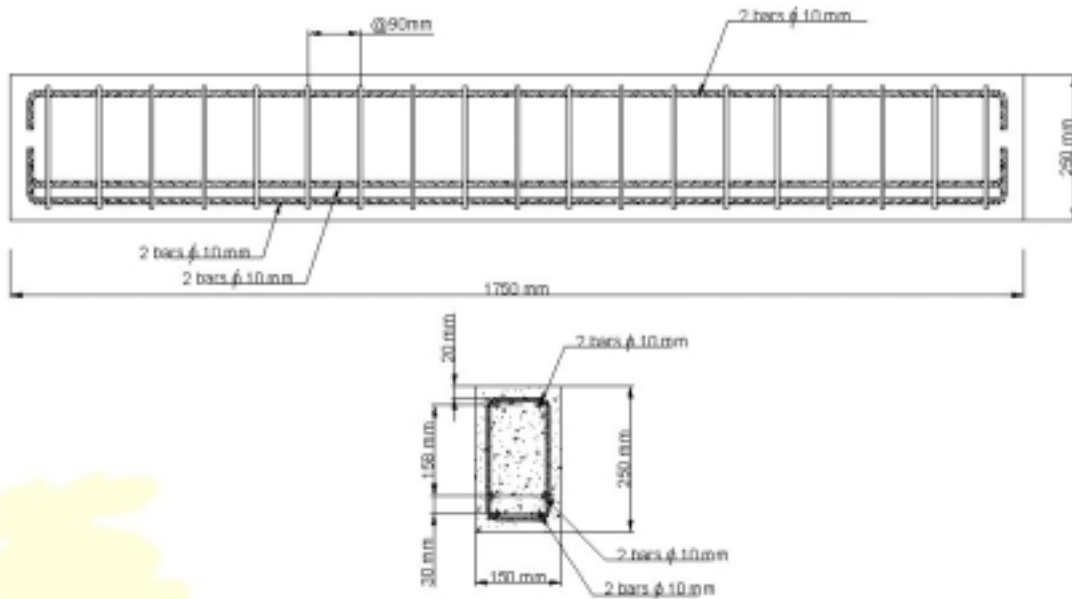
Fig. 6.4.1 Geometry and reinforcement of the beams

Component	Kg/m^3	
	Concrete 20 MPa	Concrete 25 MPa
Sand 0/5	892,5	850
Sand 0/2	200	200
Gravel 5/12	87,5	87,5
Gravel 12/25	800	815
Cement I / 42.5R	271,5	300
Additive PF75	2,17	2,4
Water	190	195

Table 6.4.3. Concrete mixture formula

The concrete mixture was designed to achieve a poor concrete [table 6.4.3]. This formula is not allowed any more by modern construction codes (now the minimum is 350 kg of cement per m^3), However, it is used to reproduce a typical concrete of the decade of 80's. An additive was used to improve consistence and to avoid segregation (water reducer PF75, courtesy of Bettor MBT).

Twenty-eight days after casting, all the beams are subjected to a preliminary loading process to induce cracks. This cracking process is aimed to helping the

artificial chemical process to attack not only the surface of the beam but also the inner part. The pre-load process consisted on two concentrated load (40 kN) applied symmetrically 400 mm from the mid span in a simple supported scheme with a distance of 1500 mm between supports. This load (57% of the ultimate) induces a quasi-generalized cracking in the central 1000 mm of the beam [figure 6.4.2 and 6.4.3].

Figure 6.4.2. Pre-cracking before chemical attack.
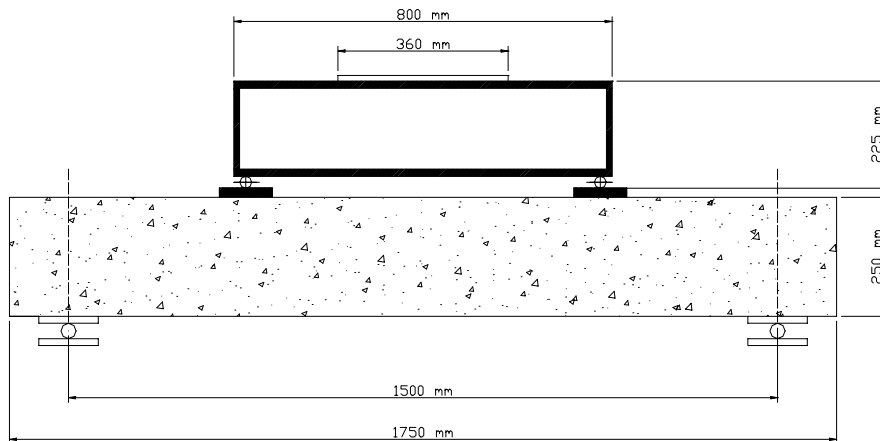
Figure6.4.3. Pre-cracking scheme before attack.

After the *cracking process* the beams were separated in to four groups: reference beams (exposed to air), sulfate attack beams (exposed to SO_4^2), chloride attack beams (exposed to Cl) and carbonation attack (exposed to CO^2). The reference beams were simply left under atmosphere action. Sulfate attack beams were subjected to cycles of 2 weeks in to a solution of 97 grams of K_2SO_4 (to obtain 5%

content of SO_4) in water and two weeks of exposition to air [figure 6.4.4]. Chloride attack beams where subjected to cycles of one week in to a solution of 5% of NaCl in water and 3 weeks exposition to air. And carbonation attack beams were subjected continuously to a 20% solution of CO_2 in air under moisture conditions between 60 and 65%. Concrete cylinders of every type were sampled from the original mixture and attacked under the same conditions of the beams [figure 6.4.5].

Figure 6.4.4. Beams subjected to attack (SO_4) inside the pool.

Figure 6.4.5. Attack containers for cylinders (SO_4).

Static tests

After 6, 12 and 24 months of attack one beam of every kind of attack and every concrete is extracted from de container and tested. A 3-point bending test was developed [figures 6.4.6 and 6.4.7]. Increasing load-unload steps were applied. The load-unload steps (6 in total) were servo-controlled applying from 1 to 6 mm of deformation at midspan [table 6.4.4]. A neoprene distribution plate was placed between the actuator and the beam to avoid deformation incompatibilities [figure 6.4.8]. Load velocity was 0.05 mm/second [figure 6.4.9].
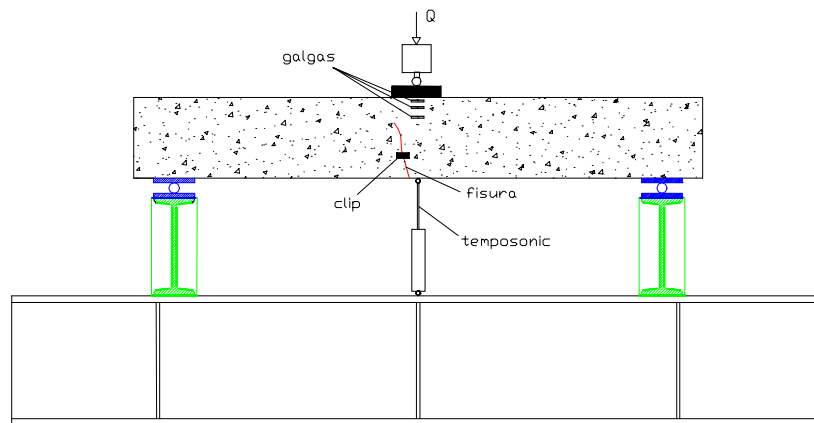
Figure 6.4.6.. Load-test configuration (static and dynamic).
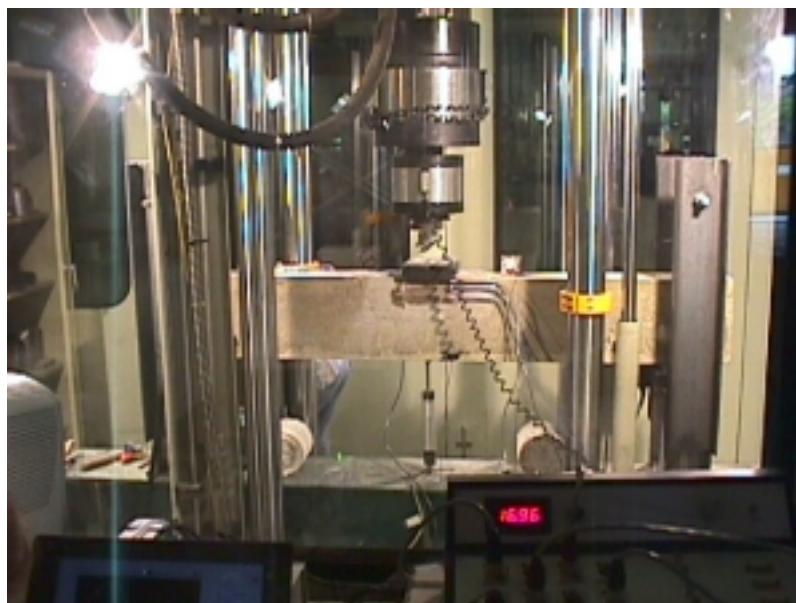
Figure 6.4.7. Load-Unload test after chemical attack.

Figure 6.4.8. Neoprene interface between actuator and beam.
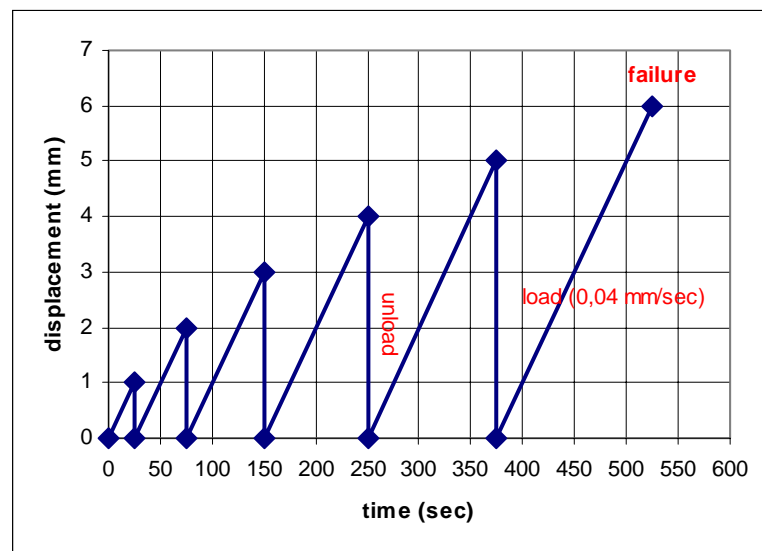
Figure 6.4.9. Load-unload process carried out in all the beams.

Beam description			Load in kN					
Attack type	Concrete type (MPa)	Time of attack	Step 1 (1 mm)	Step 2 (2 mm)	Step 3 (3 mm)	Step 4 (4 mm)	Step 5 (5 mm)	Step 6 failure
Reference	20	28 days	8,49	20,86	35,71	52,63	69,42	106,90
Reference	25	28 days	10,42	26,43	43,12	59,89	75,38	101,93
Reference	20	6 months	5,88	11,58	19,91	31,14	46,59	103,02
Reference	25	6 months	10,49	24,97	41,93	60,09	77,92	106,70
SO4	20	6 months	11,08	23,91	36,82	50,78	65,74	95,68
SO4	25	6 months	14,45	25,18	38,87	53,64	66,42	-
CL	20	6 months	15,91	31,15	46,13	59,49	72,27	101,81
CL	25	6 months	7,57	18,67	30,58	43,79	56,61	101,70
Reference	20	12 months	7,41	19,71	36,09	53,37	68,50	100,41
Reference	25	12 months	7,73	20,15	35,62	51,44	66,37	-
SO4	20	12 months	9,22	26,12	58,51	61,76	74,77	98,58
SO4	25	12 months	11,05	28,23	46,32	62,68	76,25	102,01
CL	20	12 months	13,00	30,22	48,18	64,65	77,91	102,65
CL	25	12 months	12,26	29,66	47,79	63,38	77,93	106,87
reference	20	24 months	4,58	14,70	29,15	45,59	61,14	107,50
reference	25	24 months	2,70	9,11	25,16	40,02	57,05	106,30
SO4	20	24 months	9,23	28,03	46,19	61,77	75,46	106,00
SO4	25	24 months	6,06	15,17	26,78	38,48	51,18	114,30
CL	20	24 months	3,55	12,41	26,47	40,44	53,91	104,00
CL	25	24 months	8,35	22,30	38,60	54,03	68,10	99,70

Table 6.4.4. Applied load in static tests for all beams

Dynamic test

The beams were dynamically tested before and after every step. Two piezo-electric accelerometers where attached at 300 and 600 mm from one of the supports. Excitation was generated with a 12-pounds impact hammer. Output-only measurements where developed for one second. Two tests were developed after every step. The objective of this set-up is to follow the evolution of frequencies during the crack appearance. The whole process is repeated after one year of attack. Two accelerometers were attached to the beam [figure 6.4.10] and the excitation is induced by a normalized impact hammer [figure 6.4.11]. Further information of the adquisition equipment is detailed in appendix A.

Figure 6.4.10. Attached accelerometers on beam's dynamic testing.

Figure 6.4.11. Excitation of the beam by hammer impact.

Materials

At the time of casting, several cylinders are sampled from the concrete used in the beam. The mission of those cylinders is to provide detailed information about the basic constitutive material of the beam. This data is fundamental when performing numerical models of the beam. Tests carried out in cylinders consist on:

1.   Uniaxial compressive strength

2.   Strain-controlled compressive tests to define strain-stress diagram

3.   Dynamic modulus test (ASTM C-215)

Uniaxial compressive strength

Two different concretes were used beams, at the time of placing the concrete in the beams; several cylinders were sampled, to control the evolution of the compressive strength of the concrete through all the chemical attack [figure 6.4.12]. The cylinders were tested at the same tame of the beams. The results for all the combinations of attack and concrete type are presented in table 6.4.5.

Concrete type	attack type	time from placing of concrete			
		1 month	6 months	12 months	24 months
		avearge compresive strength (MPa)			
20 Mpa Concrete	Sulfates attack	-	26,6	27,5	34,5
	Chlorides attack	-	27,2	27,7	31,1
	Reference beams	23,5	26,8	27,7	30,8
25 Mpa Concrete	Sulfates attack	-	34,7	34,1	35,5
	Chlorides attack	-	32,1	33,3	36,9
	Reference beams	28,8	32,6	33,4	35,1

Table 6.4.5. Evolution of concrete strength for all types of concrete and attacks.

Figure 6.4.12. Compressive test on a 6-month SO₄ attacked cylinder.

Strain-controlled compressive tests

The load was controlled by the mean value of three longitudinal vertical strain transducers, obtaining a post-pick behavior of the concrete [figure 6.4.13]. The load velocity is 0.001 mm/second between the plates. The maximum strength matched the simple uni-axial tests. The maximum load was achieved at a reasonable strain of 0,2% [figure 6.4.14]. A discrete idealization of the results was performed and used furthermore in the numerical simulation. Identified average static modulus is 32,2 GPa. for *20-MPa* concrete, and 33,6 GPa for *25-MPa* concrete.
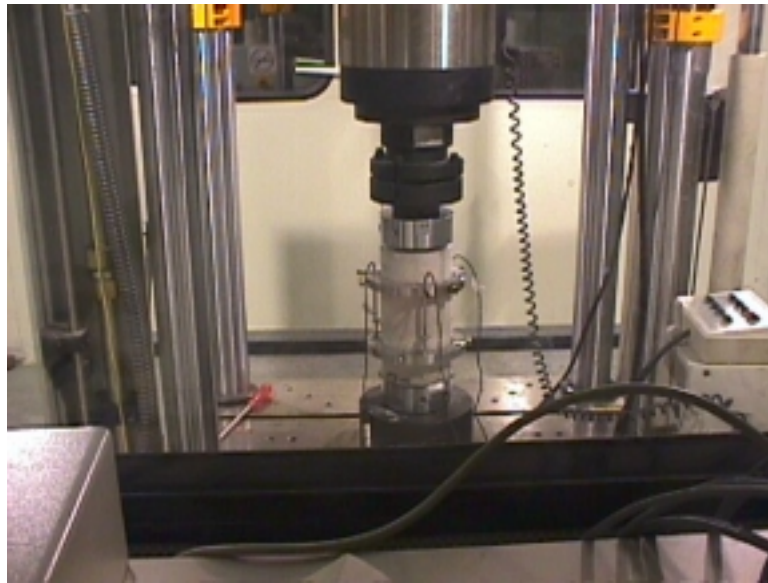
Figure 6.4.13. Strain-controlled tests for modulus in cylinders.
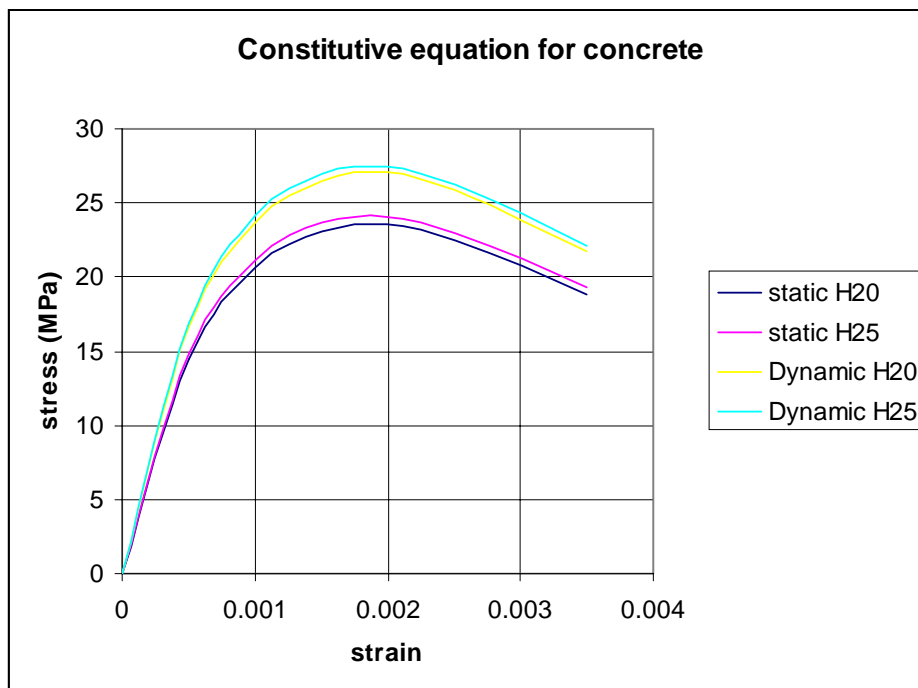
Figure 6.4.14. Constitutive equation of concrete used on modeling.

Dynamic modulus test

The test was carried out following the recommendations of ASTM C-215. Fourteen different tests were developed (seven for each kind of concrete) in cylinders [figure 6.4.15]. Identified average dynamic modulus is 36 GPa. for *20-MPa* concrete, and

37 GPa for *25-MPa* concrete.. A 10% increment is observed from static to dynamic modulus, in concordance with available literature and codes [section 3.3.3.]. Table 6.4.6 presents some examples of the calculations of dynamic modulus in *20-MPa* concrete. Table 6.4.7 is analogue to 6.4.6 but related to *25-MPa* concrete.

Figure 6.4.15. Dynamic-modulus testing of cylinders (C215 test of ASTM).

H20	x mm	y (high) mm	y2 (high) mm	z mm	weith kp	density kp/m3	identified frequency hz	dynamic E modul MPa
test								
1	150,00	300,00	300,00	150,00	12,00	2.263,54	6.695	36.525
2	150,00	300,00	300,00	150,00	12,00	2.263,54	6.700	36.580
3	150,00	300,00	300,00	150,00	12,00	2.263,54	6.710	36.689
4	150,00	300,00	300,00	150,00	12,00	2.263,54	6.610	35.604
5	150,00	300,00	300,00	150,00	12,00	2.263,54	6.600	35.496
mean	150	300	300	150	12	2.264	6.663	**36.179**

Table 6.4.6. Calculation of Dynamic strain modulus for20MPa-concrete

H25	x mm	y (high) mm	y2 (high) mm	z mm	weith kp	density kp/m3	identified frequency hz	dynamic E modul MPa
test								
1	150,00	300,00	300,00	150,00	12,00	2.263,54	6.745	37.073
2	150,00	300,00	300,00	150,00	12,00	2.263,54	6.745	37.073
3	150,00	300,00	300,00	150,00	12,00	2.263,54	6.747	37.095
4	150,00	300,00	300,00	150,00	12,00	2.263,54	6.755	37.183
5	150,00	300,00	300,00	150,00	12,00	2.263,54	6.750	37.128
mean	150	300	300	150	12	2.264	6.748	**37.110**

Table 6.4.7. Calculation of Dynamic strain modulus for25MPa-concrete

6.4.3. Results

Three point bending test with increasing load-unload steps was used to characterize the beams. Dynamic properties were evaluated after every load-unload cycle. The test was developed in every beam (every kind of concrete and every kind of chemical process) after 6, 12 and 24 months of attack. By this way, the evolution of dynamic parameters was followed by comparing frequencies with the reference beams (undamaged). Details of the methodology are presented further on.

Results are available for only two kinds of attack (sulfates and chlorides). CO_2 attack was not possible to implement during the first year because limitations on hermetic containers produced an important escape of the gas. Several isolated-designs were tested with not success.

After two year of chemical attack it is not possible to observe reduction on dynamic stiffness due to chemical attack. Actually, a slightly increment of the stiffness is observed, probably due to the saturation of the beams during the first months after casting. The applied chemical agent seems to be not aggressive enough to deteriorate the stiffness of the beams after two years of exposition. However, a strong deterioration is observed when the beams are retired from the aggressive agents. Figure 6.4.16 shows the appearance of a beam subjected to sulphates attack after 12 months. Figure 6.4.17 presents the aspect of chloride-attacked beams after 12 months of aggression.

Figure 6.4.16. External face of a SO$_4$-attacked beam (plaster formation).

Figure 6.4.17. Corrosion of the shear reinforcement after 12-months of chlorides attack.

Results are available for the test after 6, 12 and 24 months of attack. Not only dynamic but also static characterization of the beams is developed (strain gauges, displacement transducers). A FFT process was developed to pick the first natural frequency from the acceleration measurements. A typical time-response of the beam and its FFT is shown in figure 6.4.18.
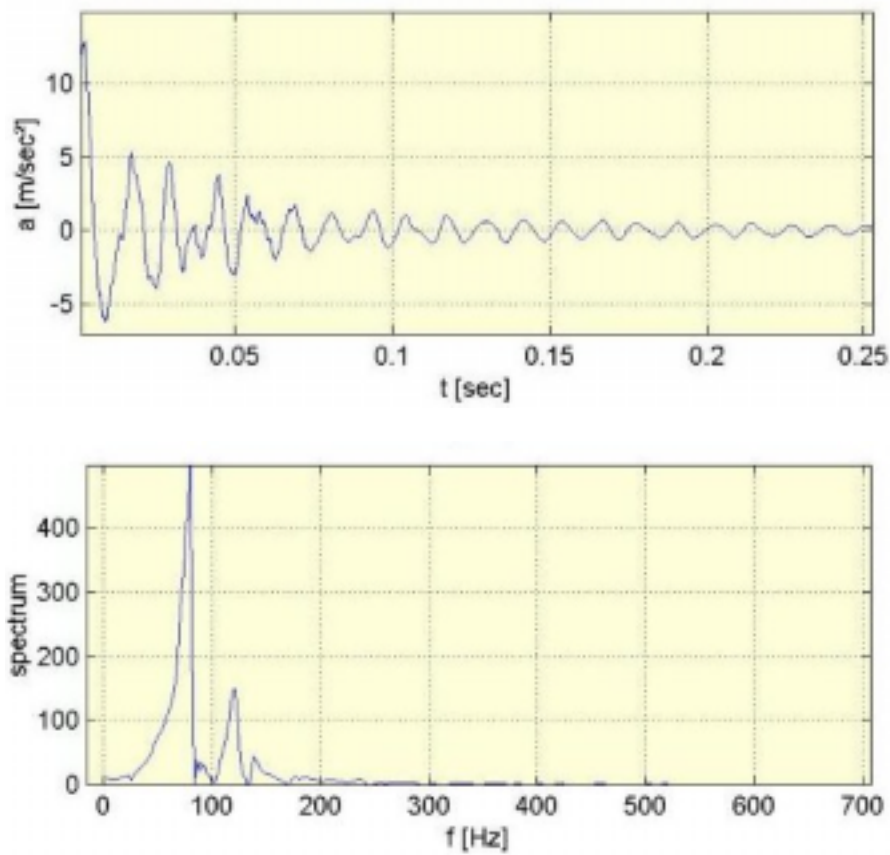
Figure 6.4.18. Typical time response and FFT of a beam.

Beam description			Experimental identified frequency (Hz)								
	Concrete	Time of	Before attack		After attack						
Attack type	type (MPa)	attack	undamaged	pre-cracked	Step 0 Unloaded	Step 1 (1 mm)	Step 2 (2 mm)	Step 3 (3 mm)	Step 4 (4 mm)	Step 5 (5 mm)	Step 6 failure
Reference	20	28 days	143	91	90	90	90	90	89	89	89
Reference	25	28 days	150	96	97	92	91	89	86	85	84
Reference	20	6 months	142	90	84	84	84	85	86	86	-
Reference	25	6 months	152	92	86	86	86	87	90	90	-
SO4	20	6 months	138	105	94	96	96	96	96	94	84
SO4	25	6 months	148	96	94	94	94	92	92	92	-
CL	20	6 months	142	101	92	92	92	92	90	90	-
CL	25	6 months	150	103	92	92	92	92	90	90	-
Reference	20	12 months	136	98	90	88	88	88	88	88	82
Reference	25	12 months	150	97	86	86	86	80	78	78	-
SO4	20	12 months	139	99	96	94	94	94	94	93	92
SO4	25	12 months	141	101	96	96	94	94	94	94	86
CL	20	12 months	140	91	98	98	98	98	98	97	86
CL	25	12 months	151	100	91	90	90	90	90	88	83
reference	20	24 months	142	97	74	76	76	76	72	76	67
reference	25	24 months	138	99	80	80	80	80	80	80	79
SO4	20	24 months	139	91	101	102	98	97	97	97	84
SO4	25	24 months	146	104	77	78	77	78	77	77	71
CL	20	24 months	140	96	76	76	78	78	75	76	70
CL	25	24 months	139	102	76	77	74	74	74	74	72

Table 6.4.8. Resume of experimentally identified frequencies.

Several problems where identified on the implementation of CO_2 attack. At the moment the process has not been effectively implemented due to the complex nature of the aggressive agent (gas form) and the difficulties on the implementation of a hermetic container. Research is carried out on this direction and the attack is at this time ready to start, but results are not available in this report.

It was possible to identify the second natural frequency only in a few beams (f2). First natural frequency (f1) was identified in all cases [table 6.4.8]. There are some cases (ej. chloride / 20 MPa / 12 months) where the beam presents an important increment in the frequency after the attack. In general not-submerged beams (reference beams) present lower frequencies than attacked beams.

6.4.4. Numerical simulation

A numerical simulation was developed to simulate the dynamic response after very load step. The numerical model does not include any chemical damage degradation, only mechanical processes are simulated. Detailed information of numerical model is presented in section 4.3.5.1. and section 5.3.

The results of the model followed the experimental data with a low dispersion. However, chemical attack was not included in the numerical simulation and therefore, the numerical results can be compared only with reference beams.

Beam description			FEM estimated frequency (Hz)							
Attack type	Concrete type (MPa)	Time of attack	undamaged	Step 0 Unloaded	Step 1 (1 mm)	Step 2 (2 mm)	Step 3 (3 mm)	Step 4 (4 mm)	Step 5 (5 mm)	Step 6 failure
Reference	20	28 days	202	97	96	96	96	96	93	-
Reference	25	28 days	204	98	98	98	98	97	93	-

Table 6.4.9. Comparison between experimental and FEM frequencies.

The model was accurate to simulate the full load process of the beams. The pre-cracking is simulated in a first step. The value of the natural frequencies, both for numerical and experimental identification, follows the same trend [table 6.4.9].

6.4.5. Discussion

The beams were subjected to 24 months of chemical attack. Dynamic testing was developed in all beams and load-unload tests were carried out following the proposed schedule. Carbonation attack was not successfully implemented, only sulphates and chloride attack were completed. Some important consideration are generated after this experimental works:

- After the attack period, variation in dynamic parameters (natural frequencies) is not clearly identified. In general, reference beams (not exposed to attack) present lower frequencies than attacked beams. The method of attack consisted in a solution of the correspondent chemical in water. The beams were cyclically submerged in this water for 6, 12 or 24 months. It is considered that the improvement in the frequencies of the attacked beams is due to the variation on curing conditions. The chemical process was initially conceived to deteriorate the properties of the materials. After two years of attack, the process did not succeed on deterioration; it has even improved the quality of the concrete. Visual inspection showed deterioration (corrosion in case of chlorides and plaster in case of sulfates), but the structural behavior of the beams (static and dynamic) did not show any important variation.

- The pre-cracking subjected all the beams to a double load of 40 kN, generating a moment with a magnitude of 58% of the ultimate. This action generated an important cracking and modified the first natural frequencies of the beams from 140 Hz to 90 Hz, approximately. The pre-cracking was intended to promote the transport of chemical agents o the inner part of the beam. However, the pre-cracking reduced the natural frequencies in such quantity that further changes due to chemical process had not resolution.

- The assessment layout proposed in Chapter 4 was successfully applied to identify the dynamic parameters suspended RC beams subjected to progressive damage by cracking. The first two natural frequencies were identified, and those frequencies were enough to update a numerical model.

- In general, an important reduction of the stiffness -and therefore of the natural frequencies- is observed after a load-cracking process. The reduction of natural frequencies achieved values around 40% for beams under ultimate loading [figure 6.4.19]. This percentage of reduction of the frequencies has agreements with previous studied cases [sections 6.2 and 6.3].
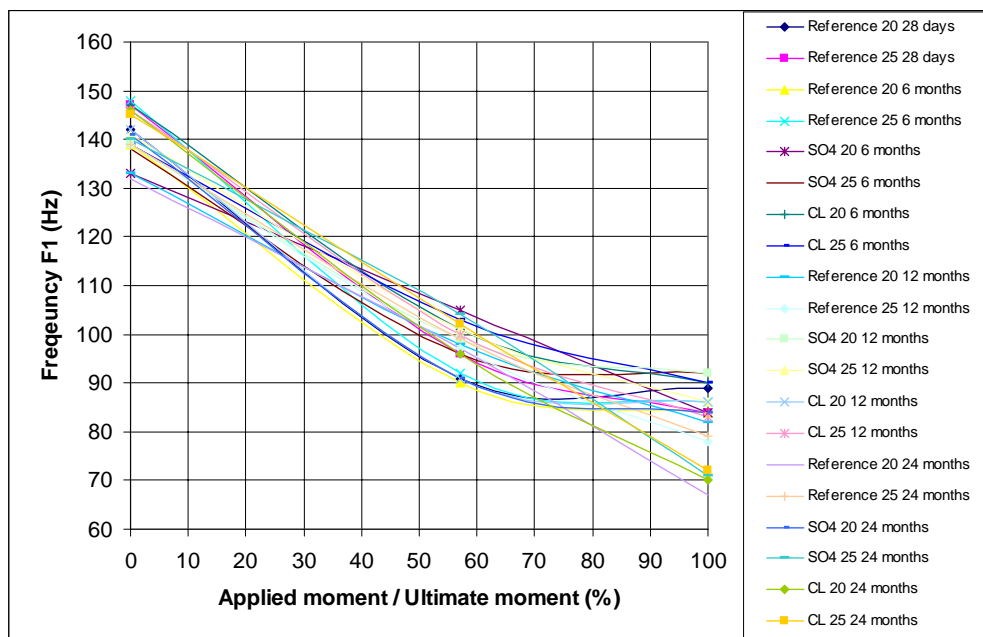
Figure 6.4.19. Evolution of the first natural frequency through the load process for all studied beams.
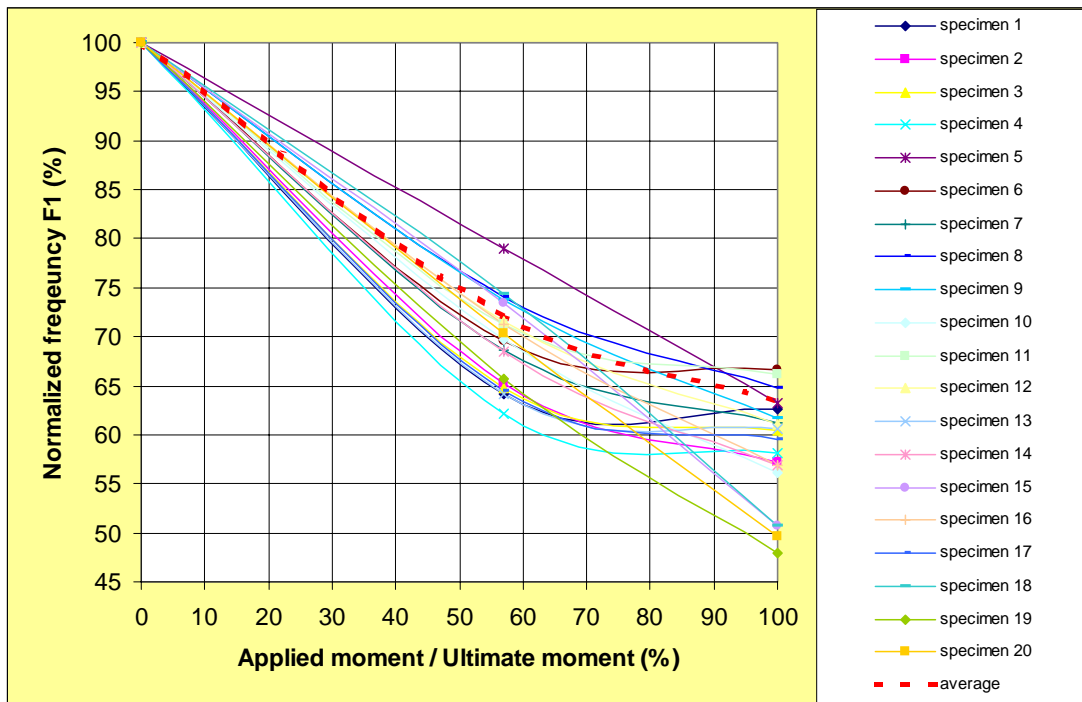
Figure 6.4.20. Comparative study of the evolution of the normalized first natural frequency through the load process for all studied beams.

- In an analogue way to sections 6.2 and 6.3, the numerical modeling was developed using material characteristics obtained from concrete cylinders. The curing and atmospheric conditions where not exactly the same for cylinders and beams (due to logistics demands). Therefore, if the model is developed using parameters measured in the cylinders, the dynamic behavior of the beam is strongly modified. This behavior does not match to the experimental one. A subject of primary importance is that the use of dynamic strain modulus, measured from concrete cylinders for the numerical simulation generates unrealistic higher values of the stiffness. It seems to be a strong influence of the scale and shape of the structure.

6.5. Influence of axial load on the dynamic response of masonry walls.

6.5.1. Introduction

In this section, an experimental program conceived to establish the relation between axial load and changes in the dynamic system characteristics of brick walls is explained. A set of three different walls are constructed and tested under different load scenarios. Tests are also carried out in constitutive materials, to identify some basic characteristics related with dynamic behavior.

An important variation of the dynamic frequencies is noticed when loading the walls. It is demonstrated that this variation is correlated with the axial load magnitude, however, the boundary conditions seems to be an important conditioning for the first load steps.

6.5.2. Materials and experimental method

The main objective of the experimental works was not related with dynamic characterization. Fifteen walls were constructed and tested to study the bi-axial behavior. Only three series of dynamic tests were carried out in two of these panels. A complete description of the experimental works aimed at characterizing bi-axial behavior of walls can be found in [Sanchez, 2001].

Description of the tested walls

The wall panels were constructed in the laboratory with a dimension of 100cm of high and 120 of wide. The bonding between bricks was made of cement-sand mortar, with 1 cm of thickness, for both horizontal and vertical joints. The wall is supported in the laboratory's reaction slab and a displacement restriction is set to avoid horizontal movements, both in the base and in the top of the wall [figures 6.5.1 and 6.5.2].

The load level was different for every panel. The panels that were dynamically tested were subjected to vertical load (uni-axial) only. Other panels were subjected to a vertical constant loading and to a variable horizontal loading (up to failure). A general view of the test is observed in figure 6.5.3.
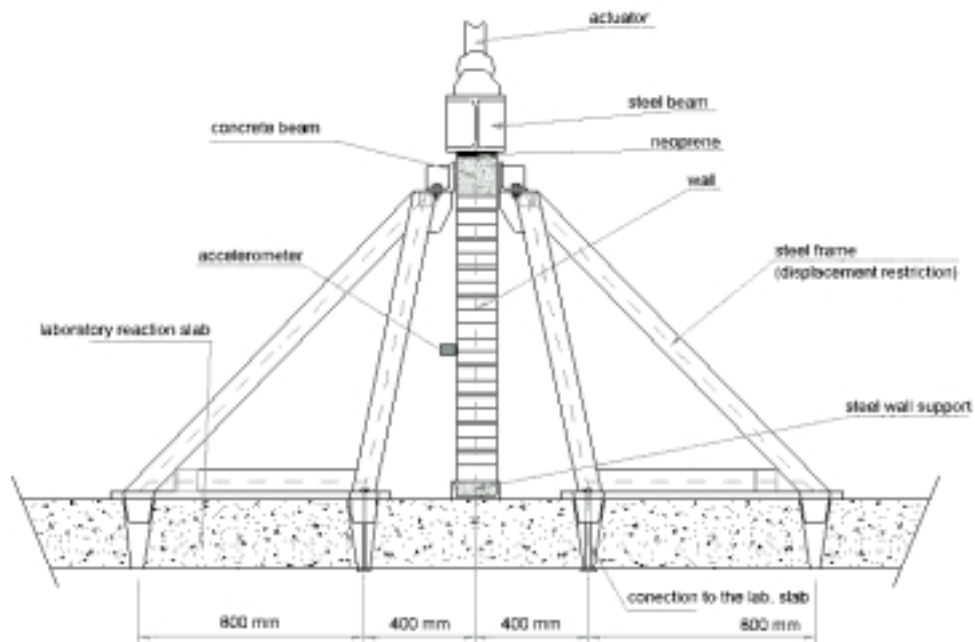
Figure 6.5.1. Configuration of the dynamic test.

Figure 6.5.2. Configuration of the dynamic tests.

Figure 6.5.3. General view of the load test.

Testing was also carried out in smaller wall specimens to identify some structural characteristics such as compressive strength or strain modulus. Two different kind of specimens were constructed and tested:

- Type I, consisted in a 3-brick array in one direction [figure 6.68, left].

- Type II, consisted in a 8-brick array in two directions [figure 6.68, right].

The average compressive strength of the wall was 1,9 MPa.
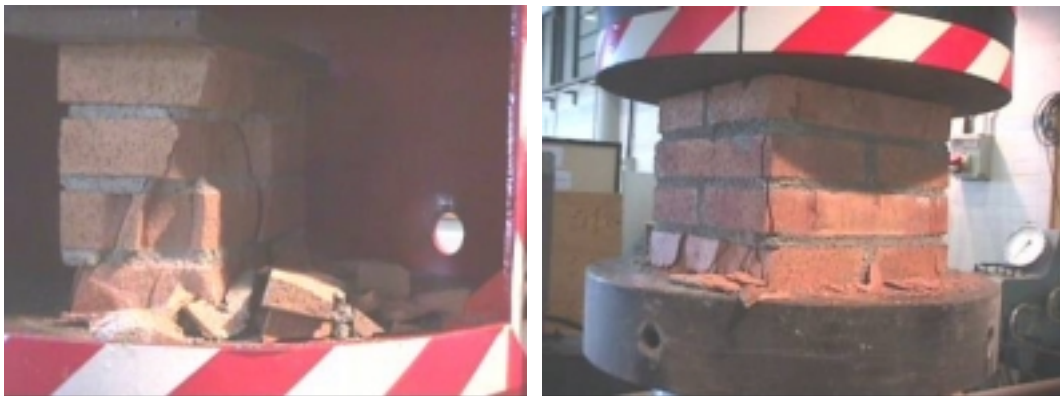
Figure 6.5.4. Wall samples subjected to uni-axial test. Type I

Material characterization test were also carried out in mortar specimens. The average compressive strength of mortar was 7,80 MPa.

Two different wall-panels were subjected to dynamic characterization. Wall 1 was subjected to increasing load steps until a maximum stress of 2,30 MPa. A detailed description of the load steps is given in table 6.5.1. The wall 1 was tested only few weeks after the construction.

Load step	Applied load (kN)	Stress (MPa)
e0	0,00	0,00
e1	30,02	0,18
e2	60,80	0,36
e3	90,00	0,54
e4	120,00	0,71
e5	150,00	0,89
e6	181,10	1,08
e7	210,50	1,25
e8	239,90	1,43
e9	269,10	1,60
e10	300,20	1,79
e11	348,80	2,08
e12	399,30	2,38

Table 6.5.1. Load steps in Wall 1.

The wall-panel 2 was subjected to dynamic characterization two times. It is worth mentioning that this panel was tested more than one year after the construction and therefore was a lot more rigid than wall 1. Once again, the panel was subjected to increasing load-steps [table 6.5.2] but the achieved stress was only 50% of the previous wall. A higher stress (similar to wall 1) could not be achieved because the panel suffered an equilibrium failure. After the first attempt, the wall was tested under the same conditions and failed again in the same configuration (rotation around the support). The lateral displacement restriction did not work properly in this test. However, the test was taken until a stress of 1,19 MPa; and the acquired data is processed and compared with the previous wall.

Load step	applied load (kN)	stress (MPa)
1	0	0.00
2	50	0.30
3	100	0.60
4	150	0.89
5	200	1.19

Table 6.5.2. Load steps in Wall 2.

6.5.4. Results

The strain modulus was measured in one panels taken until ultimate vertical load. The modulus suffered important changes while the applied load was modified. The modulus suffered an important hardening process [first half of the figure 6.5.5.]. After 500 kN of load (a stress of approximately 4,0 MPa) the wall started to loose stiffness and the strain modulus decreased [figure 6.5.5]. In this example, the hardening process described in section 5.5.2 is identified for this kind of constructive members. The phenomena consist in a stiffening of the wall until a 50-60% of the ultimate load, and then a reduction of the stiffness while cracks start to appear.
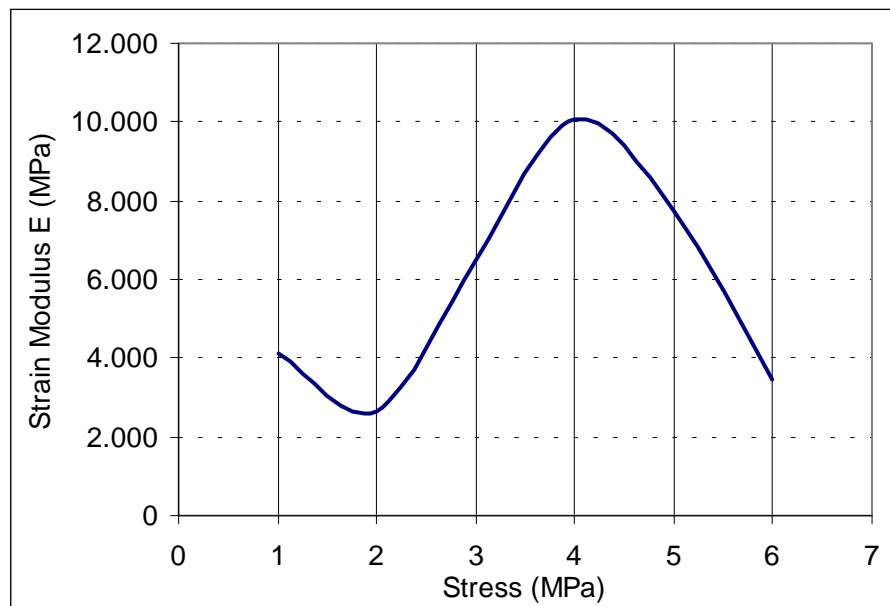
Figure 6.5.5. Experimental strain modulus vs. applied load.
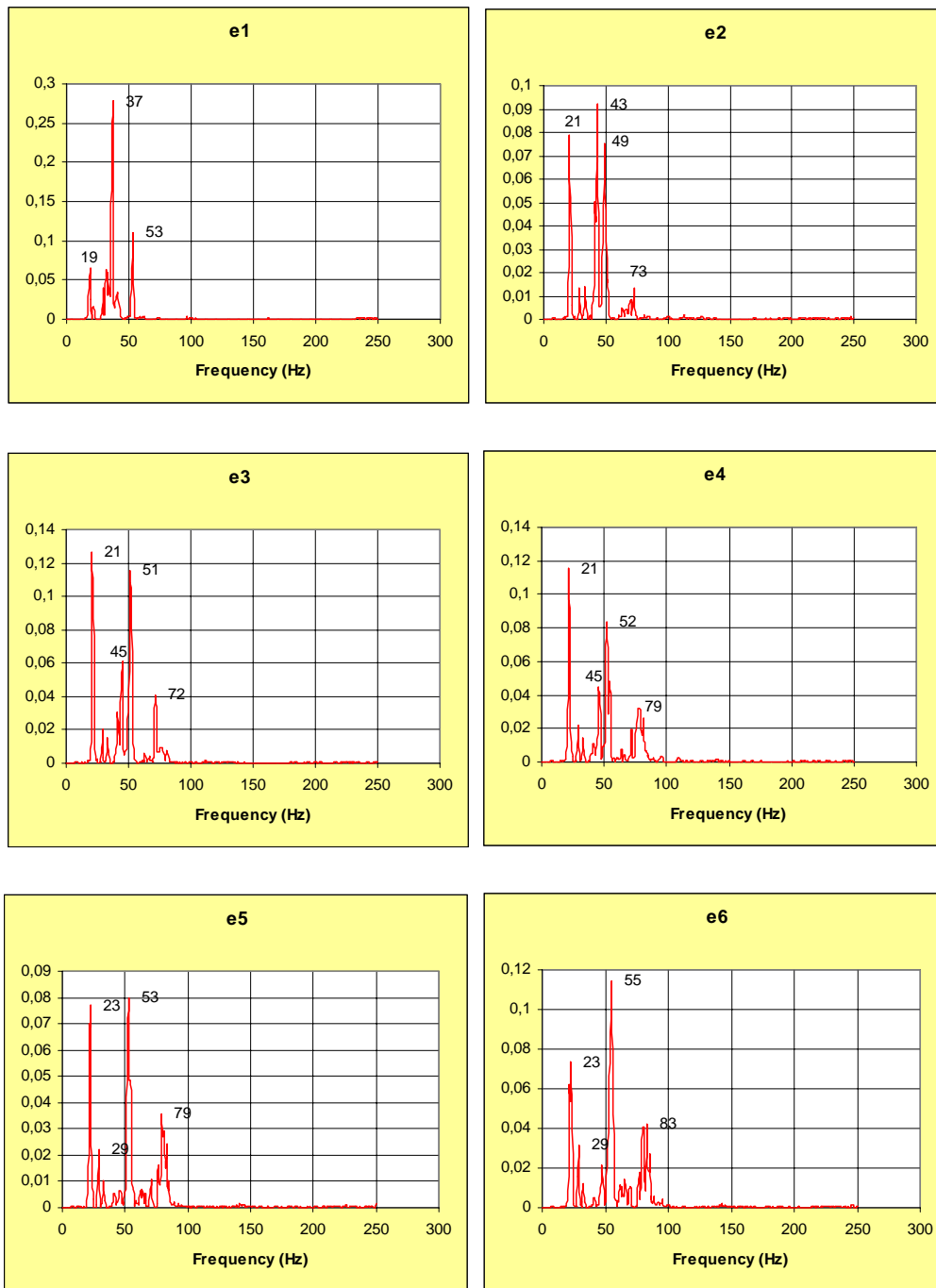
Figure 6.5.6.a Evolution frequency-domain spectra in Panel 1 through the first six load steps.
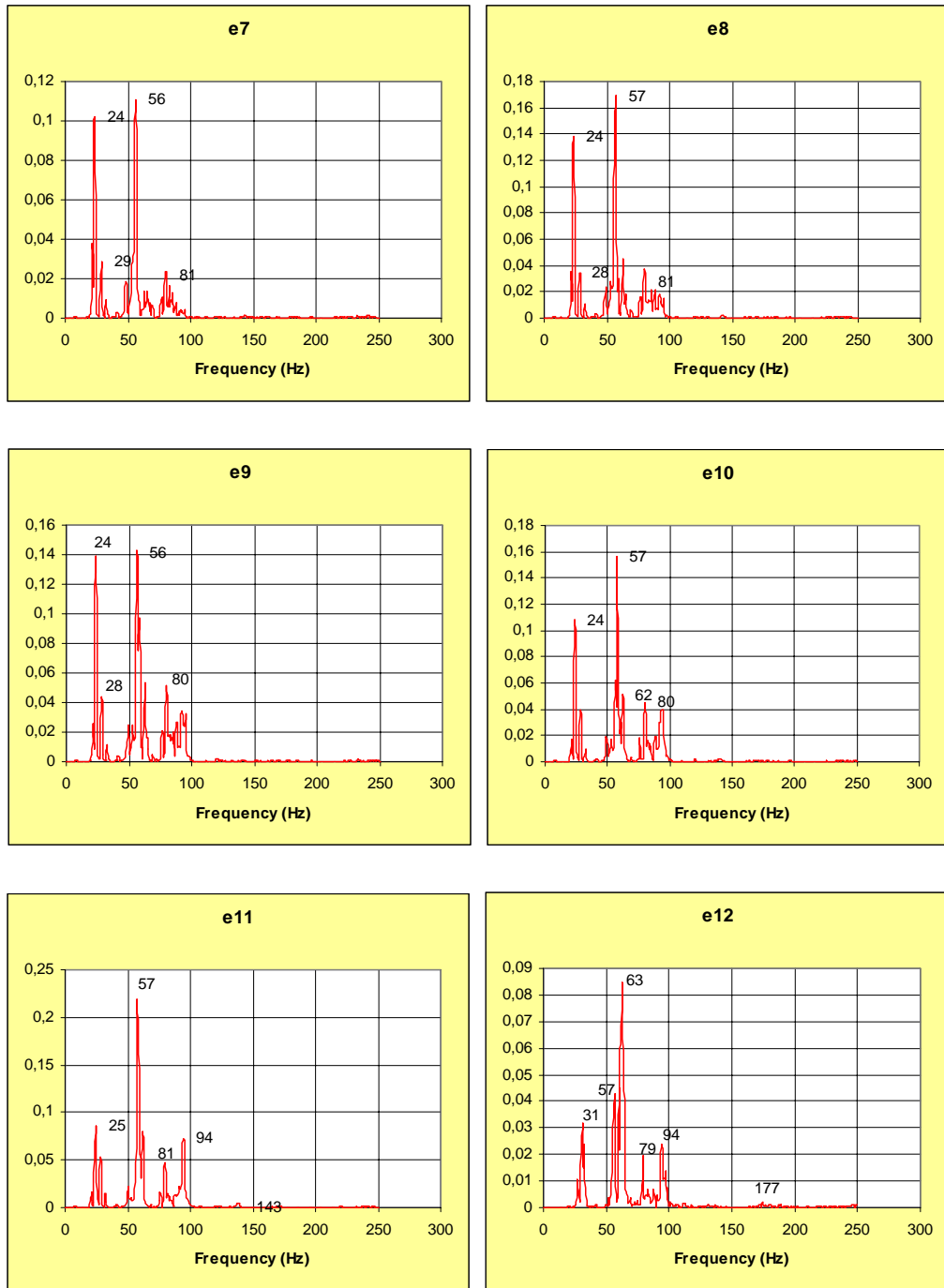
Figure 6.5.6.b Evolution frequency-domain spectra in wall-panel 1 through the

final six load steps.

The natural frequencies are evaluated after every load increment. Here, contrarily to the technique applied in concrete beams, the load is not released after every step step, because the objective of dynamic testing is precisely to identify axial load. Three natural frequencies are easily recognizable by identifying the picks in the frequency domain spectra. In figure 6.5.6a and 6.5.6b the evolution of the natural frequencies is plotted for every load steps (12 in total).

A clear increment of the first frequency is observed from step 1 (e1) to step 12 (e12). The value is modified from 37 to 63 Hz. Another frequency can be clearly followed, varying from 72 to 80 Hz. The variation of the first two natural frequencies is showed in figure 6.5.7. Other frequencies are identified for particular load steps but cannot be followed through the full load process.
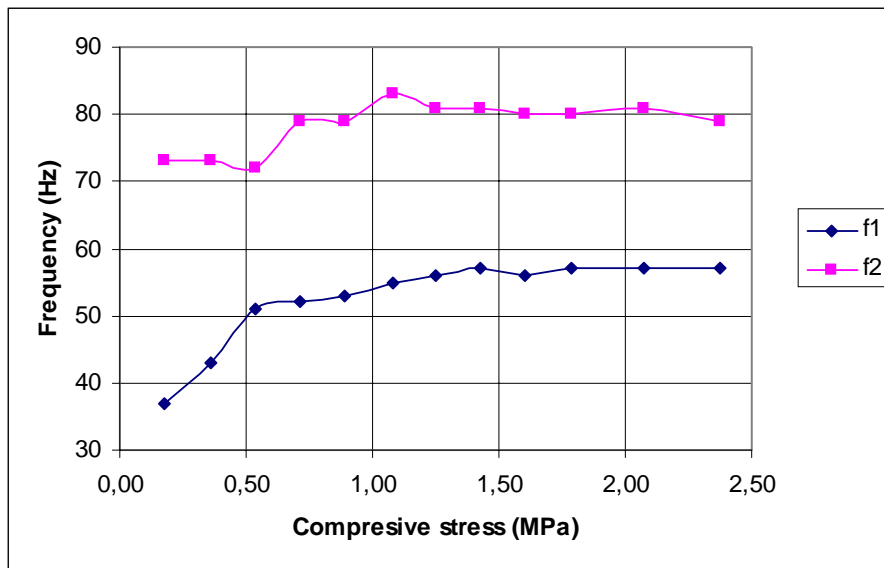
Figure 6.5.7. Evolution of the first two natural frequencies in Wall-panel 1 through the loading process.

The numerical values of the identified frequencies of wall 1 are presented in table 6.5.3.

Load step	Applied load (kN)	Stress (MPa)	Identified frequency (Hz)	
			f1	f2
e1	30,02	0,18	37,0	73,0
e2	60,80	0,36	43,0	73,0
e3	90,00	0,54	51,0	72,0
e4	120,00	0,71	52,0	79,0
e5	150,00	0,89	53,0	79,0
e6	181,10	1,08	55,0	83,0
e7	210,50	1,25	56,0	81,0
e8	239,90	1,43	57,0	81,0
e9	269,10	1,60	56,0	80,0
e10	300,20	1,79	57,0	80,0
e11	348,80	2,08	57,0	81,0
e12	399,30	2,38	57,0	79,0

Table 6.5.3. Identified frequencies in Wall 1.

The second wall-panel was tested two times. As mentioned before, an equilibrium failure has taken place at a stress around 1,2 MPa (test A) in the first attempt and the test has to be repeated with the same result (test B). Therefore, only five load steps were applied. If the frequency domain diagrams are studied, a clear pick of 50 Hz is detected for all the load-steps. This frequency remains stable (with not variation) for all the load stages. Another two natural frequencies can be clearly identified; the first one oscillates from 74 to 98 Hz and the second one is located in a range between 290 and 332 Hz [figures 6.5.8. and 6.5.9].

The evolution of the identified frequencies of wall panel 2 (test A and B) is shown in figures 6.5.10 and 6.5.11 respectively (first frequency is not plotted because it remains constant in a value of 50 Hz).
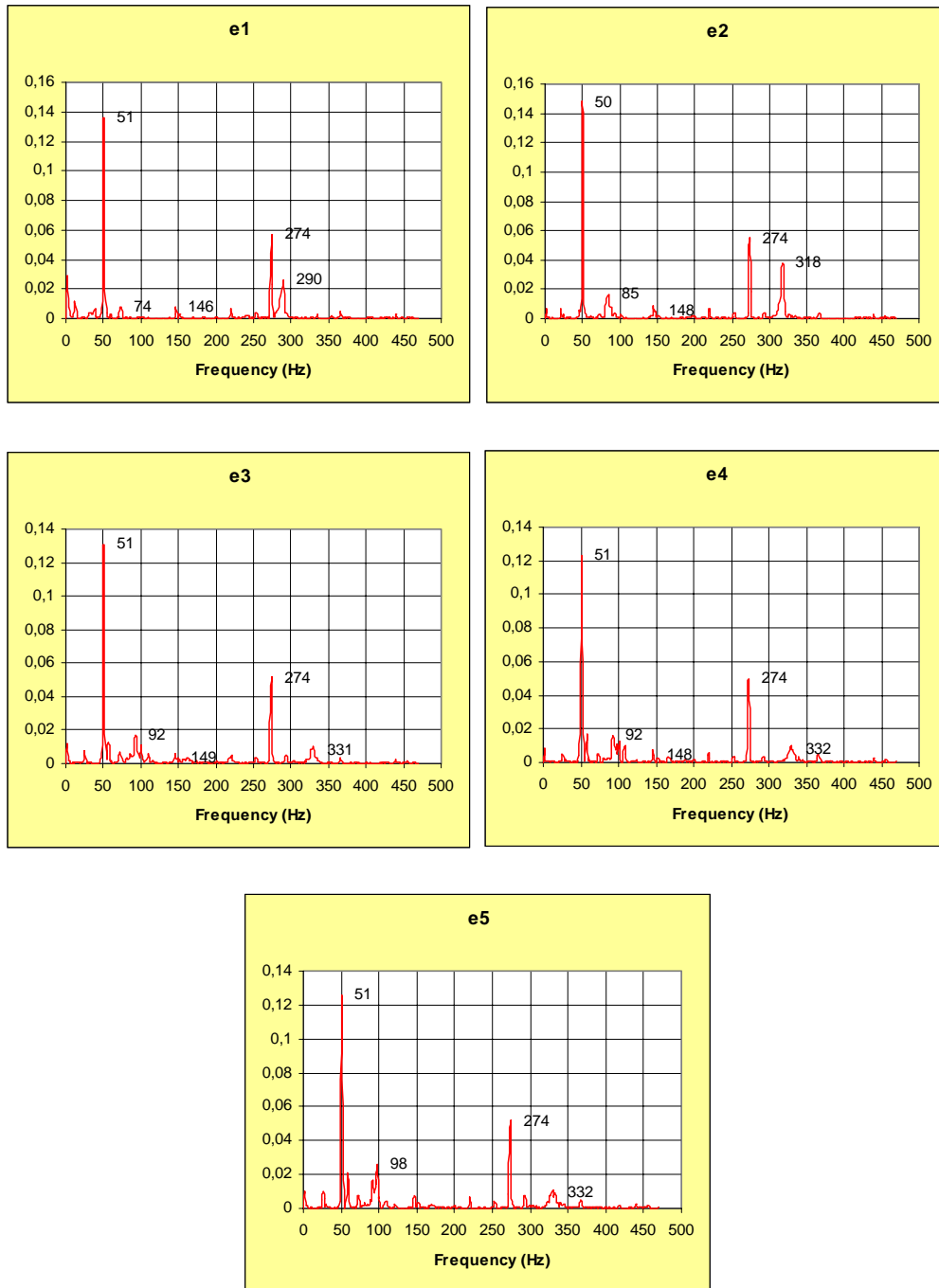
Figure 6.5.8. Evolution frequency-domain spectra in Panel 2 (test A) through the loading process (five steps).
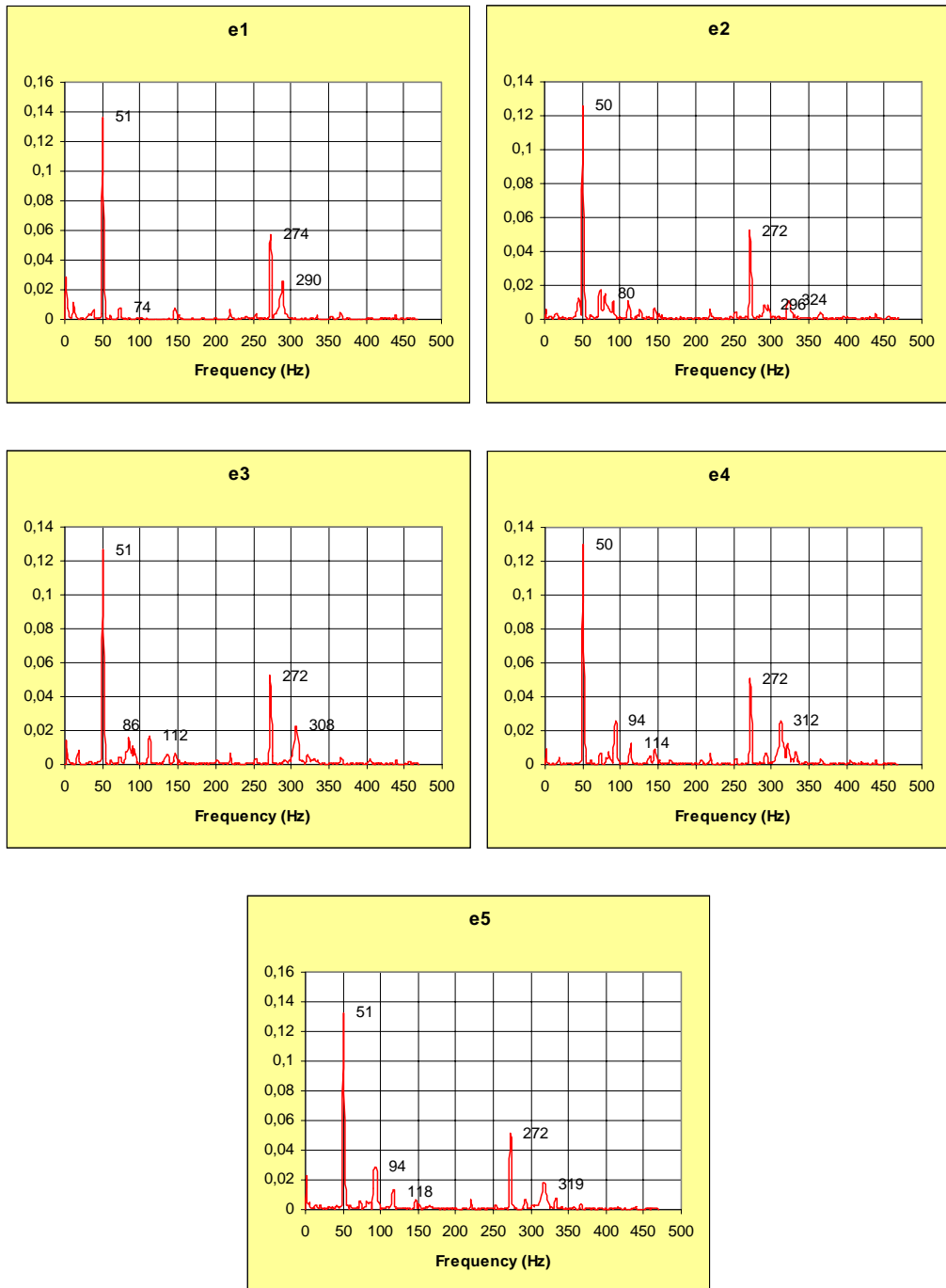
Figure 6.5.9. Evolution of frequency-domain spectra in Panel 2 (test B) through the loading process (five steps).
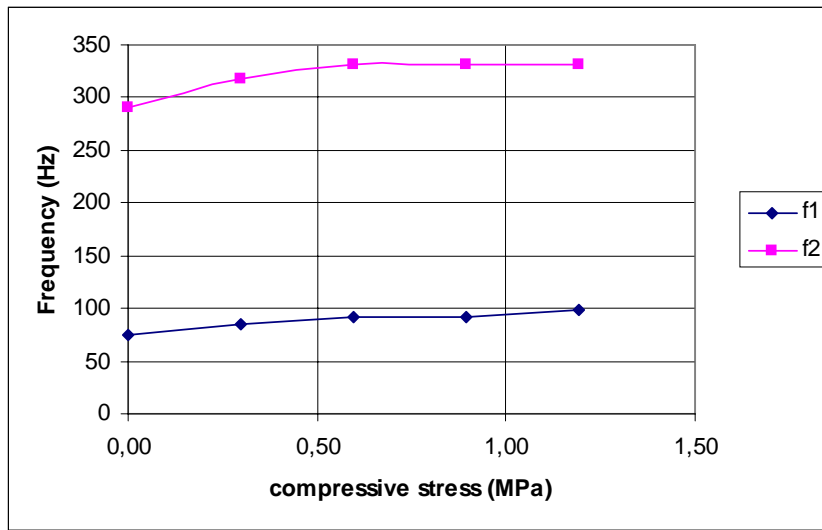
Figure 6.5.10. Evolution of the natural frequencies in Panel 2 (test A) through the loading process (five steps).
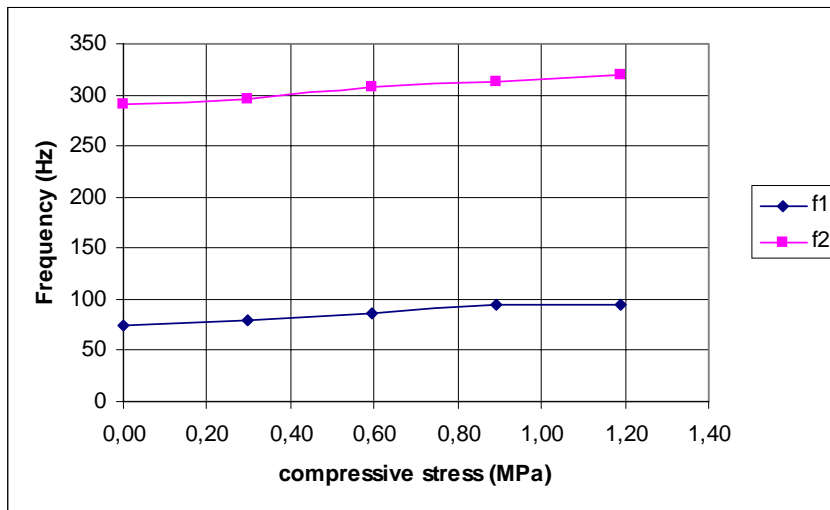
Figure 6.5.11. Evolution of the natural frequencies in Panel 2 (test B) through the loading process (five steps).

The numerical variation of the identified frequencies of wall panel 2 (tests A and B) is presented in tables 6.5.4 and 6.5.5. respectively.

Load step	applied load (kN)	stress (MPa)	Identified frequency (Hz)	
			f1	f2
1	0	0,00	74	290
2	50	0,30	85	318
3	100	0,60	92	331
4	150	0,89	92	332
5	200	1,19	98	332

Table 6.5.4. Identified frequencies in Wall 2, test A.

step	applied load (kN)	stress (Mpa)	Identified frequency (Hz)	
			f1	f2
0	0	0,00	74	290
1	50	0,30	80	296
2	100	0,60	86	308
3	150	0,89	94	312
4	200	1,19	94	319

Table 6.5.5. Identified frequencies in Wall 2, test B.

6.5.4. Numerical model

A numerical model was developed to calculate the natural frequencies. The model was defined with shell element for the wall and beam-type elements for the superior concrete and steed distribution beams [figure 6.5.12]. The model had 1000 DOF's. The contour condition were defined as follows:

- The inferior nodes (in contact with the laboratory reaction slab) were pinned (displacement restricted in x, y and z)

- The superior nodes, in contact with the distribution beams and the steel frame were restricted to z displacement.

The model was subjected only to gravitational loads and its natural frequencies are evaluated. The first 8 modal shapes and associated natural frequencies are presented in figure 6.5.13.
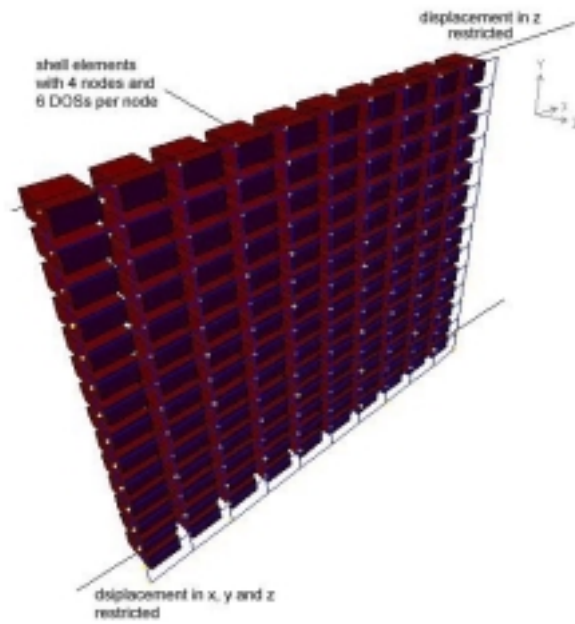
Figure 6.5.12. Numerical model and contour conditions of the tested panel.

| Mode 1; 58 Hz. | Mode 2; 73 Hz | Mode 3; 110 Hz. | Mode 4; 170 Hz. |

| Mode 5; 185 Hz. | Mode 6; 200 Hz | Mode 7; 233 Hz. | Mode 8; 313 Hz. |
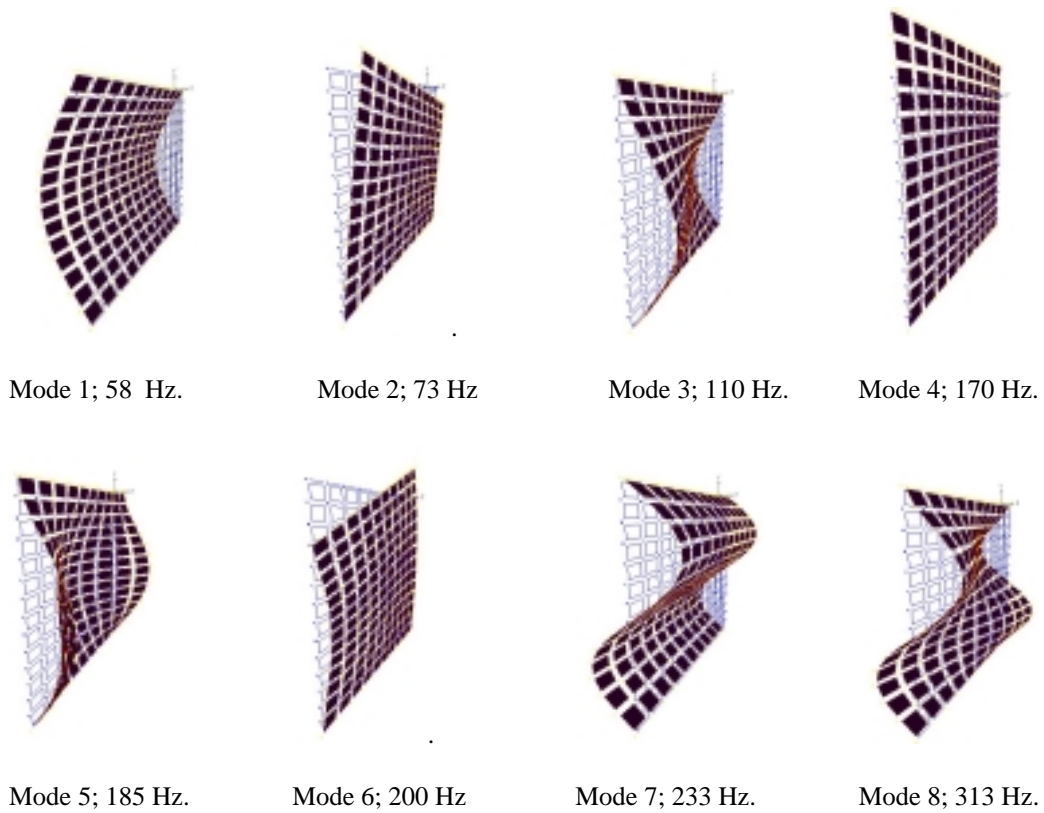
Figure 6.5.13. First eight numerical modal shapes and natural frequencies of the

tested panel.

A parametrical study was developed to characterize the influence of contour conditions in the natural frequencies of the wall panel. Different support conditions in the top and in the bottom of the wall were combined from pinned to clamped conditions. The three first natural frequencies were evaluated for every combination [table 6.5.6].

spring K	top support			
(kN/Rad)	pinned	100	500	clamped
First flexural frequency (Hz)				
pinned	58,1	67,1	79,4	90,9
100	67,1	75,8	88,5	101,0
500	79,4	88,5	102,0	116,3
clamped	90,9	101,0	116,3	131,6
Second flexural frequency (Hz)				
pinned	185,2	185,2	185,2	188,7
100	192,3	192,3	192,3	192,3
500	200,0	200,0	200,0	200,0
clamped	208,3	208,3	208,3	212,8
Third flexural frequency (Hz)				
pinned	232,6	243,9	263,2	294,1
100	243,9	256,4	277,8	303,0
500	263,2	277,8	294,1	333,3
clamped	294,1	303,0	333,3	370,4

(The three sub-blocks are grouped under "Bottom support" on the left.)

Table 6.5.6. Parametrical influence of contour conditions in the first three natural frequencies. FEM values.

The influence of the contour conditions can also be presented in a graphical way. In figure 6.5.14, the first natural frequency is plotted vs. variation if the top and bottom supports. The panel can modify its frequencies up to 240% of the initial value when contour conditions are modified. The second and third natural frequencies are studied in an analogue form [figures 6.5.15 and 6.5.16, respectively]. Second and third natural frequencies resulted to be less sensitive to the variation of the support conditios.
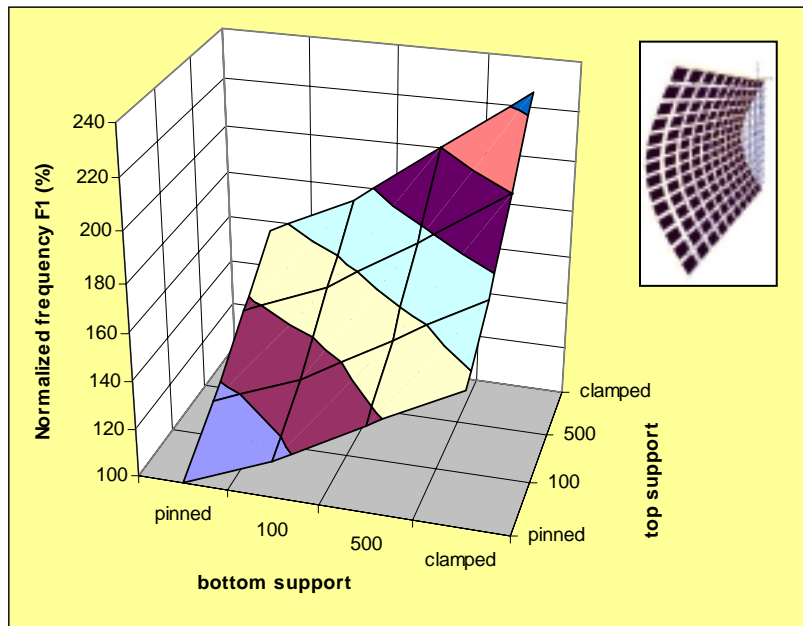
Figure 6.5.14. Parametrical study of the influence of boundary conditions in the first flexure natural frequency of the panel.
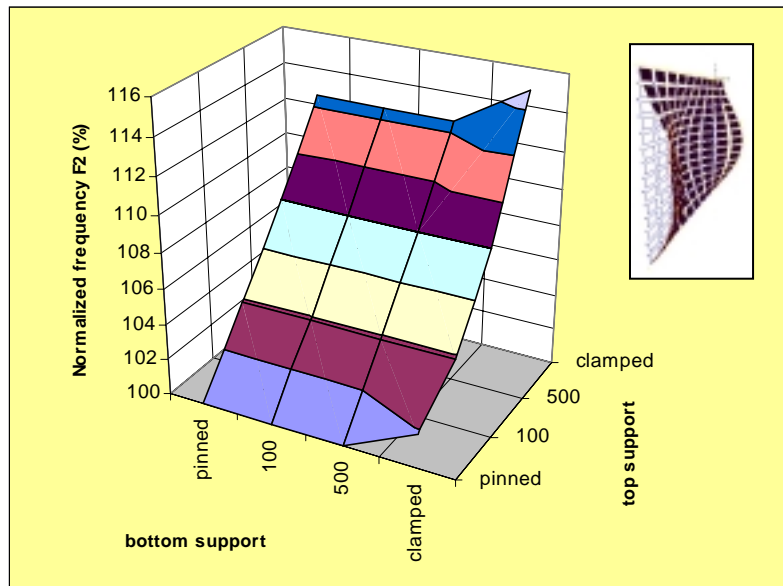
Figure 6.5.15. Parametrical study of the influence of boundary conditions in the second flexure natural frequency of the panel.
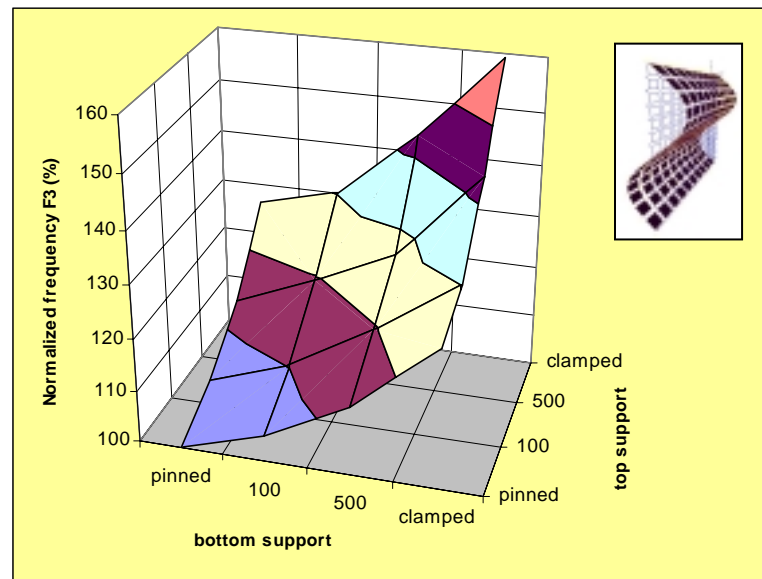
Figure 6.5.16. Parametrical study of the influence of boundary conditions in the third flexure natural frequency of the panel.

6.5.5. Discussion

A series of brick-wall panels were tested dynamically under different load levels and an important increment of the natural frequency values is observed in all the cases. An important influence of the axial load on the dynamic response of the walls was identified. This variation is related to a modification of the contour conditions.
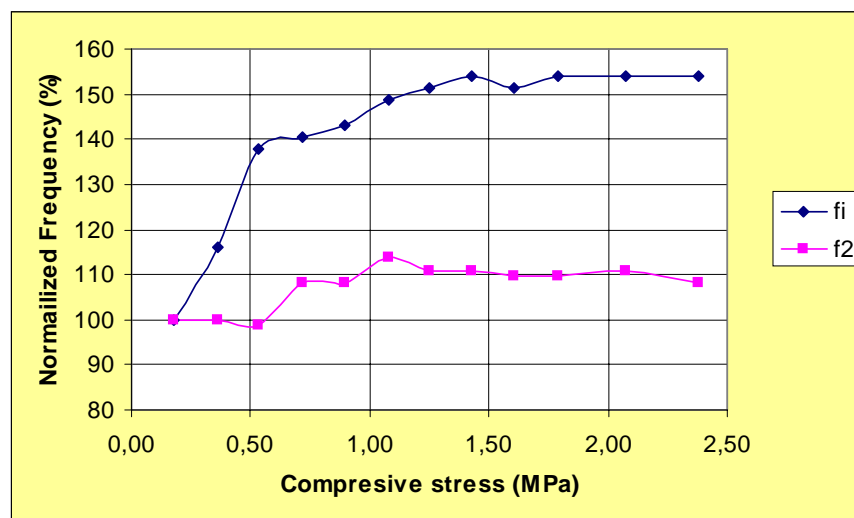
Figure 6.5.17. Experimental evolution of the first two identified frequencies of the wall through the load process. Panel 1.

In figure 6.5.17, the variation of the first and second natural frequencies of the wall-panel 1 vs. the increment in the applied stress is plotted. The first frequency increases gradually up to 155% of its initial value. The second frequency is less dependent of the induced stress.
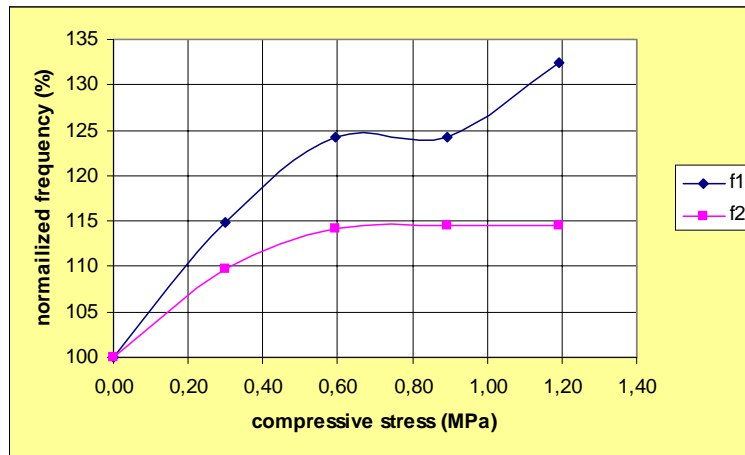
Figure 6.5.18. Experimental evolution of the first two identified frequencies of the wall through the load process. Panel 2, test A.
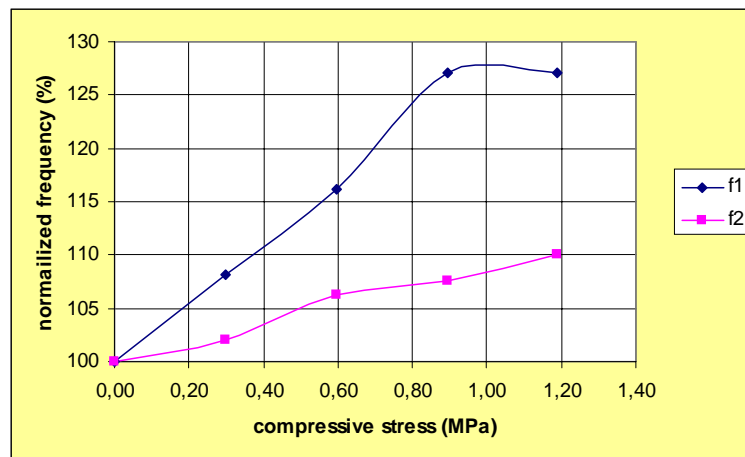
Figure 6.5.19. Experimental evolution of the first two identified frequencies of the wall through the load process. Panel 2, test B.

The wall panel 2 presents a similar behavior, the first frequency grows until a 132% of its initial value (for test A) for a stress of 1,2 MPa. The second identified frequency is again less sensitive to modifications of the axial load. The test is

developed two times in the same conditions and with similar results [figures 6.5.18 for the first attempt and 6.5.19 for the second one].

It was observed in all the cases that the first natural frequency was more sensitive to changes in the axial load. This fact is corroborated by the parametrical study where it is shown that the first frequency can be modified up to 230% of its initial value when boundary conditions are modified. Other subsequent frequencies are less sensitive to the change in boundary.

The experimental works permits to conclude that the application of axial load in a masonry element leads to a modification in its contour conditions, and furthermore to a modification in its dynamic properties. In the studied case, the wall suffered an important modification of its dynamic properties when axial load was applied. A relation between the applied stress and the variation in the frequency was found [figures 6.5.17, 6.5.18 and 6.5.]. This kind of graphs can be used in both directions: identify axial load from known frequencies or identify frequencies from known loads. The method relies in the development of a FEM to study parameter sensitivity and to find the relation between load and frequencies in very particular case.

6.6. Influence of axial load on dynamic parameters of stone columns.

6.6.1. Introduction

In this section, an experimental program conceived to establish the relation between axial load and changes in the dynamic system characteristics of stone piers is explained. The experimental campaign is developed under the frame of the study of the Cloister of Girona (described in detail further in section 7.2.1). The experimental works were carried out in collaboration with professor Miquel Llorens and the University of Girona.

The objective of the present experimental program is analyzing the variation of the natural frequencies in stone members that are subjected to axial load. A stone specimen, obtained from the same origin of the piers of Cloister of Girona is tested under different load scenarios. An important variation on the first natural frequency was observed. Another studied parameter was the ratio between first and second natural frequencies. This parameter was founded helpful when identifying contour conditions.

The hypothesis is that certain homogeneous and composite materials (as stone or brick masonry) present a hardening phenomenon under certain load conditions. This hardening is translated in to a change of modulus of deformation under different load ranges. The aim of this study is to use dynamic information as a tool to identify the strain modulus and subsequently the load conditions of the structure.

6.6.2. Materials and experimental method

Description of the tested columns

A full-scale model of the columns was constructed using stone taken form the original quarry. Although the origin is same, it must be noted that the time exposition to atmosphere conditions of the laboratory specimen is obviously very reduced compared to the ancient columns of the cloister. The specimen was installed in a press machine, supported in two steel plates with not restriction to rotation. The section of the column was circular with a diameter of 15 cm and an area of about 177 cm2

In an analogue way to tests in the cloister, impulsive force was generated by a soft single impact applied at the mid-span of the specimen. The column was subjected to an increasing axial load varying from 0 to 260 kN. Stresses due to axial load varied from 0 to 14.7 MPa [figure 6.6.1]. The application of the load was divided into steps of 20 kN. (14 steps) and evaluation of dynamic properties was done at the end of every step, under static load.

One accelerometer was attached to the column using a stiff connection to avoid decoupling effects [figure 6.6.2].

Figure 6.6.1. Loading process of the stone column.

The dynamic modulus of deformation was evaluated by means of the same technique used for concrete cylinder specimens [ASTM C215, figure 6.6.3]. A value of 37,600 MPa was thus measured.

Figure 6.6.2. Quartz accelerometer attached to the tested stone column.

Figure 6.6.3. Stone cylinder (15x30 cm) suspended to identify dynamic strain

modulus (ASTM C-215)

6.6.3. Results

The frequencies of the column are evaluated for every different load step. The load is sustained while the test is developed. The energy of the test is dissipated in less than 1/10 sec and two pick are easily recognizable in the frequency domain graph [figure 6.6.4]. A clear variation of natural frequencies was observed during the test [table 6.6.1]. First, a descending slope was presented during the first two load steps [figures 6.6.5 and 6.6.6]. Then, the frequencies showed a clear increasing trend. It is well known that the theoretical proportion between the second and first natural frequencies F2/F1 presents a constant value of 2.75 for double fixed support condition and 4.0 for a double free support condition in column-type elements [figure 6.6.8]. On the tests carried out, a variation between the ratios F2/F1 vs. applied load is clear only for the first two load steeps. Further on, the relationship between F2/F1 and the applied load remains more or less horizontal [figure 6.6.7]. This clearly shows that the support conditions at the ends of the column changed only during the first two steps to then stabilize in the form of a partial clamping. Further on, variation in frequencies is mostly to the variation of the modulus of elasticity (a hardening process).

applied load (kN)	F1 frecuency (Hz)	F2 frecuency (Hz)	F2/F2
6	759	2756	3,63
21	755	2430	3,22
41	722	2167	3,00
61	744	2265	3,04
81	744	2318	3,12
100	754	2415	3,20
120	759	2420	3,19
140	771	2460	3,19
160	774	2530	3,27
181	780	2565	3,29
201	791	2580	3,26
220	804	2590	3,22
240	808	2603	3,22
260	814	2624	3,22

Table 6.6.1. Identified frequencies.
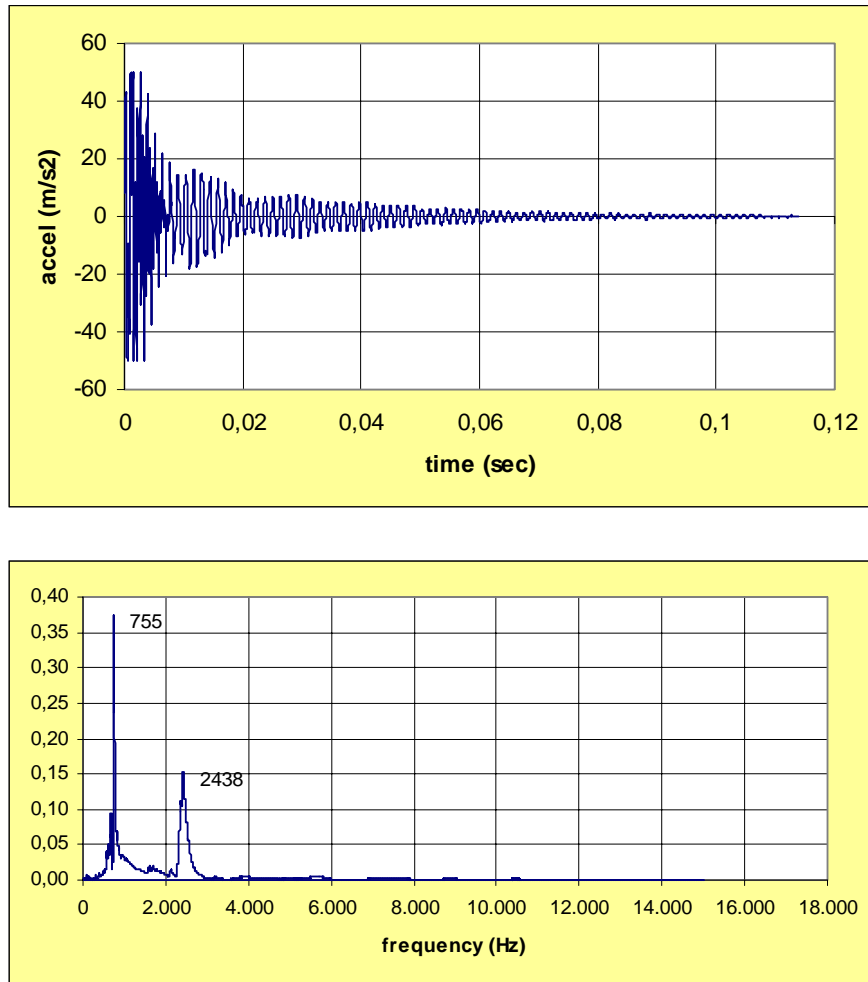
Figure 6.6.4. Typical time-domain (above) and frequency-domain (below)

spectrums.
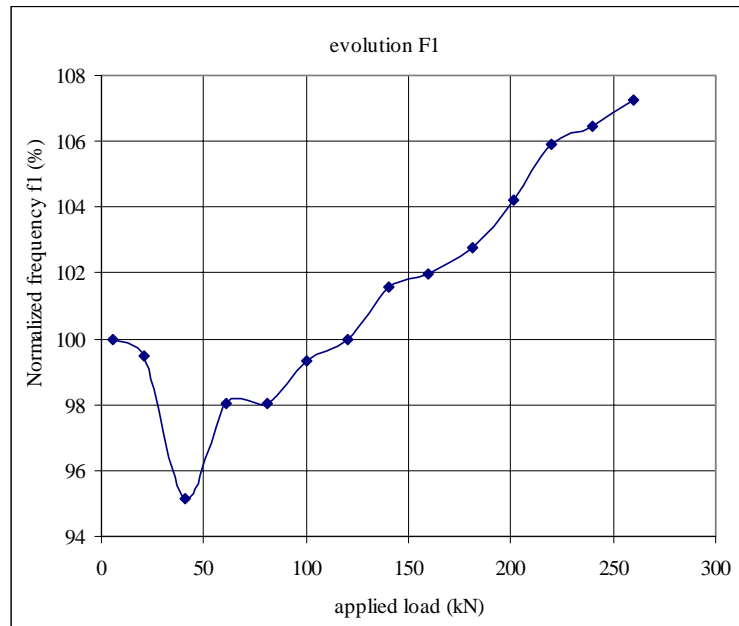
Figure 6.6.5. Evolution of the first natural frequency vs. applied axial load.
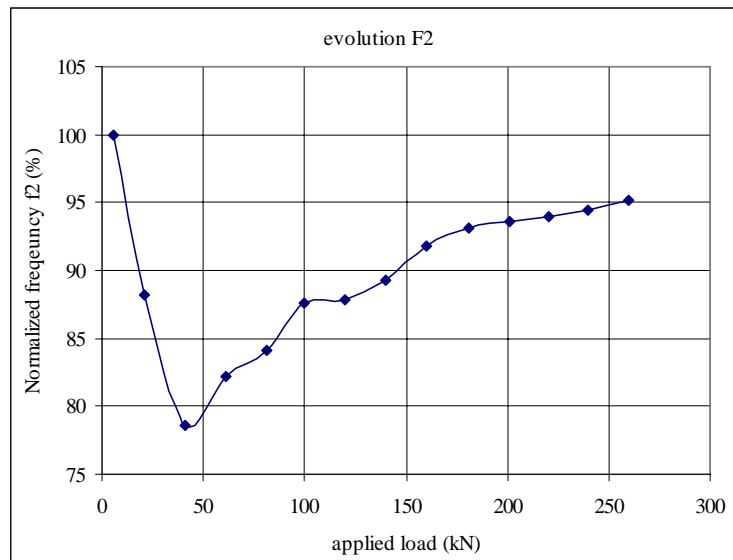
Figure 6.6.6. Evolution of the second natural frequency vs. applied axial load.
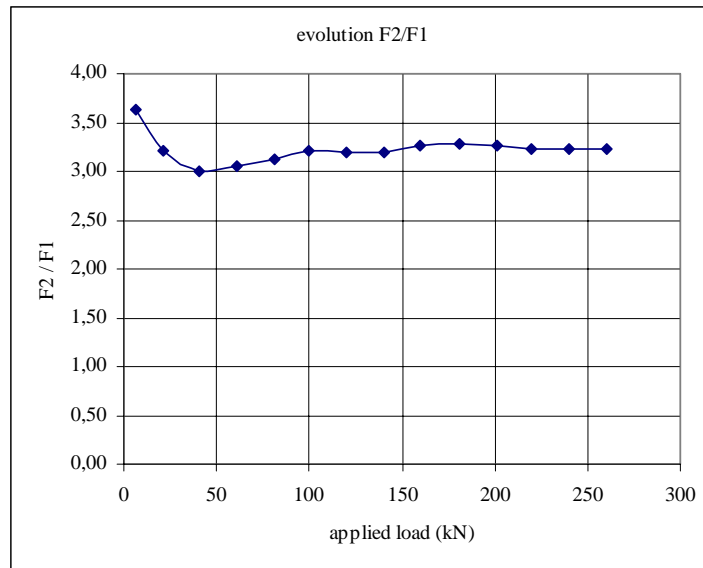
Figure 6.6.7. Relationship between the ratio F2/F1 and the applied axial load.
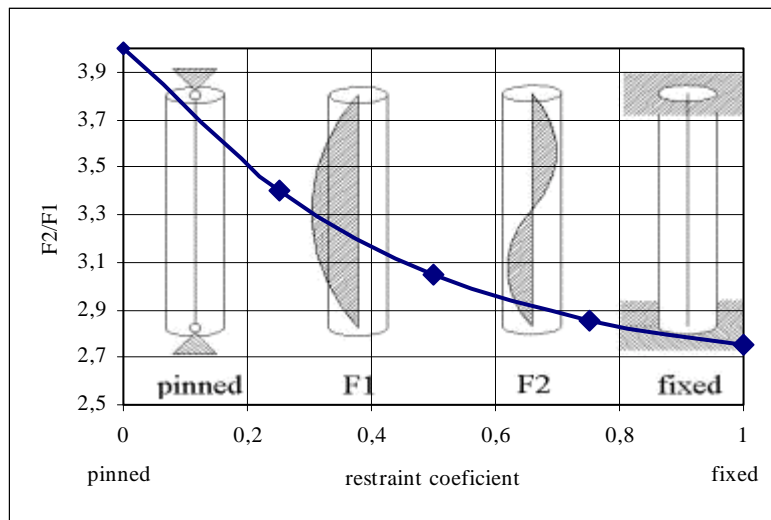
Figure 6.6.8. Theoretical relationship between first and second natural frequencies
(F2/F1) vs. a clamping coefficient

6.6.4. Discussion

A stone specimen was subjected to an increasing load test. Dynamic properties were measured for every load scenario applying the method proposed in chapter 4. A clear relationship between the axial load and the dynamic response of a stone column was identified. This variation is related to a hardening phenomena frequently identified in masonry structures.

It was possible to establish a relationship between applied load and frequency values [figures 6.6.5 and 6.6.6]. This kind of graphics can be used to identify the axial load starting from a known frequency. It is necessary to develop a calibration for every particular case; however, once the relationship is calibrated, systematic dynamic testing can be enough to identify the acting axial load.

The variation of dynamic parameters of masonry constructive members and its relation with axial loading seems to be a good alternative to identify load levels in compressed structures (not only brick walls, but also stone specimens) by measuring their dynamic response. A numerical model has to be developed and optimized for every particular case; however, when the model and the experimental results present a good correlation, the model has adequate predictive capacity.

seven

Field Studies

7.1. Introduction

In this chapter, a series of field studies are presented. The objective of those works is to confirm the assessment capacity of the proposed dynamic layout. The chapter is divided in two mayor subjects: Concrete slabs and masonry building components.

In the first part, three different concrete building are systematically inspected by means of dynamic testing. The followed methodology consists in inspecting the slabs by developing several dynamic tests and optimising a numerical model by using the identified natural frequencies.

The second part consists in three different applications of dynamic assessment addressed to historical masonry buildings. The objective of the tests is identifying the current structural condition of masonry components. Studied members include stone piers, load-caring walls and stone cantilever beams.

By developing field studies, the practical implementation of the test is corroborated, new possibilities for the test are identified and some implementation problems are detected.

7.2. Concrete Slabs

7.2.1. Pre-stressed slab (*Retie*)

7.2.1.1. Introduction

Dynamic forces applied in or in the neighborhood of buildings can lead to structural damage, mal- functioning of sensitive equipment and discomfort to people. When

the vibration is considerably magnified (e.g. resonance effects of floors), adding of damping to the structure is an effective method to reduce the level of vibration. Viscoelastic materials are generally used as an instrument to increase the amount of damping in the structure. Even that the aim of this research work is not related with viscoelastic materials, the method applied to characterize the slab is the one proposed in the thesis. The works were developed in Belgium with the support of the structural mechanic section on the K.U. Leuven during the stay developed by the doctoral candidate in 1999.

The constrained-layer damping (CLD) method involves sandwiching a viscoelastic-damping medium between two stiff outer layers. The influence of the addition of a sandwich layer system on the dynamic behavior of a complex structure can be accurately predicted by a finite element analysis. In order to obtain a substantial increase of damping of the considered structure (e.g. floor slab) the eigenfrequency of the sandwich system should be tuned to the eigenfrequency of this structural component. An important aspect in the accuracy of the efficiency prediction is a good modeling of the structure. Although the mathematical framework to calculate the dynamic response is well established (finite element method), there are many uncertainties, which can only be resolved by experimental investigation. Typically boundary conditions and present damping are parameters, which can only be determined by experiments. A modal model of the structure can be obtained by a system identification method in the time of the frequency domain. The process to update a numerical model of the slab is the one proposed in Chapter 4.

Finite element programs are used to build a spatial model or a modal model of the investigated system. By comparing the properties of the finite element model with the results obtained from a system identification procedure, more accurate boundary conditions and material properties can be deduced.

In this example, a practical *in-situ* test case is described. The building of interest is located at a high-traffic road in Retie, Belgium. The vibration levels in the house are high according to the owner of the building. First, vibration measurements are performed to evaluate the level of vibration in the building according to the DIN

norm 4150 (part 2) and to determine the dominant frequencies of the vibration. Next, a modal analysis is performed to determine if resonance of the floor is the cause of the high vibration level.

As mentioned before, even that the objective of this thesis is not related with CLD energy dissipaters, the technique used to identify dynamic properties of the slab is a basic concern. The main objective of this field-study is carry out a model updating using two different data: the acquired with seven measurement points and the acquired with one accelerometer. The hypothesis is that only one accelerometer is enough to identify natural frequencies and therefore to carry out a model updating process.

7.2.1.2. Method

Description of the building

The building of interest [Figure 7.1] is a house located at the "Molsebaan 43" to Retie. The "Molse- baan" is an intensively used road between *Turnhout* and *Mol*. The front wall of the house is located at 18.50 m from the central axis of the road.

The house has two levels above a semi basement cellar, which is used as a studio. A general base slab is used as foundation for the house. The walls are made in masonry. The floor of interest (test floor) is located in the living room of the building. This floor is made of prestressed *Stalton* beams (a typical constructive method of Belgium). Intermediate members made of burnt clay are used to fill the empty space between the *Stalton* beams [Figure 7.2.]. A concrete topping of 4 cm is used to interconnect the different beams.

Figure 7.1. General view of the analyzed house.
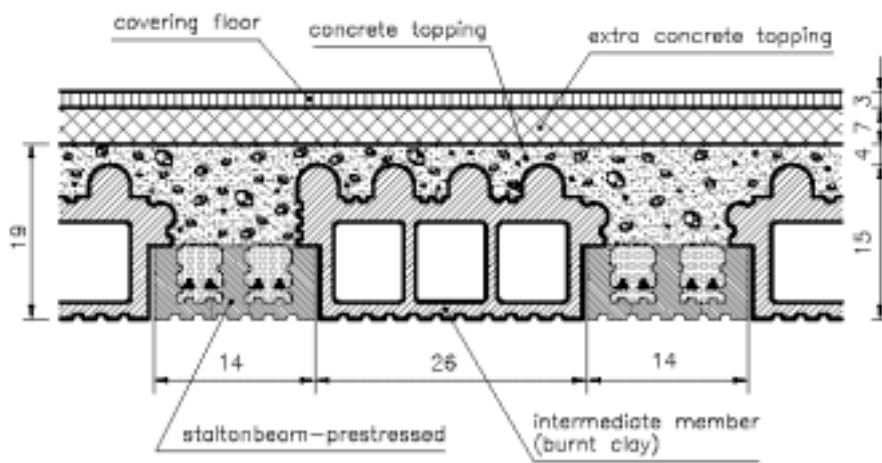
Figure 7.2. Cross-section of the test floor
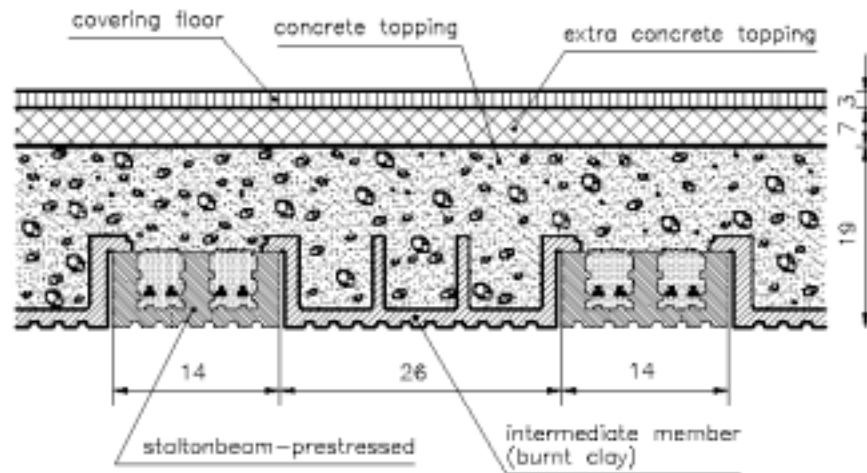
Figure 7.3. Longitudinal section of the stiffening beam

In the long direction of the floor, a stiffening beam is constructed at the central axis. It is made by filling an intermediate member with concrete [Figure 7.3].

During construction, it was already detected that the level of vibration of the floor was too high. The owner of the building decided to put an extra concrete topping of 7 cm thickness on top of the floor. Finally, a cover of 3 cm is used as finishing layer. The finished slab still present high levels of vibration detected by the users.

In Belgium, no standard exists to evaluate the vibration level in a built environment according to disturbance to people. Therefore, the German standard DIN-4150-2 [1] *"Ersch.utterungen in Bauwesen, Einwirkungen auf Menschen in Geb.auden"* was used in this report. The measurements were performed on Wednesday 22 December 1999 between 3.30 PM and 5.00 PM.

The measurement setup for evaluating the vibration level consists of 8 accelerometers [figure 7.4], a KEMO VBF 35 filter unit, a 16 bit acquisition card and a portable PC. The accelerometers 1 till 7 are located at the ceiling of the basement cellar. The accelerometer 8 is located at the floor of the basement cellar. At the location of accelerometer 8, there is an interconnection between the base slab of the house and the foundation slab of an exterior wall.

Figure 7.4. Deployment of dynamic sensors in the slab

Conditioning of the signals

A multi-channel analog filter/amplifier KEMO VBF 35 unit is used to filter the data. This is a computer optimized pass band filter, which is at up to the cut-off frequency and has a stop band of 85 dB starting at two times the cut-off frequency. Its response shape is very similar to an elliptic filter. The cut-off frequency used was 250 Hz. A 16-bit data-acquisition card (Daqbook 216) combined with the Dasy-lab software is used to obtain digital data. The sampling frequency is 1000 Hz; e.g. the Nyquist frequency is 500 Hz. The data was recorded during two periods of about 10 minutes. Afterwards, the data was spit into traffic passages of about 20 sec., which have been identified by using a trigger.

In the DIN-4150-2 standard, two evaluation periods exists when vibration due to traffic is examined: daytime (6.00 AM till 10.00 PM) and nighttime (10.00 PM till 6 PM). In table 3.2, the characteristic evaluation values are indicated for residential buildings.

According to the DIN-4150-2 standard, there is disturbance to people if the maximum value (KB_{Fmax}) is larger than A_o for the corresponding measurement period. If the KB_{Fmax} value is always smaller than the threshold value A_u, then there is no disturbance to people according to the standard. If the KB_{Fmax} value is between A_u and A_o, then an effective value KB_{FTr} for the evaluation period has to be calculated. If KB_{FTr} is larger than A_r, then there is also disturbance to people.

If the duration of the measurements is smaller than the evaluation period, then it is possible to make an extrapolation of the measurement time, if the period measured is representative for the whole evaluation period.

Because the level of vibration in the building clearly causes disturbance to people, it is interesting to compare the vibration levels with those that produce damage according to the Dutch SBR standard part 1. The sensors used, however, were not located in the most critical points of the structure as recommended in the SBR standard part 1.

From the results, it was concluded that the level of vibration in the building is smaller than the threshold values for damage according to the *"SBR richtlijn 1"*. The dominant frequency of the floor is about 14.4 Hz. At the intersection of the foundation slab of the house and the foundation slab of the exterior wall, a dominant frequency of 11 Hz was measured.

Modal analysis

Stochastic subspace identification method was used to determine the eigenfrequencies, the damping ratios and the mode shapes of the floor of the living room. Two loading cases were considered: (1) impact [figure 7.5] on the test floor and (2) ambient vibration.

In the next paragraphs, the test setup, the recording, the analysis of the signals in the frequency domain and the processing of the data for the impact case will be described. Afterwards, the results for all loading cases will be summarized. Finally, the finite element modeling of the test building will be discussed.

Figure 7.5 Excitation of the slab by impact-hammer.

The test setup

To obtain the eigenfrequencies and the damping ratios a test with a small number of measurement points is sufficient. For accurate determination of the mode shapes a rather large data set is necessary. A detailed analysis of the natural frequencies is important when the experimental determination of the boundary conditions is a subject of interest. A critical phase of the test is to find the equilibrium between simplicity (lowest number of sensors) and valuable information (reliable data).

Seven accelerometers were spread over the test floor. An impact hammer was used to excite the test floor [figure 7.5]. The lowest mode shapes can be determined by this test setup.

Analysis of the signals in the frequency domain

An analysis of the recorded signals was performed in the frequency domain. This was made to check the quality of the data. Also, it provided a first indication about the eigenfrequencies of the structure. The filtered responses in the frequency domain are shown in figure 7.6. for the test floor.

(accelerometer 1)

(accelerometer 2)

(accelerometer 3)

(accelerometer 4)

(accelerometer 5)

(accelerometer 6)
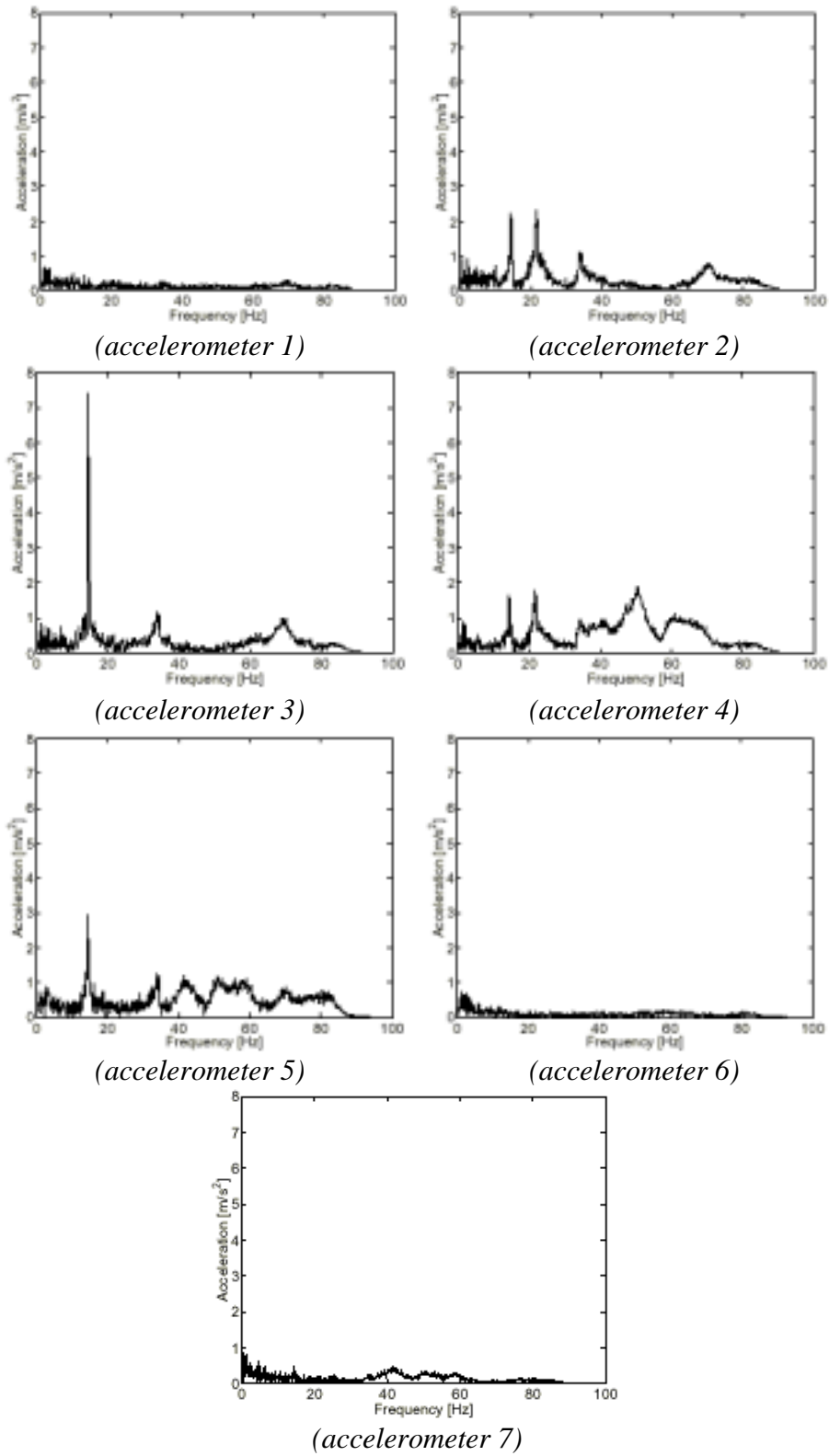
(accelerometer 7)

Figure 7.6. Some examples of experimental frequency domain (seven simultaneous accelerometers).

The response for the lower frequencies was better identified in accelerometer 3 [figure 7.6]. Sharp peaks in the frequency domain occur at 14.4, 34, and 70 Hz. The peak value at 14.4 Hz is dominant for the sensors 3 and 5 located along the center axis of the floor (long direction). The peak value at 21.5 Hz is dominant for the sensors 2 and 4. The first peak refers to the 1-1 bending mode of the tested floor, the second to the 1-2 bending mode of the foundation floor. The peak value at 34 and 70 Hz refer to the bending modes 1-3 and 1-5 of the tested floor.

Here, and in concordance with the method proposed in chapter 4, the use of only few accelerometers (2 or 3) would be sufficient to identify the first few natural frequencies of the slab. However, redundancy in the monitored points is always helpful but not strictly necessary.

7.2.1.3. Results

First, the data obtained by excitation of the test floor by impact were processed. The filtered time signals are used as input for the stochastic subspace method. The data was resampled at 200 Hz using an 8_{th} order low-pass Chebyshev type I filter. A zero-phase digital filtering technique has been used. Those mathematical procedures ere implemented in the used system-identification software [Peeteres, 2000 and Peeters and De Roeck 1999].

Several impacts were measured. For the modal analysis, only the not-contaminated data by influence of passing traffic was considered.

The lowest eigenfrequencies were identified by the stochastic subspace method. The eigenfrequencies and damping parameters are summarized in table 7.1. Also the mean value and the standard deviation are indicated in the same table.

impact	mode 1		mode 2		mode 3	
	[Hz]	[damp.]	[Hz]	[damp.]	[Hz]	[damp.]
2	14.50	0.80	21.60	2.40	33.90	2.20
3	14.40	1.10	21.60	3.10	33.90	1.50
6	14.50	1.30	21.60	3.30	34.00	1.50
7	14.40	1.80	21.70	2.50	33.80	2.00
8	14.50	0.80	21.60	2.70	33.90	1.60
9	14.50	0.80	21.70	3.30	34.10	2.20
10	14.40	1.30	21.60	3.00	33.90	2.00
average	**14.50**	**0.80**	**21.60**	**2.90**	**33.90**	**1.86**
sdv	0.06		0.05		0.09	

Table 7.1. Identified frequencies and damping ratios

Conclusion of the modal analysis

The stochastic subspace method can be used to determine the eigenfrequencies, damping parameters and mode shapes of test floor. Eight eigenfrequencies were detected in the frequency range between 0 and 100 Hz. Modes 1, 2, 3 and 5 could be identified. For the exact identification of the other mode shapes, more sensors would be needed.

7.2.1.4. Numerical simulation

The system identification procedure results in an experimental model of the test floor. Physical parameters as eigenfrequencies, damping ratios and mode shapes are determined. In this section theoretical values of eigenfrequencies and modal shapes are obtained by a finite element modeling of the test floor. The influence of parameter such as the covering floor, the concrete topping and the extra concrete topping, the Stalton beams and the stiffening beam, on the dynamic behavior of the test floor is examined.

Also the boundary conditions of the floor are examined by comparing experimental and computational results of eigenfrequencies.

Geometric and material characteristics

A cross-section of the test floor and a longitudinal section of the stiffening beam are given respectively in figures 7.2 and 7.3. The floor is made of prestressed *Stalton* beams with a width of 14 cm and a height of 6 cm. Intermediate members are made

of burnt clay with a width of 26 cm and a height of15 cm are used to fill the empty space between the Stalton beams. A concrete topping of 4 cm is used to interconnect the different Stalton beams. The owner of the building decided to put an extra concrete topping of 7 cm thickness on top of the floor. Finally, a covering layer of 3 cm is used as finishing layer.

In the long direction of the floor, a stiffening beam is constructed at the central line. It is made by filling an open intermediate member with concrete. Consequently, the stiffening beam is interrupted by 'cracks' with a height of 6 cm at regular positions.

The density of the concrete is about 2500 kg/m^3. The Young modulus of the concrete E is estimated between 30000 N/mm^2 and 35000 N/mm^2.

The element types

For the modeling of the floor, two element types are used. The (extra) concrete topping is modeled with elastic shell elements, which have both bending and membrane capabilities. This element type has four nodes and six degrees of freedom at each node.

The *Stalton* beams and the stiffening beam are modeled with 3-D beam elements. The element is a uni-axial element with tension, compression, torsion and bending capabilities. The element has two nodes and six degrees of freedom at each node. The element permits the end nodes to be offset from the centroidal axis of the beam. Also, the effect of shear deformation is available.

The finite element model is represented in figure 7.7.
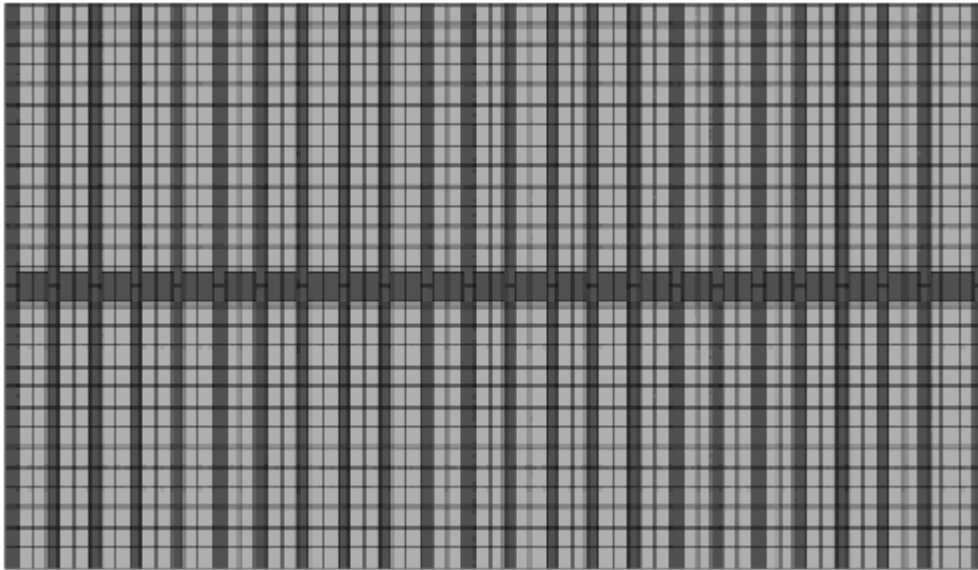
Figure 7.7. FEM of the evaluated slab

Figure Finite element model geometry

The covering floor, the concrete topping, the extra concrete topping and the intermediate members made of burnt clay are modeled with elastic shell elements. The thickness of the elements has been determined by the thickness of the concrete topping and the extra concrete topping (= 11 cm). The mass of the covering floor, the concrete filling and the intermediate members has been included in the elastic shell elements by increasing the density of the elements.

The connection between the floor and the outer wall is considered to be hinged in the long direction of the floor and to be clamped in the short direction.

The *Stalton* beams are modeled with 3-D beam elements. The height of the beam equals 15 cm and the effective width of the beam equals 11 cm. The density of the *Stalton* beam has been increased to take the real section of the Stalton beam into account. The offset of the nodes from the centroidal axis of the Stalton beam equals 15 cm. The connection between the Stalton beam and the outer wall is modeled as a hinge.

The stiffening beam is modeled with 3-D beam elements. This beam is simulated by filling up open intermediate members. As a consequence, the stiffening beam is a

beam with cracks, which have a regular spacing pattern. Therefore, the height of the stiffening beam has been reduced to 11 cm. The width of the stiffening beam equals 29.6 cm. The density of the stiffening beam has been increased to take the real section of the stiffening beam into account.

The offset of the nodes from the centroidal axis of the stiffening beam equals 11 cm. The connection between the stiffening beam and the outer wall is clamped.

Modal analysis

The subspace iteration technique has been used to determine the eigenfrequencies and the corresponding mode shapes of the test floor. The eigenfrequencies obtained by the finite element analysis and the experimentally determined eigenfrequencies are listed in table 7.2. A good agreement is found when comparing the experimental and calculated eigenfrequencies. FEM modal shapes are plotted in figure 7.8.

mode	Experimental frequency (Hz)	FEM frequency (Hz)
1	14.50	14.50
2	21.50	21.50
3	33.90	34.00
4	47.60	48.20
5	50.50	
6	50.20	52.00
7	59.70	58.70
8	68.30	
9	69.30	69.80
10	82.50	81.00

Table 7.2. Comparison between experimental and FEM identified frequencies.

mode 1   *mode 2*

mode 3   *mode 4*

mode 5   *mode 6*

mode 7   *mode 8*

mode 9   *mode 10*
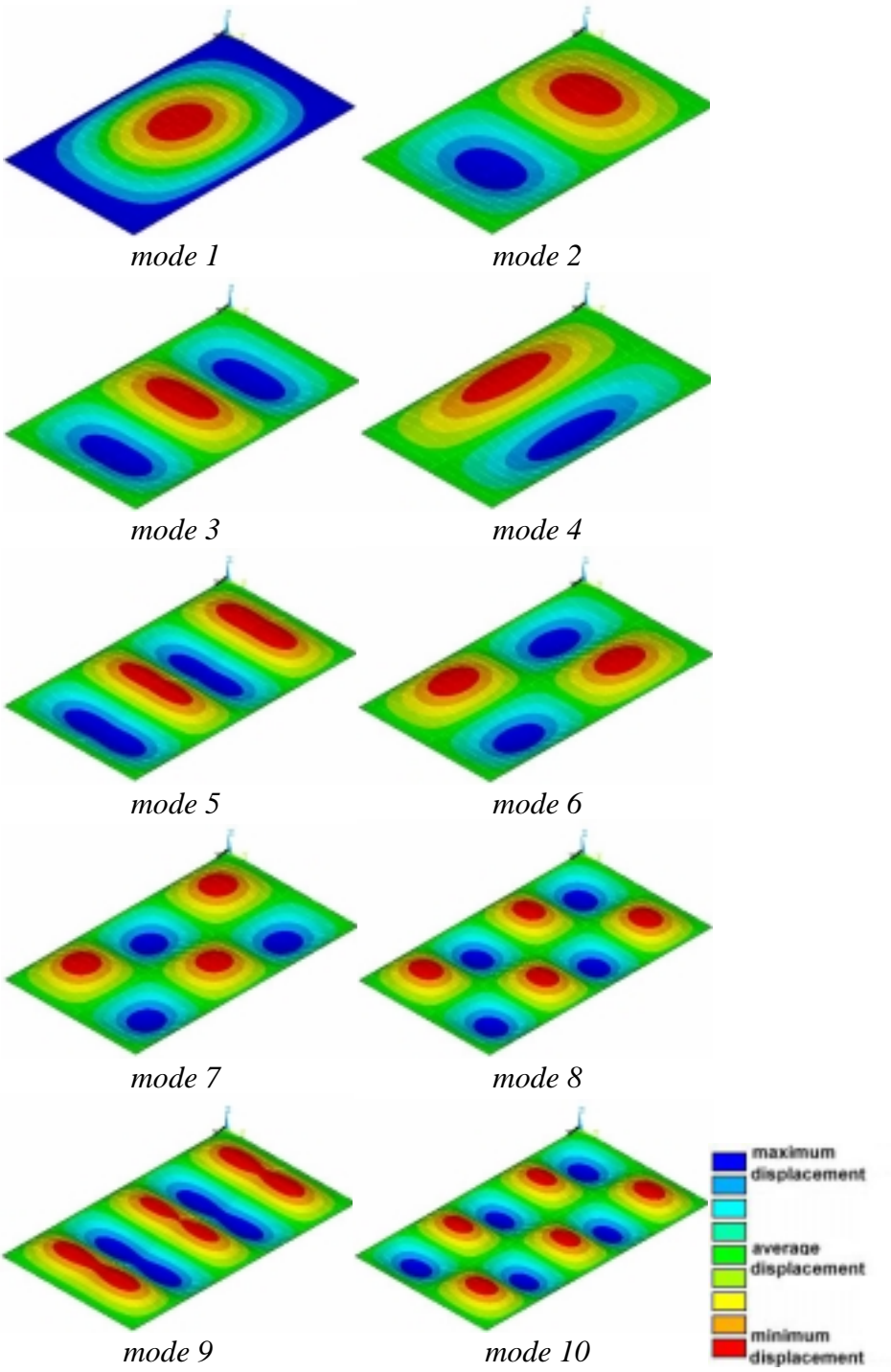
Figure 7.8. FEM modal shapes.

7.2.1.5. Discussion

After a preliminary investigation, it was found that the vibration level of the floor in the living room due to the traffic is high according to the German norm. A modal analysis has been performed to obtain the dynamic characteristics of the floor. The first eigenfrequency of the floor is 14.5 Hz and the damping ratio of this eigenmode is 0.5 %. Seven measurement points were used to identify not only the natural frequencies but also the first few modal shapes. However, the use of only one well-situated sensor was enough to identify the first few natural frequencies.

The quantity and accuracy of identified modal shapes was strictly dependent of the number of sensors attached to the structure. However, if a low number of sensors (one or two) are used, a good identification of firs natural frequencies can be developed. If the numerical model is updater using frequency-only values (excluding modal shapes) the use on few sensors is effective and represents a big save on equipment and testing time.

The test floor has been modeled with a finite element program [Ansys, 1996]. For the model, the eigenfrequencies and the mode shapes have been calculated and compared with results obtained from measurements. A good comparison has been found between the experimental determined eigenfrequencies and the numerical determined eigenfrequencies. A more detailed measurement grid is however necessary to compare the mode shapes more exactly.

Dynamic assessment was an effective method to characterize a prestressed concrete slab. This type of structures does not suffer an important reduction of stiffness due to cracking, presenting a linear behavior. A numerical model can be easily updated by comparing experimental and calculated natural frequencies.

7.2.2. Concrete framed multi-storey building *(La Pau)*

7.2.2.1. Introduction

For medium-rise (6-15 floors) housing buildings, the process of characterizing the full structure can be very repetitive. When an important pathology is detected in one point of the building, a typical procedure to ensure the security is to develop an inspection through the full structure. The inspection is normally carried out with a combination of visual and destructive techniques. The gap between those two methods is very wide. Visual inspection is a subjective process strongly dependent of the experience of the technicians. Destructive methods such as core sampling or load testing are expensive procedures to be developed in the locations of the structure. An intermediate technique that matches objective measurements and simple procedures was necessary.

In this example, a housing building was subjected to an intense inspection. Several dynamic tests were carried out in the concrete slabs with the objective of identify the structural conditions. Load tests were also developed in the same locations to calibrate and compare the results with the dynamic ones.

The studied building was located in Barcelona and suffered high aluminum-cement pathology. The authorities in charge of the maintenance decided to demolish the building. At the time of the inspection, the building was already empty, with not dead-loads or inhabitants interference. This fact allowed not only the development of several dynamic tests, but also many destructive load tests to compare the results.

Although that the objective of this thesis is not related with aluminum-cement pathologies, the study of this particular case was a great opportunity to validate the proposed methodology [chapter 4] by comparing the results with direct observations.

In the next paragraphs, the test setup, the data acquisition and the analysis of the signals in the frequency domain will be described. Afterwards, the results for all loading cases will be summarized and compared with a finite element simulation.

7.2.2.2. Method

Description of the building

The structure of interest [Figure 7.9] is an apartment-building located at *La Pau* neighborhood in Barcelona. The building has 15 levels above and a semi-basement cellar, which is used as a storage and machinery-house. The structure is based in concrete frames. However, several masonry walls are present in every floor, adding stiffness to the slabs. All the tests were carried out in the floor between 5th and 6th levels. This floor is made of prestressed beams; lighten members made of burnt clay and a compression layer [figure 7.10].
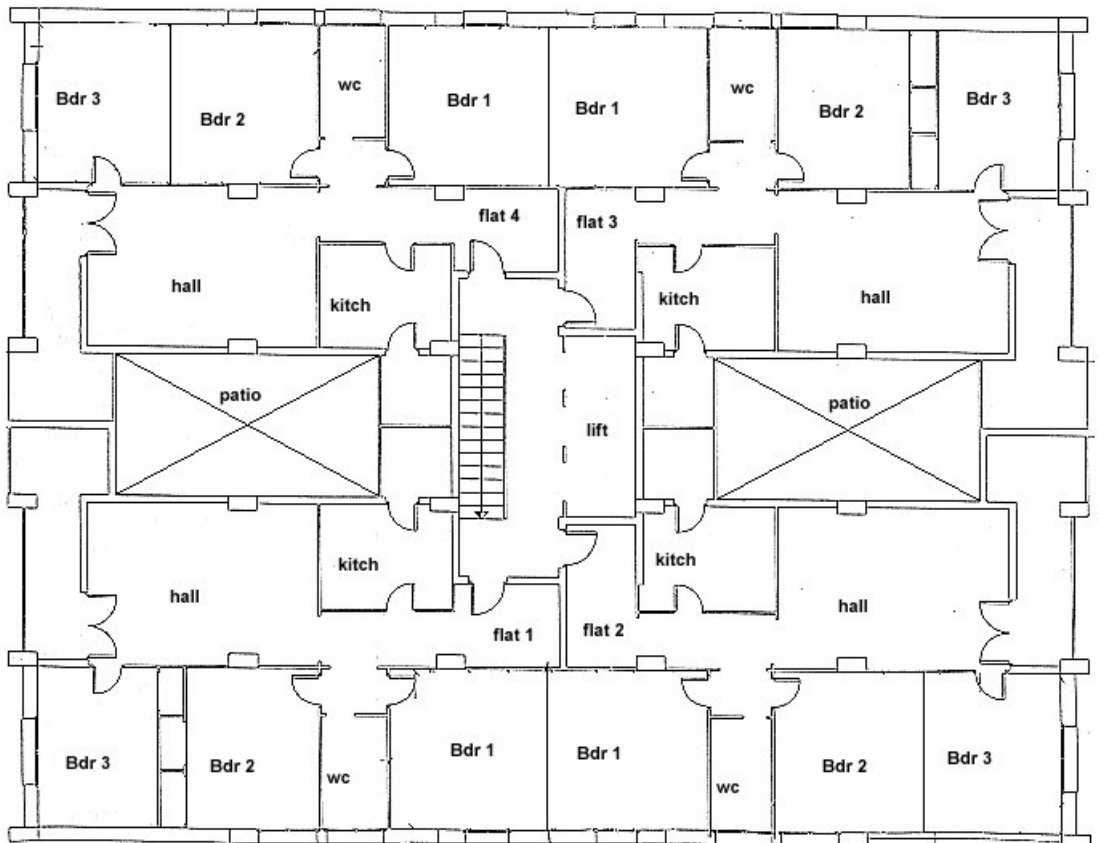
Figure 7.9. General plan of the studied building.
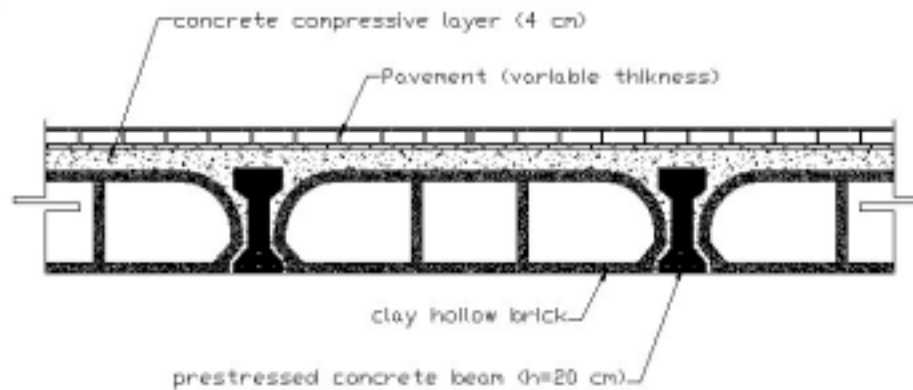
Figure 7.10. Cross-section of the tested floor

Dynamic tests

Sixty-four dynamic tests were carried out in three days. The building has four flats per level. A complete study of level 6 (slab between fifth and sixth floor) was carried out including the four flats. Every flat has a symmetric space distribution [figure 7.9.] and consist mainly in five spaces: Hall, kitchen, and bedrooms 1, 2 and 3. Other smaller spaces such as toilet or terrace were not characterized.

To obtain the basic eigenfrequencies, a test with a small number of measurement points is sufficient. For accurate determination of the mode shapes a rather large data set is necessary. In the purpose of this particular case, one dynamic sensor was enough to acquire dynamic data. The dynamic test was developed in all the slabs independently. The test equipment was reset every time that a location change was needed. Detailed information of the method is given in Chapter 4.

For all the cases, the accelerometer was attached to the center of the slab. Excitation was induced by different means; however, the most simple and effective resulted to be a person-jump.

The test length last 3 seconds, but a complete dissipation of the energy took place in less than 1 second.

Static load-tests

Sixteen static load test were carried out in different slabs. The static load test consisted in the application of a concentrated load at the midspan of the central prestressed beam. Displacements were measured vs. load application. This test produces a direct measurement of the stiffness of the slab.

The loading velocity varied from 1 kp/sec (the test length lasted 180 minutes) to 4 kp/sec (the test length was 25 minutes). For all the cases the maximum achieved load was 150 kN. The maximum deformation oscillates for all the cases between 0,2 and 0,25 mm depending on the loading speed [figure 7.11].
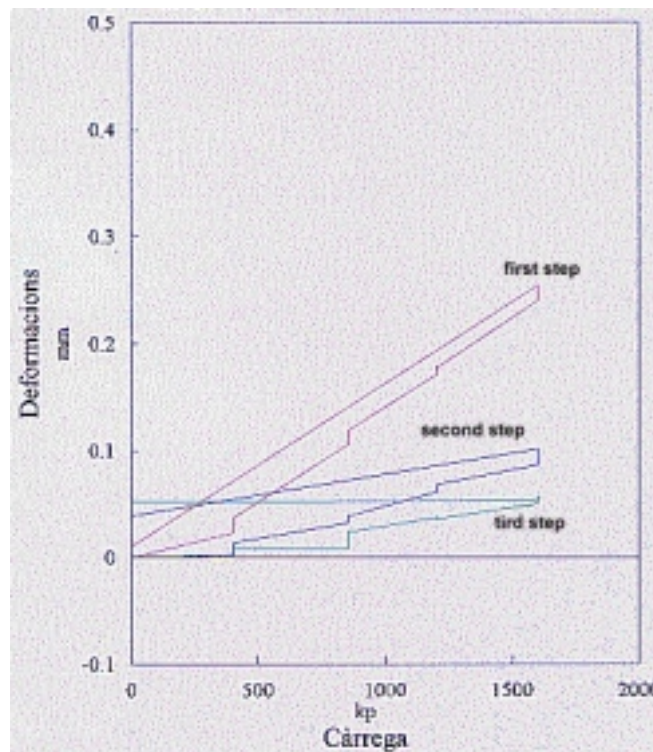
Figure 7.11. Static load test results. Load vs. midspan displacemen.

7.2.2.3. Results

First, the data obtained by excitation of the test floor by impact were processed. The lowest eigenfrequencies were identified by a simple FFT. Table 7.4 shows the identified frequencies for the 64 tests.

test number	test location flat	space	Identified frequency (Hz)	test number	test location flat	space	Identified frequency (Hz)
1	1	Bdr 1	52	33	3	Bdr 3	52
2	1	Bdr 1	52	34	3	Bdr 3	52
3	1	Bdr 1	53	35	1	Bdr 1	52
4	1	Bdr 2	53	36	2	Bdr 2	52
5	1	Bdr 2	53	37	2	Bdr 2	50
6	1	Hall	46	38	2	Bdr 3	52
7	1	Hall	46	39	2	Bdr 3	52
8	1	Bdr 3	52	40	2	Bdr 1	52
9	1	Bdr 3	52	41	2	Bdr 1	52
10	1	Kitch	75	42	4	Bdr 2	50
11	1	Kitch	75	43	4	Bdr 2	52
12	4	Hall	46	44	4	Bdr 3	60
13	4	Bdr 3	52	45	4	Bdr 3	60
14	4	Bdr 2	53	46	4	Bdr 1	41
15	4	Bdr 1	50	47	4	Bdr 1	41
16	4	Kitch	75	48	3	Bdr 1	41
17	2	Bdr 2	54	49	3	Bdr 1	41
18	2	Bdr 1	54	50	4	Bdr 3	57
19	2	Bdr 2	54	51	4	Bdr 3	57
20	2	Hall	46	52	4	Bdr 2	57
21	2	Hall	46	53	4	Bdr 2	57
22	2	Bdr 3	52	54	4	Bdr 1	57
23	2	Bdr 4	53	55	4	Bdr 1	57
24	2	Kitch	74	56	3	Bdr 1	41
25	2	Kitch	74	57	3	Bdr 1	41
26	3	Bdr 1	48	58	3	Bdr 1	41
27	3	Bdr 2	52	59	2	Bdr 3	50
28	3	Bdr 2	52	60	2	Bdr 2	50
29	3	Kitch	75	61	2	Bdr 1	52
30	3	Kitch	75	62	1	Bdr 1	51
31	3	Hall	46	63	1	Bdr 1	51
32	3	Hall	46	64	1	Bdr 1	51

Table 7.4. Experimentally identified frequencies

From identified frequencies [table 7.4] a clear pattern was identified: all bedroom-spaces had similar frequencies. All kitchen spaces presented as well the same frequency value and finally all the hall frequencies had a similar value. Some dispersion is noticed, especially for bedroom 1/flat 3, bedroom 3/flat 4 and bedroom 1/flat 4. This deviation of the average frequencies suggested a spatial condition of the previously mentioned spaces. A deeper inspection was developer and it was found that an important addition of mass (double pavement) was present for the spaces with a frequency below the average. The case with a frequency above the average could not be explained.

7.2.2.4. Numerical simulation

The system identification procedure results in an experimental model of the test floor. Physical parameters as eigenfrequencies are determined. In this section theoretical values of eigenfrequencies and modal shapes are obtained by a finite element modeling of the test floor. The influence of parameter such as the covering pavement or the concrete topping on the dynamic behavior of the test floor is examined. Also the boundary conditions of the floor are examined by comparing experimental and computational results of eigenfrequencies.

Geometric and material characteristics

A cross-section of the test floor is given in figure 7.10. The floor is made of prestressed beams with a width of 8 cm and a height of 20 cm. Intermediate members are made of burnt clay with a width of 70 cm and a height of 20 cm and are used to fill the empty space between the prestressed beams. A concrete topping of 4 cm is used to interconnect the different beams.

The density of the concrete is about 2400 kg/m^3. The Young modulus of the concrete E is estimated between 34000 N/mm^2 for the prestressed beams and 24000 N/mm^2 for the compressive layer.

The element types

For the modeling of the floor, two element types are used. The concrete topping is modeled with elastic shell elements, which have both bending and membrane capabilities. This element type has four nodes and six degrees of freedom at each node.

The prestressed beams are modeled with vertical elastic shell elements. This element type has again four nodes and six degrees of freedom at each node. The material properties are changed for this kind of element, from core testing, the Strain modulus of the prestressed beams is known.

Three different models were developed following the geometry and support conditions of the bedrooms, hall and kitchen. The model correspondent to the hall is presented in figure 7.12.

Figure 7.12. FEM of the evaluated hall slab

modal shape 1

modal shape 2

modal shape 3

Figure 7.13. First three modal shapes of hall slab model.

In figure 7.13, the first three calculated models are plotted. However, the experimental test could identify only the frequency associated to the first mode.

Experimental and FEM results were easily updated. A good correlation between experimental and theoretical eigenfrequencies was achieved in few attempts by updating the strain modulus of the two different kinds of concrete (beams and compressive layer).

space	FEM frequency *f1*	Experimental average frequency *f1*
bedrooms	52.0	52.0
hall	46.0	46.0
kitchen	74,6	74.0

Table 7.5. Comparison between experimental and FEM eigenfrequencies.

7.2.2.5. Discussion

The test floor has been modeled with an elastic FEM program. For the model, the eigenfrequencies and the mode shapes have been calculated and compared with results obtained from measurements.

A good comparison has been found between the experimentally determined eigenfrequencies and the numerically calculated ones. A more detailed measurement grid is however necessary to compare the mode shapes.

After comparing the experimental and theoretical frequencies, some slabs showed a disturbance. Those slabs deserved special attention and the cause of the disturbance was discovered: an important addition of mass by attaching several pavement layers.

The load tests were also numerically simulated in the updated model, finding a good correspondence between experimental and theoretical deformations. The slabs suffered a deformation of 0,25 mm after applying a load of 150 kN at midspan. This deformation corresponds to the experimental one [figure 7.10].

The main conclusion of this example is that a simple dynamic test is enough to identify the first few natural frequencies of a concrete slab. This identified value serves to develop a model optimizing process. Once the model is updated, the fundamental parameters of the slab (such as strain modulus and support conditions) are known. More complex method like load tests can be used only eventually to calibrate and validate the dynamic methodology. The use of dynamic techniques to characterize a building may represent a drastic reduction of the testing costs.

7.2.3. Concrete framed multi–storey building (*Manresa*)

7.2.3.1. Introduction

For low-rise (until six floors) office buildings, the process of characterizing the full structure can be very repetitive, similarly to the example presented in [7.1.2.]. When a local structural failure is detected in the building, a typical procedure to ensure the security is to develop a detailed inspection through the full structure. This inspection is normally carried out with a combination of visual and destructive techniques. There is a big gap in the complexity between those two methods. Visual inspection is a subjective process strongly dependent of the experience of the technicians. Destructive methods such as core sampling or load testing are expensive procedures to be developed in all the locations of the structure and have a strong impact in the usage of the building. An intermediate technique that matches objective measurements and simple procedures was necessary.

In this example, an office building was subjected to an intense inspection. Several dynamic tests were carried out in the concrete slabs with the objective of identify the structural conditions. The studied building was located in Manresa, Spain, and suffered a normal deterioration for its age (more than 35 years). The structure is based on concrete frames and a one-direction slab with cast-in-place beams. The authorities in charge of the maintenance decided to demolish the building. At the time of the inspection, the building was already empty, with not dead-loads or inhabitants interference. This fact allowed not only the development of several dynamic tests, but also a destructive coring to identify the slab morphology.

The study of this particular case was a good opportunity to validate the proposed methodology [chapter 4]. Structural details from the constructor were available; therefore, a detailed model was developed and updated using the dynamic information.

In the next paragraphs, the test setup, the data acquisition and the analysis of the signals in the frequency domain will be described. Afterwards, the results for all dynamic tests will be summarized and compared with a finite element simulation.

Figure 7.14. Main façade of the studied building.

7.2.3.2. Method

Description of the building

The structure of interest [Figure 7.14] was a departmental-store building located at central *Manresa*, 40 km west of Barcelona. The building has 6 levels above and a basement, which was used as a storage and lift-machinery-house. The structure was based in concrete frames. All the tests were carried out in the floors between 2nd, 3rd and 4th levels (2 slabs). This floor is made of cast-in-place beams, lighten members made of hollow brick and a concrete compression layer [figure 7.15].
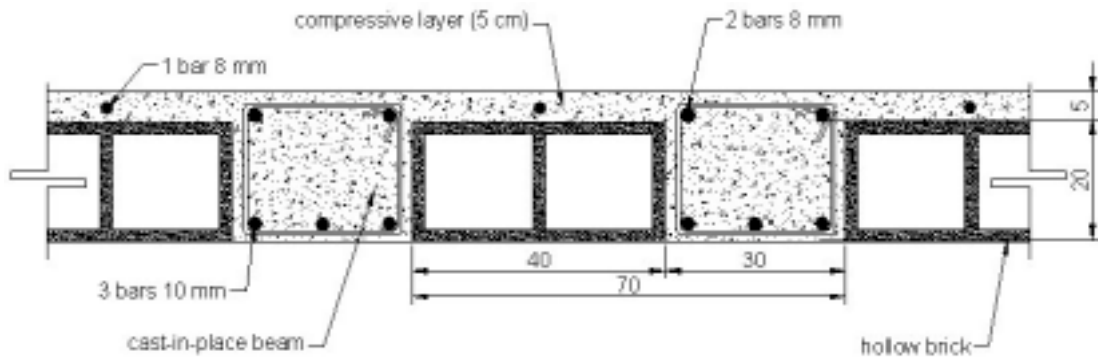
Figure 7.15. Cross-section of the tested floor
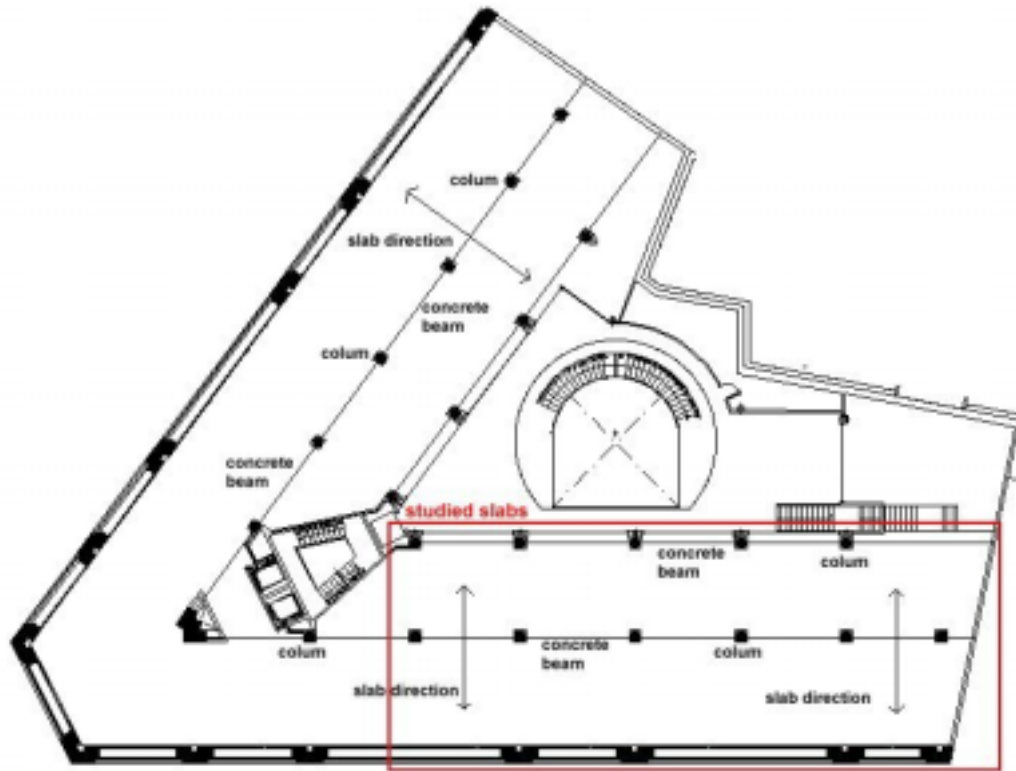
Figure 7.16. Location of the evaluated slabs in a general plan of the building

Dynamic tests

Twenty different slabs were evaluated in two levels (ten per level). Two dynamic tests were carried out in every slab producing a total of forty tests. The zone of the evaluated slabs is marked in figure 7.16. Both evaluated floors (2^d and 3^d) had identical distribution.

To obtain the basic eigenfrequencies, a test with a small number of measurement points is sufficient. For accurate determination of the mode shapes a rather large data set is necessary. In the purpose of this particular case, two dynamic sensors were enough to acquire dynamic data. The dynamic test was developed in all the slabs independently. The test equipment was reset every time that a location change was needed. Detailed information of the method is given in Chapter 4.

For all the cases, one accelerometer was attached to the center of the slab [figure 7.17, above] and the other to one quarter of the span. Excitation was induced by different means; however, the most simple and effective resulted to be a hammer impact. The slab was not in an optimum condition to be tested because heavy rubbish was accumulated is some places, adding unknown mass to the structure [figure 7.17, below].

Figure 7.17. Accelerometer attached to the slab(above) and view of the tested slabs(below)

The entire tests had a length of 1 second; a complete dissipation of the energy took place almost completely in this period [figure 7.18]. The natural frequencies were extracted by pick-picking from the frequency domain plot. It is worth to mention that at the time of testing, the building was subjected to a strong noise vibration caused by demolition machinery. This noise could not be avoided and polluted some of the response measurements.
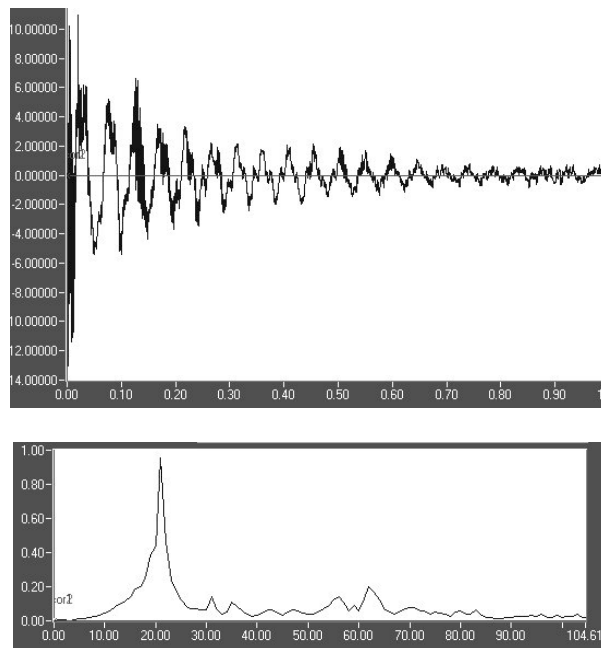
Figure 7.18. Data acquisition. Time domain (above) and FFT (below)

7.2.3.3. Results

First, the data obtained by excitation of the test floor by impact were processed. The lowest eigenfrequencies were identified by a simple FFT. Figure 7.19 shows the results of 20 tests developed in the second floor. Figure 7.20 present the identified frequencies of 20 tests carried out in the third floor.
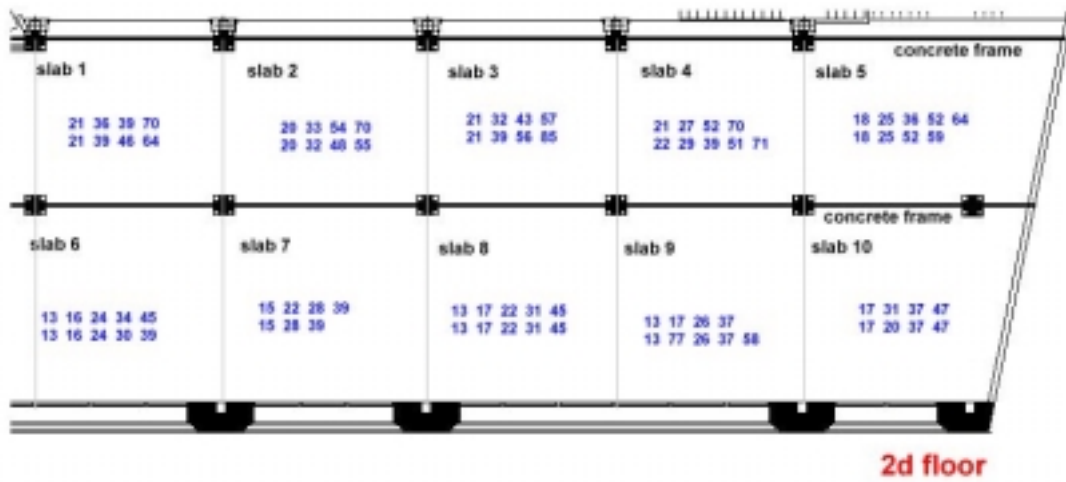
Figure 7.19. Frequencies identified in second floor (20 tests)
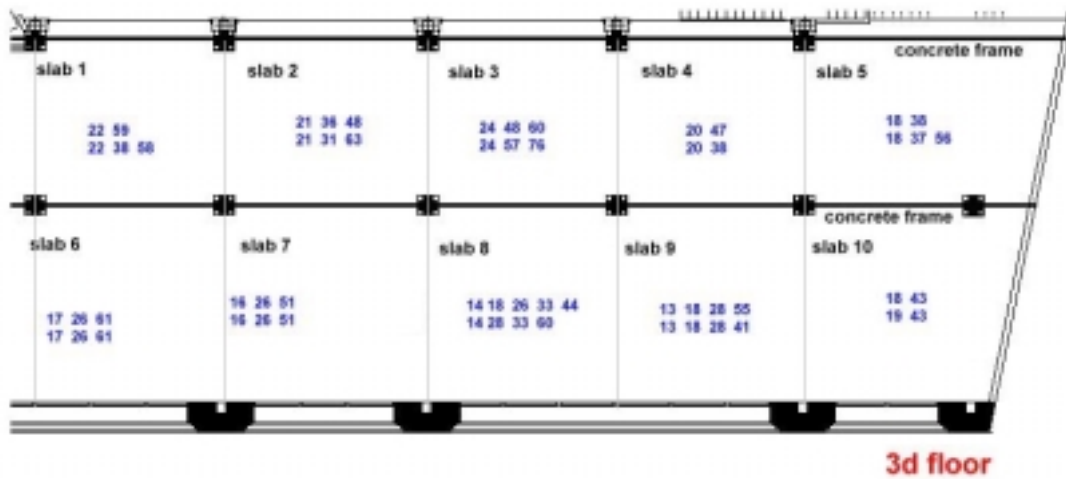
Figure 7.20. Frequencies identified in third floor (20 tests)

From identified frequencies [figures 7.19 and 7.20] a clear pattern was identified: a repetitive frequency around 21 Hz is identified for most of the cases. However, a high dispersion is noticed in other identified frequencies.

7.2.3.4. Numerical simulation

The dynamic testing of the twenty slabs resulted in an experimental model of the test floor. Physical parameters as eigenfrequencies are determined. In this section theoretical values of eigenfrequencies and modal shapes are obtained by a finite element modeling of the test floor. The influence of parameter such as the covering pavement participation or the stiffness of the concrete frames on the dynamic behavior of the test floor is examined. Also the boundary conditions of the floor are examined by comparing experimental and computational results of eigenfrequencies.

Geometric and material characteristics

A cross-section of the test floor is given in figure 7.15. The floor is made of *cast-in place-beams* with a width of 30 cm and a height of 25 cm. Intermediate members are made of hollow brick with a width of 40 cm and a height of 20 cm and are used to fill the empty space between the beams. A concrete topping of 5 cm is used to interconnect the different beams. Finally, a 4-cm ceramic pavement is added to the slab adding more mass than stiffness.

The density of the concrete is about 2400 kg/m^3. The Young modulus of the concrete E is estimated between 30000 N/mm^2 for the beams and compressive layer. The density of pavement is about 2000 kg/m^3.

The element types

For the modeling of the floor, three element types are used. The concrete topping is modeled with elastic shell elements, which have both bending and membrane capabilities. This element type has four nodes and six degrees of freedom at each node. The beams (slab and frame beams) are modeled with vertical elastic shell elements. This element type has again four nodes and six degrees of freedom at each node. The geometry is identical for the first eight slabs and different for the other two [figure 7.16]. The model correspondent to any of the first eight slabs is presented in figure 7.21.
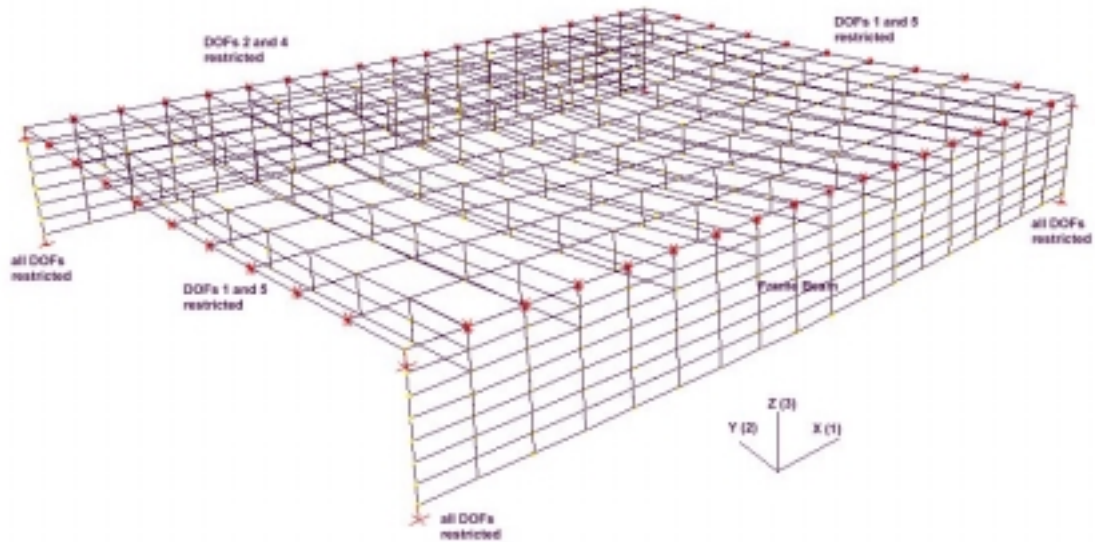
Figure 7.21. FEM of a slab with a typical geometry.

modal shape 1; f1=22 Hz   modal shape 2; f2=25 Hz

modal shape 3; f3=27 Hz   modal shape 4; f4=32 Hz

modal shape 5; f5=42 Hz   modal shape 5; f5=53 Hz
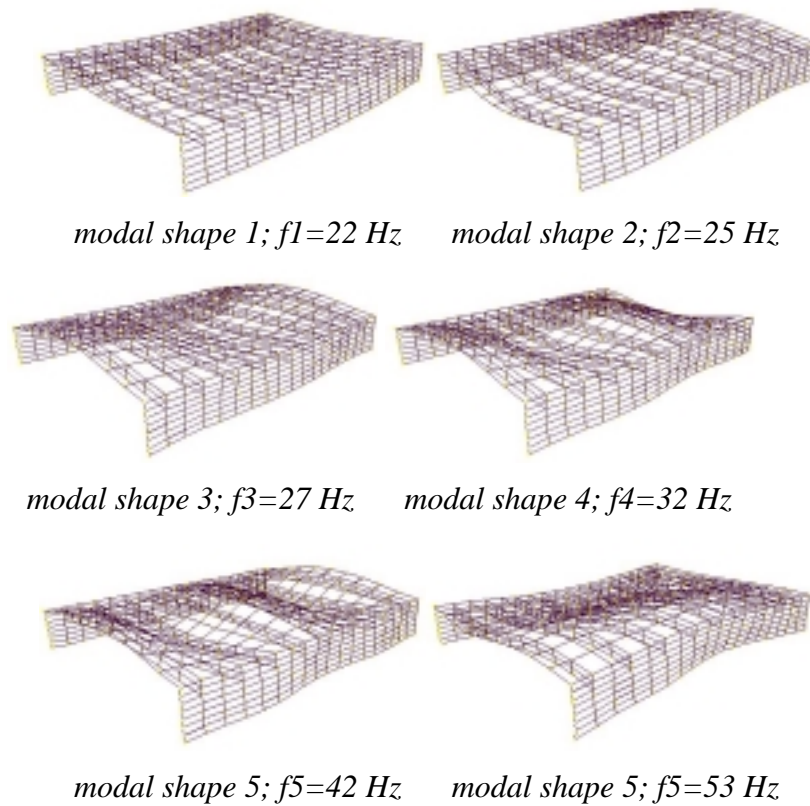
Figure 7.22. First six modal shapes and eigenfrequencies of a slab with typical

dimensions.

In figure 7.22, the first six calculated models are plotted. However, in some cases the experimental test could identify more frequencies.

Experimental and FEM results were easily updated. A good correlation between experimental and theoretical eigenfrequencies was achieved in few attempts by updating the strain modulus of the concrete (beams and compressive layer) and the contour conditions.

7.2.3.5. Discussion

Forty dynamic tests were carried out, two per slab in twenty different slabs. The results can allow some important considerations:

- The tested floor has been modeled with an elastic FEM code. It was possible to model the slabs as single elements; however, modeling the boundary beams was necessary to obtain the lower frequency values. The continuity was modeled by restricting some degrees of freedom in the contour nodes.

- A good comparison has been found between the experimentally determined eigenfrequencies and the numerically determined eigenfrequencies.

- A more detailed measurement grid is necessary to identify the modal shapes.

- The main conclusion of this example is that a simple dynamic test is enough to identify the first natural frequency of a concrete slab. This identified value serves to develop a model updating process. Once the model is updated, the fundamental parameters of the slab (such as strain modulus and support conditions) are identified.

7.3. Masonry elements

7.3.1. Stone piers in the cloister of Girona Cathedral

7.3.1.1. Introduction

The wish for scientific and respectful strategies for the study and preservation of historical constructions has promoted the development of a wide variety of effective non-destructive or quasi-non destructive tools of inspection (such as endoscopies, electromagnetic tomography or flat jack test). Those techniques can be used to obtain information about the internal composition of the structural elements or about the mechanical properties of the existing fabrics. Among these methods, dynamic identification, based on the measurement of the vibration response, constitutes one of the more versatile, fully non-destructive techniques of inspection. Dynamic identification can be used to monitor the structure both locally (aiming at the identification of a properties of a single element or part) and globally (aiming at the characterization of overall properties). The method is based in the fact that modal parameters (notably frequencies, mode shapes, and modal damping) are functions of the physical properties of the structure (mass, damping, and stiffness). In particular, dynamic identification can be used for health monitoring, since the changes in the physical properties due to damage will cause, at its turn, detectable changes in the modal response.

In the case of historical constructions, dynamic evaluation presents additional advantages besides its fully non-destructiveness. An advantage is found in the possibility to repeat the test many times and thus to extend it to a large number of similar structural elements. This is clearly illustrated by Ellis [1989] usage of the dynamic test to evaluate the integrity of 534 stone pinnacles of the Palace of Westminster in London based on wind excitation and laser remote measurements.

The architectural and historical value of the columns prevented the application of some conventional tests (core extraction or static load testing), which would have caused some deterioration, however limited. Because of that, dynamic test was preferred and executed by attaching dynamic sensors to the columns and exciting them by means of hammer impact. Historical research was conducted to locate the origin of the stone and a few new specimens were extracted from the original quarry in order to develop the parallel laboratory research. The activities carried out in laboratory [section 6.6] included static uniaxial compression tests, dynamic modulus measurement and a full-scale load increasing dynamic test). It must be mentioned that the tests were developed in recently extracted stone, with no influence of age.

Figure 7.23. General view of the cloister and tested columns.

The cathedral, originally was started to build during 11th century, is the result of the superposition of different architectural styles since the first known Romanesque

building, which was consecrated in 1038. It offers four architectural styles: Romanesque, Gothic, Renaissance and Baroque, which is not a very frequent occurrence.

The cloister [figures 7.23 and 7.24], built during 11th and 12th centuries, represents fully the spirit of the Romanesque era, conserved entirely, despite the fact that some double columns and capitals display signs of erosion which affects the limestone rock, sculptured to create a series of Biblical representations which form a valuable part of the Catalan Romanesque period. They belong to the previous cathedral, of which only the old bell tower is conserved. The tower ("Tower of Carlemany"), built during 11th century, serves today as the buttress of the Gothic nave.

Figure 7.24. General views of the cloister and tested columns.
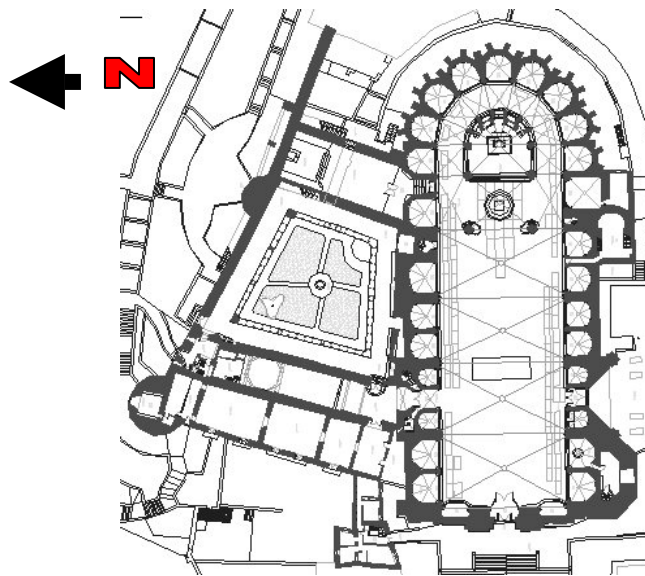
Figure 7.25. Overview of the Cathedral and Cloister.

The Gothic nave, which is the widest in the world and measures 22.98 meters, is at the same time, the widest of any style, excepting that of St. Peter's in Rome (which measures 25 meters). While the construction of a temple with three naves was initiated, the proposal to continue it with only one nave caused the suspension of the works and motivated an intermittent discussion between those in charge and the technicians, which lasted fifty years. In 1417, the Cathedral Chapter held a meeting with the masters of the works and infamous experts. After hearing their opinion, the Chapter was inclined towards the single-nave plan, which converted the Cathedral into a unique monument in the history of world Gothic architecture.

Figure 7.26. Cloister view with the Cathedral behind.
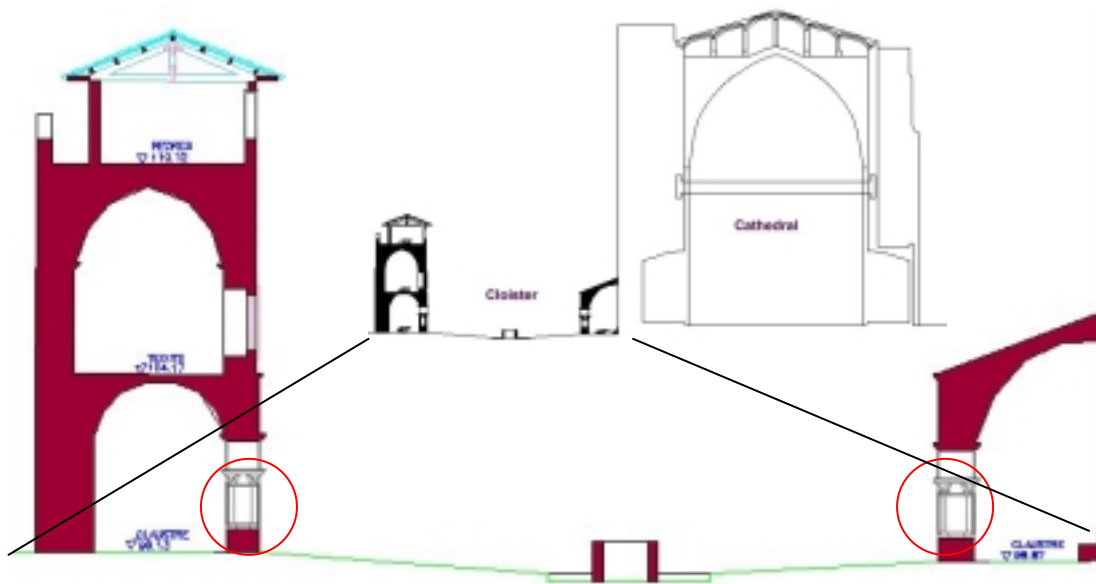
Figure 7.26. Detail of Cloister and evaluated columns.

7.3.1.2. Method

The cloister of the cathedral is nowadays subject to an important project of restoration requiring a general study of the structural state of the columns. It was decided to develop only non-destructive evaluation. By this way, dynamic evaluation was an alternative and the first testing campaign is presented in the next paragraphs.

The four sides of the cloister were fully tested, including 74 columns that were tested twice yielding 148 dynamic tests. No significant variation between the results obtained in the two tests carried out on each column was observed. Dissipation of the impact energy took place in about 0.3 seconds. One mode was always clear and in some cases, the second mode was observed.

The generation of impulsive force was caused through a 10-pounds hammer applied at mid-span of every column with a single impact. A dynamic transducer consisting of a ceramic accelerometer was attached in horizontal direction [Figure 7.28].

Figure 7.28. Acquisition system (left) and accelerometer attached on a column (right)

A clear pattern was observed on the time-response diagram of every column. Very clean time responses were extracted. A typical example of those plots is presented in figure 7.29. Data acquisition was developed using a routine of Labview code, on an interval of one second, and acquiring at a frequency of 30,000 Hz.
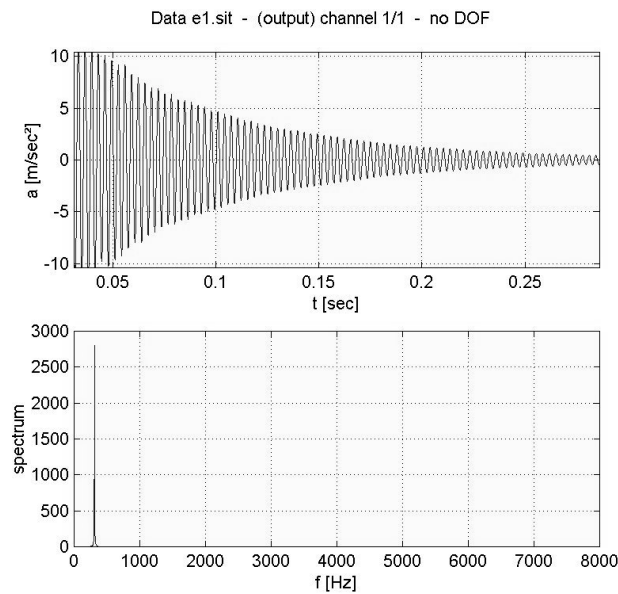
Figure 7.29. Typical time-response of a column (above) and FFT diagram (below).

7.3.1.3. Results

After obtaining the first natural frequency for every column, a clear trend can be observed in every side of the cloister. For the south side, small variations are observed between all the evaluated columns (less than 4%) except for the columns on axis 10 [table 7.7 and figure 7.30]. As it can be observed in figure 7.23, columns are displayed by pairs, and the frequencies of two twin columns were always the same. This proves that variation in frequencies is mostly due to location than to material or geometrical parameters.

axis	column	f1	f2	f2/f1	column	f1	f2	f2/f1
1	1	268	813	3,03	2	268	812	3,03
2	3	282	813	2,88	4	282	813	2,88
3	5	271	813	3,00	6	271	812	3,00
4	7	283			8	284	813	
5	9	267	813	3,04	10	267	813	3,04
6	11	274	821	3,00	12	272	816	3,00
7	13	271	813	3,00	14	270	812	3,01
8	15	270	810	3,00	16	270	811	3,00
9	17	280	810	2,89	18	281	810	2,88
10	19	318	810	2,55	20	317	810	2,56

Table 7.7. Frequencies identified in-situ (South side of the cloister)
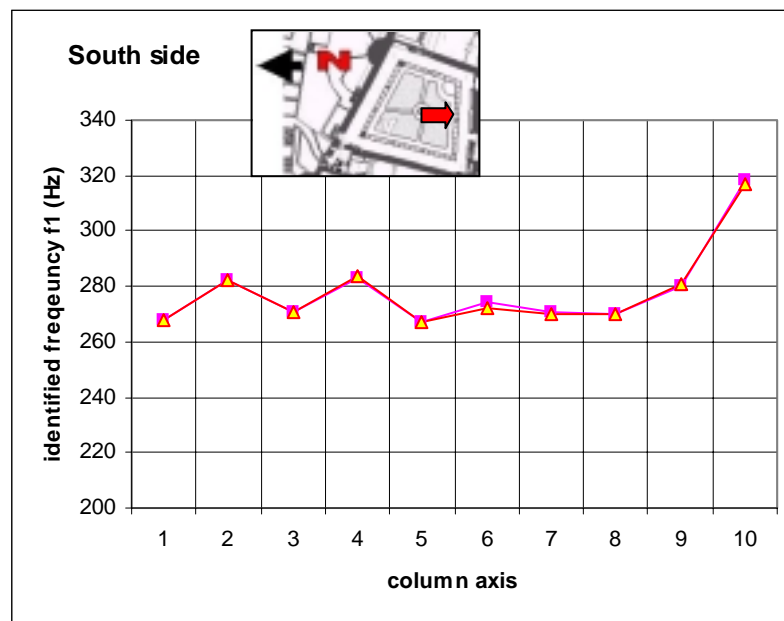
Figure 7.30. First frequency identified in the cloister columns (South side).

The east side count only with six axes (12 columns). A reduction of the frequencies is observed in central columns [table 7.8 and figure 7.31]. Once again, two twin columns always share the same frequency probing that the variation in frequencies is mostly due to location than to material or geometrical parameters.

axis	column	f1	f2	f2/f1	column	f1	f2	f2/f1
11	21	309	821	2,66	22	309	818	2,65
12	23	308	816	2,65	24	308	814	2,64
13	25	306	815	2,66	26	306	814	2,66
14	27	288	816	2,83	28	288	814	2,83
15	29	305	813	2,67	30	306	813	2,66
16	31	324	812	2,51	32	324	812	2,51

Table 7.8. Frequencies identified in-situ (East side of the cloister)
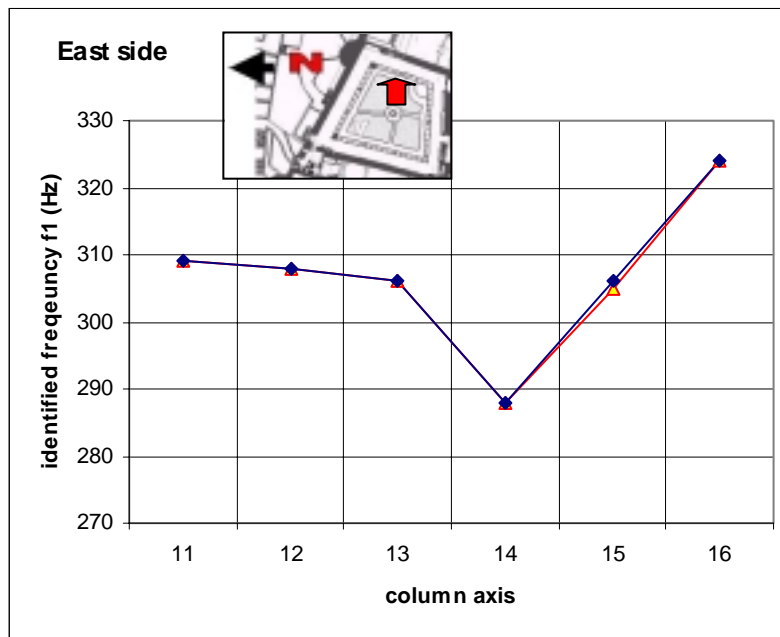
Figure 7.31. First frequency identified in the cloister columns (East side).

The north side counts 18 columns. An identified general trend is a reduction of the frequencies in central columns [table 7.9 and figure 7.32]. Once again, two twin columns always share the same frequency probing that the variation in frequencies is mostly due to location than to material or geometrical parameters.

axis	column	f1	f2	f2/f1	column	f1	f2	f2/f1
17	33	324	811	2,50	34	325	821	2,53
18	35	321	817	2,55	36	319	813	2,55
19	37	271	813	3,00	38	278	811	2,92
20	39	270	811	3,00	40	270	811	3,00
21	41	270	811	3,00	42	270	811	3,00
22	43	301	811	2,69	44	301	-	
23	45	313	811	2,59	46	313	811	2,59
24	47	329	812	2,47	48	329	811	2,47
25	49	328	812	2,48	50	328	813	2,48

Table 7.9. Frequencies identified in-situ (North side of the cloister)
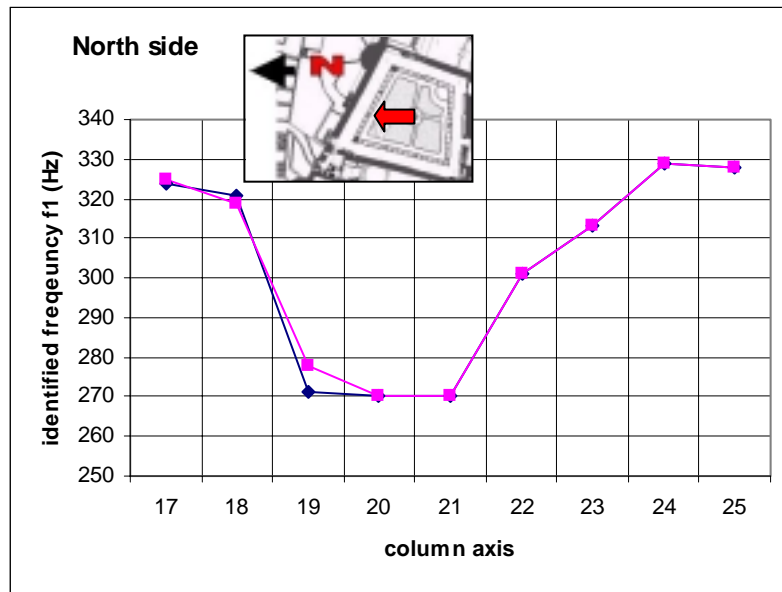
Figure 7.32. First frequency identified in the cloister columns (North side).

Finally, the west side of the cloister counts with 12 axes (24 columns). An identified general trend is again a reduction of the frequencies in central columns [table 7.10 and figure 7.33]. Once again, an in concordance with previous the sides, two twin columns always share the same frequency; therefore, in the entire cloister the variation in frequencies is not related to material or geometrical parameters.

axis	column	f1	f2	f2/f1	column	f1	f2	f2/f1
26	51	316	950	3.01	52	316	950	3.01
27	53	311	935	3.01	54	311	948	3.05
28	55	315	940	2.99	56	315	940	2.98
29	57	279	838	3.00	58	281	870	3.10
30	59	270	830	3.07	60	265	800	3.02
31	61	270	800	2.96	62	270		
32	63	252			64	250		
33	65	286	857	3.00	66	286	918	3.21
34	67	286	923	3.23	68	285	965	3.39
35	69	293	910	3.11	70	292	877	3.00
36	71	309	925	2.99	72	309	925	2.99
37	73	308	922	3.00	74	308		

Table 7.10. Frequencies identified in-situ (West side of the cloister)
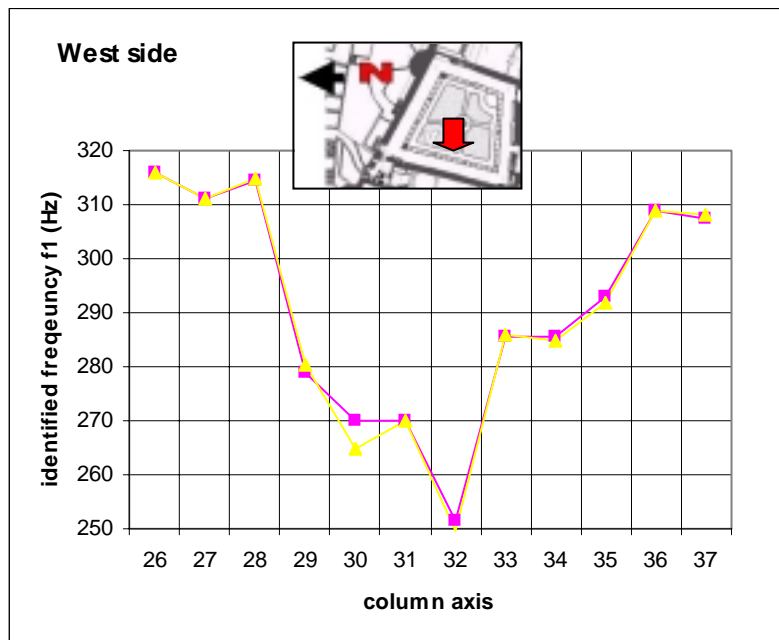
Figure 7.33. First frequency identified in the cloister columns (West side).

7.3.1.4. Numerical simulation

A simple numerical model was created to assessing the accuracy of the identification method. The model consisted of a simple column with variable support conditions at the ends. The modulus of deformation was estimated from the value obtained experimentally as dynamic modulus. A satisfactory agreement was obtained between the analytical prediction of the first natural frequencies and the measures obtained experimentally in the cloister.   The agreement was obtained assuming fixed condition at the ends of the columns.
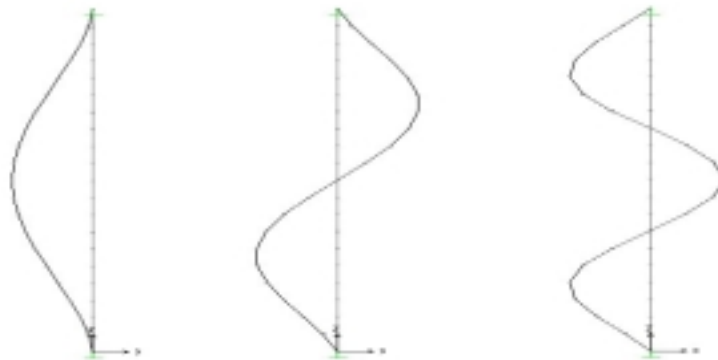
Figure 7.34. First modes of vibration predicted by the analytical model ,
corresponding to frequencies F1=370 Hz (left); F2=909 Hz (middle); F3=1700 Hz
(right).

7.3.1.5. Discussion

The present study constitutes a first approach of a more general investigation aimed at assessing the condition of stone columns, based on dynamic identification. In particular, the study has shown it feasible to correlate the load sustained by the stone columns with their measured natural frequencies. A test developed in laboratory [section 6.6] showed that a clear variation in natural frequencies appears when increasingly loading a stone column with a hydraulic actuator. The variation of the natural frequencies can be caused, in principle, either by a modification of the supporting conditions or by a modification of the intrinsic stiffness of the specimen with the amount of load.   As is well known, a modification of the support conditions would force a variation of the ratio between the first two natural

frequencies. In the case of the tested columns, the fact that the ratio between the two first natural frequencies did not vary significantly through the loading process showed that the variation of the absolute values was essentially due to the non-linearity of the stress-strain response of the material, i. e, the alteration of the stiffness with the load. Columns with visible cracks showed a sensible decrease in frequency, due to loss of inertia. Further investigation is needed (and now being undertaken) to define a clear relation between natural frequencies and axial load in columns of the cloister.

The vast majority of the tested columns showed a clear trend do reduce the frequencies when approaching to middle section of the cloister length. The reason to this phenomenon has not been clearly established yet. An accepted hypothesis is that an arch mechanism is developed in the wall above the columns. This arch displaces a part of the vertical loads to the edges of the cloister (to the columns near to the corners). However, further research is needed to validate this hypothesis.

The dynamic assessment of the columns permitted to draw the conclusion that certain members are holding a higher load than others are. This fact was corroborated with the assessment of a column with evident damage (a transversal crack in axis 32, west side). The test was able to identify a general load pattern in the cloister. The columns with higher frequencies are likely to be loaded in a higher ratio than the specimens with lower frequency values.

Dynamic testing of the stone columns was strictly non-destructive, a valuable characteristic when evaluation historical buildings. Any other structural assessment technique would cause damage to the evaluated members.

7.3.2. Load stone wall in Gaudi's *Palau Güell*

7.3.2.1. Introduction

The evaluation of existing structures and buildings with the use of non-destructive and quasi-non destructive inspection has been largely promoted and developed in the last years. Such techniques include respectively endoscopies, sonic and ultrasonic tests, electromagnetic and sonic tomography, dynamic tests, radar emission on one hand and flat-jack tests, borehole dilatometer, etc, on the other. Many authors researched the different available techniques [see section 3.6.6] in order to assess their feasibility and their reliability on detecting the internal composition and consistency of masonry, identifying the damage and measuring the mechanical parameters of the tested elements. In particular, the need of scientific and respectful strategies for the analysis and the preservation of historical construction encouraged the use of such inspecting techniques.

Among these inspection techniques, one of the fully non-destructive and completely viable for the application on ancient constructions is the dynamic identification, based on the measurement of the response to ambient or forced vibration. The method is based on the fact that the modal parameters (natural frequencies, mode shapes, modal damping) are function of the physical properties of the structure (mass, damping and stiffness). Therefore, dynamic tests can be used for the identification of local (in single elements) or global (for the characterization of a whole structure) properties, and for the medium to long term monitoring of buildings. A complete review of the state of the art on damage identification and health monitoring was developed in Chapter 3.

In the presented study, dynamic inspections were applied to a stonewall in the entrance of the Palau Güell in Barcelona. The wish of preserving the integrity of the wall, in fact, avoided the use of some conventional totally or slightly destructive tests, such as static load or flat-jack testing. On the bases of a previous investigation [Ellis, 1998], where the variation of natural frequencies and of frequency domain shapes with the level of load acting on stone elements was analysed, dynamic tests

were applied not only for damage identification, but also for the performance assessment of the different blocks. The analysis of the response of the 33 stones that constitute the wall to dynamic excitation, allowed expressing some qualitative evaluations on the whole wall conditions.

The Palau Güell was built between 1885 and 1889 and represents the transition, in Gaudí's architecture, from the Moorish style to the Gothic one. Actually this palace, which despite a plant of only 12x18 m rises for 6 floors, evokes and sums different architectonical and decorative styles, resulting in an eclectic building. Two external views of the Palau Güell can be seen in the following Fig. [7.35].

During the erection of the palace, the project varied many times. This fact led to a not integral structural design of the building, which nowadays is reflected in various structural problems. Therefore, high compressive stresses, differential settlements, flexural cracking, characterize the palace from a technical point of view. Moreover, different and often experimental constructive techniques were employed. Brick masonry walls, columns and vaults, refined and even illogical stone stereotomy in limestone elements, load bearing steel beams, false capitals turned upside down, which bear and melt into the architraves, all contribute in making the Palau Güell a very complex building.

Figure 7.35. View of the palace from down under (left); its famous doorway (right).

7.3.2.2. Method

The attention was focused on a very peculiar load bearing wall of the Palau Güell. This wall is found at the mezzanine, between the ground and the noble floors, and rises on three stone columns that separate different areas in the palace hall. Therefore, one side of the wall, namely the "internal side", closes the area of an office that is located at the mezzanine. The other side, the so-called "external" one, free stands over the entrance (see Fig. [7.36]).

Figure 7.36. View of the entrance and of the studied wall from another room.

This stone wall is not homogeneous as it could seem. About half of it, in fact, is made of massive and hybrid stone blocks, while the other half is constituted of brick masonry, simply covered with stones plates on the external side, in order to assure an uniform view when entering the palace. The hybrid stones are made of two covering stone plates, on the two sides of the wall, about 4 to 5 cm thick, and an internal layer of poor mortar. All the massive and covering stones come from a limestone quarry in Garraf (Catalunya, Spain) that was property of the family Güell. A passing-trough crack, on the whole height of the wall, marks the separation between the two portions of the wall, the brick and the stone made. Very often this crack affects the nearby stones, dividing them into separate pieces. In particular, the

massive stone that presents the worst conditions is divided into three main pieces and is characterized by the out-of-plane expulsion of material (see Fig. [7.37]). Moreover, frequent displacement of the stones, with the consequent opening and detachment of mortar joints, was observed.

Figure 7.37. The "exploded" stone.

In this area, an extensive dynamic tests campaign was performed. The experimental testing was not focused on the behaviour of the whole wall, but on the performance of the blocks under real service conditions. The aim was to find out, considering the actual crack pattern, which stones can and how do they bear the high vertical loads from the upper beam down to the architrave and columns. Two kinds of tests were carried out: "one-sensor" tests were performed with an impact hammer and one piezoelectric accelerometer. The stones were hit and the dynamic excitation was detected on the same face of the wall. "Double-sensor" tests were performed with the use of two accelerometers, simultaneously placed on the two accessible faces of the stones. They allowed detecting the dynamic response of the two sides of the blocks to the same impact, in order to develop comparative analyses. In particular, the peak frequencies, the frequency domain shapes, the time domain responses and the level of damping ratio were analyzed. In the frequency domain, the analyses

were performed between 0 and 5000 Hz. The range between 0 and 500 Hz, in fact, can be considered typical of the first modes of vibration of the wall, as shown by numerical modelling, while for highest frequencies, namely from 1 to 8 kHz, the stone modes can be detected. The elastic waves generated were amplified, processed with an analogical-digital converter and then recorded with a portable PC. About 160 "one-sensor" and 120 "double-sensor" tests were carried out. A scheme of the performed tests can be seen in Fig. [7.38].

Single test; one-sensor   **Double test; double-sensor**
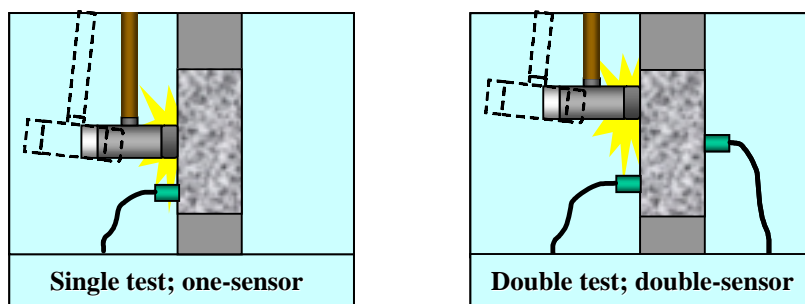
Figure 7.38. Scheme of the dynamic tests performed.

At last, to validate the hypotheses generated by dynamic testing, the results of some corings that had been already executed were considered. These holes had been cored on the internal side of the wall, in correspondence of the joint between the stone and the brick masonry, in order to detect whether the stones were massive or hybrid. Other corings were executed to complete the analysis. An accurate geometrical survey was carried out, too. Finally, a simple numerical model was performed in order to validate the hypothesis about the frequency range to be analized.

7.2.2.3. Results

In particular, the peak frequencies analysis was performed in order to make a first rough evaluation of the integrity of the blocks. Some cracked blocks, together with some others that apparently presented good conditions, were tested changing the position of the accelerometer from test to test. In the case of un-cracked stones, an accurate repetition of peak frequencies in the 0-5000 Hz spectrum was detected, even though the amplitudes of some peaks were different (see Fig. [7.39], right). On the contrary, the frequency response of damaged stones did not allow finding any

similarity in the peak frequencies. Moreover, it showed strong differences in the global frequency domain shapes (Fig. [7.39], left). Therefore, the recurrence of peak frequencies revealed to be a valid tool for the damage identification. The simple repetition of the tests, if carried out also on apparently healthy blocks, can help in internal damage identification, for a first performance assessment of the stones.
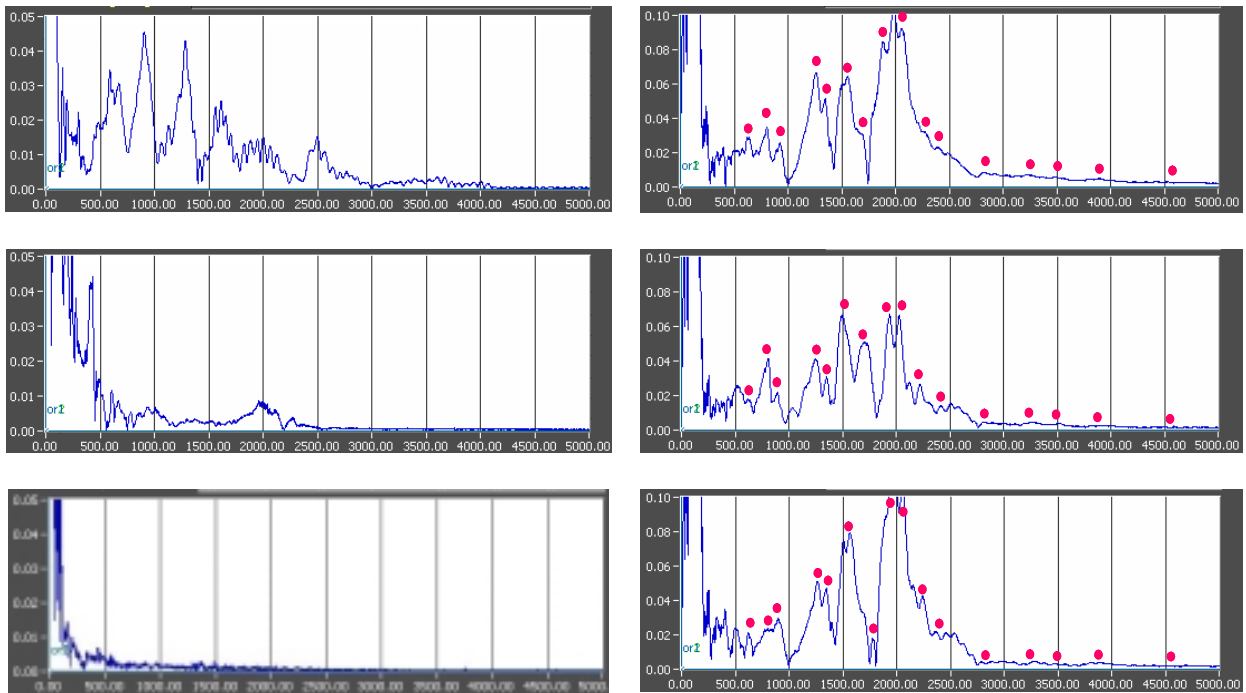
Figure 7.39. Different peak frequencies for a cracked stone (left); repetition of peaks (marked with the red points) for an un-cracked stone (right).

Complementary to the study of peak frequencies was the analysis of the damping ratio, which was implemented in a very simple way. The velocity of energy dissipation after the hammer impact, in fact, is proportional to the damping properties of the excited material. In case of presence of cracks and discontinuities, the energy can be also dissipated by friction. Therefore, high damping ratios in the time domain response of stones were related to the presence of cracks or discontinuities, while low damping ratios were used to hypothesize a good shape of stone (see Fig. [7.40]). In this regard, with this first analysis it was not possible to distinguish between cracked and hybrid stones, that is to say between the different

causes of higher damping ratios (cracks or discontinuities). For example, in the case of the three time domain responses reported in Fig. [7.40], with the outcomes of the subsequent geometrical survey and coring, it was found that the stone characterized by low damping ratio was massive, and the two stones characterized by high damping ratios were respectively massive but cracked (left-below diagram) and un-cracked but hybrid (right-below diagram).
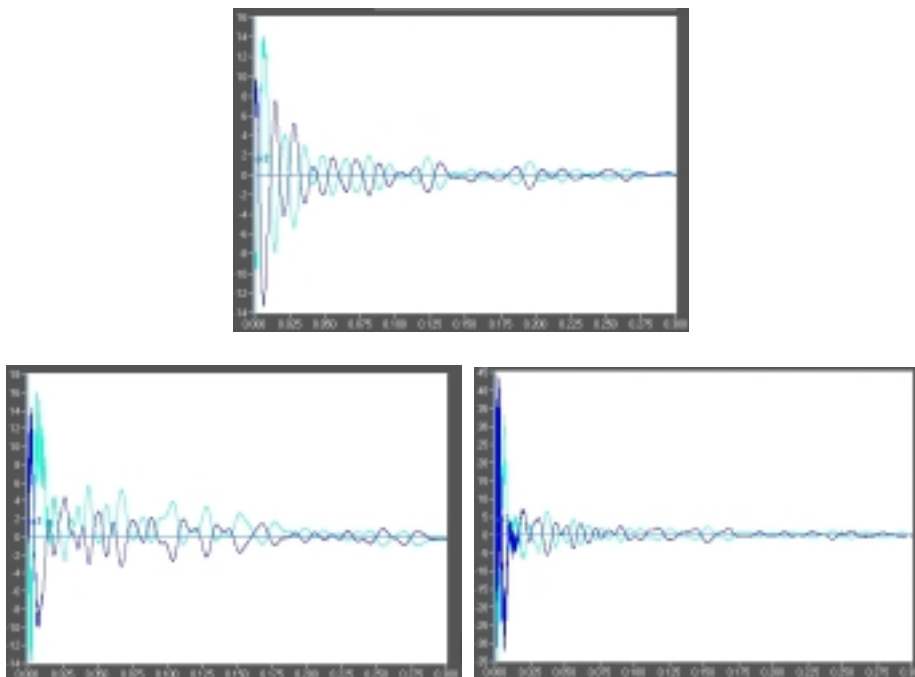
Figure 7.40. Different time domain responses: low (above) and high (below) damping ratios.

In connection with a first assessment of the stones, not only damage identification was relevant, but also, exactly, the knowledge of blocks typology, considering their different (massive and hybrid) and unknown nature. In this regards, a comparative analysis of the time domain response of the two faces of the stones, detected by double-sensor testing, was developed. In Fig. [7.41] the results of two of these analyses is shown.
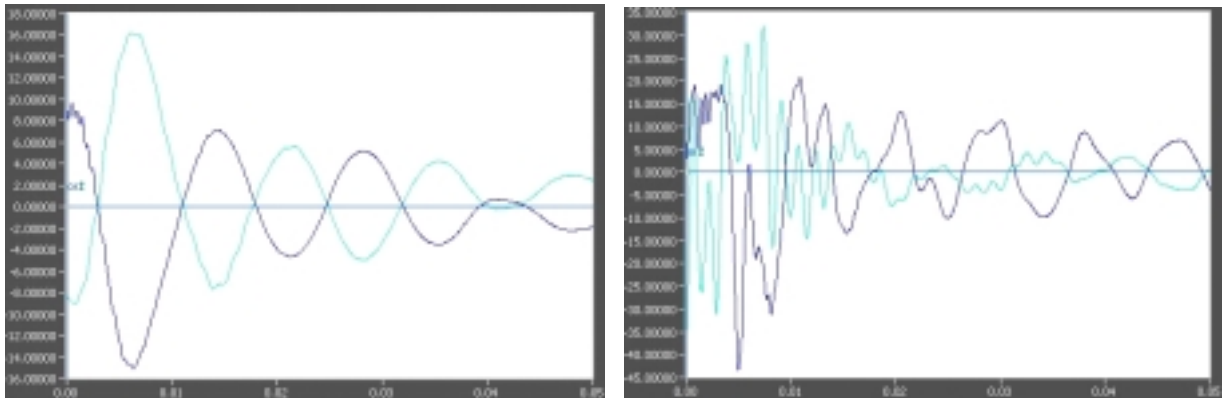
Figure 7.41. Time domain responses of the two faces of a block: case of a massive stone (left) and of a hybrid stone (right).

The two lines in each diagram show the response of the two surfaces of the blocks. A quasi perfect symmetrical behaviour of the faces, which revealed that accelerations on the two sides of the blocks were inverted, was found for some stones. Vice versa, a different path of the accelerations, showing a completely independent response of the two sides of the blocks to the same impulse, was found for others. The hypothesis that the two behaviours corresponded respectively to massive or hybrid blocks were made, and was subsequently confirmed by the evidence of the performed coring and geometrical survey (see Fig. [7.42]).

By analyzing the frequency domain shapes, finally, a hypothesis on the boundary conditions of the stones was planted. Two main cases were detected by applying one-sensor tests. The frequency domain of the stones presented a flat or a chaotic shape (see Fig. [7.43]). This path was related to the effectiveness of the stones confinement, that is to say the existence of a good or poor boundary and the presence of a high or low degree of compression loading.
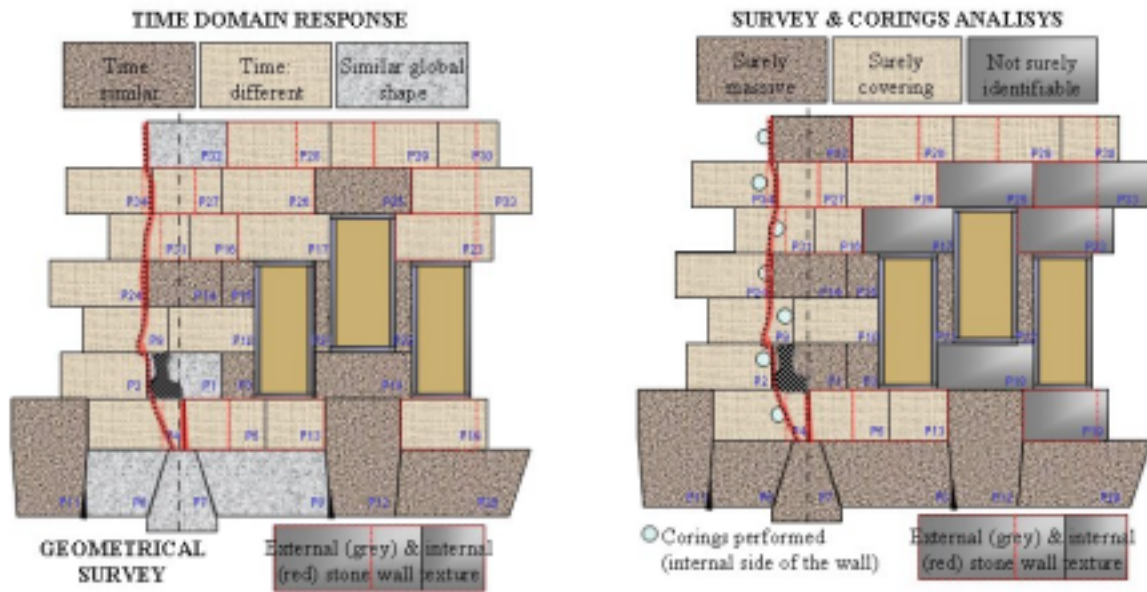
Figure 7.42. Hypotheses on the nature of the blocks made by time domain response analysis (left) and by geometrical surveying and coring (right).
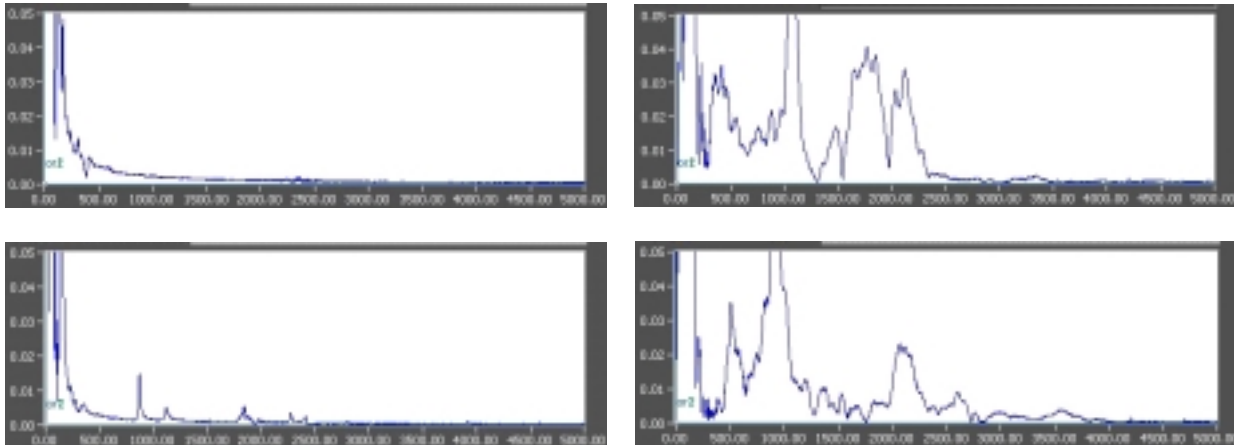
Figure 7.43. Flat (left) and chaotic (right) frequency domain shapes.

Moreover, with the use of double-sensor tests, stones showing different behaviour on the two faces were found. These cases, in general, corresponded to hybrid blocks, where the two external stone plates are separated by a layer of poor mortar (10 cm thick) and provided of no connection. Therefore, a different performance of the two surfaces of the blocks is essentially possible. In the case of the exploded stone, on the contrary, the different behaviour was related to the condition of its external surface that was actually loose and could not be confined nor loaded. It

showed, in fact, a chaotic frequency domain shape, despite the presence of a high compression rate still loading the unharmed parts of the block.

After grouping the different kinds of stones with reference to the boundary conditions found, the performance of the whole wall was evaluated. As it can be seen in Fig. [7.44], a distribution of confined or partially confined stones was found (colours from red to pink). This distribution revealed to be compatible with possible loading levels in the wall. In fact, the two vertical areas characterized by flat frequency domain shapes, were located in correspondence of the application of vertical loads coming from the upper floor. In particular, the area where the straight line is drawn is characterized for bearing a steel beam, whose evaluated transmitted load is equal to 730 kN, and for ending, in the lower part, in correspondence of one of the supporting columns. Finally, the capital and all the stones of the architraves, presented the most clean flat frequency domain shape, which is in perfect agreement with the expected concentration of compressive loads there.
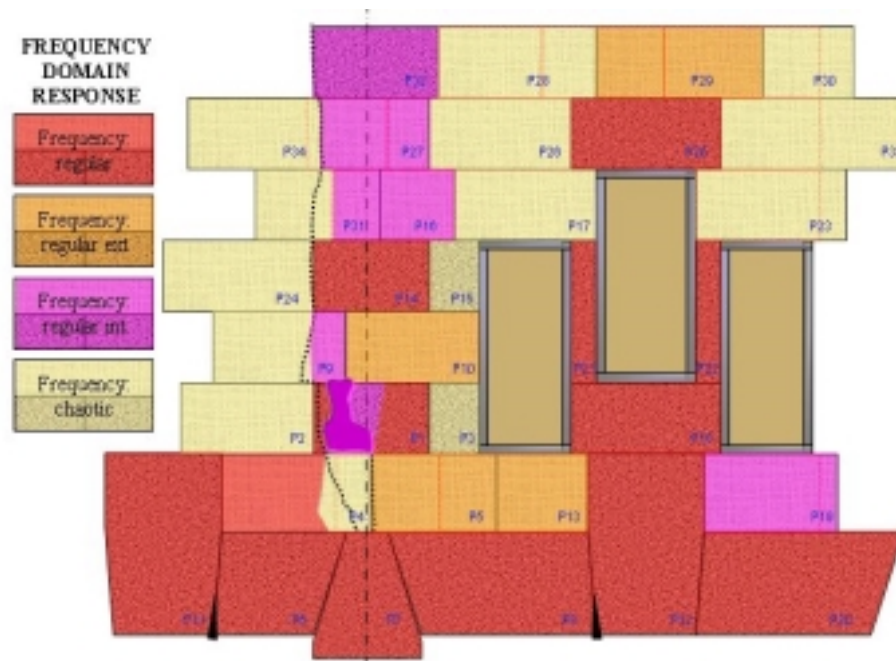
Figure 7.44. Results of the hypotheses that exists a relationship between the load distribution and the different frequency domain shapes detected on the wall.

7.2.2.4. Numerical simulation

A simple analytical model was created to assess the reliability of the starting hypothesis. The model consisted of a column, representing a portion of the tested wall, with a double fixed support condition at the ends. It was used to verify that, to identify the behaviour of the stones, the lower frequencies did not have to be considered, being typical of the structure mode of vibration. The modulus of elasticity was estimated from available data about the Garraf stone, and was taken equal to 38 GPa. A satisfactory agreement was found between the analytically predicted values of the first natural frequencies and those experimentally measured by dynamic testing in the Palau Güell. The first natural frequencies found by means of this simple analytical model were F1=63 Hz, F2=170 Hz, F3=323 Hz.

7.2.2.5. Discussion

In the presented field study a first attempt is made, inside a more general investigation, of using dynamic testing for the performance assessment of load bearing masonry under actual service conditions. In particular, the condition of the tested wall was investigated by checking the single constituent materials, represented by different kinds of stone blocks. The simple qualitative evaluation of the results obtained during the non-destructive testing campaign, allowed formulating different hypotheses about the composition and the structural behaviour of the wall. The gathered information was completely confirmed by the evidence of some inspections and by the outcomes of numerical modelling.

The nature of each of the 33 blocks tested, massive stone or hybrid block, was identified by detecting anomalies in the time domain response. Regarding the frequency domains, the presence of evident and numerous frequencies, which constituted a chaotic domain shape, did not allow the detection of damage by studying natural frequencies shifts. This chaotic pattern in the range 0-5000 Hz was related to the possibility that the boundary conditions of the stones were not good and the block excitation not fairly good dissipated by the whole structure in the first natural frequencies. The identification of the confinement of blocks led to a qualitative evaluation of their loading condition. Some anomalies detected with this

kind of analysis revealed also the presence of internal damage in few stones. Finally, the simultaneous testing on the two surfaces of the wall revealed to be easy to perform and reliable in results. Various different pieces of information were collected thanks to double testing.

The available dynamic information was enough to understand the full condition of the wall and to outline a clear loading bajada from the upper beam to the column below. This path followed the pattern of the mentioned crack and produced dangerous stress concentrations. On the bases of these results, considering also the presence of badly damaged stones, the possibility of operating a proper strengthening intervention is being taken into account. The dynamic investigation proposed has been therefore useful for a performance assessment of the studied wall. On the other hand, further investigation is needed in order to develop the proposed analyses and to numerically define the found relationships.

7.3.3. Stone cantilevers in Notre Dame of Laken, Belgium

7.3.3.1. Introduction

The church was built in 1854, during the reign of King Leopold I, to commemorate the death of his wife Louise-Marie of Orléans, Belgium's first queen. The construction continued until 1908. At the moment the church is again under renovation. One of the major subjects of this renovation is the reinforcement of stone cantilevers.

During the last decade, some structural accidents have taken place by the falling of stone pieces from the church's façade. The stones of the façade have been subjected an aggressive atmospheric action and have suffered important deterioration. As a result of this deterioration some specimens have lost the connection and have precipitated to the ground, in some cases from 100 m. high [figure 7.44].
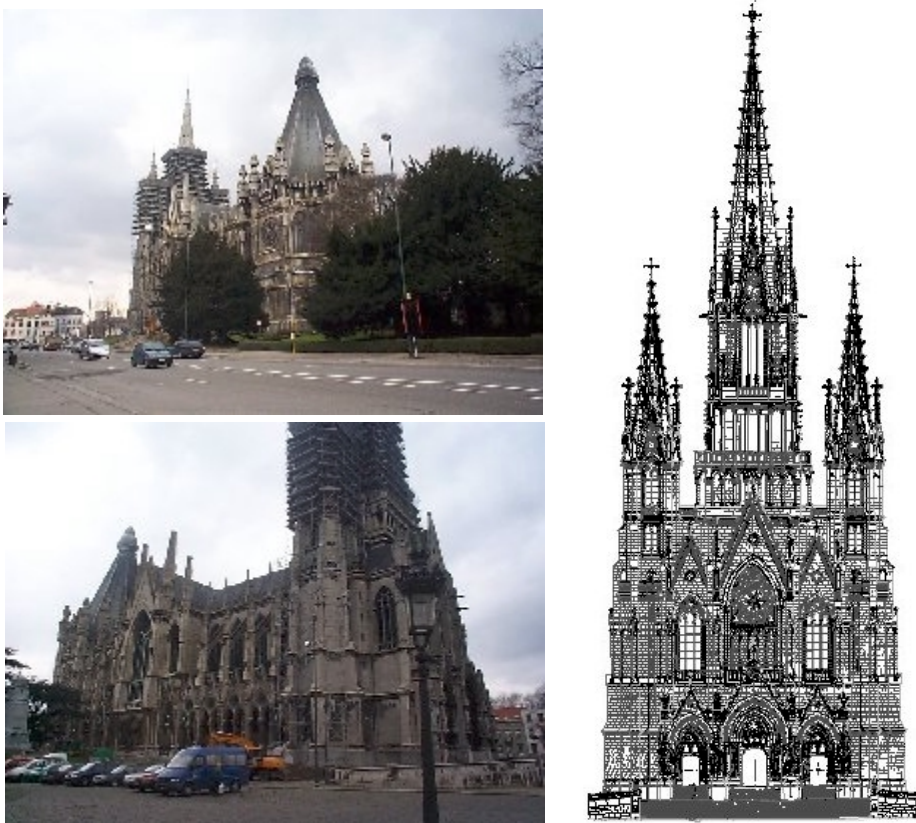
Figure 7.44. A general view of the church (left) and a An artist representation of the façade (rigth).

This local collapse did not cause any personal injuries, however, the church's administration decided to set a framework around the towers [figure 7.45] to sustain the stones, causing a very important architectural degradation. The frameworks did not have a permanent character, and were implemented only while any other permanent solution was found.

The Catholic University of Leuven was required to develop a research on the stability of the façade. Due to the great historical value of the church, a non-destructive identification technique was required to characterize the façade stones. Dynamic testing was considered a good alternative and was developed in seven stones in a first approach.

A description of the experimental work carried out to study the stones and the process of the acquired data is described in this section.

Figure 7.45. Frameworks deployed to avoid stone falling (right).

7.3.3.2. Method

The first step consisted in a visual inspection of the stones and the identification of the previous structural accidents. The original place of the precipitated stones was identified [figure 7.46]. The failure was produced by a crack in the stones. The connection to the façade was solid and did not present any visual defects; therefore, the pathology was more related to the material than to the construction process.

Figure 7.46. Original location of precipitated stones.

Seven different stone-cantilever beams were evaluated. All the beams were situated at the same level and around the same tower. To obtain the basic eigenfrequencies, a test with a two or four measurement points was considered sufficient. The process of the data was developed in situ; therefore only one test was recorded for every beam. The test equipment was reset every time that a location change was needed. Detailed information of the method is given in Chapter 4.

When torsion modes were subject of interest, four accelerometers were attached to the beam [figure 7.47], two accelerometers were attached to the end corners and other two to both support sides. All accelerometer were attached in a vertical position.

A different configuration of sensors was implemented when the torsional modes were not monitored. In this configuration two accelerometers are attached to the beam, one at every end, and above the central axis [figure 7.48].

Figure 7.47. Instrumentation of the beams.

Figure 7.48. Instrumentation of one stone with 2 sensors.

The data-acquisition setup consisted in a KEMO VBF 35 filter unit, a 16 bit acquisition card and a portable PC [figure 7.49].

Figure 7.49. Data acquisition system.

Some stones presented important visual characteristics: Stone number 7 was sustained in a steel tube, probably because it showed an important crack and it was in a high risk of failure [figure 7.50, right]. Stone no. 2 also showed an important crack, but probably related to any mechanical abrasion [figure 7.50, left].

Figure 7.50 Stone-beam 2 (right) and 7 (left).

Dynamic tests

The entire tests had a length of 0.2 seconds; a complete dissipation of the energy took place completely in this period [figure 7.18]. The natural frequencies were extracted by pick-picking from the frequency domain plot [figure 7.51].
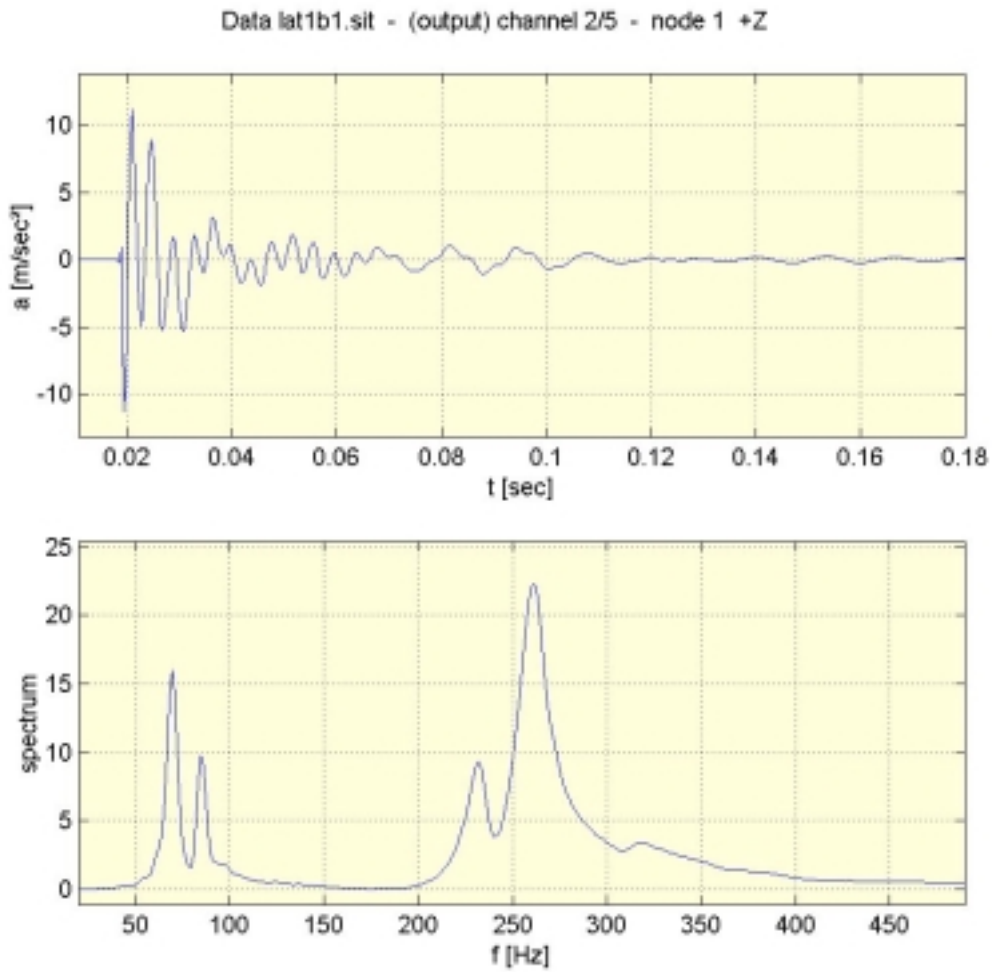
Figure 7.51 Typical data acquisition in time domain (above) and frequency domain (below)

7.3.3.3. Results

The data obtained by excitation of the beam by impact were processed. The typical frequencies are repeated in all beams with a small deviation. Table 7.11 presents all the obtained results. Support spring and first bending frequencies presented almost not variation [figure 7.52]; however, the first torsional frequency oscillated around 250 Hz with an important deviation [figure 7.52].

Stone-beam	Support spring		Bending		Torsion		Torsion 2		Bending 2	
	f (Hz)	Damp. (%)	f (Hz)	Damp. (%)	f (Hz)	Damp. (%)	f (Hz)	Damp. (%)	f (Hz)	Damp. (%)
1	69.7	4.7	84.8	2.7	231.4	4.6	259.7	3.6		
2	61.3	2.3	75.4	2.3	209.3	6.8			308.3	4.0
3	63.5	6.0	75.9	2.9	252.0	8.7				
4	66.9	2.7	96.5	2.7	313.4	4.5				
5	69.0	4.0	89.5	3.5	267.0	6.2				
6	76.5	5.5	93.4	2.0	284.3	4.2			441.4	7.1
7	68.9	3.4	82.6	4.7	240.8	6.8	290.2	13.8		

Table 7.11 Identified frequencies in all specimens
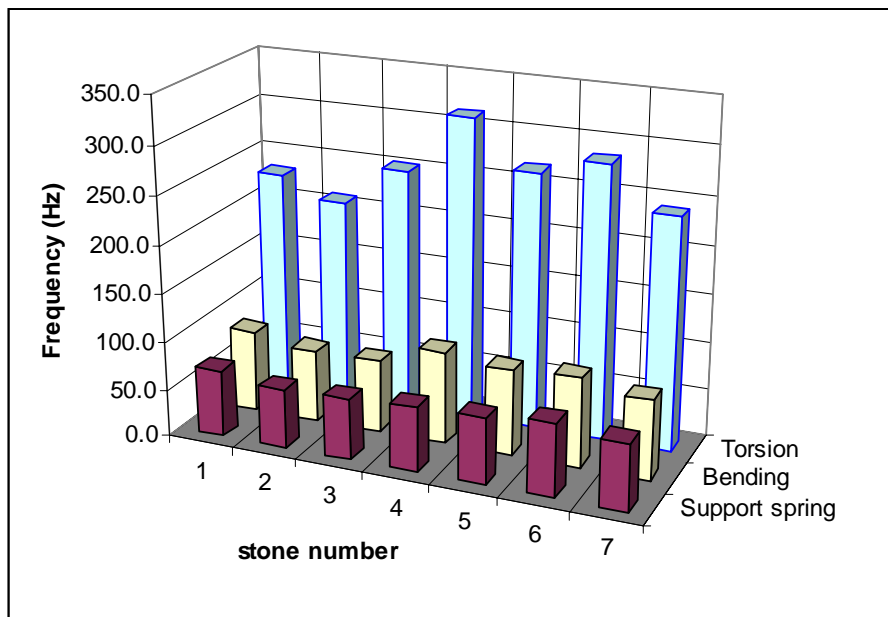
Figure 7.52. First three identified frequencies

7.3.3.4. Numerical simulation

Geometric and material characteristics

A simple elastic FE model was developed to simulate the behavior of the stone beams.

The density of the stone is 2200 kg/m^3 and the Young modulus E is estimated around 25000 N/mm^2. The clamping coefficient is unknown, as a first approach a full-clamped condition is assumed and gradually released to match the experimental values.

The element types

Linear elements are implemented. A dense mesh would be useless because a low number of points are monitored. A model with 6 nodes and 6 DOFs per node would be accurate enough. The lowest frequency of the model is a rigid-body vibration. The stone oscillates around the support axis [figure 7.53].
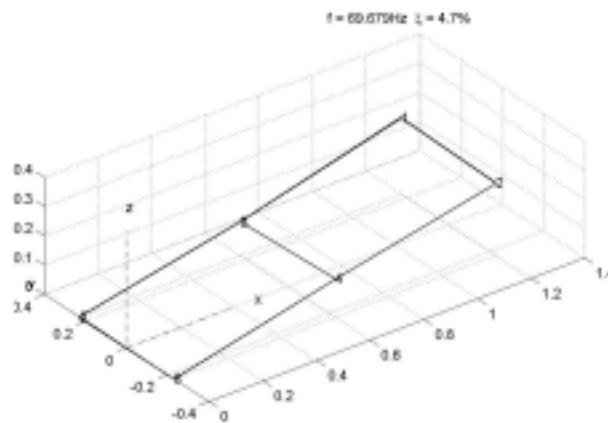
Figure 7.53. Support-spring mode

The second natural frequency is related with a flexure mode. While the support remains rigid, the stone-beam vibrated whit a flexion-shape [figure 7.54, left]. Another natural frequency (the fifth) is also related with flexure [figure 7.54, right].
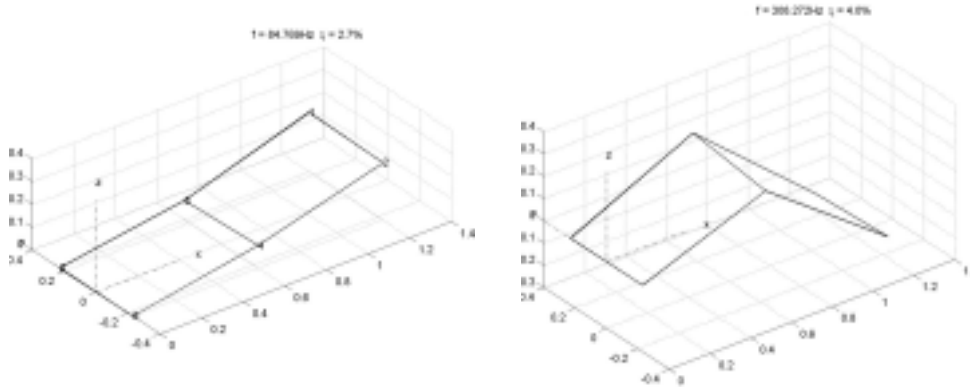
Figure 7.54. Bending Modes

Another kind of modeshapes is related with torsion. Figure 7.55 shows the calculated shapes. The third natural frequency of the beam is related with torsion.
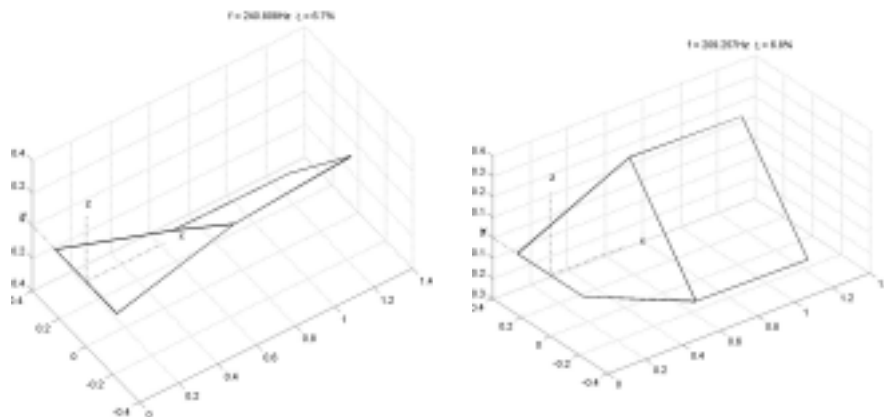
Figure 7.55. Torsional Modes

The process of model updating was very simple, and after a few attempts, a perfect approach was achieved. The low number of unknown variables helps the process of updating to be simple and accurate.

7.3.3.5. Discussion

Several dynamic tests were carried out in the façade of the Church of Laken. A dynamic characterization of seven stone-cantilever beams was successfully developed. The dynamic test has given valuable information to identify not only the strain modulus of the material but also the support conditions.

The tested floor has been modeled with an elastic FEM code. For the model, the eigenfrequencies and the mode shapes have been calculated and compared with results obtained from measurements. A perfect comparison has been found between the experimental determined eigenfrequencies and the numerical ones. A more detailed measurement grid is however necessary to identify higher frequencies and more complex mode shapes.

The main conclusion of this example is that a simple dynamic test is enough to identify the first few natural frequency of a stone beam. This identified value serves to develop a model updating process. Once the model is updated, the fundamental parameters of the structural member are identified (such as strain modulus and support conditions).

eight

C o n c l u s i o n s   a n d   f i n a l   r e m a r k s

8.1. Partial conclusions

This research has explored the applicability of a simple structural evaluation technique for building components such as masonry elements (load bearing walls, columns) or concrete elements (slabs and beams) based on the identification of their dynamic properties.

The works developed include a *state-of-the-art* review, a parametrical sensitivity study, a series of experimental works under laboratory conditions and a series of field studies implementing dynamic testing for different purposes.

In the following paragraphs, particular conclusions for the different aspects of this research are presented.

8.1.1. On the *State-of-the-art*.

- Available literature shows a significant development on dynamic identification algorithms and equipments. Damage or fault detection, as determined by changes in the dynamic properties or response of structures, is a subject that has received considerable attention from the engineering academic community. The interest in the ability to monitor a structure and detect damage at the earliest possible stage was observed pervasive throughout the civil, mechanical and other engineering fields.

- A topic of primary importance is the dependence on prior test information for the detection and location of damage. Many algorithms of the literature have been developed by presuming that access to data from the undamaged structure is available. Often, the lack of availability of this type of data can make a method impractical for certain applications. While it is doubtful that all dependence on prior models and data can be eliminated, certainly steps can and should be taken to minimize the dependence on such information.

- Type, number and location of sensors is an important issue that has not been addressed sufficiently in the current literature. Techniques that are to be seriously considered for implementation in the field, should demonstrate that they can perform well under the limitations of a small number of measurement locations.

- A topic that is a point of controversy among many researchers is the general level of sensitivity that modal parameters have to small alterations in a structure. Much of the evidence on both sides of this disagreement is anecdotal because it is only demonstrated for specific structures or systems and not proven in a fundamental sense.

- The amount of literature related to damage detection using shifts in natural frequencies is quite large. The observation that changes in structural properties cause changes in vibration frequencies was the impetus for using modal methods for damage identification and health monitoring. However, it should be noted that frequency shifts have significant practical limitations for applications to certain type of structures. Therefore, different identification algorithms based in changes on modal shapes, mode shape curvature, strain mode shape or dynamic flexibility, are more adequate for certain specific applications.

In general terms, sufficient evidence exists to promote the use of measured vibration data for the detection of damage in structures, but a lack of specific applications is observed in the literature. Additionally, it is concluded that research

should be focused more on testing of real structures in their operating environment, rather than laboratory tests of representative structures. If specific techniques can be developed to quantify and extend the life of structures, the investment made in this technology will clearly be worthwhile.

8.1.2. On the numerical modeling of the vibration response

In general, it was shown that non-linear parameters, like tension stiffening or constitutive equations of materials, are fundamental when damage models are studied. Also, the support condition results to be fundamental when modelling all types of structural members. Finally, the load-induced hardening phenomenon in masonry structures may be a key issue when attempting to model such king of structures. Nevertheless, particular conclusions to the parametrical study are:

- The numerical model showed its adequacy for the simulation of the dynamic response of structural members, allowing its use for the sensibility studies and also for the identification process.

- In concrete members, tension stiffening was determinant to simulate the evolution of the natural frequencies through a cracking process. However, the tension stiffening parameters (such as tensile strength or maximum tensile strength) should be selected carefully, because they are critical for the behaviour of the concrete member after the appearance of the first crack.

- For masonry members, it was found that the hardening process plays a fundamental role. The modification of strain modulus or contour conditions due to loading influenced seriously the dynamic properties of evaluated building components.

8.1.3. On the parametrical study

A parametrical sensitivity study of the most important parameters when modeling concrete or masonry structures was developed. The dynamic response of the models

was sensitive to the parametrical variation in a different extent. The study of the influence of different parameters has allowed some conclusions:

- Parameters such as dead load, boundary conditions, strain modulus, reinforcement ratio or geometry properties have a direct influence in the dynamic response of the structural component. A clear relationship between the variation of those parameters and the dynamic response of the member is found. The parametrical study has allowed to determinate the relationship which characterizes this influence.

- Orthotropy in the geometry of concrete slabs (one way-slabs) has an important influence on its dynamic behaviour. While the first natural frequency is strongly dependent of the stiffness in the principal direction, subsequent frequencies are dependent of the ratio between the principal and secondary stiffness. This permits to formulate specific applications to determinate the characteristics of orthotropy of the slab.

- An intermediate FE mesh resolution is able to obtain similar results than refined meshes. The use of a medium-refined mess (less than 100 DOF's for beams and 1.000 for slabs) is enough to simulate accurately the dynamic behaviour of the evaluated member.

8.1.4. On the dynamic assessment of building components

In general terms, all the works carried out in this thesis have contributed to the conclusion that dynamic testing is a promising technique to characterize constructive members. Concrete beams, RC and prestressed slabs, masonry brick-walls and stone columns were subjected to dynamic assessment obtaining valuable information related to their structural state. Some particular conclusions can be drawn for every kind of building component:

8.1.4.1 Concrete beams

- Stiffness degradation (due to flexural cracking) in RC beams produced an important reduction of the frequencies (reaching 40%).

A relationship between damage due to cracking and variation in natural frequencies was observed in the different experimental works. This relationship can be used to identify the level of cracking from known natural frequencies.

- A numerical model including tension stiffening was accurate to simulate the evolution of the natural frequencies when damage due to cracking was induced. The proposed model was very sensitive to the tension stiffening parameters. Tension stiffening values proposed by other authors for the study of static tests [i.e Van Greunen, 1979; Kang, 1977 or Berzegar-Jimshidi, 1980] resulted accurate also for the simulation of the dynamic response of RC beams.

- The use of a suspended configuration of the test improved dramatically the acquired signal condition. The laboratory works carried out in this research, suggest that a reduction of the noise by setting soft springs to the beam supports can lead to a much more accurate identification.

- The possibility of identifying damage due to chemical attack (such as that due to chlorides or sulphates) requires the condition to have experienced either reduction of the section of steel or cracking of concrete. Otherwise, as shown by the experiments carried out in to the frame of the present research, no variation can be detected in the dynamic response.

8.1.4.2. Concrete slabs

It is possible to carry out a systematic recognition of large slab surfaces in buildings using dynamic assessment. The test shows a high repeatability, making possible to develop over hundred dynamic tests in one journey. If the acquired data are treated adequately, the tests can allow conclusions of the structural state of the slabs at low cost (if compared with traditional destructive techniques).

Dynamic identification of concrete slabs was successful in all the cases studied. In particular, the following conclusions can be drawn:

- Prestressed and reinforced concrete slab can be studied by two different test lay-outs:

    o a deployment of multiple sensors with identification of frequencies and modal shapes

    o a reduced version using only one sensor and measuring only natural frequencies

    The first approach is able to identify not only the first few natural frequencies but also the modal shapes associated to them. The second approach cannot identify modal shapes; however, the first few natural frequencies can be identified and a numerical model can be updated using this information. Parameters such as contour conditions or strain modulus of the materials are identified with both approaches, but the use on only one accelerometer represents an important time and equipment reduction.

- The test can be used systematically through several slabs (i.e. sections 7.1.2 and 7.1.3), giving a complete panorama of the structural condition of the slabs of the building. By optimising a numerical model with the dynamic information, parameters such as strain modulus of the concrete, support conditions or participation of pavement can be identified.

- By studying the proportion between the two first identified frequencies, it is possible to identify the ratio between the longitudinal and transversal stiffness in an orthotropic concrete slab. By using the criteria proposed in the parametrical study (section 5.4.7), the proportion between longitudinal and transversal stiffness can be identified. The knowledge of the orthotropic properties of the slab, allows the characterization of the capacity of distribution of concentrated loads between the slab nerves.

- A simulation of static tests can be developed in the optimised numerical model. Once the model has achieved a good level of dynamic prediction, static processes can also be simulated with success.

- It was demonstrated that the use of dynamic testing is a good alternative for the systematic recognition of concrete slabs. However, more direct methods, such as load tests or core extraction are always necessary to calibrate the identification procedure. Dynamic assessment presents the advantage of inspecting the building in a wider extant than if only traditional inspection methods are used.

8.1.4.3. Masonry members

Dynamic testing in masonry members is a promising alternative for non-destructive assessment. It was demonstrated that the dynamic properties of the members may be strongly related to the axial load to which they are subjected. A series of dynamic tests may allow the detection of qualitative variations in the load applied to the members and, if a previous calibration is available, even identify the load actually supported by the member.

- A relationship between axial load and dynamic properties of masonry members exists in many cases. The variation of the natural frequencies can be due to two facts: modification of the boundary conditions or load-induced hardening processes. Studying the proportionality between the first and second natural frequencies can lead to a differentiation between those two possible factors. This differentiation was carried out with success in specimens subjected to increasing loads under laboratory conditions.

- The characterization of the internal morphology of a multi-layer load-bearing wall can be carried out by dynamic assessment. Dynamic testing may succeed to identify loader or unloaded blocks and to distinguish between solid or hollow members existing in the wall (as described in the study of Palau Güell). By means of comparing the stiffness of every stone,

the load level can also be identified. The proposed methodology is strictly non-destructive and at the same time affordable and effective.

- For the case of stone members subjected to flexure (as shown in the study of *Laken church*), dynamic testing was able to characterize a series of stone cantilever beams. The strain modulus of the material, the clamping coefficient and the absence of cracks were identified through dynamic assessment. The test did not cause any deterioration to the structure and produced valuable information for a model optimisation.

8.2. Global conclusions

The present research has contributed to ascertain that dynamic testing is a valuable tool to assess the structural conditions of single concrete or masonry building elements such as concrete beams, concrete slabs, masonry walls or stone piers.

Experimental works and field studies have permitted to conclude that a combined implementation of a simple dynamic testing and numerical modelling is able to characterize the current structural conditions of a building component. The information acquired with the proposed layout leads to the identification of characteristics such as boundary conditions, cracking levels, geometry properties or levels of axial loading.

By comparing systematically the experimental and the numerically produced frequencies, it can be concluded that a detailed numerical model is able to predict the dynamic response of the studied component. This prediction is accurate not only for undamaged conditions, but also for different damage scenarios. The prediction capacity of the model is strongly dependent of the calibration of the constitutive equations of the materials. A good approximation was achieved by including tension stiffening in the case of concrete members and a *hardening equation* in the case of masonry structural members.

8.3. Further research

This thesis is intended to contribute to the application of dynamic testing as an identification technique for building components. Nevertheless, this work is only a

particular approach to the more wide field of construction engineering. Future research is certainly needed to obtain a robust, automatic, generally applicable monitoring system. Some fields in which further research is needed are:

- Sensor technology. Dynamic identification is strictly related with the technology of the sensors. While sensors are improving, dynamic identification techniques will improve for sure. A potential application of dynamic testing is definitely related with wireless communications and GPS (global positioning systems). In the near future, the resolution of GPS will certainly achieve such sensibility that dynamic identification will be possible by using global position sensors.

- The dynamic identification and model updating of historical constructions. Dynamic testing is a good alternative for approaching to the knowledge of these complex structures. Modelling historical building is a hard process; therefore, dynamic techniques are a good manner of interact with the structure and allow some quasi-direct retrofit.

- In this thesis, relatively small building components were studied. Excitation techniques fur such structures can be simply carried out by hammer impact. However, when larger structures are studied, the source of excitation can be a complex factor. Environmental excitation presents a good alternative for this problem; however, further research on this field is needed, especially when studying masonry historical buildings.

a

Dynamic equipment

Measurement and post processing equipment

Seismic accelerometer. Piezotronics mod. 393C.

0.454 kg stainless steel attached to a quartz transducer.

Sensibility: 1.0 Volt/g

Frequency range =.025 a 800 Hz.

Ceramic accelerometer. Piezotronics mod. 393A.

 0.210 Kg (7.4 Oz) stainless steel attached to a ceramic transducer.

Sensibility = 1.0 Volt/g.

Frequency range = 0.5 a 2000 Hz.

12-pounds impact hammer mod.

Signal conditioner / Amplifier Piezotronics Mod. F482A16.

Four channel amplifier digitally controlled with self-feeding. Every channel admits variable increments (1x, 10x, 100x) and detects failures and overloading per channel..

National Instruments CB-40 Connector Block.

Analog format connector to data acquisition card.

Acquisition system

- Vibration measure and analysis integrated system (Sistema integrat de mesura i analisi de vibracions SIMAV):

Software application designed to acquire and process dynamic information up to 4 different sensors. The system resolution is limited by the acquisition buffer (30,000 points). The software was designed and developed for this particular propose by the Thermal Engines department of the Technical University of Catalonia (UPC)

- National Instruments DAQCard 1200:

Plugged to a PCMCIA port of a conventional Piii notebook computer.

Signal post-process system

Software application MACEC V. 2.0, developed by the Civil Engineering Department of the catholic University of Leuven, Belgium. MACEC is a dynamic parameter identification toolbox for Matlab.

b

P a r a m e t r i c a l   s t u d y   d a t a

Mass per node. (kg mass)		f1	f2	f3
2.92	= 4 Gravity	40.9	154.0	316.0
2.19	3 G	47.3	178.0	365.0
1.46	2 G	58.0	218.0	447.0
0.73	1 G	82.0	308.6	632.8
0.37	1/2 G	107.0	402.0	825.0
0.18	1/4 G	151.3	569.0	1167.0

Table B.1. Influence of mass on natural frequencies.

REINFORCEMENT		INTACT		Q= 20.0 kN		Q= 40.0 kN		Q= 60.0 kN	
Tensile Bars	Area (cm^2)	f_1 (Hz)	f_2 (Hz)	f_1 (Hz)	f_2 (Hz)	f_1 (Hz)	f_2 (Hz)	f_1 (Hz)	f_2 (Hz)
2ϕ6	0,56549	53,356	200,9	52.135	200.10	FAILURE		FAILURE	
2ϕ8	1,00531	53,786	202,44	52.727	201.83	FAILURE		FAILURE	
2ϕ10	1,57079	54,296	204,27	53.409	203.81	FAILURE		FAILURE	
2ϕ12	2,26195	54,866	206,3	54.162	206.01	44.645	192.71	FAILURE	
2ϕ14	3,07876	55,478	208,48	54.936	208.29	48.042	198.84	FAILURE	
2ϕ16	4,02124	56,113	210,74	55.723	210.63	50.430	203.64	44.674	187.61
2ϕ18	5,08938	56,756	213,01	56.490	212.96	52.480	207.73	47.493	194.89
2ϕ20	6,28318	57,391	215,25	57.224	215.22	54.162	211.14	49.883	201.49
2ϕ24	8,047787	58,596	219,47	58.557	219.47	56.632	216.76	53.553	210.90

Table B.2. Influence of tensile steel reinforcement on natural frequencies.

REINFORCEMENT		UNLOADED		Q= 20.0 kN		Q= 40.0 kN		Q= 60.0 kN	
Compression Bars	Area (cm^2)	f_1 (Hz)	f_2 (Hz)	f_1 (Hz)	f_2 (Hz)	f_1 (Hz)	f_2 (Hz)	f_1 (Hz)	f_2 (Hz)
2ϕ6	0,56549	55.646	209.06	55.234	208.95	50.022	201.92	FAILURE	
2ϕ8	1,00531	56.113	210.74	55.723	210.63	50.430	203.64	44.674	187.61
2ϕ12	2,26195	57.298	214.96	56.960	214.88	51.572	208.07	45.498	191.49
2ϕ14	3,07876	57.974	217.36	57.664	217.30	52.203	210.56	45.922	193.60
2ϕ16	4,02124	58.679	219.86	58.399	219.81	52.846	213.13	46.329	195.72
2ϕ18	5,08938	59.397	222.40	59.143	222.36	53.452	215.68	46.698	197.78
2ϕ20	6,28318	60.113	224.91	59.879	224.88	54.062	218.20	47.050	199.72
2ϕ24	8,04779	61.488	229.72	61.288	229.70	55.158	222.88	47.606	203.12
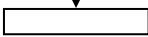
Table B.3. Influence of compressive steel ratio on natural frequencies.

Support stiffness (kp-m / Rad)	Unloaded			Q=50.0 kN		
	f_1 (Hz)	f_2 (Hz)	f_2 / f_1	f_1 (Hz)	f_2 (Hz)	f_2 / f_1
Free	56.11	210.740	3.756	46.72	195.14	4.2
5.0E5	79.69	238.330	2.991	77.51	236.92	3.1
2.0E6	101.41	273.120	2.693	99.66	271.87	2.7
3.0E6	106.77	283.160	2.652	104.72	281.42	2.7
5.0E6	112.12	293.770	2.620	109.69	291.29	2.7
Clamped	122.83	316.590	2.577	118.95	311.09	2.6

Table B.4. Influence of clamping on natural frequencies.

Dynamic modulus (MPa)	Unloaded		Q=20.0 kN		Q=40.0 kN		Q= 60.0 kN	
	f_1 (Hz)	f_2 (Hz)	f_1 (Hz)	f_2 (Hz)	f_1 (Hz)	f_2 (Hz)	f_1 (Hz)	f_2 (Hz)
10000	51.397	192.85	51.160	192.81	47.320	187.94	42.596	175.83
11000	53.489	200.79	53.183	200.72	48.751	194.96	43.600	181.19
12000	55.500	208.41	55.129	208.32	50.039	201.61	44.433	186.17
13000	57.438	215.76	57.005	215.64	51.355	208.11	45.256	190.77
14000	59.312	222.85	58.811	222.69	52.542	214.28	45.936	195.00
15000	61.126	229.72	60.561	229.53	53.653	220.09	46.611	199.24
16000	62.888	236.39	62.261	236.16	54.778	225.75	47.255	203.12
17000	64.600	242.87	63.915	242.61	55.821	231.20	47.706	206.91
18000	66.268	249.18	65.526	248.88	56.835	236.51	48.066	210.41
19000	67.894	255.33	67.098	255.00	57.819	241.67	48.438	213.74
20000	69.482	261.34	68.630	260.97	58.765	246.75	48.687	216.95

Table B.5. Influence of Strain modulus on natural frequencies.

Concentrated load		
Applied Load (kN)		
	f_1 (Hz)	f_2 (Hz)
0.0	56.114	210.74
5.0	56.114	210.74
10.0	56.114	210.74
15.0	56.114	210.74
20.0	55.723	210.63
25.0	54.991	209.87
30.0	54.153	208.54
35.0	52.408	206.63
40.0	50.476	203.77
45.0	48.786	200.18
50.0	47.326	196.11
55.0	46.013	191.98
60.0	44.828	188.04
65.0	43.846	184.16
70.0	FAILURE	

Table B.6. Influence of cracking on natural frequencies.

Distributed Load (kN/m)	f_1 (Hz)	f_2 (Hz)
0.0	56,114	210,74
50.0	56,114	210,74
100.0	55,416	210,06
150.0	53,494	205,3
200.0	48,358	194,43
250.0	44,988	182,27
300.0	42,525	172,83
350.0	40,652	165,56
400.0	FAILURE	

Table B.7. Influence of cracking on natural frequencies.

% Tensile capacity of concrete	Q=20.0 kN		Q=40.0 kN		Q= 60.0 kN	
	f_1 (Hz)	f_2 (Hz)	f_1 (Hz)	f_2 (Hz)	f_1 (Hz)	f_2 (Hz)
5 %	53.356	207.58	44.628	185.78	40.767	168.50
6 %	54.684	209.35	46.623	193.57	41.998	175.34
7 %	55.274	210.26	48.622	199.52	43.353	181.75
8 %	55.723	210.63	50.431	203.64	44.675	187.61
9 %	56.008	210.73	52.089	206.31	46.037	192.74
10 %	56.114	210.74	53.433	207.88	47.462	197.21
11 %	56.114	210.74	54.336	208.82	48.718	200.75
12 %	56.114	210.74	54.750	209.52	49.954	203.43
13 %	56.114	210.74	55.069	210.02	51.268	205.45
14 %	56.114	210.74	55.326	210.35	52.312	206.93
15 %	56.114	210.74	55.559	210.56	53.288	207.88

Table B.8. Influence of tensile capacity of concrete on natural frequencies.

TENSION STIFFENING	Q=20.0 kN		Q=40.0 kN		Q= 60.0 kN	
	f_1 (Hz)	f_2 (Hz)	f_1 (Hz)	f_2 (Hz)	f_1 (Hz)	f_2 (Hz)
1.0 E-3	55.512	210.58	43.405	193.88	FAILURE	
2.0 E-3	55.658	210.62	48.782	201.72	41.483	179.80
3.0 E-3	55.700	210.63	49.951	203.05	43.613	185.24
4.0 E-3	55.721	210.63	50.381	203.90	44.574	187.4
5.0 E-3	55.733	210.64	50.658	203.89	45.132	188.56
6.0 E-3	55.741	210.64	50.832	204.08	45.480	189.28
7.0 E-3	55.746	210.64	50.952	204.22	45.716	189.77
8.0 E-3	55.75	210.64	51.040	204.31	45.887	190.13
9.0 E-3	55.754	210.64	51.106	204.39	46.017	190.40
2.0 E-2	55.756	210.64	51.158	204.45	46.120	190.62

Table B.9. Influence of tension stiffening on natural frequencies.

Density (Lb/in^3 E-4)	f1	f2	f3	f4	f5
1.50	73	223	457	957	1239
2.00	63	193	396	829	1073
2.25	60	182	373	782	1013
2.50	56	173	354	741	960
3.00	52	158	323	676	876

Table B.10. Influence of the material density on the first five natural frequencies.

Volume steel / Volume concrete	f1	f2	f3	f4	f5
4.25E-03	59,9	180	372	777	1003
5.67E-03	59,96	181	372.5	779	1007
8.50E-03	60	182	373	782	1013
1.28E-02	60,15	184	375	787	1022
1.70E-02	60,20	186	376	791	1030

Table B.11. Influence of reinforcement on the first five natural frequencies
(Unloaded condition).

Damaged state (Load=500 Lb)					
Volume concrete / Volume steel	f1	f2	f3	f4	f5
4.25E-03	52	164	351	730	901
5.67E-03	53	167	353	740	920
8.50E-03	55	172	358	756	950
1.28E-02	57	177	362	767	975
1.70E-02	58	180	365	777	992

Table B.12. Influence of reinforcement on the first five natural frequencies (After
point-loading of 500 Lb)

Modulus (Lb/in^2)	f1	f2	f3	f4	f5
2.15E+06	44	133	270	569	740
3.15E+06	52	160	326	684	887
4.15E+06	60	182	373	782	1013
5.15E+06	67	202	416	869	1124
6.15E+06	72	220	454	948	1226

Table B.13. Influence of strain modulus on the first five natural frequencies.

Applied load (Lb)	f1	f2	f3	f4	f5
0.00	60	182	373	782	1013
500.00	55	172	358	756	950
800.00	50	157	343	684	866
1000.00	40	143	337	592	768
1100.00	failure				

Table B.14. Influence of cracking on the first five natural frequencies.

Tension stiffening branch amplitude	f1	f2	f3	f4	f5
5.00E-04	49	157	346	710	849
1.00E-03	53	167	353	742	919
2.00E-03	55	172	358	756	950
4.00E-03	55	174	360	759	960
8.00E-03	56	175	360	762	962

Table B.15. Influence of tension stiffening branch on the first five natural frequencies.

references

ACI [1985]. "Strength Evaluation of Existing Concrete Bridges." American Concrete Institute Special Publication 88.

ACI [1968]. "*Guide for making a Condition Survey of concrete in service*." American Concrete Institute, Committee 201.

ACI Committee 201. [1991]. "Guide of durable concrete." ACI Materias Journal. 88[5], 544-582.

Actis, R.L. and A.D. Dimarogonas, [1989], "Non-Linear Effects due to Closing Cracks in Vibrating Beams," ASME Design Engineering Division Publication DE–Structural Vibration and Acoustics, 18[3], 99–104.

Aktan, A.E., K.L. Lee, C. Chuntavan and T. Aksel, [1994], "Modal Testing for Structural Identification and Condition Assessment of Constructed Facilities," in Proc. of 12th International Modal Analysis Conference, 462–468.

Alampalli, S., G. Fu, and E.W. Dillon, [1995], "On the Use of Measured Vibration for Detecting Bridge Damage," in Proc. Fourth International Bridge Engineering Conference, 125–137.

Allbright, K., K. Parekh, R. Miller, and T.M. Baseheart, [1994], "Modal Verification of a Destructive Test of a Damaged Prestressed Concrete Beam," Experimental Mechanics, 34[4], 389–396.

Ambrosini D, Luccioni B and Danesi R. [1999] "Theoretical-experimental damage determination in prestressed concrete beams" Proceeding of International symposium on NDT, 1999, Santa Maria, Brazil

American Society of Civil Engineers Committee on Bridge Safety, [1980] "*A Guide For Field Testing of Bridges*", New York.

ASTM [1983]. "*Corrosion of Metals in Association with Concrete*." ASTM Special *Technical Publication 818*.

ASTM [1987c]. "*Standard Test Method for Pulse Velocity through Concrete:* ASTM C597-83." ASTM Annual Book of Standards, 4.02.

ASTM [1987f]. "S*tandard test method for half cell potentials of uncoated reinforcing steel in concrete:* ASTM C876-87." ASTM Annual Book of Standards, 4.02.

Avitabile, P. [1998] "Modal space, back to the basis". Experimental Techniques, by the Society for Experimental Mechanics. July/August

Baker, A. F. [1986]. "*Potential mapping techniques*." Proceedings of Seminar on Corrosion in Concrete, Monitoring Surveying and Control by Cathodic Protection

Balis Crema, L., A. Castellani and G. Coppotelli, [1995], "Generalization of Non Destructive Damage Evaluation Using Modal Parameters, in Proc. of the 13th International Modal Analysis Conference, 428–431.

Balis Crema, L., F. Mastroddi, [1995], "Frequency-Domain Based Approaches for Damage Detection and Localization in Aeronautical Structures," in Proc. of the 13th International Modal Analysis Conference, 1322–1330.

Baruch, M. and I.Y. Bar Itzhack, [1978], "Optimum Weighted Orthogonalization of Measured Modes," AIAA Journal, 16[4], 346–351.

Barzegar-Jamshidi, F and Schonobrich, W. [1980] "Non-linear fdinite element analysis of reinforced concrete under short term monotonic loading" Structural research serie no. 530, University of Illinois, Urbana, November.

Bazant, Z. P., and Oh, B. [1984]. ''Deformation of progressively crackingreinforced cracking reinforced concrete beams.'' *ACI J.*, 81[3], 268–278.

Begg, R.D., A.C. Mackenzie, C.J. Dodds, and O. Loland, [1976], "Structural Integrity Monitoring Using Digital Processing of Vibration Signals," in Proc. 8th Annual Offshore Technology Conference, Houston, TX, 305–311.

Bensalem A, Fairfield C and Sibbald A [1995] "Non-destructive testing for arch bridge assessment", Proceedings of the First International Conference on Arch Bridges, Bolton, UK. 3-6 September.

Berman, A. and E.J. Nagy, [1983], "Improvement of Large Analytical Model Using Test Data," AIAA Journal, 21[8] 1168–1173.

Bishop, C.M., [1994], "Neural Networks and Their Applications," Review of Scientific Instrumentation, 65[6], 1803–1832.

Biswas, M., A. Pandey, and S. Bluni, [1994], "Modified Chain-Code Computer Vision Techniques for Interrogation of Vibration Signatures for Structural Fault Detection," Journal of Sound and Vibration, 175[1], 89–104.

Biswas, M., A.K. Pandey and M.M. Samman, [1990], "Diagnostic Experimental Spectral/Modal Analysis of a Highway Bridge," Modal Analysis: The International Journal of Analytical and Experimental Modal Analysis, 5, 33–42.

Bridge Inspection Panel [1984]. "*Bridge Inspection Guide.*" Department of transport, Scottish Development Department, Welsh Office, Department of the environment for Northern Ireland, HMSO.

Brock, J.E., [1968], "Optimal Matrices Describing Linear Systems," AIAA Journal, 6[7], 1292–1296.

BSI BS 1881 [1988b]. "*Testing Concrete.* Part 204: *Recommendations for the use of electromagnetic covermeters.*" BSI, London.

BSI BS 1881 [1986c]. "*Testing Concrete.* Part 203: *Recommendations for Measurements of Velocity of Ultrasonic Pulses in Concrete.*" BSI, London.

BSI, B. 1. [1986a]. "*Testing Concrete.* Part 201: *Guide to the use of Non-Destructive Tests for Hardened Concrete.*" BSI, London.

BSI, B. 6. [1981]. "*Guide to the assessment of Concrete Strength in Existing Structures.*" BSI, London.

Budipriyanto, A. and A.S.J. Swamidas, [1994], "Experimental and Analytical Verification of Modal Behaviour of Uncracked/Cracked Plates in Air and Water," in Proc. of the 12th International Modal Analysis Conference, 745–752.

Building Research Establishment [1977]. "*Determination of chloride and cement content in hardened Portland cement concrete*." Information Paper IP 13/77, BRE, London.

Campbell-Allen, D. a. R. H. [1991]. Concrete structures: materiasl, maintenance and repair., Longman Scient. and Research., U.S.

Canet, J.M. y Barbat, A. [1988], "Estructuras sometidas a acciones sísmicas. Cálculo por ordenador.", published by Centro Internacional de Métodos Numéricos.

Cantor, T. R. [1984]. "*Review of penetration radar as applied to the non-destructive testing of concrete*." In situ Non-destructive testing of concrete, American Concrete Institute Special Publication 82, 581-602.

Careira, D. J., and Chu, K.-H. [1986]. ''Stress-strain relationship of re-inforcedconcrete in tension.'' *ACI J.*, 83[1], 21–28.

Casas, J. R. [1995] "Dynamic Modeling of Bridges: Observations from Field Testing," Transportation Research Record, 1476.

Casas, J.R. and . Aparicio A.C, [1994], "Structural Damage Identification from Dynamic-Test Data," Journal of Structural Engineering, 120[8], 2437–2450.

Casas, J.R., [1988], "El estudio de la respuesta dinámica como método de inspección y control de tableros de puentes de hormigón armado y pretensado" Ph.D. dissertation. Technical University of Catalunya, Spain.

Casas, J.R., [1994], "An Experimental Study on the use of Dynamic Tests for Surveillance of Concrete Structures," Materials and Structures, 27[174], 588–595.

Cawley, P. and R.D. Adams, [1979a], "The Locations of Defects in Structures from Measurements of Natural Frequencies," Journal of Strain Analysis, 14 [2], 49–57.

Cement and Concrete Association [1988]. "*The diagnosis of Alkali-Silica Reaction,* Report of working party." Cement and Concrete Association, Wexham Springs.

Ceravolo, R. and A. De Stefano, [1995], "Damage Location in Structures Through a Connectivistic Use of FEM Modal Analyses," Modal Analysis: The International Journal of Analytical and Experimental Modal Analysis, 10[3],176.

Chance, J., G.R. Tomlinson, and K. Worden, [1994], "A Simplified Approach to the Numerical and Experimental Modeling of the Dynamics of a Cracked Beam," in Proc. Of the 12th International Modal Analysis Conference, 778–785.

Chen, H.L., C.C. Spyrakos, and G. Venkatesh, [1995], "Evaluating Structural Deterioration by Dynamic Response," Journal of Structural Engineering, 121[8], 1197–1204.

Chen, J.-C. and J.A. Garba, [1988a], "On-Orbit Damage Assessment for Large Space Structures," AIAA Journal, 26[9], 1119–1126.

Chen, J.-C. and J.A. Garba, [1988b], "Structural Damage Assessment Using a System Identification Technique," from Structural Safety Evaluation Based on System Identification Approaches, H.G. Natke and J.T.P. Yao, Eds., Friedr. Vieweg & Sohn, Braun-schweig, Wiesbaden.

Chen, Y. and A.S.J, Swamidas, [1996], "Modal Parameter Identification for Fatigue Crack Detection in T-Plate Joints," in Proc. 14th International Modal Analysis Conference, 112–118.

Chen, Y., and A.S.J. Swamidas, [1994], "Dynamic Characteristics and Modal Parameters of a Plate with a Small Growing Surface Crack," in Proc. of the 12th International Modal Analysis Conference, 1155–1161.

Choudhury, A.R. and J. He, [1996], "Structural Damage Location Using Expanded Measured Frequency Response Function Data," in Proc. of the 14th International Modal Analysis Conference, 934–942.

Chowdhury, M.R. and M. Ramirez, [1992], "A Comparison of the Modal Responses for Defective Versus Nondefective Concrete Test Beams," in Proc. of the 10th International Modal Analysis Conference, 508–515.

Clark, L. A., and Cranston, W. B. [1979]. ''The influence of bar spacingon tension stiffening in reinforced concrete slabs.'' *Proc., Int. Conf. onConcrete Slab*s, 118–128.

Clark, L. A., and Speirs, D. M. [1978]. ''Tension stiffening in reinforcedconcrete beams and slabs under short-term load.'' *Tech. Rep. No. 42.52*1, Cement and Concrete Association, London.

Clough, R.W. y Pienzen, J. [1993], Dynamic of structures. McGraw-Hill, International Editions, Civil Engineering Series.

Concrete Society [1987]. " *Concrete core testing for strength*." Report of working party, Technical report 11, Concrete Society..

Concrete Society [1988]. "*Permeability testing of site concrete, a review of methods and experience*." Report of a Working Party, Technical Report 31, Concrete Society.

Cooley, J. W. and Turkey, J. W. [1965]. "An algorithm for the machine calculation of Complex Fourier Series"; Mathematics and Computation. 19[90], 297-311.

Cope, R. J. [1986]. ''Nonlinear analysis of reinforced concrete slabs. "*Computer modelling of RC structure*s", Pineridge, Swansea, U.K., 3–43.

Coppolino, R.N. and S. Rubin, [1980], "Detectability of Structural Failures in Offshore Platforms by ambient Vibration Monitoring," in Proc. 12th Annual Offshore Tech. Conf., 4, 101–110.

Cost, [2000]. "System Identification & Structural Health Monitoring", Proceedings of the Conference on System Identification & Structural Health Monitoring. Madrid, Spain, June 2000.

Crisfield, M. A, [1982] "Variable Step-Length for Nonlinear Structural Analysis," Report 1049, Transport and Road Research Lab., Crowthorne, England.

Crohas, H. and P. Lepert, [1982], "Damage-Detection Monitoring Method for Offshore Platforms is Field-Tested," Oil & Gas Journal, February 22, 94–103.

Damjanic, F., and Owen, D. R. J. [1984]. ''Practical considerations formodelling of post-cracking concrete behaviour for finite-element anal-ysisof reinforced concrete structures.'' *Proc., Int. Conf. on Comp.-AidedAnal. and Des. of Concrete Struct*., Pineridge, Swansea, U.K.,693–706.

Doebling S. W., Farrar C. R., Prime M. B., and Shevitz D. W. [1996] "*Damage Identification and Health Monitoring of Structural and Mechanical Systems From Changes in Their Vibration Characteristics: a Literature Revie*w". Research report LA-13070-MS, ESA-EA Los Alamos National Laboratory, Los Alamos, NM, USA.

Doebling, S.W., [1995], Measurement of Structural Flexibility Matrices for Experiments with Incomplete Reciprocity, Ph. D. Dissertation, University of Colorado, Boulder, CO, Department of Aerospace Engineering Sciences, CU-CAS-95-10.

Doebling, S.W., [1996], "Damage Detection and Model Refinement Using Elemental Stiffness Perturbations with Constrained Connectivity," in Proc. of the AIAA/ASME/AHS Adaptive Structures Forum, 360–370, AIAA-96-1307.

Doebling, S.W., F.M. Hemez, M.S. Barlow, L.D. Peterson, and C. Farhat, [1993a], "Damage Detection in a Suspended Scale Model Truss Via Model Update," in Proc. Of the 11th International Modal Analysis Conf., 1083–1094.

Doebling, S.W., F.M. Hemez, M.S. Barlow, L.D. Peterson, and C. Farhat, [1993b], "Selection of Experimental Modal Data Sets for Damage Detection Via Model Update," in Proc. of 34th AIAA/ASME/ASCE/AHS/ASC Structures, Structural Dynamics, and Materials Conference, 1506–1517, AIAA-93-1481-CP.

Doebling, S.W., L.D. Peterson, and K.F. Alvin, [1995], "Measurement of Static Flexibility Matrices for Experiments with Incomplete Reciprocity," in Proc. of 36th AIAA/ASME/ASCE/AHS/ASC Structures, Structural Dynamics, and Materials Conference, 2777–2791, AIAA-95-1092-CP.

Doebling, S.W., L.D. Peterson, and K.F. Alvin, [1996], "Estimation of Reciprocal Residual Flexibility from Experimental Modal Data," AIAA Journal, to appear.

Dong C., P.Q. Zhang, W.Q. Feng, and T.C. Huang, [1994], "The Sensitivity Study of the Modal Parameters of a Cracked Beam," in Proc. of the 12th International Modal Analysis Conference, 98–104.

Dos Santos, J.M.C. and D.C. Zimmerman, [1996a], "Damage Detection in Complex sructures Using Component Mode Synthesis and Residual Modal Force Vector," in proc. of the 14th International Modal Analysis Conference, 1299–1305.

Dos Santos, J.M.C. and D.C. Zimmerman, [1996b], "Structural Damage Detection Using Minimum Rank Update Theory and Parameter Estimation," in Proc. of the AIAA/ASME/AHS Adaptive Structures Forum, 168–175, AIAA-96-1282.

Duggan, D.M., E.R. Wallace, and S.R. Caldwell, [1980], "Measured and Predicted Vibrational Behavior of Gulf of Mexico Platforms," in Proc. 12th Annual Offshore Tech.Conf., 92–100.

Elkordy, M.F., K.C. Chang, and G.C. Lee, [1993], "Neural Network Trained by Analytically Simulated damage States," ASCE Journal of Computing in Civil Engineering,7[2], 130–145.

Elkordy, M.F., K.C. Chang, and G.C. Lee, [1994], "A Structural Damage Neural Network Monitoring System," Microcomputers in Civil Engineering, 9, 83–96.

Ellis, B. R. [1998]. "Non Destructive dynamic testing of stone pinnacles of the palace of Westminister." Proceedings of Proceedings of the institution of Civil Engineers, Structures and Buildings UK

Farrar, C.; Duffey, A.; Cornwell, P. and Doeblinng, S. [1999] "Excitation methods for bridge structures", Proceedings of International Modal Analysis Conference, Kissimmee, FL, Feb.

Farrar, C.R. and K.M. Cone, [1995], "Vibration Testing of the I-40 Bridge Before and After the Introduction of Damage," in Proc. 13th International Modal Analysis Conference, 203–209.

Farrar, C.R., W.E. Baker, T.M. Bell, K.M. Cone, T.W. Darling, T.A. Duffey, A. Eklund, and A. Migliori, [1994], "Dynamic Characterization and Damage Detection in the I-40 Bridge Over the Rio Grande", Los Alamos National Laboratory report LA-12767-MS.

Figg, J. W. A. M. A. F. [1985]. "*Concrete in oceans*." *Technical report No. 10,* Offshore Technology Report OTR 84/205, HMSO, London..

FIP [Federation Internationale de la Precontrainte] [1986]. "*Inspection and maintenance of reinforced and prestressed concrete structures*." Thomas Telford, London. 7pp..

Fox, C.H.J., [1992], "The Location of Defects in Structures: A Comparison of the Use of Natural Frequency and Mode Shape Data," in Proc. of the 10th International Modal Analysis Conference, 522–528.

Friswell M.I. and Mottershead J.E. [1995] "Finite Element Model Updating in Structural Dynamics". Kluwer Academic Publishers, Dordrecht, The Netherlands.

Friswell, M.I., J.E.T. Penny and D.A.L. Wilson, [1994], "Using Vibration data and Statistical Measures to Locate Damage in Structures," Modal Analysis: The International Journal of Analytical and Experimental Modal Analysis, 9[4], 239–254.

Fritzen, C.P., S. Seibold and D. Buchen, [1995], "Application of Filter Techniques for Damage Identification in Linear and Nonlinear Mechanical Structures," in Proc. of the 13th International Modal Analysis Conference, 1874–1881.

Gates, J.H., [1976], "California's Seismic Design Criteria for Bridges," ASCE Journal of Structural Engineering, 102, 2301–2313.

Gattermayerova, H. and Bayer, J. A. K. J. [1998]. "Dynamic test and Verifications of Mechanical Properties of a Panel Building." Proceedings of Saving building in Central and Eastern Europe, IABSE Colloquium , Berlin 4-5 June

Genovese, F. a. V. F. [1998]. "Identification of dynamic characteristics of masonry building." Proceedings of European Conference on Earthquake Engineering Paris

Ghaboussi, J., and Sidarta, D. E. [1998]. ''New nested adaptive neural networks [NANN] for constitutive modeling.'' *Int. J. of Comp. andGeotechnic*s, 22[1], 29–52.

Ghaboussi, J., Garrett, J. H., Jr., and Wu, X. [1991]. ''Knowledge-basedmodeling of material behavior with neural networks.'' *J. Engrg. Mech.*,ASCE, 117[1], 132–153.

Ghaboussi, J., Pecknold, D. A., Zhang, M., and HajAli, R. M. [1996]. ''Neural network constitutive models determined from structural tests.''*Proc., 11th ASCE Engrg. Mech. Conf*., ASCE, New York, 701–704.

Gilbert, R. I. [1988]. *Time effects in concrete structure*s, Elsevier Science,Amsterdam.

Gilbert, R. I. and R. F. Warner, [1978] "Tension Stiffening in Reinforced Concrete Slabs," Journal of the Structural Division, American Society of Civil Engineers, vol. 104, ST12, pp. 1885-1900.

Gorlov, A.M., [1984], "Disaster of the I-95 Mianus River Bridge–Where Could Lateral Vibration Come From?," ASME Journal of Applied Mechanics, 51, 694–696.

Gudmundson, P., [1982], "Eigenfrequency Changes of Structures Due to Cracks, Notches, or other Geometrical Changes," Journal of the Mechanics and Physics of Solids, 30[5], 339–353.

Gudmundson, P., [1983], "The Dynamic Behavior of Slender Structures with Cross-Sectional Cracks," Journal of the Mechanics and Physics of Solids, 31, 329–345.

Gysin, H.P., [1986], "Critical application of an Error Matrix Method for Location of Finite element Modeling Inaccuracies," in Proc. of the 4th International Modal Analysis Conference, 1339–1351.

Hand, F. D., D. A. Pecknold, and W. C. Schnobrich, [1973] "Nonlinear Analysis of Reinforced Concrete Plates and Shells," Journal of the Structural Division, American Society of Civil Engineers, vol. 99, ST7, pp. 1491-1505.

Hearn, G. and R.B. Testa, [1991], "Modal Analysis for Damage Detection in Structures," Journal of Structural Engineering, 117[10], 3042–3063.

Helene, P. [1993]. Corrosion of reinforcement steel bars study [In Portugese], Technical University of Sau Paulo., Sau Paulo, Brasil.

Hemez, F.M. and C. Farhat, [1995], "Structural Damage Detection via a Finite Element Model Updating Methodology," Modal Analysis: The International Journal of Analytical and Experimental Modal Analysis, 10 [3], 152–166.

Hemez, F.M., [1993], Theoretical and Experimental Correlation Between Finite Element Models and Modal Tests in the Context of Large Flexible Space Structures, Ph. D. Dissertation, Dept. of Aerospace Engineering Sciences, University of Colorado, Boulder, CO.

Hendry, A. W. A. R. R. [1985]. "*Acoustic emission observations on a stone masonry bridge loaded to failure*." Proceedings of Proceedings of the 2nd International Conference on Structural Faults and Repair Engineering Technics Press, Edinburgh 285-91

Hibbit, Karlsson and Sorensen. [1995]. "Abaqus Standar User manual." Hibbit, Karlson and Sorensen, Inc. Printed in USA, 1995.

Hilleborg, A. [1982]. ''The influence of tensile toughness of concrete onthe behaviour of reinforced concrete structures.'' *Proc., 9th FIP Congr.*,Federation Internationale de la Precontrainte, 157–164.

Hinkle, J.D., S.W. Doebling, and L.D. Peterson, [1995], "The Effects of Gravity Preload on the Flexibilities of a Precision Deployable Structure," in Proc. of 36th AIAA/ASME/ASCE/AHS/ASC Structures, Structural Dynamics, and Materials Conference, 2465–2473, AIAA-95-1440-CP.

Hinton, E., H. H. Abdel Rahman, and O. C. Zienkiewicz, [1981] "Computational Strategies for Reinforced Concrete Slab Systems," International Association of Bridge and Structural Engineering Colloquium on Advanced Mechanics of Reinforced Concrete, pp. 303-313, Delft.

Hogg, R.V. and Craig, A.T. [1978] "Introduction to Mathematical Statistics", fourth edition. Macmillan.

Hop, T. [1991]. "Effect of degree of prestressing and age of concrete beams on frequency and damping of their free vibration." Materials and structures, 210-220.

Huang, C. S. , Yang, Y. B. , Lu, L. Y. , and Chen, C. H. [1999] *Earthquake Engineering & Structural Dynamics* 28, 857-878

Ismail, F., A. Ibrahim, and H.R. Martin, [1990], "Identification of Fatigue Cracks from Vibration Testing," Journal of Sound and Vibration, 140, 305–317.

Jauregui, D.V. and C.R. Farrar, [1996a], "Damage Identification Algorithms Applied to Numerical Modal Data From a Bridge," in Proc. 14th International Modal Analysis Conference, 119–125.

Jerath S., Shibani M.M. [1984] "Dynamic Modulus for Reinforced Concrete Beams."ASCE Journal of Structural Engineering, June, Vol 110 No 6

Jokubatis, V. [1967]. ''Regular and accidental crack influence on deflec-tionsof reinforced concrete beams subjected to short-term loading.''PhD thesis, Kaunas Politechnical Institute, Lithuania [in Lithuanian].

Jones, D. S. a. O. C. W. [1978]. "*The practical aspects of load testing.* " The Structural Engineer, 56 A [12], 353-6.

Ju, F. and M. Mimovich, [1986], "Modal Frequency Method in Diagnosis of Fracture Damage in Structures," in Proc. of the 4th International Modal Analysis Conference,1168–1174.

Kabe, A.M., [1985], "Stiffness Matrix Adjustment Using Mode Data," AIAA Journal, 23[9], 1431–1436.

Kaklauskas G and Ghaboussi J, [2001] "Stress-strain relations for cracked tensile concrete from RC beam tests "ASCE Journal of Structural Engineering; Jan; Vol 127 No 1

Kaklauskas, G. [1999]. ''Universal constitutive model for flexural rein-forcedconcrete members.'' *Rep. No. A-329*, Lithuanian State Scienceand Studies Foundation, Vilnius, Lithuania.

Kaklauskas, G., Ghaboussi, J., and Hawkins, N. M. [1997]. ''Determi-nationof stress-strain curves for concrete from RC beam tests.'' *Proc.,5th Int. Conf. Modern Build. Mat. and Technique*s, 128–145.

Kaklauskas, G., Ghaboussi, J., and Wu, X. [1998]. ''Neural network mod-ellingof tension stiffening effect for R/C flexural members.'' *Proc.,Euro-C 1998 Conf. on Comp. Modelling of Concrete Struct*., Balkema,Rotterdam, The Netherlands, 823–832.

Kam, T.Y. and T.Y. Lee, 1992, "Detection of Cracks in Structures Using Modal Test Data," Engineering Fracture Mechanics, 42[2], 381–387.

Kammer, D. C., [1988], "Optimal Approximation for Residual Stiffness in Linear System Identification," AIAA Journal, 26[1], 104–112.

Kang, Y. J. [1977] "Non-linear geometric, material and time dependent analysis of concrete frames"; UC-SESM Report No. 77-1, Division of structural engineering and structural mechanics, University of California, Berkeley, January.

Kaouk, M. and D.C. Zimmerman, [1993], "Evaluation of the Minimum Rank Update in Damage Detection: An Experimental Study," in Proc. of the 11th International Modal Analysis Conference, 1061–1067.

Kaouk, M. and D.C. Zimmerman, [1994a], "Structural Damage Assessment Using a Generalized Minimum Rank Perturbation Theory," AIAA Journal, 32[4], 836–842.

Kaouk, M. and D.C. Zimmerman, [1994c], "Structural Damage Detection Using Measured Modal Data and No Original Analytical Model," in Proc. of the 12th International Modal Analysis Conf., 731–737.

Kaouk, M., [1993], Finite Element Model Adjustment and Damage Detection Using Measured Test Data, Ph. D. Dissertation, Dept. of Aerospace Engineering Mechanics and Engineering Science, Univ. of Florida, Gainesville, FL.

Kashangaki, T.A-L., [1991], On-Orbit Damage Detection and Health Monitoring of Large Space Trusses–Status and Critical Issues, NASA report TM-104045.

Kashangaki, T.A-L., S.W. Smith, and T.W. Lim, [1992], "Underlying Modal Data Issues for Detecting Damage in Truss Structures," in Proc. of 33rd AIAA/ASME/ ASCE/AHS/ASC Structures, Structural Dynamics and Materials Conf., 1437–1446, AIAA-92-2264-CP.

Kato, M. a. S. S. [1986]. "Vibration of PC bridge during failure process." Journal of Structural Engineering, ASCE, 112[7], 1692-1703.

Keiller, A. P. [1982]. "*A preliminary investigation of test methods for the assessment of strength of in-situ concrete.*" Technical Report 551, Cement and Concrete Association, Wexham Spring, September.

Kenley, R.M. and C.J. Dodds, [1980], "West Sole WE Platform: Detection of Damage By Structural Response Measurements," in Proc. of the 12th Annual Offshore Technology Conference, 111–118.

Kim, H.M. and T.J. Bartkowicz, [1993], "Damage Detection and Health Monitoring of Large Space Structures, Sound and Vibration, 27[6], 12–17.

Kim, J.-T., and N. Stubbs, [1993], Assessment of the Relative Impact of Model Uncertainty on the Accuracy of Global Nondestructive Damage Detection in Structures. Re-port prepared for New Mexico State University.

Ko, J. M., C. W. Wong, and H. F. Lam, [1994], "Damage Detection in Steel Framed Structures by Vibration Measurement Approach," in Proc. of 12th International Modal Analysis Conference, 280–286.

Koh, C.G., L.M. See and T. Balendra, [1995], "Damage Detection of Buildings: Numerical and Experimental Studies," Journal of Structural Engineering, 121[8], 1155–1160.

Kong, F., Z. Liang, and G.C. Lee, [1996], "Bridge Damage Identification Through Ambient Vibration Signature," in Proc. 14th International Modal Analysis Conference, 717–724.

Krawczuk, M. and W.M. Ostachowicz, [1992], "Parametric Vibrations of a Beam with Crack," Archive of Applied Mechanics, 62, 463–473.

Kropp [1995]. Chlorides in Concrete. Performance Criteria for Concrete Durability., RILEM Technical Committee.

Kudva, J., N. Munir, and P. Tan, [1991], "Damage Detection in Smart Structures Using Neural Networks and Finite Element Analysis," in Proc. of ADPA/AIAA/ASME/SPIE Conference on Active Materials and Adaptive Structures, 559–562.

Kuns, J. T. a. E. J. W. [1985]. "*Remote sensing techniques applied to bridge deck evaluation.*" American Concrete Institute Special Publication, 88-25[237-59].

Lam, H.F., J.M. Ko, and C.W. Wong, [1995], "Detection of Damage Location Based on Sensitivity Analysis," in Proc. of the 13th International Modal Analysis Conference, 1499–1505.

Law, S.S., P. Waldron, and C. Taylor, [1992], "Damage Detection of a Reinforced Concrete Bridge Deck Using the Frequency Response Function," in Proc. of the 10th International Modal Analysis Conference, 772–778.

Lawrence, C. D. [1981]. "*Durability of concrete: Molecular transport processes and test methods*." Technical Report 544, Cement and Concrete Association, Wexham Springs.

Liang, Z., M. Tong, and G.C. Lee, [1995], "Modal Energy Measurement of a Long Steel Bridge," in Proc. 13th International Modal Analysis Conference, 226–232.

Lifshitz, J.M. and A. Rotem, [1969], "Determination of Reinforcement Unbonding of Composites by a Vibration Technique," Journal of Composite Materials, 3, 412–423.

Lin R.M. and D.J. Ewins, [1990], "On the Location of Structural Nonlinearity from Modal Testing–A Feasibility Study," in Proc. of the 8th International Modal Analysis Conference, 358–364.

Lin, C. S. and A. C. Scordelis, [1975] "Nonlinear Analysis of Reinforced Concrete Shells of General Form," Journal of the Structural Division, American Society of Civil Engineers, vol. 101, pp. 523-238.

Lin, C. S. and A. C. Scordelis, [1975] "Nonlinear Analysis of Reinforced Concrete Shells of General Form," Journal of the Structural Division, American Society of Civil Engineers, vol. 101, pp. 523-238.

Ljung, L. [1987]. System Identification, Prentice-Hall, New Jersey.

Loland, O. and J.C. Dodds, [1976], "Experience in Developing and Operating Integrity Monitoring System in North Sea," in Proc. of the 8th Annual Offshore Technology Conference, 313–319.

Maeck J., De Roeck G., [2002] "Damage assessment of a gradually damaged RC beam using dynamic system identification", Proceedings IMAC 20, International Modal Analysis Conference, Los Angeles, California, USA, February.

Maeck, J. and De Roeck G. [1999a]. "Damage identification in reinforced concrete structures by dynamic stiffness determination." Engeneering structures, 22.

Maeck, J. and De Roeck G. [1999b]. "Detection of damage in civil engineering structures by direct stiffness derivation." Proceedings of Proceedings of the fourth European Conference on Structural Dynamics, EURODYN 99, Czech Republic

Maeck, J. and De Roeck G.. [1999c]. "Dynamic bending and torsion stiffness derivation from modal curvatures and torsion rates." Journal of Sound and Vibration, 225[1], 153-170.

Malhorta, V. M. [1991].Proceedings of the second Internat Conference. Montreal, Canada.

Man, X.T., L.M. McClure, Z. Wang, R.D. Finch, P.Y. Robin, and B.H. Jansen, [1994], "Slot Depth Resolution in Vibration Signature Monitoring of Beams Using Frequency Shift," Journal of the Acoustic Society of America, 95[4], 2029–2037.

Manning, D. G. [1985]. "*Detecting Defects and Deterioration in Highway Structures*." National Cooperative Highway Research Program: Transportation Research Board, Washington, DC., 118.

Manning, D. G. and Holt, F. B. [1980]. "*Detecting delamination in concrete bridge decks*." Concrete International,[November], pp. 34-41.

Manning, D.G. and Bye, D.H.[1983]. "*Bridge deck rehabilitation manual*, part 1, condition surveys ." Research and Development Branch, Ontario Ministry of Transportation and Communications..

Manning, R., [1994], "Damage Detection in Adaptive Structures Using Neural Networks,"in Proc. of 35th AIAA/ASME/ASCE/AHS/ASC Structures, Structural Dynamics, and Materials Conference, 160–172.

Mayes, R.L., [1992], "Error Localization Using Mode Shapes–An Application to a Two Link Robot Arm," in Proc. 10th International Modal Analysis Conference, 886–891.

Mayes, R.L., [1995], "An Experimental Algorithm for Detecting Damage Applied to the I-40 Bridge over the Rio Grande," in Proc. 13th International Modal Analysis Conference, 219–225.

Mazurek, D.F. and J.T. DeWolf, [1990], "Experimental Study of Bridge Monitoring Technique," ASCE Journal of Structural Engineering, 116, 2532–2549.

McConnell, K. G. [1995] *Vibration Testing Theory and Practic*e, John Wiley and Sons, Inc., NY

McGowan, P.E., S.W. Smith, and M. Javeed, [1990], "Experiments for Locating Dam-age Members in a Truss Structure," in Proc. 2nd USAF/NASA Workshop on System Identification and Health Monitoring of Precision Space Structures, 571–615.

McNeice, A. M., [1967] "Elastic-Plastic Bending of Plates and Slabs by the Finite Element Method," Ph. D. Thesis, London University.

Meneghetti, U. and A. Maggiore, [1994], "Crack Detection by Sensitivity Analysis," in Proc. of the 12th International Modal Analysis Conference, 1292–1298.

Menzies, J. B. [1978]. "*Load testing of concrete building structures*." The Structural Engineer, 56 A [12], 347-52.

Migliori, A., T.M. Bell, R.D. Dixon, R. Strong, [1993], Resonant Ultrasound Non-Destructive Inspection, Los Alamos National Laboratory report LA-UR-93-225.

Mkalar, P. F. W. R. E. S. B. R. a. C. V. P. [1984]. "*Acoustic emission behavior of concrete*." In-situ Non-destructive Testing of Concrete American Concrete Institute Special Publication , 82, 619-37.

Montgomery, F. R. a. A. A. [1985]. "*Early experience with a new concrete permeability apparatus*." Proceedings of Proceedings of the 2nd International Conference on Structural Faults and Repairs, Engineering Techincs Press, Edinburgh 359-63

Moore, W. M. S. G. a. M. L. J. [1973]. "*An instrument for detecting delamination in concrete bridge decks*." Highway Research Board, Washington, DC., 541, 44-52.

Morsch, E. [1909]. *Concrete-steel constructio*n, McGraw-Hill New York

Mottershead, J. E. & Friswell, M. I. [1993] "Model updating in structural dynamics: a survey". J. Sound Vib. 162, 347{375.

Mottershead, J. E. & Friswell, M. I. [eds] [1998] "Model updating." Mech. Syst. Signal Process. 12[1].

Narkis, Y., [1994], "Identification of Crack Location in Vibrating Simply Supported Beams," Journal of Sound and Vibration, 172[4], 549–558.

Nataraja, R., [1983], "Structural Integrity Monitoring in Real Seas," in Proc. 15th Annual Offshore Tech. Conference, 221–228.

Neville, A. M. [1995]. Properities of Concrete, Pearson Education Limited, England.

Nwosu, D.I., A.S.J. Swamidas, J.Y. Guigne, and D.O. Olowokere, [1995], "Studies on Influence of Cracks on the Dynamic Response of Tubular T-Joints for Nondestructive Evaluation," in Proc. of the 13th International Modal Analysis Conference, 1122–1128.

Oliveira, D.V., [2003] "Experimental and numerical analysis of blocky masonry structures under cyclic loading. Ph.D. Dissertation, Universidade do Minho, Guimarães, Portugal.

Oller, E.; Salcedo, J; Cobo, D. and Marí., A.R. [2001] "Flexural Strengthening of Reinforced Concrete Beams with Externally Bonded CFRP laminates". Seminario Composites in Construction [CCC2001], organizado por Universidad de Porto, [Octubre].

Olson, L. D. and Wrigh, C. C. [1990]. "Nondestructive testing for repair and rehabilitation." Concrete International. Design and construction., 58-64.

Osegueda, R.A., P.D. Dsouza, and Y. Qiang, [1992], "Damage Evaluation of Offshore Structures Using Resonant Frequency Shifts," Serviceability of Petroleum, Process, and Power Equipment, ASME PVP 239 /MPC 33, 31–37.

Pandey, A.K., and M. Biswas, [1994], "Damage Detection in Structures Using Changes in Flexibility," Journal of Sound and Vibration, 169 [1], 3–17.

Papadakis, V. G., Roumeliotis, A. P., and Fardis, M. N. a. V. C. G. 1. [1996]. "Mathematical modelling of chloride effect on concrete durability and protection measures." Proceedings of International Conference. Concrete in the service of mankind. Dundee, UK.

Pape, D.A., [1993], "A Modal Analysis Approach to Flaw Detection in Ceramic Insulators," in Proc. of the 11th International Modal Analysis Conference, 35–40.

Park, Y.S., H.S. Park, and S.S. Lee, [1988], "Weighted-Error-Matrix Application to Detect Stiffness Damage-Characteristic Measurement," Modal Analysis: The International Journal of Analytical and Experimental Modal Analysis, 3[3], 101–107.

Peeters, B. [2000]. "System identification and damage detection in civil engineering", Ph.D. dissertation, Civil Engineering Department, Catholic University of Leuven, Belgium.

Peeters, B. and De Roeck, G [1999b]. "Experimental dynamic analysis of a steel mast excited by wind load." Proceedings of Structural dynamics - EURODYN 99 Rotterdam 1075-1080

Peeters, B. and De Roeck, G [1999b]. "Reference-based stochlastic suspsace identification for output-only modal anaysis." Mechanical systems and signal procesing, 13[6], 855-878.

Peeters, B. and De Roeck, G. [1999a]. "Experimental dynamic analysis of a steel mast excited by windload."1075-1080.Conference proceedings

Peeters, B. and De Roeck, G. [2000]. "Reference based stochastic subspace identification in civil engineering." Inverse problems in engineering, 8[1], 47-74.

Peeters, B; Abdel Wahab, M., G. De Roeck, J. De Visscher, W.P. De Wilde, J.-M. Ndambi, J. Vantomme, [1996] "Evaluation of structural damage by dynamic system identification", Proceedings of ISMA 21, the 21th International Seminar on Modal Analysis [edited by P. Sas], pp. 1349-1361, Katholieke Universiteit Leuven, Belgium, 18-20 September.

Penny, J.E.T., D.A.L. Wilson, and M.I. Friswell, [1993], "Damage Location in Structures Using Vibration Data," in Proc. of the 11th International Modal Analysis Conference, 861–867.

Perchard, D.R., and A.S.J. Swamidas, [1994], "Crack Detection in Slender Cantilever Plates Using Modal Analysis," in Proc. of the 12th International Modal Analysis Conference, 1769–1777.

Peterson, L.D., K.F. Alvin, S.W. Doebling, and K.C. Park, [1993], "Damage Detection Using Experimentally Measured Mass and Stiffness Matrices," in Proc. of 34th AIAA/ASME/ASCE/AHS/ASC Structures, Structural Dynamics, and Materials Conference, 1518–1528, AIAA-93-1482-CP.

Peterson, L.D., S.W. Doebling and K.F. Alvin, [1995], "Experimental Determination of Local Structural Stiffness by Disassembly of Measured Flexibility Matrices," in Proc. of

36th AIAA/ASME/ASCE/AHS/ASC structures, Structural Dynamics, and Materials Conference, 2756–2766, AIAA-95-1090-CP.

Petroski, H. J. and J. L. Glazik, [1980], "Effects of Cracks on the Response of Circular Cylindrical Shells," Nuclear Technology, 5, 303–316.

Popovics S., Rose J.L., Popovics J.S. [1990] ".The Behavior of Ultrasonic Pulses in Concrete." Cement and Concrete Research; Mar; Vol 20 No 2

Poston R.W., Withlock A. R. and Kesner K.E., [1995] "Condition assessment using non-destructive evaluation" Concrete International, Jul.

Prakhya, G. K. V., and Morley, C. T. [1990]. ''Tension stiffening andmoment-curvature relations for reinforced concrete elements.'' *ACIStruct. J*., 87[5], 597–605.

Prentis, J. M. [1951]. ''Distribution of concrete stress in reinforced andprestressed concrete beams when tested to destruction by a pure bend-ingmoment.'' *Mag. of Concrete Res*., 2[5], 73–77.

Prime, M.B. and D.W. Shevitz, [1996], "Linear and Nonlinear Methods for Detecting Cracks in Beams, in Proc. of the 14th International Modal Analysis Conference," 1437–1443.

Prion, H.G.L., C.E. Ventura and M. Rezai, [1996], "Damage Detection of Steel Frame By Modal Testing," in Proc. 14th International Modal Analysis Conference, 1430–1436.

Raghavendrachar, M. and A. E. Aktan, [1992], "Flexibility by Multireference Impact Testing for Bridge Diagnostics," ASCE Journal of Structural Engineering, 118, 2186–2203.

Regourd [1983]. "Durability Phisyco-Chemical and biological processes related to concrete." Proceedings of Workshop on Durability of Concrete Structures. CEB, RILEM. Copenhagen, Denmark. Pp. 49-71.

Richardson, M.H. and M.A. Mannan, [1992], "Remote Detection and Location of Structural Faults Using Modal Parameters," in Proc. of the 10th International Modal Analysis Conference, 502–507.

Richardson, M.H., [1980], Detection of Damage in Structures from Changes in their Dynamic [Modal] Properties- A survey, NUREG/CR-1431, U.S. Nuclear Regulatory Commission, Washington, D.C.

Rizos, P.F., N. Aspragathos, and A.D. Dimarogonas, [1990], "Identification of Crack Location and Magnitude in a Cantilever Beam from the Vibration Modes," Journal of Sound and Vibration, 138[3], 381–388.

Rostam, S. [1992]. Tecnología Moderna de durabilidad., Cuadernos Intemac No. 5., Madrid, España.

Rytter, A., [1993], Vibration Based Inspection of Civil Engineering Structures, Ph. D. Dissertation, Department of Building Technology and Structural Engineering, Aalborg University, Denmark.

Saitoh, M. and B.T. Takei, [1996], "Damage Estimation and Identification of Structural Faults Using Modal

Salane, H.J., J.W. Baldwin, and R.C. Duffield, [1981], "Dynamics Approach for Monitoring Bridge Deterioration," Transportation Research Record, 832, 21–28.

Salawu, O.S. and C. Williams, [1994], "Damage Location Using Vibration Mode Shapes," in Proc. of 12th International Modal Analysis Conference, 933–939.

Salawu, O.S. and C. Williams, [1995], "Bridge Assessment Using Forced-Vibration Testing," Journal of Structural Engineering, 121[2], 161–173.

Salawu, O.S., [1994], "Nondestructive Evaluation of Constructed Facilities Using Vibration Testing," Insight, 36[8], 611–615.

Salawu, O.S., [1995], "Nondestructive Assessment of Structures Using the Integrity Index Method Applied to a Concrete Highway Bridge," Insight, 37[11], 875–878.

Samman, M. M. and M. Biswas, [1994], "Vibration Testing for Nondestructive Evaluation of Bridges," Journal of Structural Engineering, 120[1], 290–306.

Samman, M.M., M. Biswas, and A.K. Pandey, [1991], "Employing Pattern Recognition for Detecting Cracks in a Bridge Model," Modal Analysis: The International Journal of Analytical and Experimental Modal Analysis, 6, 35–44.

Sanchez, D. [2001] "Determinación experimental de la envolvente de rotura biaxial en muros de obra de fabrica", Undergraduate thesis, Deparment of Construction engineering, UPC, September.

Sanders, D., R.N. Stubbs, and Y.I.Kim, [1989], "Global Nondestructive Damage Detection in Composite Structures," in Proc. of the 7th International Modal Analysis Conference, 1501–1507.

Sanders, D., Y.I. Kim and R.N. Stubbs, [1992], "Nondestructive Evaluation of Damage in Composite Structures Using Modal Parameters," Experimental Mechanics, 32, 240–251.

Savage, R. J. [1985].*Proceedings of the 2nd International Conference on Structural Faults and Repair*, Engineering Technics Press, Edinburgh 255-64

Schnobrich, W. C. [1985]. ''The role of finite-element analysis of rein-forcedconcrete structures.'' *Proc. of Seminar Sponsored by Japan Soc. for Promotion of Sci. and U.S. Nat. Sci. Found.*, ASCE, New York, 1–24.

Shen, M.H.H. and Y.C. Chu, [1992], "Vibrations of Beams with a Fatigue Crack," Computers & Structures, 45[1], 79–93.

Shirole, A.M. and R.C. Holt, [1991], "Planning for a Comprehensive Bridge Safety Assurance Program," Transportation Research Record, 1290 , 39–50.

Sibbald, A., A. Bensalem, and C.A. Fairfield, [1995], "NDT of Arch Bridges," Insight, 37[11], 864–870.

Sigmund, V. a. H. K. [1998]. "Dynamic Characteristics as indicators of structural integrity." Proceedings of Saving building in Central and Eastern Europe, IABSE Colloquium Berlin

Sigmund, V. A. Herman. K. [1998]. "Dynamic Characteristics as indicators of structural integrity." Conference proceedings of Saving Buildings in Central and Eastern Europe, IABSE, Berlin 4-5 June.

Silva, J.M.M. and A.J.M.A. Gomes, [1990], "Experimental Dynamic Analysis of Cracked Free-free Beams," Experimental Mechanics, 30[1], 20–25.

Silva, J.M.M. and A.J.M.A. Gomes, [1994], "Crack Identification of Simple Structural Elements Through the use of Natural Frequency Variations: The Inverse Problem," in Proc. of the 12th International Modal Analysis Conference, 1728–1735.

Simmermacher, T., D.C. Zimmerman, R.L. Mayes, G.M. Reese and G.H. James, [1995], "Effects of Finite Element Grid Density on Model Correlation and Damage Detection of a Bridge," in Proc. of 36th AIAA/ASME/ASCE/AHS/ASC Structures, Structural Dynamics and Materials Conference, 2249-2258.

Skjaerbaek, P.S., S.R.K. Nielsen, and A.S. Cakmak, [1996], "Assessment of Damage in Seismically Excited RC-Structures from a Single Measured Response," in Proc. Of the 14th International Modal Analysis Conference, 133–139.

Slastan, J. a. Foissner. P. [1995]. "Masonry building dynamic characteristics evaluation by means of ambient vibration." Proceedings of 10th European Conference on Earthqueke Engineering Rotterdam

Slastan, J., and S. Pietrzko, [1993], "Changes of RC Beam Modal Parameters Due to Cracks," in Proc. of the 11th International Modal Analysis Conference, 70–76.

Slater, G.L., and S. Shelley, [1993], "Health Monitoring of Flexible Structures Using Modal Filter Concepts," SPIE Smart Structures and Intelligent Systems, 1917, 997– 1007.

Smith, S.W. and C.A. Beattie, [1991a], Model Correlation and Damage Location for Large Space Truss Structures: Secant Method Development and Evaluation, NASA-CR- 188102.

Smith, S.W. and P.E. McGowan, [1989], "Locating Damaged Members in a Truss Structure Using Modal Test Data: A Demonstration Experiment," in Proc. of 30th AIAA/ASME/ASCE/AHS/ASC Structures, Structural Dynamics and Materials Conf., AIAA-89-1291-CP.

Spyrakos, C., H.L. Chen, J. Stephens, and V. Govidaraj, [1990], "Evaluating Structural Deterioration Using Dynamic Response Characterization," Proc. Intelligent Structures, Elsevier Applied Science, 137–154.

Srinivasan, M.G. and C.A. Kot, [1992], "Effects of Damage on the Modal Parameters of a Cylindrical Shell," in Proc. of the 10th International Modal Analysis Conference, 529–535.

Stain, R. T. [1982]. "*Integrity Testing*." *Civil Engineering*, 54-9.

Stubbs, N. A. O. R. [1990]. "Global Non-destructive damage evaluation in solids." International Journal of Analytical and Experimental Modal Analysis , 5[2], 67-79.

Stubbs, N. and R. Osegueda, [1990a], "Global Non-Destructive Damage Evaluation in Solids," Modal Analysis: The International Journal of Analytical and Experimental Modal Analysis, 5[2], 67–79.

Stubbs, N. and R. Osegueda, [1990b9, "Global Damage Detection in Solids–Experimental Verification," Modal Analysis: The International Journal of Analytical and Experimental Modal Analysis, 5[2], 81–97.

Stubbs, N., J.-T. Kim, and C.R. Farrar, [1995], "Field Verification of a Nondestructive Damage Localization and Severity Estimation Algorithm," in Proc. 13th International Modal Analysis Conference, 210–218.

Stubbs, N., J.-T. Kim, and K. Topole, [1992], "An Efficient and Robust Algorithm for Damage Localization in Offshore Platforms," in Proc. ASCE Tenth Structures Congress, 543–546.

Stubbs, N., T.H. Broome and R. Osegueda, [1990], "Nondestructive Construction Error Detection in Large Space Structures," AIAA Journal, 28[1], 146–152.

Swamidas, A.S. and Y. Chen, [1992], "Damage Detection in a Tripod Tower Platform [TTP] Using Modal Analysis," ASME Offshore Technology, 1-B, 577–583.

Tang, J.P., and K.-M. Leu, [1991], "Vibration Tests and Damage Detection of P/C Bridges," Journal of the Chinese Institute of Engineers, 14, 531–536.

Tesinas muros

Todd, M. D., C. C. Chang, G. A. Johnson, S. T. Vohra, J. W. Pate and R. L. Idriss [1999] "Bridge Monitoring Using a 64-Channel Fiber Bragg Grating System," *Proceedings of the 17th International Modal Analysis Conferenc*e, Kissimmee, FL, pp. 1719-1725

Toksoy, T. and A.E. Aktan, [1994], "Bridge-condition Assessment by Modal Flexibility," Experimental Mechanics, 34, 271–278.

Tomlinson, G. R. [1994]. "Linear or non-linear – That is the question." 19th International Seminar on Modal Analysis, Leuven, Belgium, September 1994, 11-32.

Tracy, J.J. and G.C. Pardoen, [1989], "Effect of Delamination on the Natural Frequencies of Composite Laminates," Journal of Composite Materials, 23, 1200–1215.

Turner, J.D. and A.J. Pretlove, [1988], "A Study of the Spectrum of Traffic-Induced Bridge Vibration," Journal of Sound and Vibration, 122, 31–42.

Van Greunen [1979] "Non-linear geometric, material and time dependent analysis of reinforced and prestressed concrete slabs and panels"; UC-SESM Report No. 79-3, Division of structural engineering and structural mechanics, University of California, Berkeley, October.

Vandiver, J.K., [1975], "Detection of Structural Failure on Fixed Platforms by Measurement of Dynamic Response," in Proc. of the 7th Annual Offshore Technology Conference, 243–252.

Vandiver, J.K., [1977], "Detection of Structural Failure on Fixed Platforms by Measurement of Dynamic Response," Journal of Petroleum Technology, March, 305–310.

Vassie, P. R. [1980]. "*A Survey of Site Tests for the Assessment of Corrosion in Reinforced Concrete*." TRRL Report 953, Department of the Environment, Department of Transport..

Verbeck, G. J. [1975]. "Mechanisms of corrosion in concrete." Corrosion of Metals in Concrete., ACI SP-49, 21-38.

Vestroni, F., Beolchini, G. C., and Antonacci, E. a. M. C. [1996]. "Identification of dynamic characteristics of masonry buildings from forced vibration test." Proceedings of Eleventh World Conference on Earthquake Engineering

Villemure, I., C.E. Ventura, and R.G. Sexsmith, [1996], "Impact and Ambient Vibration Testing To Assess Structural Damage In Reinforced Concrete Frames," in Proc. 14th International Modal Analysis Conference, 1178–1184.

Wang, W. and A. Zhang, [1987], "Sensitivity Analysis in Fault Vibration Diagnosis of Structures," in Proc. of 5th International Modal Analysis Conference, 496–501.

Wenner, F. [1915]. "*A Method of Measuring earth resistivity*." Bulletin of the Bureau of Standards, 12, 415-538.

West, W.M., [1984], "Illustration of the Use of Modal Assurance Criterion to Detect Structural Changes in an Orbiter Test Specimen," in Proc. Air Force Conference on Aircraft Structural Integrity, 1–6.

Whittome T.R., and C.J. Dodds, [1983], "Monitoring Offshore Structures by Vibration Techniques," in Proc. of Design in Offshore Structures Conference, 93–100.

Williams, A. [1986]. ''Tests on large reinforced concrete elements sub-jectedto direct tension.'' *Tech. Rep. No. 42.562*, Cement and ConcreteAssociation, London.

Wojnarowski, M.E., S.G. Stiansen and N.E. Reddy, [1977], "Structural Integrity Evaluation of a Fixed Platform Using Vibration Criteria," in Proc. 9th Annual Offshore Tech. Conf., 247–256.

Wolff, T. and M. Richardson, [1989], "Fault Detection in Structures From Changes in Their Modal Parameters," in Proc. of the 7th International Modal Analysis Conference, 87–94.

Wu, X., J. Ghaboussi, and J.H. Garrett, [1992], "Use of Neural Networks in Detection of Structural Damage," Computers and Structures, 42[4], 649–659.

Yuen, M.M.F., [1985], "A Numerical Study of the Eigenparameters of a Damaged Cantilever," Journal of Sound and Vibration, 103, 301–310.

Zhang, Z. and A.E. Atkan, [1995], "The Damage Indices for Constructed Facilities," in Proc. of the 13th International Modal Analysis Conference, 1520–1529.

Zimmerman, D. C., M. Kaouk, and T. Simmermacher, [1995b], "On the Role of Engineering Insight and Judgement Structural Damage Detection," in Proc. of the 13th International Modal Analysis Conf., 414–420.

Zimmerman, D.C. and M. Kaouk, [1994], "Structural Damage Detection Using a Minimum Rank Update Theory," Journal of Vibration and Acoustics, 116, 222–230.

Zimmerman, D.C., S.W. Smith, H.-M. Kim, and T.J. Bartkowicz, [1996], "Spacecraft Applications for Damage Detection Using Vibration Testing," in Proc. of the 14th International Modal Analysis Conference, 851–856.